

Envisat MERIS

Geometry Handbook

name
function
company

date
signature

prepared by

Serge RIAZANOFF
Engineer
VisioTerra
Serge.Riazanoff@visioterra.com



checked by

Stéphane MBAYE
Engineer
GAEL Consultant
Stephane.Mbaye@gael.fr

authorized by

Christophe DEMANGE
Director
GAEL Consultant
Christophe.Demange@gael.fr

approved by

Steven DELWART
Project Manager
ESA-ESTEC
Steven.Delwart@esa.int

DOCUMENT STATUS SHEET

Issue	Date	Comments	Author
1.0	16/08/2004	Draft 1 - Creation of the document – Orthorectification results	S. Riazanoff
1.0	19/08/2004	Draft 2 – Level 1B model, performances, disparity analysis	S. Riazanoff
1.0	19/08/2004	Draft 3 – Orthorectification application	S. Riazanoff
1.0	23/08/2004	Comparison BEAM vs. MERSYN	S. Riazanoff
1.1	29/10/2004	Comments Marc BOUVET on 20/09/2004	S. Riazanoff
1.2	08/11/2004	Release 02.04 of MERSYN – Appendix C	S. Riazanoff
		Benchmark – Appendix D	S. Riazanoff
1.3	16/11/2004	Section 5 – GETASSE30 Quality Control	S. Riazanoff
1.4	03/01/2005	Comments of Norman Fomferra – Eq. 2, 6a and 6b, Appendix E, MERSYN program version 02.05	S. Riazanoff
1.5	06/05/2005	Completion of document – Chapter 5.2. Comparison of GETASSE30 with GPS points	S. Riazanoff

TABLE OF CONTENTS

1 INTRODUCTION.....	7
1.1 PURPOSE OF THIS DOCUMENT.....	7
1.2 DOCUMENT OVERVIEW.....	7
1.3 APPLICABLE DOCUMENTS.....	8
1.4 REFERENCE DOCUMENTS.....	8
1.5 ABBREVIATIONS AND ACRONYMS.....	9
1.6 DEFINITIONS.....	10
2 MERIS LEVEL 1B GEOMETRY	11
2.1 MERIS INSTRUMENT.....	11
2.2 PROCESSING LEVELS.....	12
<i>MERIS Level 1B product grid and tie-point grid.....</i>	13
<i>Along-track tie-points.....</i>	15
<i>Across-track tie-points.....</i>	16
<i>Bi-linear interpolation within « tie-point facets ».....</i>	16
<i>Parallax estimate at tie-points.....</i>	18
<i>Projection of MERIS pixels to the level 1B product grid.....</i>	19
2.3 MERIS FR AND RR LEVEL 1B PRODUCTS.....	20
3 ORTHORECTIFICATION APPLICATION.....	21
3.1 OVERALL ARCHITECTURE.....	21
<i>Use case 1 – Minimum radiance synthesis.....</i>	22
<i>Use case 2 – Maximum NDVI synthesis.....</i>	22
<i>Use case 3 – Orthorectified mapping.....</i>	22
<i>Digital elevation data.....</i>	23
<i>Workflow.....</i>	24
<i>Check parameters and initialise application.....</i>	25
<i>Build up the segment boundary.....</i>	25
<i>Compute intersections of current line vs. boundary.....</i>	26
<i>Read or initialise to background synthesis line.....</i>	26
<i>Retrieve the antecedent (l,p) within the 1B product.....</i>	26
<i>Read MDS(16) flags and check pixel validity.....</i>	26
3.2 PREDICTION/CORRECTION ALGORITHM.....	27
<i>Prediction/correction principle.....</i>	28
3.3 DIRECT LOCATION MODEL.....	29
<i>Retrieving tie-point facet.....</i>	29
<i>Geodetic coordinates interpolation.....</i>	30
<i>Viewing angle interpolation.....</i>	30
<i>Compute and apply the geodetic correction.....</i>	30
3.4 INVERSE LOCATION MODEL.....	31
<i>Retrieving the tie-point facet.....</i>	31
<i>Retrieving offsets within the facet</i>	31
4 ORTHORECTIFICATION RESULTS	33
4.1 MERIS SCENE IN INPUT.....	33
4.2 DIGITAL ELEVATION MODELS.....	35
<i>DEM Italy.....</i>	35
<i>SRTM.....</i>	35
4.3 REFERENCE IMAGE – THE LANDSAT TM MOSAICSNA.....	36
4.4 SUPERIMPOSABILITY – VISUAL CHECKING.....	37
<i>Comment of animation 02 – No orthorectification.....</i>	38
<i>Comment of animation 03 – Altitudes from tie-points grid.....</i>	38
<i>Comment of animation 04 and 05 – Altitudes from DEM Italy.....</i>	39
<i>Comment of animation 06 – Altitudes from DEM SRTM</i>	39
<i>Conclusions.....</i>	40
4.5 RUN-TIME PERFORMANCES.....	41

<i>Performance of the prediction/correction algorithm.....</i>	41
<i>Access time to DEMs.....</i>	41
4.6 DISPARITY ANALYSIS.....	41
<i>Better correlation of SRTM DEM synthesis</i>	42
<i>Global displacement.....</i>	42
4.7 COMPARISON WITH BEAM / VISAT	47
4.8 BENCHMARK.....	49
5 GETASSE30 QUALITY CONTROL.....	50
5.1 COMPARISON WITH EUROPE09.....	51
<i>Visual inspection</i>	52
<i>Statistics of image difference.....</i>	54
5.2 COMPARISON WITH EUVN GEODESIC POINTS.....	59
<i>Description of reference data.....</i>	59
<i>Quality control results.....</i>	62
APPENDIX A MERIS SCENE FR ITALY	66
A.1 DECODING LOG.....	66
APPENDIX B - ORTHORECTIFICATION LOGS.....	74
B.1 NO ORTHORECTIFICATION.....	74
B.2 ALTITUDES FROM TIE-POINT GRID.....	74
B.3 DEM ITALY.....	76
B.4 DEM SRTM	77
B.5 DEM GETASSE30.....	78
APPENDIX C - MERS YN SOURCE CODE.....	80
APPENDIX D - ORTHORECTIFICATION BENCHMARK.....	94
D.1 BENCHMARK POINTS DISTRIBUTION.....	95
D.2 BENCHMARK VALUES.....	96
APPENDIX E - TIE-POINT VALUES.....	98
E.1 SCENE01-01/MER_FR_1PNUPA20030921_092217_000000982020_00079_08149_0354.N1	98
E.2 SCENE01-02/MER_FR_1PNUPA20030921_092220_000000982020_00079_08149_0398.N1	100
E.3 SCENE01-03/MER_FR_1PNUPA20030921_092327_000000982020_00079_08149_0394.N1	100
E.4 SCENE01-04/MER_FR_1PNUPA20030921_092341_000000982020_00079_08149_0534.N1	100
E.5 SCENE01-05/MER_FR_1PNUPA20030925_103640_000000982020_00137_08207_0539.N1	100
E.6 SCENE01-06/MER_FR_1PNUPA20030926_100615_000000982020_00151_08221_0538.N1	101
E.7 SCENE01-07/MER_FR_1PNUPA20031010_092709_000000982020_00351_08421_0536.N1	101
E.8 SCENE01-08/MER_FR_1PNUPA20031010_092717_000000502020_00351_08421_0453.N1	101
E.9 SCENE01-09/MER_FR_1PNUPA20031207_104236_000000982022_00180_09252_0537.N1	101
E.10 SCENE01-10/MER_FR_1PNUPA20031208_101129_000000982022_00194_09266_0535.N1....	102
E.11 SCENE02-01/MER_FR_1PNDPA20040302_103942_000000982024_00409_10483_1126.N1....	102
E.12 SCENE02-02/MER_FR_1PNDPA20040302_103942_000000982024_00409_10483_1130.N1....	102
E.13 SCENE02-03/MER_FR_1PNDPA20040302_104117_000000982024_00409_10483_1131.N1....	102
E.14 SCENE02-04/MER_FR_1PNPDE20040328_102200_000000982025_00280_10855_0002.N1....	103
E.15 MER_RR_1PNPDK20030408_093303_000023202015_00208_05773_0848.N1	103
APPENDIX F - QUALITY CONTROLS OF ACE AND GETASSE30.....	106
F.1 DIFFERENCES BETWEEN GPS POINTS AND ACE DEM – NEAREST NEIGHBOUR.....	106
F.2 DIFFERENCES BETWEEN GPS POINTS AND GETASSE30 DEM – NEAREST NEIGHBOUR.....	108
F.3 DIFFERENCES BETWEEN GPS POINTS AND GETASSE30 DEM – NEAREST NEIGHBOUR.....	110
F.4 DIFFERENCES BETWEEN GPS POINTS AND GETASSE30 DEM – NEAREST NEIGHBOUR.....	113

LIST OF FIGURES

fig. 1 - Artist view of Envisat satellite.....	7
fig. 2 - MERIS instrument (red) on Envisat (http://envisat.esa.int/dataproducts/meris/CNTR3-1-1.htm).....	11
fig. 3 - MERIS FOV, camera tracks, pixel enumeration and swath dimension http://envisat.esa.int/dataproducts/meris/CNTR3-1-3.htm	11
fig. 4 - Functional Breakdown for Level 1B processing algorithm (R-3).....	12
fig. 5 - Satellite fixed coordinate system (R-3).....	13
fig. 6 - MERIS level 1B grid and tie-point grid.....	14
fig. 7 - MERIS frames and tie frames (R-3).....	15
fig. 8 – tie-points pointing direction (R-3).....	16
fig. 9 - Interpolation within a “tie-point facet” (R-3).....	17
fig. 10 - Parallax estimation principle (R-3).....	18
fig. 11 - MERIS pixel location (R-3).....	19
fig. 12 - MERIS synthesis March-April 2003	21
fig. 13 - Minimum radiance synthesis parameters.....	22
fig. 14 - Maximum NDVI synthesis parameters.....	22
fig. 15 - Orthorectified mapping parameters.....	22
fig. 16 - MERSYN overall workflow	24
fig. 17 - Segment boundary of a MERIS RR segment.....	25
fig. 18 - Processing only pixels inside boundary.....	25
fig. 19 - Computing the output image size.....	25
fig. 20 - Segment crossing the -180°/+180° meridian.....	26
fig. 21 - Direct and inverse location models.....	27
fig. 22 - Example of prediction/correction refinements.....	28
fig. 23 - prediction/correction algorithm.....	29
fig. 24 - Retrieving tie-points facet order.....	31
fig. 25 - Facet in the level 1B grid referential (left) and in the geodetic referential (right).	31
fig. 26 - Point inside the latitude and longitude ranges but outside the facet.....	32
fig. 27 - Intersections method.....	32
fig. 28 - Level 1B MERIS scene	33
fig. 29 - MERIS footprint overlaid on SRTM elevations	34
fig. 30 - DEM Italy (250 metres).....	35
fig. 31 - SRTM W020N90 tile	35
fig. 32 - Landsat TM mosaic	36
fig. 33 - REGIST application (snap01_REGIST.gif).....	37
fig. 34 - MERIS (snap02_REGIST_Flicker_no-ortho_meris.gif)	37
fig. 35 - Landsat (snap02_REGIST_Flicker_no-ortho_tm.gif).....	37
fig. 36 - Parallaxes error due to the precision of the DEM(s).....	39
fig. 37 - West offset along the coastline	40
fig. 38 - No-orthorectification – Highest confidence (red) and 95% tie-points.....	45
fig. 39 – Orthorectification from SRTM DEM – Highest confidence (red) and 95% tie-points.....	46
fig. 40 - REGIST application (snap11_REGIST.gif).....	47
fig. 41 - BEAM (snap12_REGIST_Flicker_x4_beams.gif)	48
fig. 42 - MERSYN (snap12_REGIST_Flicker_x4_mersyns.gif)	48
fig. 43 - BEAM (snap13_REGIST_Flicker_x4_beams.gif)	48
fig. 44 - MERSYN (snap13_REGIST_Flicker_x4_mersyns.gif)	48
fig. 45 - BEAM (snap04_REGIST_Flicker_14_beams.gif)	49
fig. 46 - MERSYN (snap04_REGIST_Flicker_14_mersyns.gif)	49
fig. 47 - BEAM (snap05_REGIST_Flicker_14_beams.gif)	49
fig. 48 - MERSYN (snap05_REGIST_Flicker_14_mersyns.gif)	49
fig. 49 - Origin of GETASSE30 data.....	50
fig. 50 - GETASSE30 over Europe	51
fig. 51 - Shading of GETASSE30 – Full image.....	52
fig. 52 - Shading of EUROPE09 – Full image.....	52

fig. 53 - Switzerland animation 01. GETASSE30 (left) and EUROPE09 (right).	53
fig. 54 - Spain animation 02. GETASSE30 (left) and EUROPE09 (right).	54
fig. 55 - EUROPE09 subtracted to GETASSE30 above EGM96 – Image of differences.	55
fig. 56 - EUROPE09 subtracted to GETASSE30 above EGM96 – Statistics.	55
fig. 57 - EUROPE09 subtracted to GETASSE30 above WGS84 – Image of differences.	56
fig. 58 - EUROPE09 subtracted to GETASSE30 above WGS84 – Statistics.	56
fig. 59 - GETOPO30_EGM96-EUROPE09 – Tile defect.	57
fig. 60 - GETOPO30_EGM96-EUROPE09 – Punctual defects.	58
fig. 61 - Site providing a collections of geodesic points.	59
fig. 62 - Distribution of GPS points over Europe.	60
fig. 63 - Distribution of the geodesic control points relatively to GETASSE30 DEM over Europe.	63
fig. 64 - Elevation errors distribution for various interpolation methods.	65
fig. 65 - Distribution of benchmark points.	95
fig. 66 - First and last viewing vectors of the first tie-points line.	98
fig. 67 - Location of the FR scene within the full swath in geodetic geometry.	98

LIST OF TABLES

table 1 - Size and number of tie-points in products.....	15
table 2 - MERIS FR and RR Level 1B product descriptions (http://envisat.esa.int/instruments/meris/data-app/prodspread.html)	20
table 3 - Run-time performances.....	41
table 4 - Statistics of elevation differences (expressed in metres).	63

1 INTRODUCTION

1.1 Purpose of this document

This document describes an accurate method to orthorectify MERIS 1B scenes or segments. This project has been performed on behalf the European Space Agency under the ESTEC contract 17944/03/NL/CO with GAEL Consultant, which has subcontracted the works to VisioTerra.

The overall contract foresees two work packages:

- WP1 - Envisat MERIS Geometry handbook describing the orthorectification algorithm providing examples of code.
- WP2 – SRTM / DEM Digital Elevation Model Quality Assessment.

Algorithms laid down in this document apply to both Full Resolution (FR) and Reduced Resolution (RR) MERIS level 1B products.



fig. 1 - Artist view of Envisat satellite.

1.2 Document overview

- Chapter 1 is the present section applicable to the overall document.
- Chapter 2 describes the MERIS level 1B geometry.
- Chapter 3 describes the orthorectification process.
- Chapter 4 gives results of the orthorectification process.
- Chapter 5 tests the quality of the GETASSE30 DEM.
- Appendix A includes the header information of the MERIS scene being tested.
- Appendix B includes the logs of the orthorectification execution.
- Appendix C provides the C-language code of MERSYN application.
- Appendix C provides the C-language code of MERSYN application.

" This document discloses subject matter in which VisioTerra has proprietary rights. Recipient of this document shall not duplicate, use or disclose in whole or in part, information disclosed here on except for or on behalf of VisioTerra to fulfil the purpose for which the document was delivered to him. "

- Appendix D details the benchmark used to orthorectify a scene over Italy.
- Appendix E logs the orthorectification correction performed on first and last pixels of some lines.
- Appendix F details the differences between GTASSE30 30 and geodesic point elevations.

1.3 Applicable documents

A-1	PO-SW-ESA-GS-1393	<i>ESTEC Contract 17944/03/NL/CO Statement Of Work</i> Issue 1, 19/11/2003 ESA - ESTEC
A-2	e-mail Steven DELWART	<i>Use of GETASSE30 DEM</i> 22/10/2004 Steven DELWART - ESA - ESTEC ..\management\mail_20041022_Delwart_GETASSE30_data_available.txt

1.4 Reference documents

This section describes the related documents and applied conventions to be considered within the present document.

R-1	PO-RS-MDA-GS-2009 (1)	<i>Envisat-1 Products Specifications Volume 1 - Introduction</i> Issue 3, Revision L – 30/01/2001 ESA – ALCATEL SPACE
R-2	PO-RS-MDA-GS-2009 (11)	<i>Envisat-1 Products Specifications Volume 11 – MERIS Products Specification</i> Issue 3, Revision J – 12/05/2003 ESA – ALCATEL SPACE http://earth.esa.int/pub/ESA_DOC/ENVISAT/MERIS/Vol11_Meris_3j.pdf
R-3	PO-TN-MEL-GS-0002	<i>MERIS Level 1 Detailed Processing Model, Parameters Data List</i> Issue 6, Revision 1 – 28/03/2003 ACRI ..\A001_REFERENCE_DOCUMENTS\ENVISAT\PO-TN-MEL-GS-0002_DPM1b_i6r1.pdf
R-4	PO-TN-MEL-GS-003	<i>MERIS Input / Output Data Definitions</i> Issue 6 revision 1 – 23/03/2003 ACRI
R-5	SRTMvsACE_draft_v3.doc	<i>Intercomparison of ACE and SRTM30 global digital elevation model at global and regional scale</i> Issue – Revision 3 – 08/10/2004 Marc BOUVET – ESA/ESTEC ..\reference_documents\SRTMvsACE_draft_v3.doc \\Leo\leo_disks\leo_2\P194_ESTEC_MERIS_GEOMETRY_H_ANDBOOKDEM_GETASSE30\doc\SRTMvsACE_draft_v3.doc

R-6 Readme_with_images.doc

GETASSE30 - Global Earth Topography and Sea Surface Elevation at 30 arc second resolution

Issue -, Revision -, 20/10/2004

Marc BOUVET – ESA/ESTEC

[..\reference_documents\Readme_with_images.doc](#)

[\\Leo\leo_disks\leo_2\P194_ESTEC_MERIS_GEOMETRY_HANDBOOK\DEM_GETASSE30\doc\Readme_with_images.doc](#)

R-7 e-mail Norman FOMFERRA

Comments on equations 6a and 6b

17/12/2004

Norman FOMFERRA – Brockman Consult

[..\management\mail_20041217_Fomferra_MERIS_Geometry_Handbook.txt](#)

Most of the fields of the MERIS 1B products required in for the orthorectification are given in the product specification document R-2 but may also be found at the following Web addresses:

- MERIS FR 1B -
http://envisat.esa.int/dataproducts/meris/CNTR6-2-1.htm#eph.meris.merisdf.1p.MER_FR_1P,
- MERIS RR 1B -
http://envisat.esa.int/dataproducts/meris/CNTR6-2-2.htm#eph.meris.merisdf.1p.MER_RR_1P.

1.5 Abbreviations and Acronyms

This section controls the definition of all abbreviations and acronyms used within this document. Special attention has been paid to adopt abbreviations, acronyms and their definitions from international standards as ISO, ANSI or ECSS.

Abbreviations and acronyms specific to Envisat/MERIS may be found at address <http://envisat.esa.int/dataproducts/meris/CNTR5-1.htm>.

ACE	Altimetry Corrected Elevations
ADSR	Annotation Data Set Record
ANSI	American National Standards Institute
DEM	Digital Elevation Model
ECSS	European Cooperation for Space Standardization
EGM96	Earth Gravity Model 1996
EO	Earth Observation
ETRS89	European Terrestrial Reference System 1989
FR	Full Resolution
GETASSE30	Global Earth Topography and Sea Surface Elevation at 30 arc second resolution
ISO	International Organization for Standardization
ITRS	International Terrestrial Reference System
ITRF	International Terrestrial Reference Frame
MDS	Measurement Data Set
MDSR	Measurement Data Set Record
MSS	Mean Sea Surface

" This document discloses subject matter in which VisioTerra has proprietary rights. Recipient of this document shall not duplicate, use or disclose in whole or in part, information disclosed here on except for or on behalf of VisioTerra to fulfil the purpose for which the document was delivered to him. "

NDVI Normalised Difference Vegetation Index

RR Reduced Resolution

SRTM Shuttle Radar Topography Mission

TBC To Be Confirmed

TM Thematic Mapper (instrument of Landsat)

WGS84 World Geodetic System 1984

1.6 Definitions

This section provides the definition of all common terms used within this document. Special attention has been paid to adopt definitions from international standards as ISO, ANSI or ECSS.

ESA also provides the following glossaries (only those interesting for this document have been selected):

- Geometry <http://envisat.esa.int/dataproducts/meris/CNTR5-2-1.htm>,
- Optics <http://envisat.esa.int/dataproducts/meris/CNTR5-2-9.htm>,
- Product <http://envisat.esa.int/dataproducts/meris/CNTR5-2-10.htm>,

geocoded An image (or more generally any EO data) is geocoded if a simple relation exists giving the geodetic coordinates (λ, ϕ) or (X,Y) of the attached geodetic system, from the coordinates of any point (i,j) of the image.

2 MERIS LEVEL 1B GEOMETRY

Scope of this section is to quickly describe the geometry of the Envisat MERIS level 1B products. A more detailed description is to be searched in document R-3. Content of this document is also presented at <http://www.envisat.esa.int/dataproducts/meris/CNTR2-6-1.htm> address.

2.1 MERIS Instrument

MERIS instrument is flown onboard the Envisat satellite (see fig. 2).

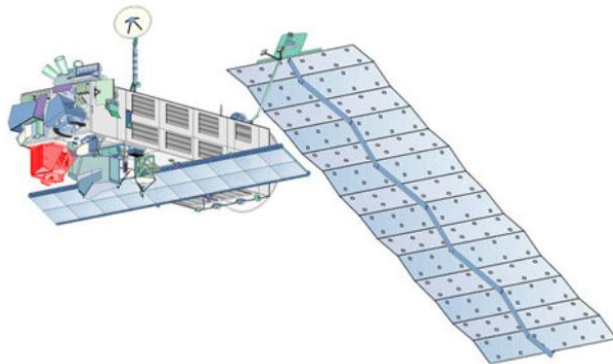


*fig. 2 - MERIS instrument (red) on Envisat
(<http://envisat.esa.int/dataproducts/meris/CNTR3-1-1.htm>)*

This push-broom instrument acquires top of atmosphere radiances in 15 visible and NIR bands and is an assembly of five (5) cameras, sometimes called *modules* because each camera is included within a module sub-system (see fig. 3).

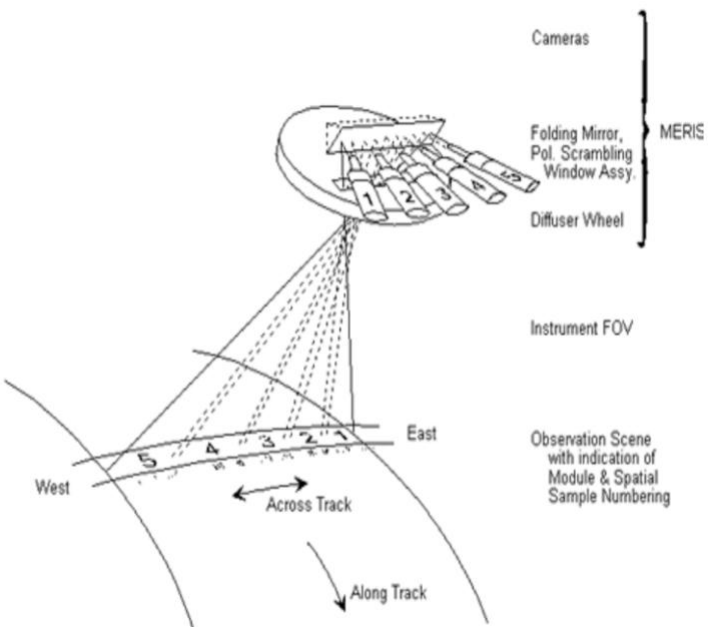


*fig. 3 - MERIS FOV, camera tracks, pixel enumeration and swath dimension
(<http://envisat.esa.int/dataproducts/meris/CNTR1-1-3.htm>)*

" This document discloses subject matter in which VisioTerra has proprietary rights. Recipient of this document shall not duplicate, use or disclose in whole or in part, information disclosed here on except for or on behalf of VisioTerra to fulfil the purpose for which the document was delivered to him. "

2.2 Processing levels

Processing from Level 0 to Level 1B includes the following tasks:

- source data packet extraction,
- saturated pixels replacement and flagging,
- radiometric processing,
- stray light correction,
- **geo-location**,
- pixel classification,
- external data assimilation,
- formatting.

Figure fig. 4 here below illustrates the workflow.

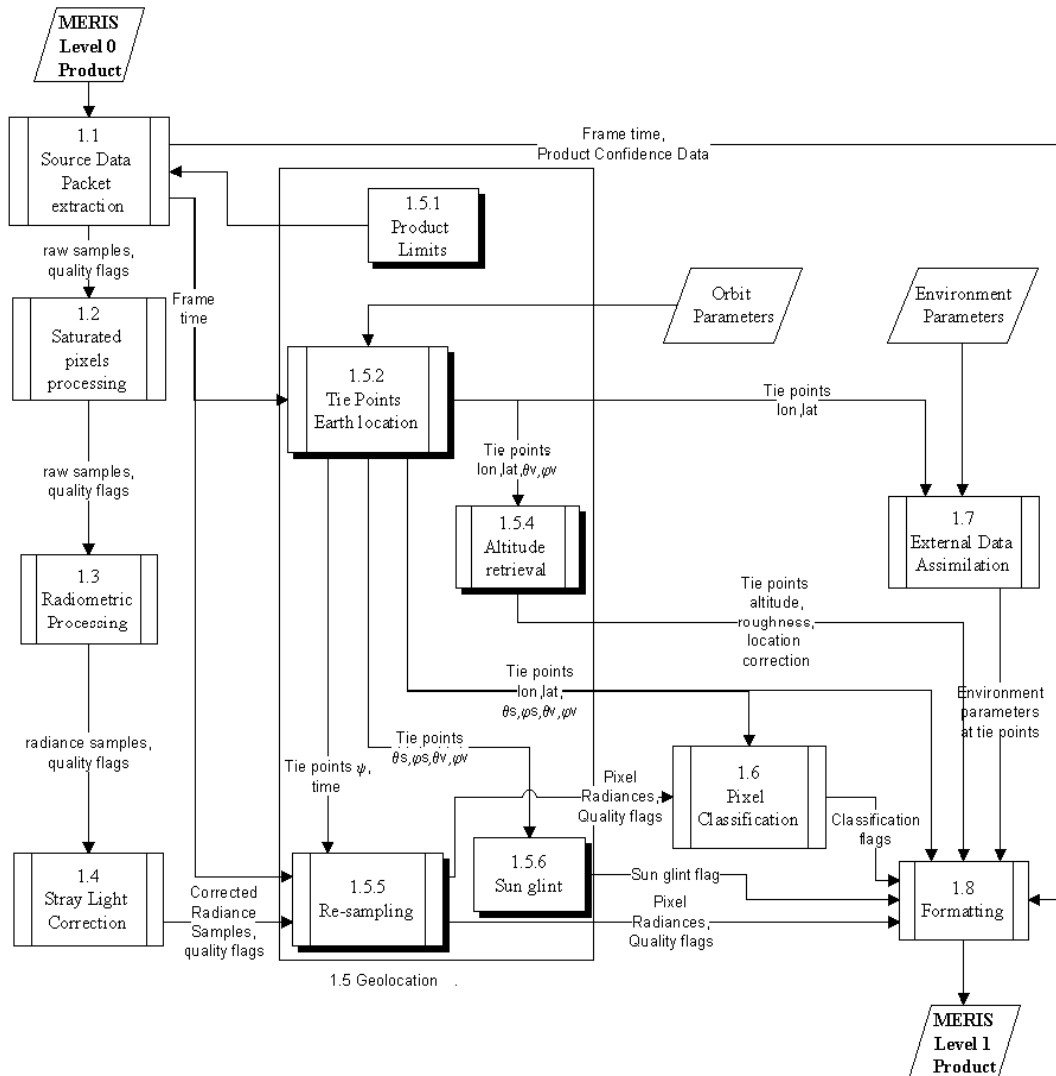


fig. 4 - Functional Breakdown for Level 1B processing algorithm (R-3).

MERIS Level 1B product grid and tie-point grid

The level 1B product grid is a geolocated system defined by the vertical projection of the satellite trajectory over the Earth. (fig. 5) defined by the velocity vector and by its perpendicular plane crossing the Earth.

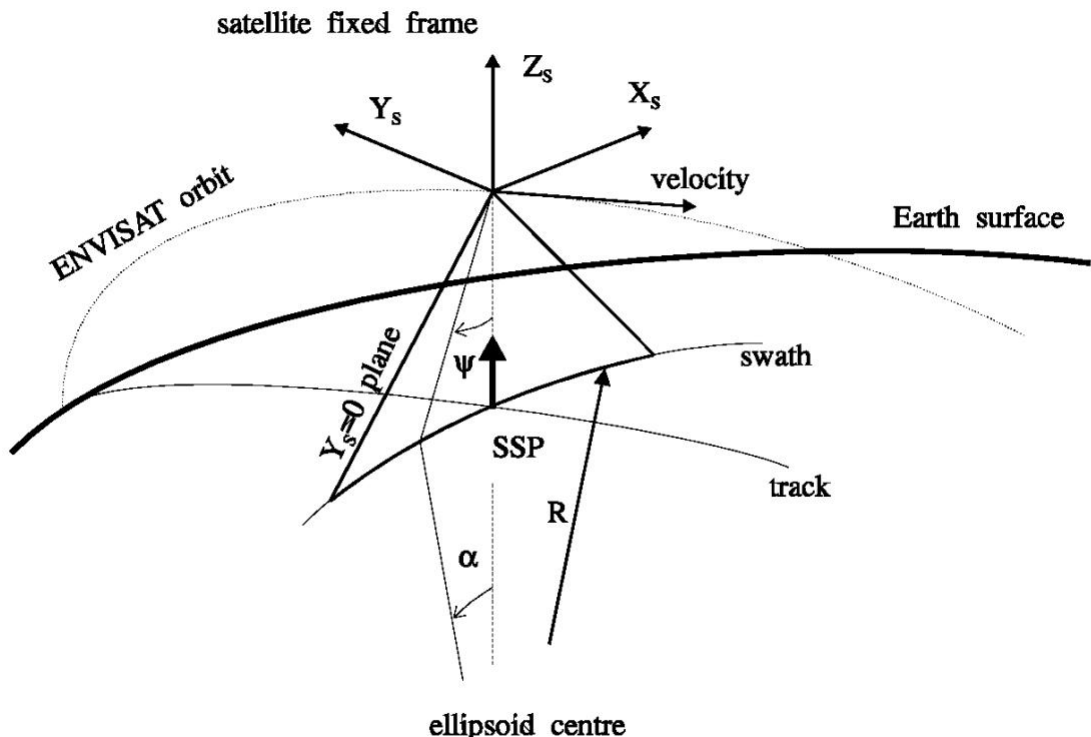


fig. 5 - Satellite fixed coordinate system (R-3).

The document “MERIS Level 1 Detailed Processing Mode” (R-3) says:

“In order to simplify product handling, the MERIS radiance samples are re-located by nearest neighbour interpolation to the MERIS product grid, which has the following characteristics (FR grid) :

- central column : sub-satellite point track on Earth;
- line orientation : perpendicular to spacecraft velocity, projected on Earth;
- columns spacing : fixed for one product, 260 m (with very small variations);
- number of columns : 4481;
- line spacing : variable with time and orbit altitude, fixed by the MERIS frame time of 0.044s (mean \approx 292 m).

“The RR-grid is a 4x4 sub-sampled version of that grid.” (R-3)

To provide geodetic information (latitude, longitude, DEM elevation and roughness), but also information relative to the acquisition conditions (sun incidence angles, viewing angles, wind directions, pressure, ozone, humidity) a **tie-point grid** is superimposed over the MERIS level 1B product grid (see fig. 6). These tie-point grid values are stored in the MERIS 1B product within the Annotation Data Set (ADS) / Tie Points Location & Corresponding Auxiliary Data (LADS).

“ This document discloses subject matter in which VisioTerra has proprietary rights. Recipient of this document shall not duplicate, use or disclose in whole or in part, information disclosed here on except for or on behalf of VisioTerra to fulfil the purpose for which the document was delivered to him. ”

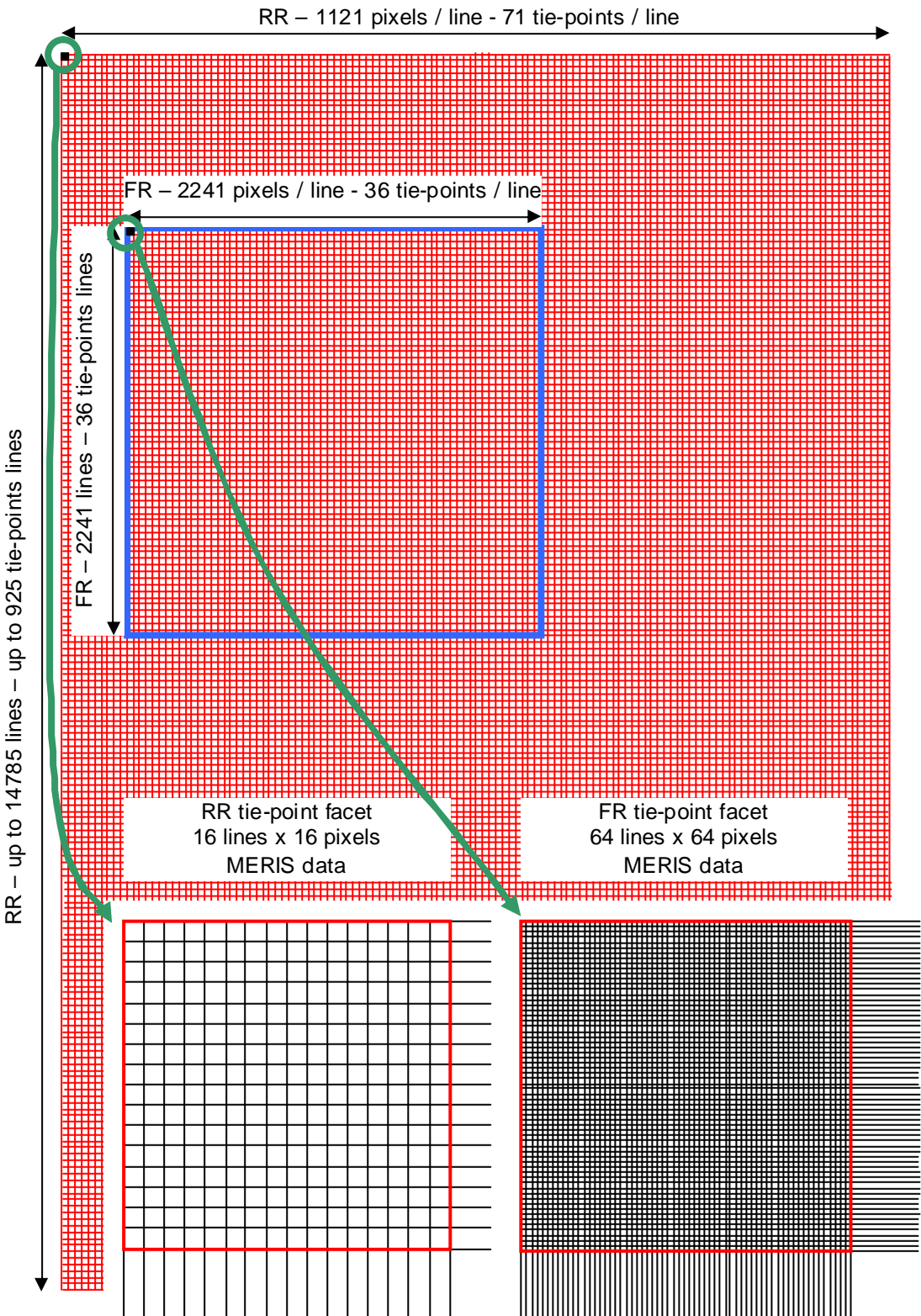


fig. 6 - MERIS level 1B grid and tie-point grid.

The tie-point grid “contains”:

- 64 lines x 64 pixels MERIS data for the FR product, and
- 16 lines x 16 pixels MERIS data for the RR product.

The size of products and the number of tie-points to be found in the Annotation Data Set are given in the table 1 below.

Product	MERIS grid		Tie-point grid	
	Line number	pixel number / line	annotation data set (ADSR) number	samples number / ADSR
MERIS RR 1B	$\leq 14785^{(1)}$	1121	≤ 925	71
MERIS FR 1B	2241	2241	36	36
MERIS FS 1B ⁽²⁾	4481	4481	71	71

(1) A full segment may match up to 43.5 minutes (a sunlight orbit) representing up to 17400 km on ground.

(2) The full resolution Full Swath will be available for the next release of the processor and all the values provided here are to be confirmed.

table 1 - Size and number of tie-points in products.

Along-track tie-points

The constant along-track sampling of 0.044 seconds produces periodic MERIS frames that contain measurements resampled on the MERIS grid. Each DF MERIS frames (DF=64 for FR and DF=16 for RR), a “tie frame” is computed giving the position of the grid along the MERIS swath (see fig. 7).

DF (ΔF in fig. 7): tie-frame spacing.

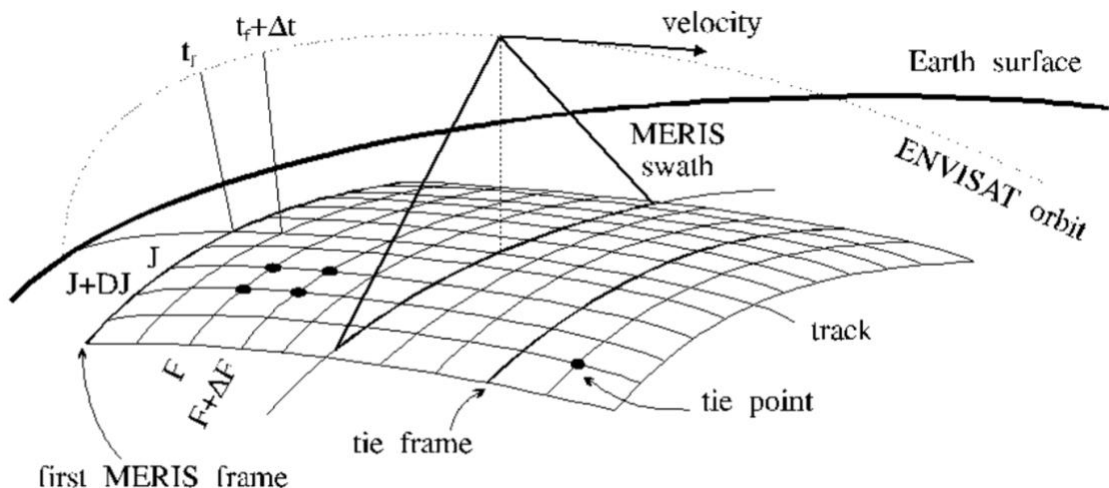


fig. 7 - MERIS frames and tie frames (R-3).

Across-track tie-points

Tie-points along the MERIS swath are sampled in order to be evenly spaced (in distance) along the swath (see fig. 8).

DJ: tie-points column spacing.

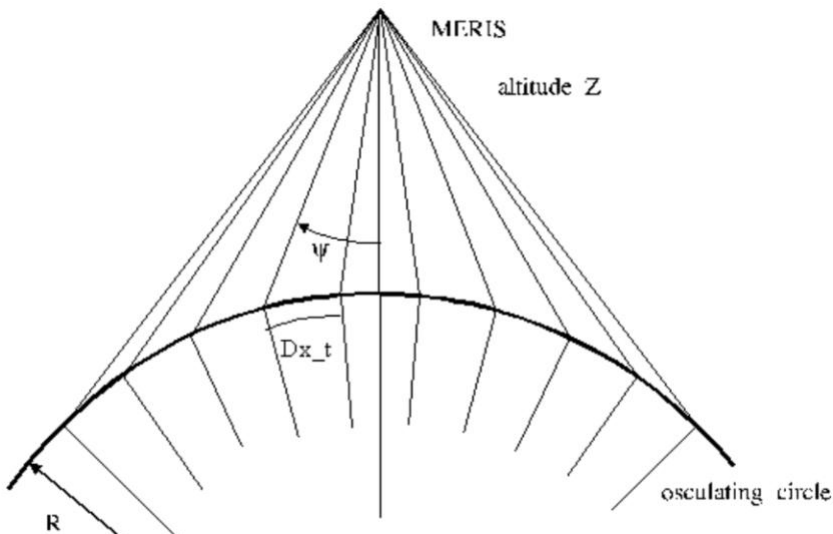


fig. 8 – tie-points pointing direction (R-3).

Bi-linear interpolation within « tie-point facets »

Let (F,J) , $(F+DF,J)$, $(F,J+DJ)$ and $(F+DF,J+DJ)$ the coordinates in the MERIS Level 1B product grid of four adjacent tie-points (see fig. 9), any ancillary value $X(F,J)$ given at the tie-point location may be interpolated within the facet at the location (f,j) using the following formula:

$$X(F+f,J+j) = \left(\frac{DJ-j}{DJ} \right) \times \left[\left(\frac{DF-f}{DF} \right) \times X(F,J) + \left(\frac{f}{DF} \right) \times X(F+DF,J) \right] \\ + \left(\frac{j}{DJ} \right) \times \left[\left(\frac{DF-f}{DF} \right) \times X(F,J+DJ) + \left(\frac{f}{DF} \right) \times X(F+DF,J+DJ) \right] \quad \text{Eq. 1}$$

Where:

- $X()$ is the measurement stored on each tie-point (latitude, longitude, DEM altitude, DRM roughness, DEM latitude correction, DRM roughness, sun zenith, sun azimuth, viewing zenith, viewing azimuth, zonal winds, meridional winds, mean sea level pressure, total ozone, relative humidity).
- (F,J) are the coordinates of the frame (along-track) and column (across-track) expressed in the product grid reference system (i.e. the line index and column index of the level 1B image).
- DF is the number of product lines (frames) between two consecutive tie-points along-track.
- DJ is the number of product pixels between two consecutive tie-points across-track.
- (f,j) are the coordinates within the tie-point facet ($f \in [0,DF[$ and $j \in [0,DJ[$). These coordinates may be float and not necessarily integer.

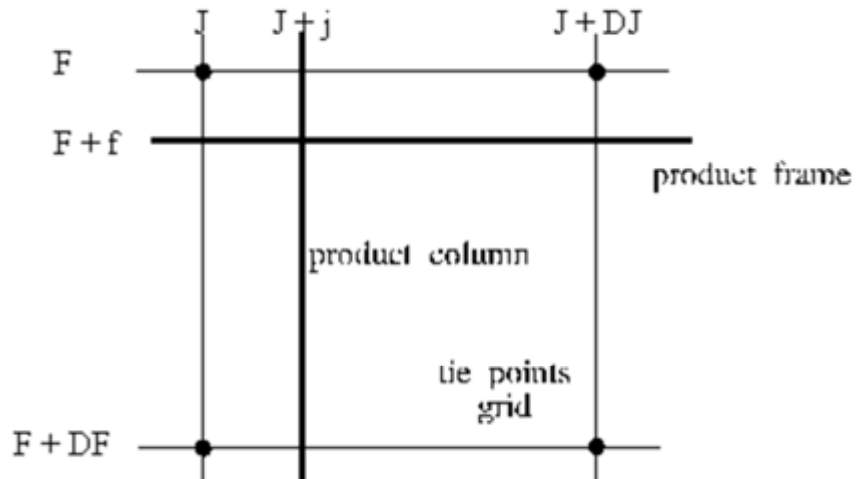


fig. 9 - Interpolation within a "tie-point facet" (R-3).

Parallax estimate at tie-points

As shown in fig. 10, the parallax may be estimated knowing the altitude and viewing angle at any point of the product grid. In particular, the geodetic correction terms ($d\text{lat}$, $d\text{lon}$) are said being computed by the formula below and stored in the Tie Points ADSR (see R-3, section 8.3.3, page 8-28):

dx	$= Z_{F,J} \times \tan(\theta_{vF,J})$	Eq. 2
$d\text{lat}_{F,J}$	$= \frac{dx \times \cos(\varphi_{vF,J})}{R_e}$	Eq. 2
$d\text{lon}_{F,J}$	$= \frac{-dx \times \sin(\varphi_{vF,J})}{R_e \times \cos(\phi_{F,J})}$	

Where:

- dx is the modulus of the parallax error.
- $d\text{lat}_{F,J}$ is the latitude correction of tie-point (F,J).
- $d\text{lon}_{F,J}$ is the longitude correction of tie-point (F,J).
- $Z_{F,J}$ is the DEM elevation of tie-point (F,J).
- $\theta_{vF,J}$ is the zenith of the viewing angle of tie-point (F,J).
- $\varphi_{vF,J}$ is the azimuth of the viewing angle of tie-point (F,J).
- $\phi_{F,J}$ is the geodetic latitude of tie-point (F,J).
- R_e is the mean Earth radius ($R_e = 6\,370\,997.0$ metres)

Examples of tie-point values and explanation relative to the way data are computed are provided in APPENDIX E. Observation of correction values for latitude and longitude shows that eq. 2 is not strictly exact (see eq. 2' in APPENDIX E).

Slightly different formulae (see eq. 6a and 6b) are proposed in sub-section “Compute and apply the geodetic correction” of section 3.3.

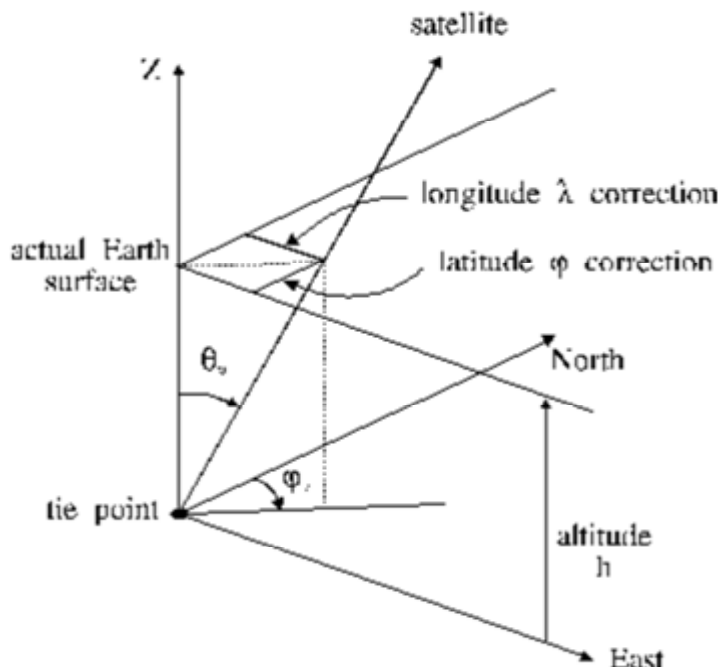


fig. 10 - Parallax estimation principle (R-3).

Projection of MERIS pixels to the level 1B product grid

After radiometric correction, each MERIS pixel P_k of the frame f is copied into the MERIS Level 1B product grid at the location of coordinates (f', j) that are the nearest integer of the projection coordinates within the tie-point facet $[F, F+DF]x[J, J+DJ]$.

These projection coordinates are computed from the (θ_k, ψ_k) viewing vector of point P_k .

The viewing vector it-self is computed from propagated ephemeris and attitude values and from the nominal values of the CCD viewing vectors.

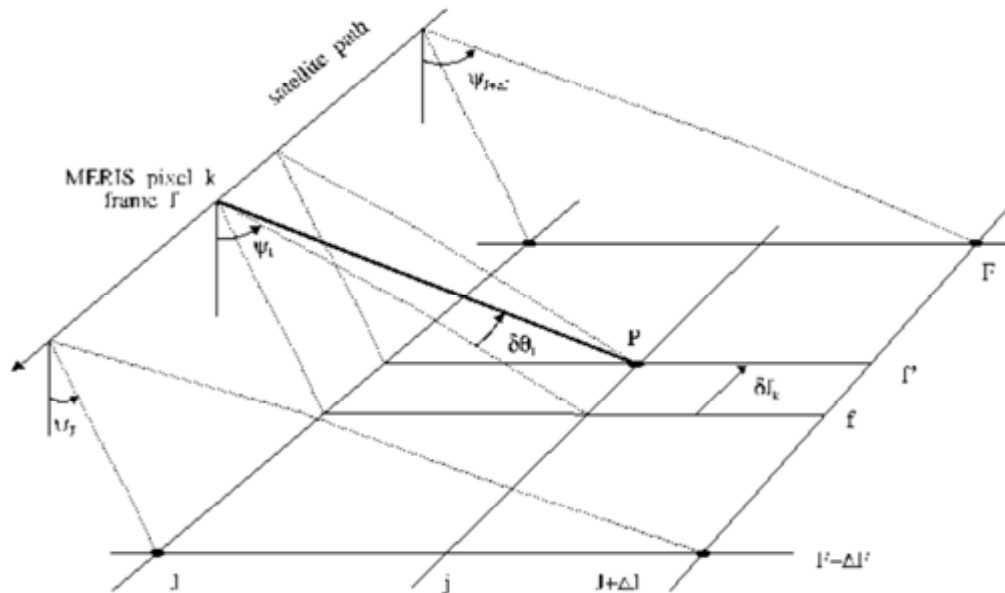


fig. 11 - MERIS pixel location (R-3).

2.3 MERIS FR and RR level 1B products

The overall characteristics of MERIS level 1B products are shown in the table here below, enabling the comparison between Full Resolution (FR) and Reduced Resolution (RR) products.

PRODUCT ID	MER_FR_1P	MER_RR_1P
NAME	Level 1b Full Resolution	Level 1b Reduced Resolution
DESCRIPTION	MERIS product calibrated and geolocated. Produced on request only Floating scene concept for distribution	MERIS product calibrated (radiance) and geolocated. Produced Systematically
COVERAGE	575 km x 575km	1150 km x 17500 km
THROUGHPUT	6 PDHS-E 3 PDHS-K	1 per orbit
GEOMETRICAL SAMPLING	300 x 300 meters resampled in a "pseudo satellite" projection along track	1.2 km x 1.2 km resampled in a "pseudo satellite" projection along track
SEGMENT SIZE	157 bytes per scene	532 Mbytes
RADIOMETRIC RESOLUTION	$1.14 \times 10^{-1} \text{ w/m}^2/\text{sr}/\mu\text{m}$ @442.5nm SSP with $Q_s=60^\circ$	$2.85 \times 10^{-2} \text{ w/m}^2/\text{sr}/\mu\text{m}$ @442.5nm SSP with $Q_s=60^\circ$
RADIOMETRIC ACCURACY	from 400 to 900 nm < 2% from 900 to 1050 nm < 5%	from 400 to 900 nm < 2% from 900 to 1050 nm < 5%
DATA SET	MPH SPH ADS MDS	MPH SPH ADS MDS
ANNOTATION DATA	Orbit state vector, Time correlation parameters, Latitude, Longitude, altitude and topographic corrections Sun azimuth, Sun elevation, view azimuth, view elevation Resampled ECMWF data: Mean Sea Level pressure, Total column ozone, Total column water vapour, Wind speed,	Orbit state vector, Time correlation parameters, Latitude, Longitude, altitude and topographic corrections Sun azimuth, Sun elevation, view azimuth, view elevation Resampled ECMWF data: Mean Sea Level pressure, Total column ozone, Total column water vapour, Wind speed,
NOTES	On demand dissemination of multiple of scenes (575km x 575km) or (296km x 296km)	Produced systematically. On demand dissemination of multiple of scenes (1150 km x 1150 km)

table 2 - MERIS FR and RR Level 1B product descriptions
<http://envisat.esa.int/instruments/meris/data-app/prodspread.html>

3 ORTHORECTIFICATION APPLICATION

Orthorectified images are corrected of the acquisition conditions (viewing geometry, platform attitude, Earth rotation and of the relief effects (parallax). Such a corrected images are perfectly superimposable whatever being their acquisition dates.

One of the principal applications of such a superimposability is the possibility to process mosaicking and more simply synthesis. For example, a synthesis of all the MERIS RR 1B segments acquired on March and April 2003 has been created by GAEL Consultant in June 2003.

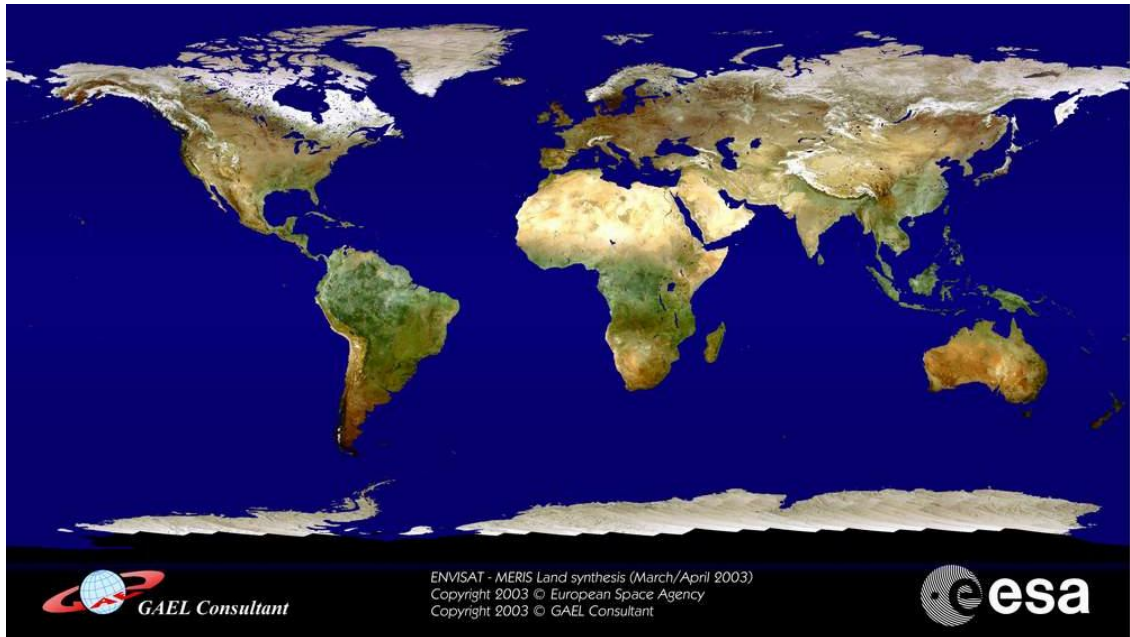


fig. 12 - MERIS synthesis March-April 2003

This project has been the opportunity to develop a first version of a synthesis process, called MERSYN. The present contract has given the possibility to refine MERSYN application extending the orthorectification process to MERIS FR.

This is the reason reader will sometimes encounter references to the synthesis process, up to the name of the provided code (MERSYN for MERIS synthesis). But the synthesis it-self is marginal; most of the code is dedicated to orthorectification that is the challenging activity.

3.1 Overall architecture

MERSYN is able to orthorectify a MERIS Level 1B scene or segment and to add it over an existing synthesis. Merging of a new MERIS pixel over an existing synthesis may be performed according to two different “selection algorithms”: “Minimum radiance” or “NDVI maximum”. The number of parameters for these two behaviour is not the same providing two use cases.

When no synthesis is provided in input, MERSYN only orthorectifies the segment or scene. This is the third use case.

* This document discloses subject matter in which VisioTerra has proprietary rights. Recipient of this document shall not duplicate, use or disclose in whole or in part, information disclosed here on except for or on behalf of VisioTerra to fulfil the purpose for which the document was delivered to him. ”

Use case 1 – Minimum radiance synthesis

In this use case the selection algorithm (« -sal » parameter) has the value “Minimum radiance” meaning that for each band b the MERIS pixel $R(b,i,j)$ will replace the synthesis pixel $S_{n-1}(b,i,j)$ only if MERIS pixel is inferior.

$$S_n(b,i,j) \leftarrow \min[R(b,i,j), S_{n-1}(b,i,j)]$$

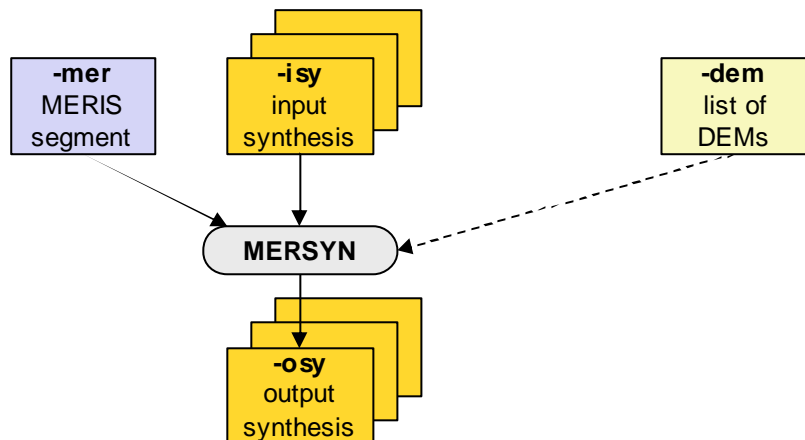


fig. 13 - Minimum radiance synthesis parameters.

Use case 2 – Maximum NDVI synthesis

In this use case the selection algorithm (« -sal » parameter) has the value “Maximum NDVI” (Normalised Difference Vegetation Index).

In this algorithm, all the bands b of a MERIS pixel $R(b,i,j)$ will replace the previous synthesis value $S_{n-1}(b,i,j)$ only if the new NDVI is greater than the previous one $NDVI_{n-1}(i,j)$.

$$NDVI_n(i,j) = \frac{R(13,i,j) - R(7,i,j)}{R(13,i,j) + R(7,i,j)}$$

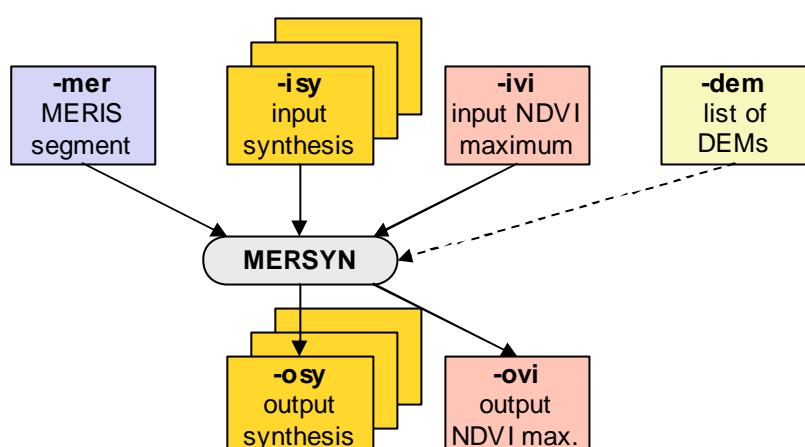


fig. 14 - Maximum NDVI synthesis parameters.

Use case 3 – Orthorectified mapping

In this use case, only the mapping is performed. The output image may be orthorectified using MERIS tie-points elevation values or one (or more) DEM(s) provided as input parameters.

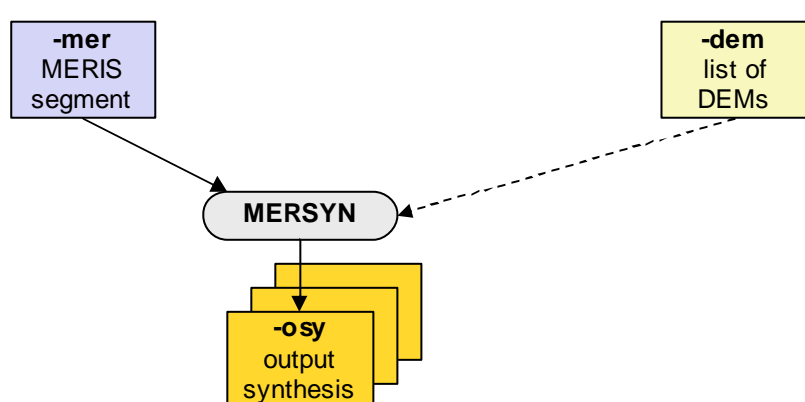


fig. 15 - Orthorectified mapping parameters.

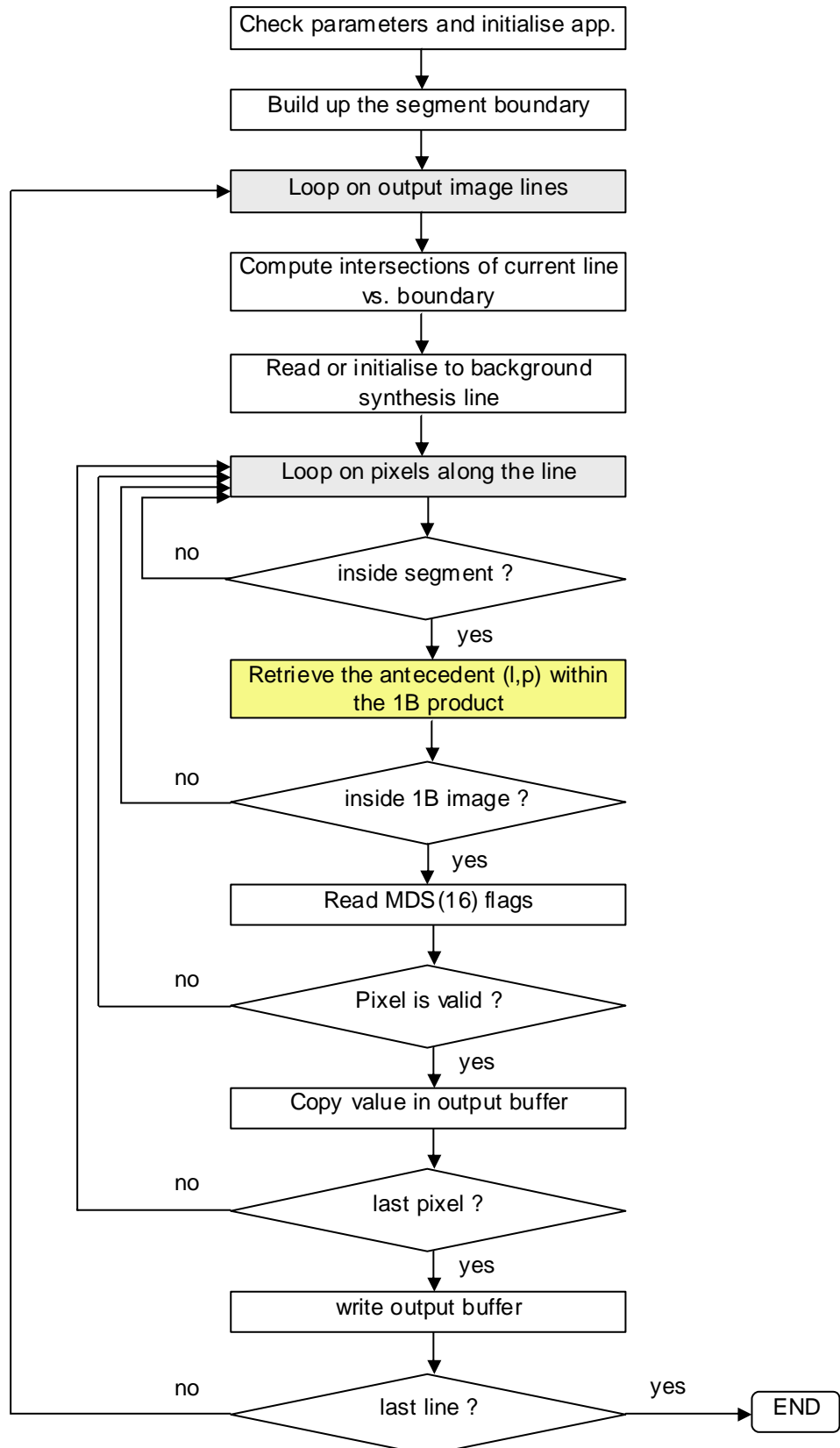
Digital elevation data

MERSYN may:

- no process any orthorectification (“-ort” parameter set to “NO”),
- uses elevation data found in tie-points auxiliary data of the product (no values given to “-dem” parameter),
- uses elevation found within the provided DEM(s) (“-dem” parameter).

More than one DEM may be provided. In such a case, for each pixel of the output geocoded image MERSYN will search for the corresponding elevation data within the first DEM in the list. If the point is outside the DEM, or if a background value (meaning no elevation) is found within this DEM, MERSYN will attempt to get elevation data from the second DEM in the list, and so on...

When more than one DEM are provided, it is recommended that all the DEM belongs to the same series; for example tiles of ACE, SRT30 or GTOPO30. When such is not the case, it is recommended to set the DEM having the greater accuracy as first DEM in the “-dem” list.

Workflow

fig. 16 - MERSYN overall workflow

Check parameters and initialise application

MERSYN checks that all the parameters have consistent values according to the three use cases. For example if a synthesis is provided in input (use cases 1 or 2), the number of channels, the projection, origin and pixel size are automatically found in the TELIMAGO header of the input synthesis and therefore these parameters shall not be provided.

MERSYN also initialise the files, reading input headers or decoding the MPH and SPH of the MERIS product in input, allocate the buffers, initialise the variables...

To minimise file access, height of input MERIS buffers shall be large enough to avoid multiple readings when processing all the pixels of one output line. Buffer height shall be greater than the tangent of the maximum NADIR inclination multiplied by the segment width.

Build up the segment boundary

The segment boundary is a closed polygon built from the geodetic information (latitude and longitude) of the tie-points located along the border of the tie-point grid. Figure fig. 17 here attached illustrates an example of MERIS RR segment boundary.

The segment boundary is used in two ways:

- Optimisation – to compute a projected product, each pixel of the output image shall be processed looking for its antecedent within the input image (see the “reverse location model” hereafter). This process is very time-consuming.

Identifying if a pixel is inside or not the segment boundary enables processing the strict minimum of output pixels. In fig. 18, only the pixels (represented in orange) located inside the segment boundary (red) among all the pixels of the full line (yellow) shall be processed.

- Output image size – in use case 3, when no synthesis is provided in input and MERSYN is used as a mapping process, the size of the output image shall be determined.

The retained size is the smallest rectangle that includes all the segment boundary (see fig. 19).

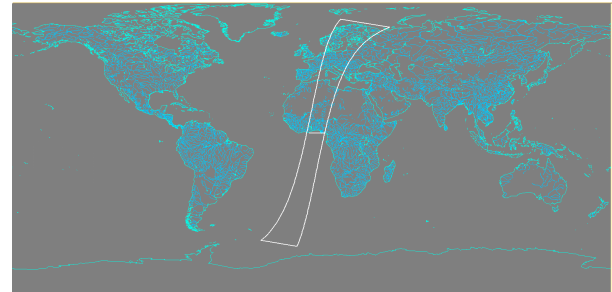


fig. 17 - Segment boundary of a MERIS RR segment.

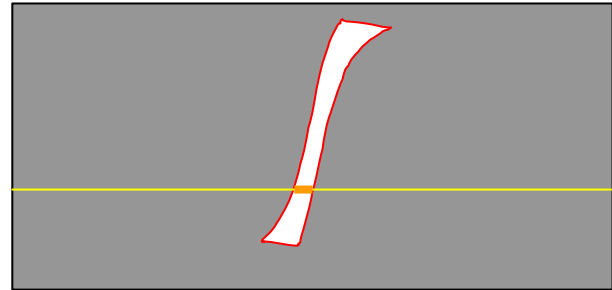


fig. 18 - Processing only pixels inside boundary.

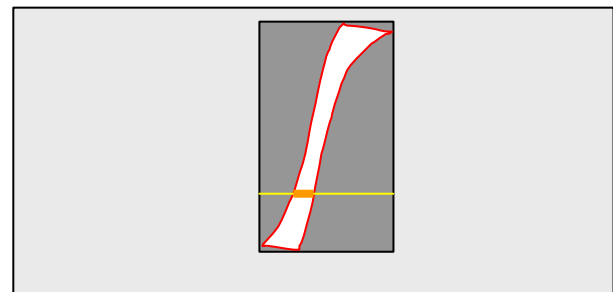


fig. 19 - Computing the output image size.

When the segment is crossing the -180° or $+180^{\circ}$ meridians (see fig. 20) and if the output projection is bounded to these meridians (case of Mercator, Plate Carrée...), the polygon shall be split in two polygons.

A generalised approach should be to enable splitting in more than two polygons in order to comply with discontinuous coordinates reference systems like the Goode-Homolosine. This approach is not supported in the current version 2.03 of MERSYN.



fig. 20 - Segment crossing the $-180^{\circ}/+180^{\circ}$ meridian.

Compute intersections of current line vs. boundary

This operation produces a series of column coordinates delimiting the segment(s) to be processed (represented in orange in fig. 18, fig. 19 or fig. 20) along the current line.

The case of only one point matching one boundary extremity shall be avoided.

Read or initialise to background synthesis line

When a synthesis is provided in input (use cases 1 or 2), the current line i is read and is copied into the output buffer. Otherwise (use case 3), the buffer of the output line is initialised with the background value meaning what no antecedent has been yet found for the output pixels.

Retrieve the antecedent (l,p) within the 1B product

The prediction/correction algorithm used to retrieve the antecedent (l,p) in level 1B image of output pixel (i,j) is fully described in section 3.2 below.

In the current version of MERSYN, only the “nearest neighbour” sampling method has been implemented, and therefore only one pixel (l,p) radiance will be copied into the output buffer. More sophisticated sampling methods could be implemented like the bi-linear interpolation requiring 2×2 pixels anchored on (l,p) or bi-cubic interpolation requiring 4×4 pixels around (l,p) .

Read MDS(16) flags and check pixel validity

The flag values matching input pixel (l,p) are read. Except for use case 3, where all the pixels shall be reported in output image, a pixel is considered as being valid if the “glint risk” (TBC), “bright” (TBC) and “invalid” flags are not set.

3.2 prediction/correction algorithm

To produce a geocoded image (see fig. 21), one must handle:

- a direct location model $f(l,p,h)$ able to compute the (λ, φ) coordinates in the Earth reference system associated to the geocoded image (i.e. the projection of the image),
- an inverse location model $f^{-1}(\lambda, \varphi, h)$ able to compute the coordinates (l, p) in the input product reference system (here a MERIS 1B product of m frames and n columns).

Both functions are useful. The direct location model enables computing the coordinates of the image boundary and therefore the size of the output image. The inverse location model forms the kernel of the geocoding processing, because it enables retrieving the antecedent of any point of the output image.

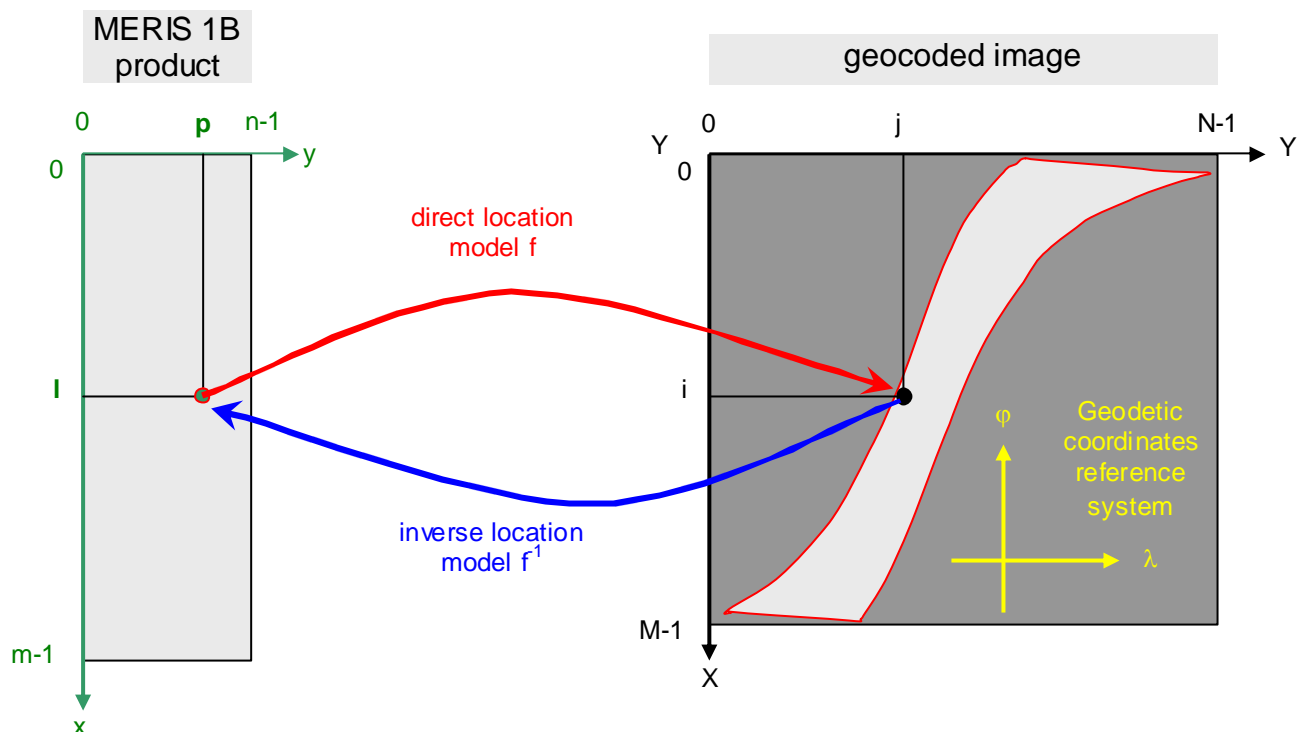


fig. 21 - Direct and inverse location models.

The basic geocoding program is given here below:

```

for i←0 to M-1 do
    for j←0 to N-1 do
         $(\lambda, \varphi) \leftarrow F_{\text{proj}}(i, j)$ 
         $(l, p) \leftarrow f^{-1}(\lambda, \varphi, h)$ 
        if  $(l, p)$  is inside the input image
             $S(i, j) \leftarrow R(l, p)$ 
        fsi
    done
done

```

Where:

F_{proj} is the function giving the Earth coordinates according to the location (i, j) in the output image.

For Cartesian projections system, this function is a simple linear formula:

$$\begin{cases} \lambda = origin_y + pixel_width \times j \\ \varphi = origin_x - pixel_height \times i \end{cases}$$

Prediction/correction principle

The prediction/correction algorithm is to be used when the direct and inverse location models have not the same accuracy. In this case, go and return to/from the output image does not enable retrieving the origin pixel.

$$f(f^{-1}) \neq Id \quad (\text{the identical function})$$

In most of the cases the direct location model is issued from a viewing model given by analytical functions and providing accurate results, while the inverse location model is only a predictor, for example estimated by a polynomial function.

In our case, the direct location model makes use of the tie-point geodetic coordinates that are supposed to have been computed with high accuracy.

Scope of the prediction/correction algorithm is to retrieve the pixel (l, p) that match the (λ, φ) by the direct location model: $f(l, p) = (\lambda, \varphi)$.

Principle is to sum a series of always-smaller corrections vectors, each one being estimated by a go and return from/to the MERIS segment to/from the geocoded image. The refinement loop is stopped when the (l_i, p_i) is close enough the first point (l_0, p_0) according to a predefined tolerance.

Figure fig. 22 illustrates the prediction/correction principle on two iterations.

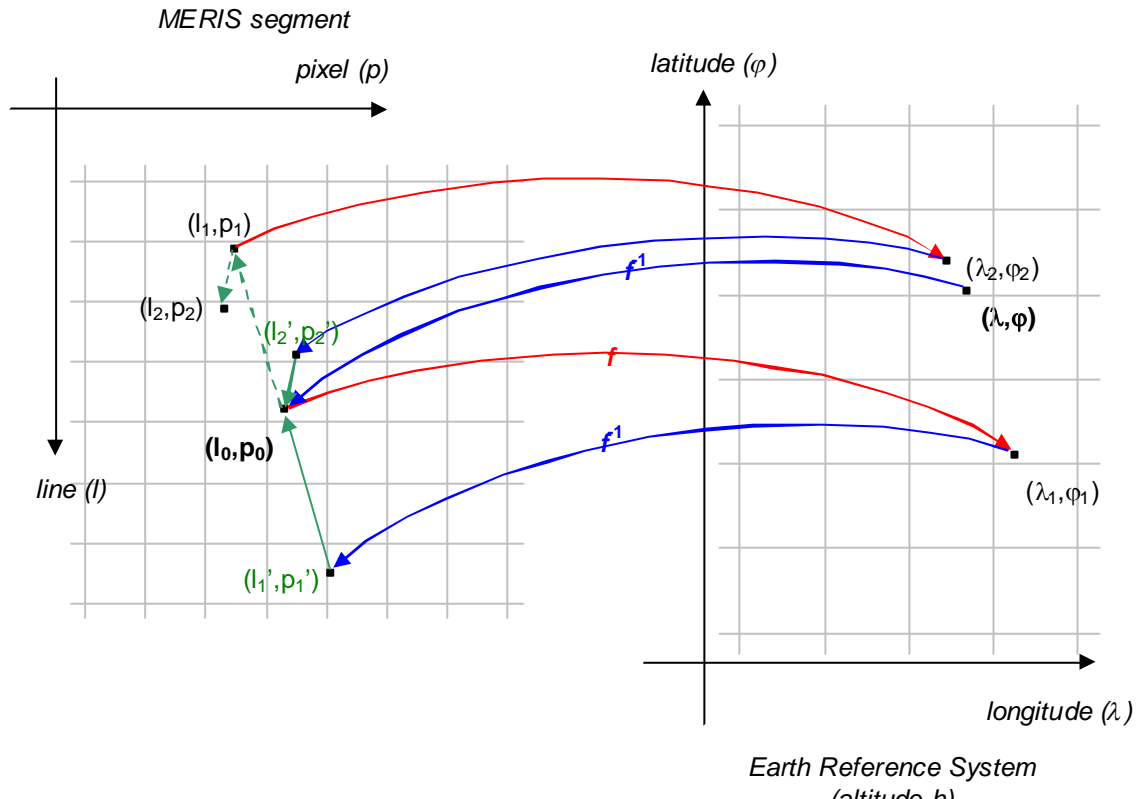


fig. 22 - Example of prediction/correction refinements.

The prediction/correction algorithm is given in fig. 23 here below.

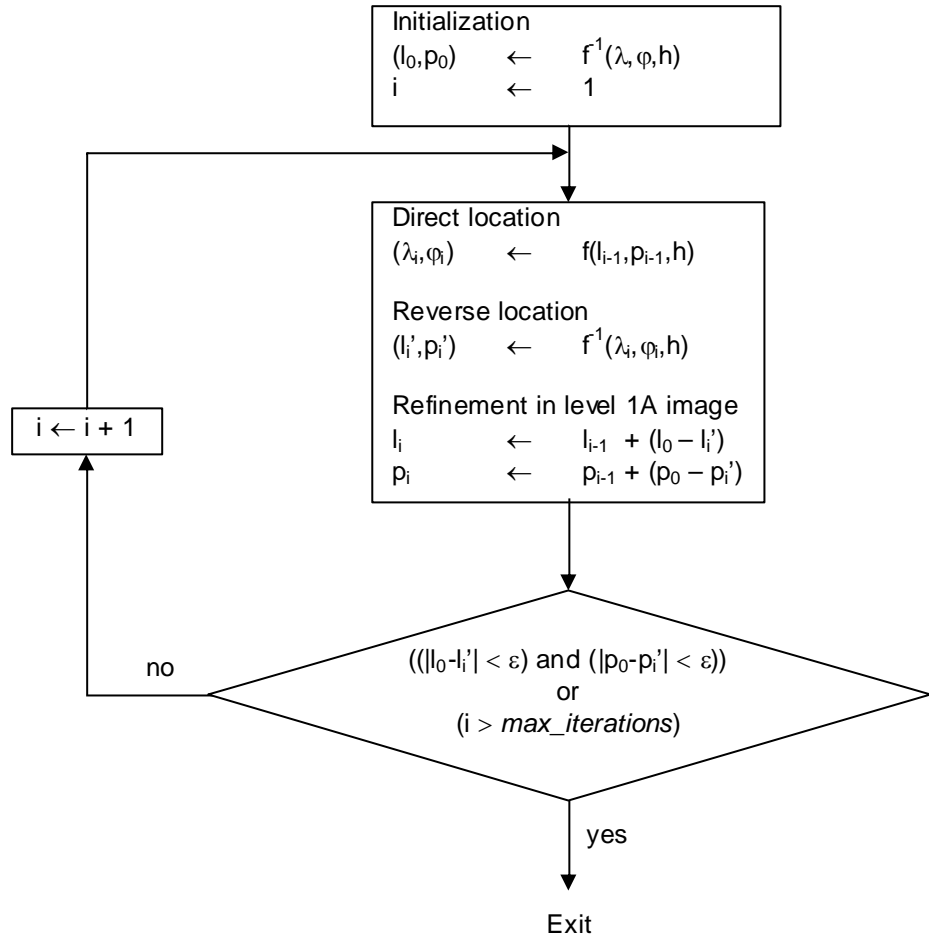


fig. 23 - prediction/correction algorithm.

3.3 Direct location model

The direct location f compute the geodetic coordinates (λ, φ) from the MERIS segment coordinates (l, p) and the altitude h . The provided geodetic coordinates are corrected of the parallax bias taking into account the viewing angle (θ_v, φ_v) and the altitude h .

Retrieving tie-point facet

Coordinates (F, J) of the upper-left tie-point of the facet containing the point (l, p) may simply be obtained dividing l and p by the number DF of frames between two consecutive tie-points and the number DJ of columns between tie-points respectively.

$$\begin{cases} F = \text{int}\left(\frac{l}{DF}\right) \\ J = \text{int}\left(\frac{p}{DJ}\right) \end{cases} \quad \text{Eq. 3a}$$

" This document discloses subject matter in which VisioTerra has proprietary rights. Recipient of this document shall not duplicate, use or disclose in whole or in part, information disclosed hereon except for or on behalf of VisioTerra to fulfil the purpose for which the document was delivered to him. "

$$\begin{cases} f &= l - F \times DF \\ j &= p - J \times DJ \end{cases} \quad \text{Eq. 3b}$$

Geodetic coordinates interpolation

The standard bi-linear interpolation (eq. 1) is applied to the longitude and latitude of the tie-points.

$$\begin{aligned} \lambda(l, p) &= \left(\frac{DJ-j}{DJ} \right) \times \left[\left(\frac{DF-f}{DF} \right) \times \text{Lon}(F, J) + \left(\frac{f}{DF} \right) \times \text{Lon}(F+DF, J) \right] \\ &\quad + \left(\frac{j}{DJ} \right) \times \left[\left(\frac{DF-f}{DF} \right) \times \text{Lon}(F, J+DJ) + \left(\frac{f}{DF} \right) \times \text{Lon}(F+DF, J+DJ) \right] \end{aligned} \quad \text{Eq. 4a}$$

$$\begin{aligned} \varphi(l, p) &= \left(\frac{DJ-j}{DJ} \right) \times \left[\left(\frac{DF-f}{DF} \right) \times \text{Lat}(F, J) + \left(\frac{f}{DF} \right) \times \text{Lat}(F+DF, J) \right] \\ &\quad + \left(\frac{j}{DJ} \right) \times \left[\left(\frac{DF-f}{DF} \right) \times \text{Lat}(F, J+DJ) + \left(\frac{f}{DF} \right) \times \text{Lat}(F+DF, J+DJ) \right] \end{aligned} \quad \text{Eq. 4b}$$

Viewing angle interpolation

The standard bi-linear interpolation (eq. 1) is applied to the viewing zenith and viewing azimuth of the tie-points.

$$\begin{aligned} \theta_v(l, p) &= \left(\frac{DJ-j}{DJ} \right) \times \left[\left(\frac{DF-f}{DF} \right) \times \theta_v(F, J) + \left(\frac{f}{DF} \right) \times \theta_v(F+DF, J) \right] \\ &\quad + \left(\frac{j}{DJ} \right) \times \left[\left(\frac{DF-f}{DF} \right) \times \theta_v(F, J+DJ) + \left(\frac{f}{DF} \right) \times \theta_v(F+DF, J+DJ) \right] \end{aligned} \quad \text{Eq. 5a}$$

$$\begin{aligned} \varphi_v(l, p) &= \left(\frac{DJ-j}{DJ} \right) \times \left[\left(\frac{DF-f}{DF} \right) \times \varphi_v(F, J) + \left(\frac{f}{DF} \right) \times \varphi_v(F+DF, J) \right] \\ &\quad + \left(\frac{j}{DJ} \right) \times \left[\left(\frac{DF-f}{DF} \right) \times \varphi_v(F, J+DJ) + \left(\frac{f}{DF} \right) \times \varphi_v(F+DF, J+DJ) \right] \end{aligned} \quad \text{Eq. 5b}$$

Compute and apply the geodetic correction

The geodetic correction formula applied to the tie-points (see eq. 2 and fig. 10 in section “Parallax estimate at tie-points” of section 2.2) are applied to the (l,p) point.

dx	$= h \times \tan(\theta_v(l, p))$	
$dlat(l, p)$	$= \frac{dx \times \cos(\varphi_v(l, p))}{R_e}$	
$dlon(l, p)$	$= \frac{dx \times \sin(\varphi_v(l, p))}{R_e \times \cos(\varphi_v(l, p))}$	

$\lambda(l, p) \leftarrow \lambda(l, p) + dlon(l, p)$		
$\varphi(l, p) \leftarrow \varphi(l, p) + dlat(l, p)$		

3.4 Inverse location model

The inverse location f^{-1} retrieves the facet (F, J) that includes the point which geodetic coordinates are (λ, φ) and computes the offset (f, j) within the facet.

Retrieving the tie-point facet

Facet retrieving is one of the most time-consumer, and therefore an optimisation is proposed assuming that processing of geocoded image is performed on contiguous points: ... (i, j) ($i, j+1$) ... ($i, N-1$) ($i+1, 1$) ...

Coordinates (F_{last}, J_{last}) of the latest facet are kept and searching is performed in this facet first (see fig. 24). In case of failure, searching is performed within the four nearest (4-connex) facets, and then within the 4 other neighbour (8-connex) facets. In case of failure, all the facets of the tie-point grid shall be inspected.

This last case is significantly time-consuming (in particular for RR products containing a large number of tie-points) and all shall be done to avoid it.

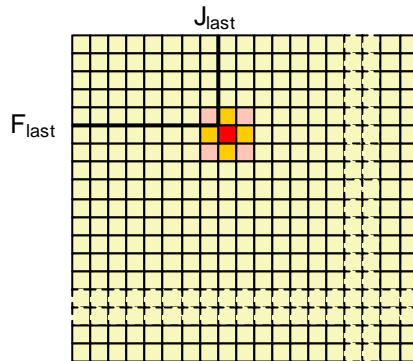


fig. 24 - Retrieving tie-points facet order.

Retrieving offsets within the facet

Facets are obviously not parallel to the geodetic reference system and placed in this referential (see fig. 25), they may have whatever pattern.

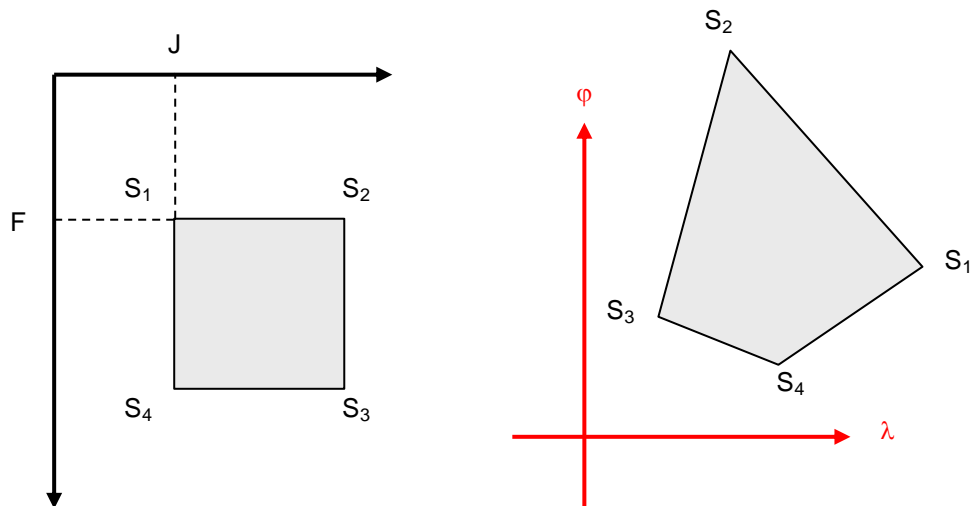


fig. 25 - Facet in the level 1B grid referential (left) and in the geodetic referential (right).

To state if a point is within a facet or not, we cannot only test that the geodetic coordinates (λ, φ) of the point are within the longitude and latitude ranges of the tie-point corners. Figure fig. 26 here below for example illustrates an example where the latitude and longitude of a point are inside the ranges defined by the tie-points but the point is outside the facet.

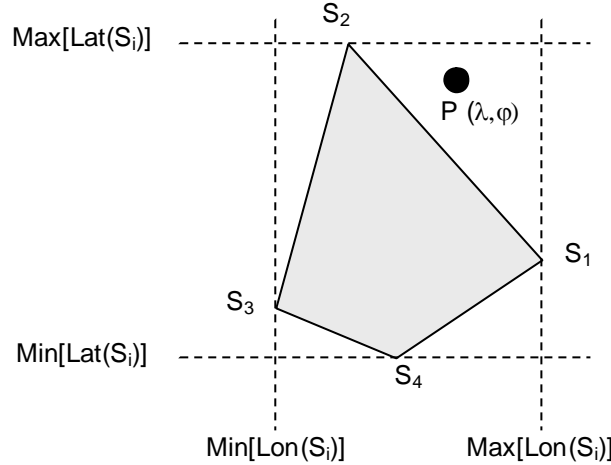


fig. 26 - Point inside the latitude and longitude ranges but outside the facet.

Algorithms exists to determine if a point is inside a polygon or not but they are time-consuming.

It is proposed to use a method illustrated in fig. 27 that:

- computes the two intersection points I_1 and I_2 of the facet opposite borders (when not parallel),
- computes the intersection I'_1 and I''_1 of (I_1P) with the two other borders,
- computes the intersection I'_2 and I''_2 of (I_2P) with the two other borders,
- checks that points I'_1 , I''_1 , I'_2 and I''_2 are inside the segments $[S_1S_4]$, $[S_2S_3]$, $[S_1S_2]$ and $[S_3S_4]$ respectively.

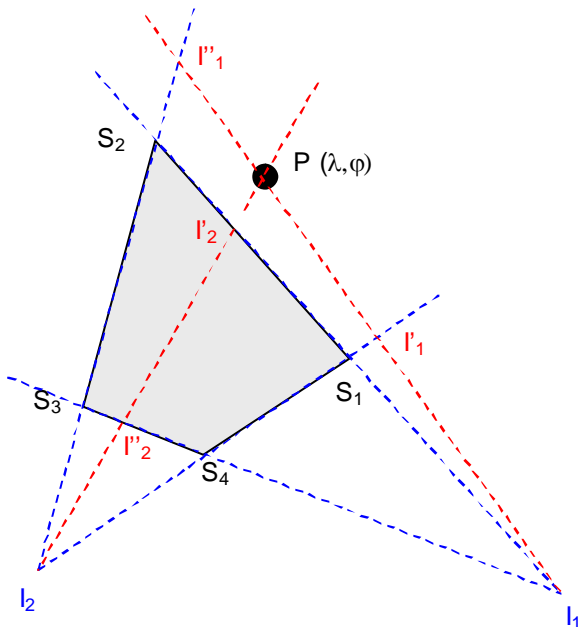


fig. 27 - Intersections method.

4 ORTHORECTIFICATION RESULTS

Images given in this section have been generated by the MERSYN process, setting different parameters like the DEM in input.

Geometry checking is performed comparing the orthorectified MERIS image mapped in "Plate Carrée" projection with ground spacing of 260 metres (FR) with reference to data like:

- Vector layers and in particular those showing the coastlines.
- Landsat TM mosaic that has been resampled to 260 metres in the same projection as for the MERIS images.

In section 4.7, a non-orthorectified scene produced by BEAM / VISAT will be compared with the same MERSYN result.

4.1 MERIS scene in input

The full resolution (FR) MERIS scene being controlled has the standard name

MER_FR__1PNUPA20030921_092341_00000982020_00079_08149_0534.N1

The geometry of the level 1B product is shown in fig. 28.

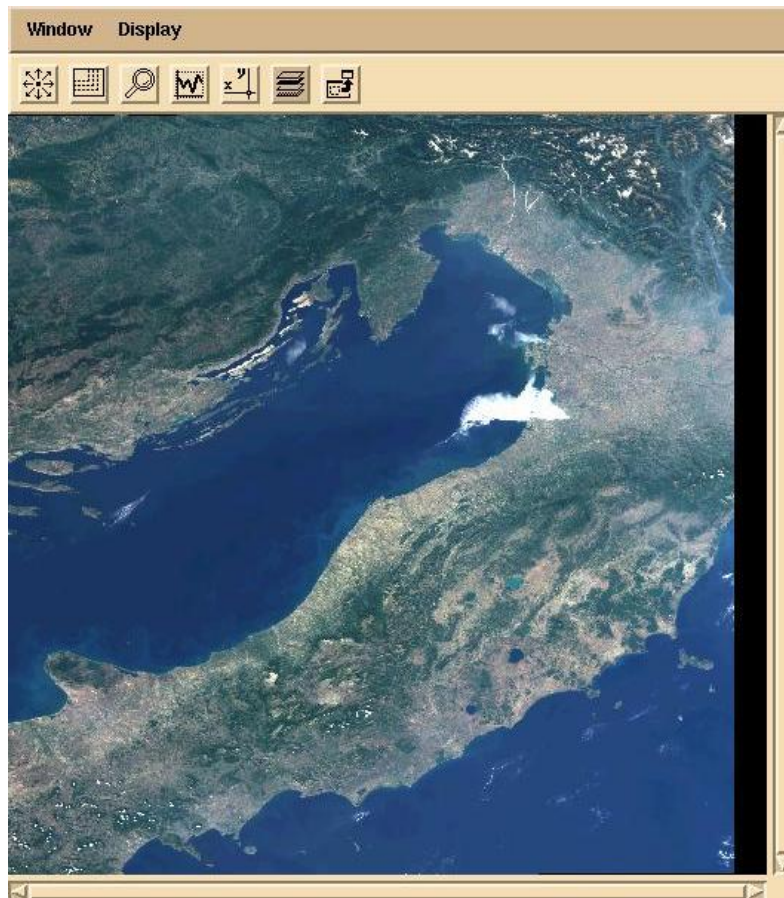


fig. 28 - Level 1B MERIS scene.

This scene has been chosen because its footprint (see fig. 29) includes terrains with very varying elevations (Alps, plain of Po, Abruzzi...).

" This document discloses subject matter in which VisioTerra has proprietary rights. Recipient of this document shall not duplicate, use or disclose in whole or in part, information disclosed hereon except for or on behalf of VisioTerra to fulfil the purpose for which the document was delivered to him. "

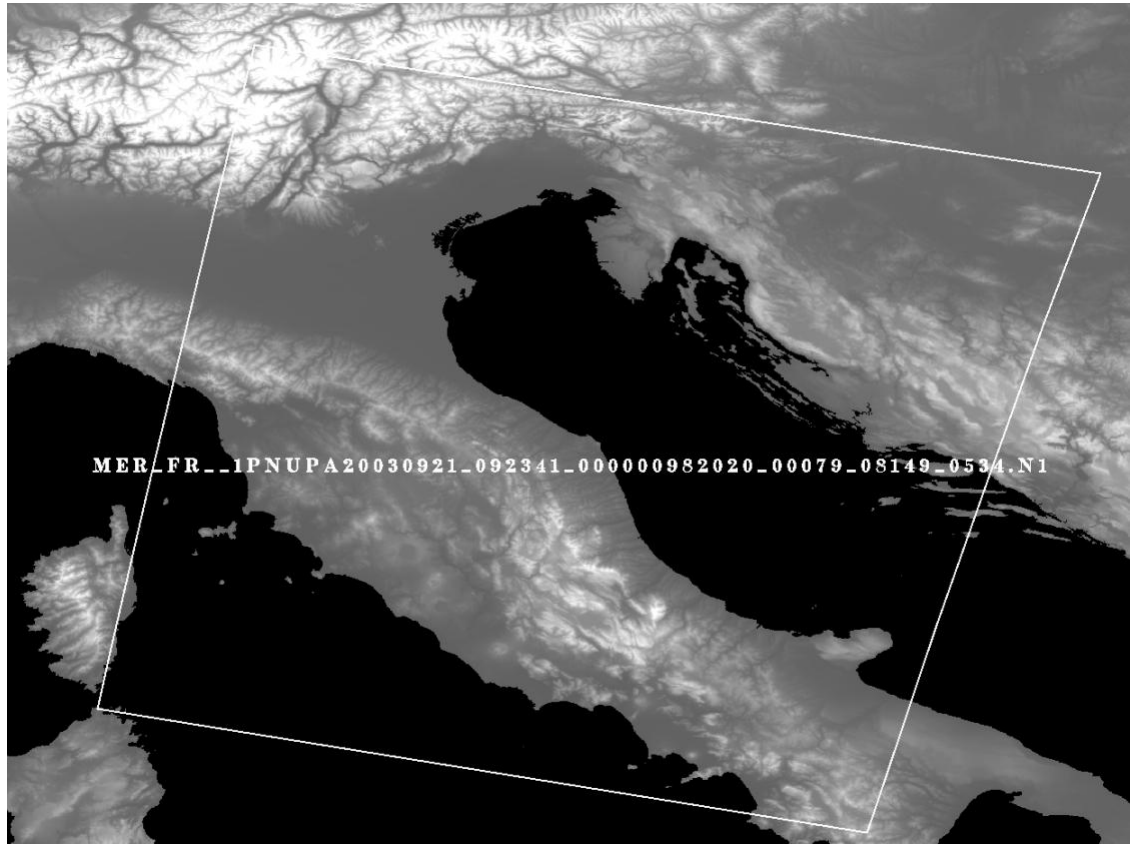


fig. 29 - MERIS footprint overlaid on SRTM elevations

In particular, Alps located at the upper-left corner of the scene are acquired with a high zenith angle. Some of the values found within the “Tie-point ADS” are given in section A.1 (Decoding log) of APPENDIX A.

DATA SET #3 - "Tie points ADS":									
No.	Date	Alt.	Rough.	Corr.	Lat.	Lon.	Sun (Zen., Azi.)	View (Zen., Azi.)	
FIRST	(Lat., Lon.)								
LAST	(Lat., Lon.)								
1	117451421.714409								
(45.909863, 18.014693)	98	3	0 1e-6	0 1e-6	(48.2, 153.6)	(0.0, 182.0)			
(47.028196, 10.603496)	1476	382	-1907 1e-6	-16512 1e-6	(51.8, 145.0)	(40.7, 99.6)			
9	117451444.240873								
(44.594348, 17.519381)	591	159	0 1e-6	0 1e-6	(47.2, 152.5)	(0.0, 181.9)			
(45.703992, 10.278711)	850	227	-1101 1e-6	-9284 1e-6	(50.8, 144.1)	(40.7, 99.6)			
17	117451466.767337								
(43.277165, 17.041762)	417	32	0 1e-6	0 1e-6	(46.1, 151.4)	(0.0, 181.9)			
(44.379209, 9.960598)	744	75	-967 1e-6	-7942 1e-6	(49.8, 143.2)	(40.7, 99.7)			

Zenith of the viewing angle of the first CCD (matching the East of the scene) is almost 0.0 meaning that pixels are located at the NADIR of the satellite, while the viewing angle of the last CCD (West of the scene) has almost the maximum value (40.7°).

The MERIS FR scene is located on the East of the track leading to the left border region, for example North of the Alps, is seen with the maximum incidence angle and therefore showing the largest parallax defect.

4.2 Digital elevation models

Two digital elevation models have been used to orthorectify the MERIS scene. These two DEMs have not the same resolution to enable comparing the influence of this feature.

DEM Italy

This 250 metres DEM has been generated by photogrammetry techniques. This DEM (see fig. 30) covers the administrative boundaries of Italy and the North of Alps.



fig. 30 - DEM Italy (250 metres)

SRTM

SRTM30 is a near-global digital elevation model (DEM) comprising a combination of data from the Shuttle Radar Topography Mission, flown on February 2000 and the U.S. Geological Survey's GTOPO30 data set. It can be considered to be either an SRTM data set enhanced with GTOPO30, or as an upgrade to GTOPO30.

SRTM is provided by tiles and its ground sampling is 30" arc (approximately 1 km resolution at Equator). The tile covering the MERIS scene (see fig. 31) is identified **W020N90** (geodetic coordinates of the upper left corner) and as an extent of 40° (West - East) by 50° (North - South).



fig. 31 - SRTM W020N90 tile

4.3 Reference image – The Landsat TM mosaicsna

The reference image used to perform controls is a mosaic of Landsat TM scenes with a resolution of 30 metres.

This reference scene has been computed by GAEI Consultant in September 1997 from 38 Landsat scenes and orthorectified using a 75 metres DEM of Italy.

Ground control points have been taken from 1:20.000 and 1:25.000 IGM maps.

The location accuracy has been controlled with a RMS error less than 50 metres.

Figure fig. 32 shows the full image (top) and a 1:100.000 display (bottom) overlaid by vector layers of the Italian provinces.

Note: Sites are now available to download orthorectified Landsat ETM+ scenes (see <http://image2000.jrc.it/> or <http://glcf.umiacs.umd.edu/index.html>).



fig. 32 - Landsat TM mosaic

4.4 Superimposability – Visual checking

A visual verification of the superimposability quality may be performed using the “Flicker” tool of REGIST application (see fig. 33). In this example, the MERIS projected image (left) is compared with the Landsat mosaic (right).

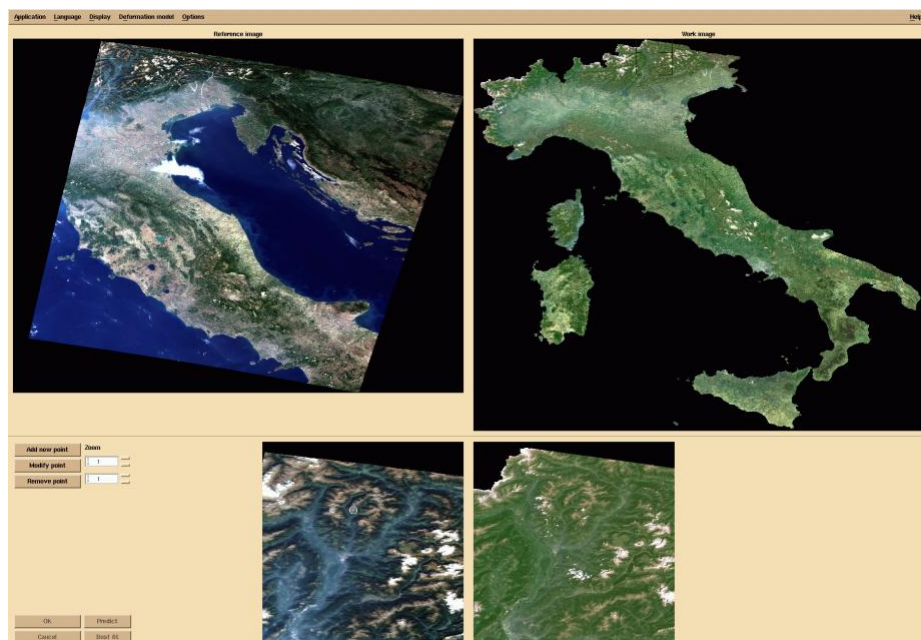


fig. 33 - REGIST application (snap01_REGIST.gif)

For the selected zone, full resolution or zoomed windows found in MERIS and Landsat are alternatively displayed within a same frame (see fig. 34 and fig. 35).

 <p>Window</p> <p>Display Swap Start Stop</p> <p>Reference Interval : 150</p> <p>Work</p>	 <p>Window</p> <p>Display Swap Start Stop</p> <p>Reference Interval : 150</p> <p>Work</p>
<p>fig. 34 - MERIS (snap02_REGIST_Flicker_no-ortho_meris.gif)</p>	<p>fig. 35 - Landsat (snap02_REGIST_Flicker_no-ortho_tm.gif)</p>

This alternative displaying (flicking) enables identifying sub-pixel displacements. Such movements cannot be observed in this document, but GIF images have been captured and stored in GIF animations that are available on demand:

- snap02_REGIST_Flicker_no-ortho_anim.gif
- snap03_REGIST_Flicker_anti-grid_anim.gif
- snap04_REGIST_Flicker_dem-italy_anim.gif
- snap05_REGIST_Flicker_dem-italy+translation_anim.gif
- snap06_REGIST_Flicker_dem-srtm+translation_anim.gif

Comment of animation 02 – No orthorectification

When no orthorectification is performed the deformations appear with the largest amplitude.

Comment of animation 03 – Altitudes from tie-points grid

When orthorectification is computed interpolating the elevation values from those found within the tie-point grid, we may observe that the bottom of the valleys are almost correctly superimposed (no movement) but the mountains are moving eastward.

Such an internal geometry defect is due to a poor accuracy of the tie-point elevations that have been computed from a 5' arc (almost 9 km along equator) DEM smoothing the picks and ridges of the mountains.

For example a point (coordinates (117,872) in the geocoded scene) has the following elevation value depending on the source, given here in increasing order of spatial accuracy:

Source	resolution	altitude
Tie-point grid	5' arc	1406.003360 m
DEM SRTM	30''	2106.815331 m
DEM Italy	250 m	2230.704269 m

The deficit of 700 metres (2106 – 1406) on pixels seen with the largest viewing zenith (40°) leads to an error of approximately 587 metres ($= \tan(40^\circ) \times 700 \text{ m}$, see eq. 2), i.e. more than two (2) pixels.

While the difference between the SRTM DEM and the accurate one (250 m) over Italy shows a deficit of 124 metres leading to a parallax error of only 104 metres, i.e. a third of the MERIS RR resolution.

Figure fig. 36 here below illustrates the parallaxes error that can be due to the accuracy of the Digital Elevation Model.

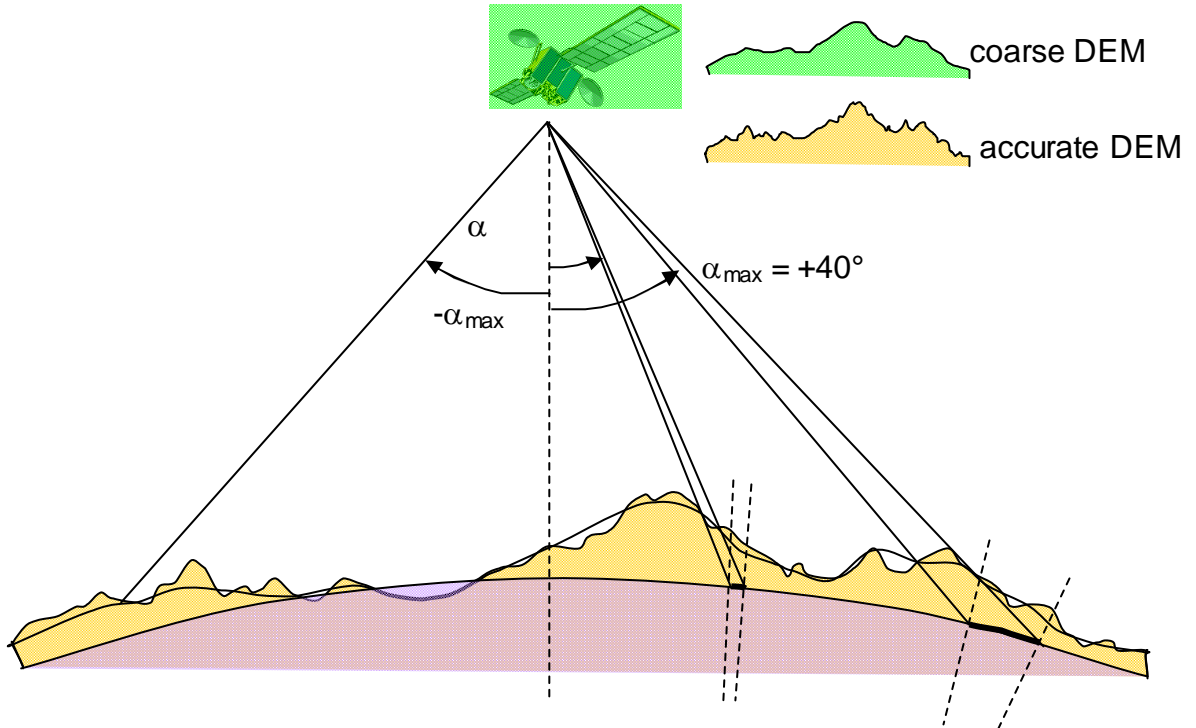


fig. 36 - Parallaxes error due to the precision of the DEM(s)

Comment of animation 04 and 05 – Altitudes from DEM Italy

When orthorectification is performed from elevation values found in DEM Italy (250 m planimetric resolution), the two images (see animation 04) are shifted in a uniform way.

Such translation has an amplitude of +1.2 pixels vertically and -4.4 pixels horizontally, leading to an error modulus of **1185 metres**.

“Moving” the orthorectified MERIS scene (i.e. just changing the origin coordinates of the upper left corner), the MERIS and Landsat scenes are perfectly superimposable (see animation 05).

Comment of animation 06 – Altitudes from DEM SRTM

Exactly the same translation defect has been observed in the MERIS scene orthorectified from elevations found within the SRTM DEM (30 “ arc planimetric resolution).

“Moving” the orthorectified MERIS scene with the same vector (+1.2,-4.4) leads to the same good result, superimposable on the Landsat mosaic.

Conclusions

From the observations detailed here above we may conclude the following three assessments.

- **Quality of the tie-point elevations** – The quality of the elevations found within the tie-point grid is not sufficient to correct parallax defect below 2 pixels error.
- **Uniform translation** – For this scene, a large translation of 1185 metres is observed leading to an absolute location accuracy of 4.5 pixels (see fig. 37). This uniform translation has been measured on only one scene and cannot be generalised for any other MERIS RR acquisition. A systematic control of a significant set of MERIS scenes is out of the scope of this handbook.
- **Quality of the DEM** – SRTM elevation data seems to be enough to efficiently orthorectify MERIS FR scenes. Results obtained are similar to those obtained with a more accurate DEM of 250 metres resolution.

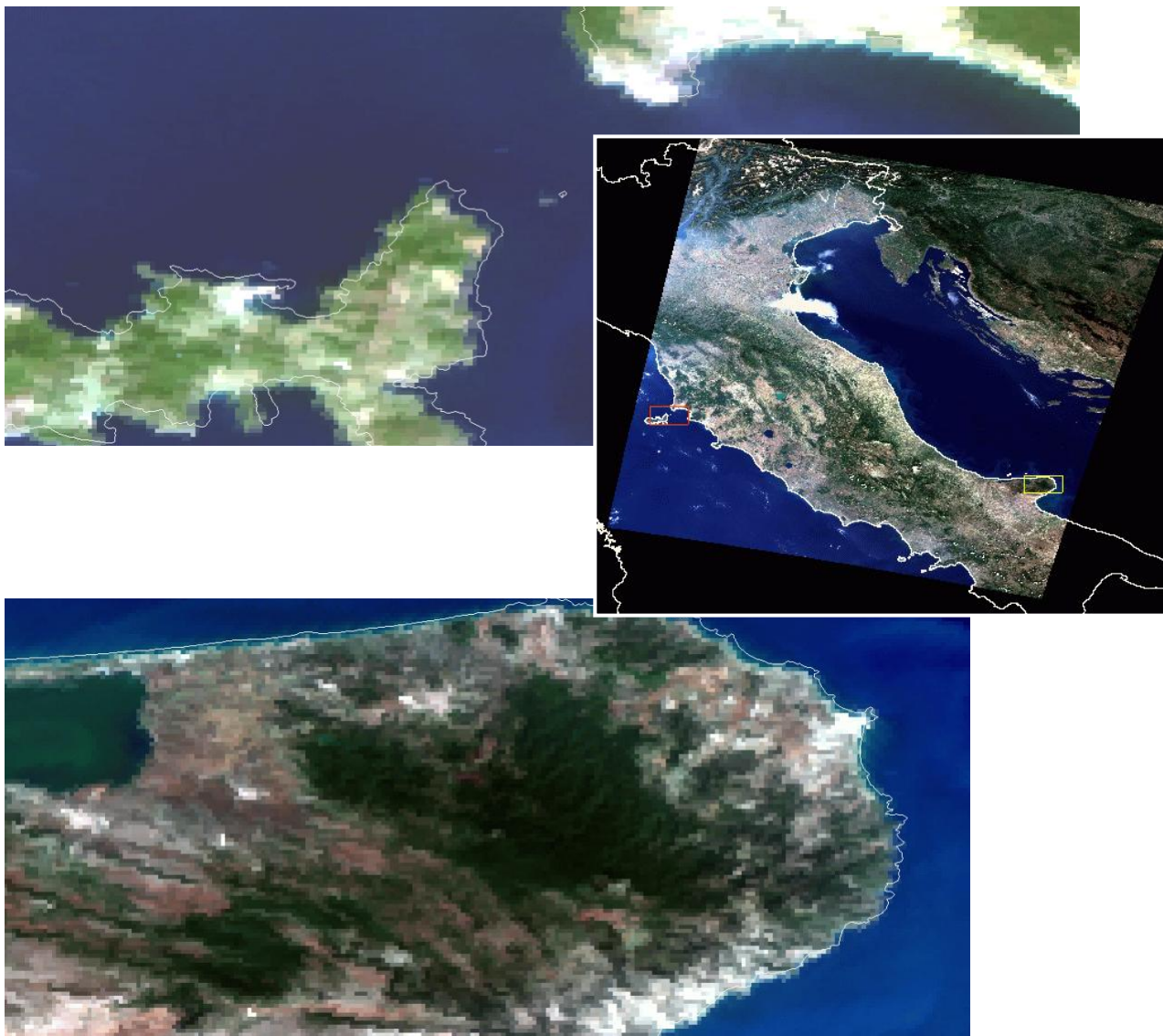


fig. 37 - West offset along the coastline

4.5 Run-time performances

Orthorectification is time consuming. Most of the time is spent to access elevation data from an external DEM, retrieve the tie-point facet including the processed point, go and return according to the prediction/correction algorithm, projection changes...

Table here below resumes the run-time and convergence performances observed for the generation of the four synthesis.

	No orthorectification	Altitudes from tie-points grid	Altitudes from DEM Italy	Altitudes from DEM SRTM
Run-time	27.700 s	68.760 s	325.960 s	304.440 s
Iteration 0	7818186 (100.0 %)	2936 (0.0 %)	2936 (0.0 %)	2936 (0.0 %)
Iteration 1	-	2852732 (36.5 %)	3008252 (38.5 %)	3034335 (38.8 %)
Iteration 2	-	4833499 (61.8 %)	4798944 (61.4 %)	4777361 (61.1 %)
Iteration 3	-	129019 (1.7 %)	8054 (0.1 %)	3554 (0.0 %)

table 3 - Run-time performances.

Performance of the prediction/correction algorithm

Performance of the prediction/correction algorithm almost doubles the execution time (68.760 seconds vs. 27.700 seconds).

We may note that only three iterations are required to converge on a precision that was set to 0.1 pixels (i.e. 26 metres maximum error between the direct and inverse location models).

Access time to DEMs

Accessing to external data almost multiply by five (x5) the execution time (325.960 seconds or 304.440 seconds vs. 68.760 seconds).

Note that a bi-linear interpolation of the DEM value being computed, a 2x2 window of elevation values shall be read for each pixel to be processed. Access to the elevation data is performed inside the prediction/correction loop.

Even if sizes of the DEMs are very close (5800 lines x 4400 pixels for the DEM Italy and 6000 lines x 4800 pixels for the DEM SRTM), the time to access DEM Italy is a little larger than the one to access DEM SRTM. This extra time is only due to the precision of the DEM (250 metres for Italy vs. 30' arc for SRTM), inducing more frequent accesses to the DEM Italy file.

4.6 Disparity Analysis

Misregistration of MERIS scene with regard to the Landsat TM mosaic may also be computed performing a disparity analysis (DISPAR process).

Research of homologous points is accomplished within an exploration window of 9 lines x 19 columns. Pattern matching is performed using the classical ZNCC (Zero mean Normalized Cross Correlation) algorithm, computing the normalised covariance within statistical window which size is 5x5.

DISPAR has been applied to the synthesis for which no orthorectification has been applied (file "synthesis_no-ortho.sta.3" and to the synthesis Orthorectified from the SRTM DEM (file "synthesis_dem-srtm.sta.3").

Obtained results are given in the logs here below. Figures fig. 38 and fig. 39 show the points or regions with the highest confidence value, the minimum threshold having been set to 95%. The vectors illustrate

" This document discloses subject matter in which VisioTerra has proprietary rights. Recipient of this document shall not duplicate, use or disclose in whole or in part, information disclosed here on except for or on behalf of VisioTerra to fulfil the purpose for which the document was delivered to him."

the tie-point automatically generated with a pixel sampling of 0.1 pixels and greater than the 95% confidence threshold.

Better correlation of SRTM DEM synthesis

The regions showing the much variation of landscape like the coastlines, the lake borders and the mountains are those in which the correlation is higher.

As expected, the better internal geometry of the orthorectified synthesis leads to more points (58 "CANDIDATE PIXELS" (*)) having a confidence index over 95% than for the non-orthorectified image (only 37 points).

Nevertheless, both scores are surprisingly low, meaning that the radiometric correlation between the band 3 of MERIS and band 1 of Landsat is poor even if both bands are centered on the blue of the visible spectrum. The same defect has been observed in the green bands (5 for MERIS and 2 for Landsat) or the red bands (7 for MERIS and 3 for Landsat).

The reasons of such a decorrelation (that could be due to the precision of the radiometric bands, their bandwidth, the different acquisition periods...) should be investigated but such an analysis is out of the scope of this document.

Global displacement

Individual displacements (dX, dY) are more scattered for the non-orthorectified scene. This defect is particularly visible within the region of North Alps (see fig. 38). Nevertheless, a global displacement noted in the previous section can be estimated by the algebraic mean of the (dX, dY) displacements:

- **(-1.029730, 2.813514)** for the non-orthorectified scene, and
- **(-0.724138, 2.591379)** for the scene Orthorectified from the SRTM DEM.

This last displacement has a modulus of **699.569 metres**.

FILE synthesis_no-ortho.sta.3

```

STATISTICAL WINDOW SIZE      = 5
EXPLORATION WINDOW HEIGHT   = 9
EXPLORATION WINDOW WIDTH    = 19
CONFIDENCE THRESHOLD       = 95.0 %

TOTAL NUMBER OF PIXELS     = 110544
IMAGE PIXELS                = 74771
CANDIDATE PIXELS (*)        = 37 (0.0 %)

TIE-POINTS                  = 37

CONFIDENCE VALUES:
MINIMUM                      = 0.000000 vs. 95.009510 (*)
MAXIMUM                      = 99.411765 vs. 99.411765 (*)
MEAN                          = 26.599705 vs. 96.399719 (*)
VARIANCE                     = 10.974342 vs. 0.013694 (*)
STANDARD DEVIATION           = 33.127544 vs. 1.170194 (*)

X DISPLACEMENT:
ON LIMIT                     = 6268 / 74771 (8.38%)
RMS                           = 1.800067 vs. 1.510951 (*)
MINIMUM                      = -4.000000 vs. -3.000000 (*)
MAXIMUM                      = 4.000000 vs. 2.000000 (*)
MEAN                          = 0.401206 vs. -1.029730 (*)
STANDARD DEVIATION           = 1.755 vs. 1.106 (*)

ORIGINAL VALUES:
RMS                           = 468.017367 vs. 392.847264 (*)
MINIMUM                      = -1040.000000 vs. -780.000000 (*)
MAXIMUM                      = 1040.000000 vs. 520.000000 (*)
MEAN                          = 104.313651 vs. -267.729730 (*)
STANDARD DEVIATION           = 456.244 vs. 287.489 (*)

Y DISPLACEMENT:
ON LIMIT                     = 3490 / 74771 (4.67%)
RMS                           = 3.620483 vs. 4.084744 (*)
MINIMUM                      = -9.000000 vs. -4.100000 (*)
MAXIMUM                      = 9.000000 vs. 8.000000 (*)
MEAN                          = 0.941761 vs. 2.813514 (*)
STANDARD DEVIATION           = 3.496 vs. 2.961 (*)

ORIGINAL VALUES:
RMS                           = 941.325648 vs. 1062.033491 (*)
MINIMUM                      = -2340.000000 vs. -1066.000000 (*)
MAXIMUM                      = 2340.000000 vs. 2080.000000 (*)
MEAN                          = 244.857819 vs. 731.513514 (*)
STANDARD DEVIATION           = 908.922 vs. 769.937 (*)

```

FILE synthesis_dem-srtm.sta.3

STATISTICAL WINDOW SIZE = 5
 EXPLORATION WINDOW HEIGHT = 9
 EXPLORATION WINDOW WIDTH = 19
 CONFIDENCE THRESHOLD = 95.0 %

TOTAL NUMBER OF PIXELS = 110544
 IMAGE PIXELS = 74723
 CANDIDATE PIXELS (*) = **58** (0.1 %)

TIE-POINTS = 58

CONFIDENCE VALUES:

MINIMUM	= 0.000000	vs.	95.003623	(*)
MAXIMUM	= 100.000000	vs.	100.000000	(*)
MEAN	= 26.689998	vs.	96.212369	(*)
VARIANCE	= 11.050492	vs.	0.016515	(*)
STANDARD DEVIATION	= 33.242281	vs.	1.285098	(*)

X DISPLACEMENT:

ON LIMIT	= 6113 / 74723	(8.18%)		
RMS	= 1.776098	vs.	1.288276	(*)
MINIMUM	= -4.000000	vs.	-3.000000	(*)
MAXIMUM	= 4.000000	vs.	2.000000	(*)
MEAN	= 0.424984	vs.	-0.724138	(*)
STANDARD DEVIATION	= 1.725	vs.	1.065	(*)

ORIGINAL VALUES:

RMS	= 461.785466	vs.	334.951772	(*)
MINIMUM	= -1040.000000	vs.	-780.000000	(*)
MAXIMUM	= 1040.000000	vs.	520.000000	(*)
MEAN	= 110.495912	vs.	-188.275862	(*)
STANDARD DEVIATION	= 448.371	vs.	277.029	(*)

Y DISPLACEMENT:

ON LIMIT	= 3246 / 74723	(4.34%)		
RMS	= 3.484071	vs.	3.703842	(*)
MINIMUM	= -9.000000	vs.	-7.000000	(*)
MAXIMUM	= 9.000000	vs.	8.000000	(*)
MEAN	= 0.800090	vs.	2.591379	(*)
STANDARD DEVIATION	= 3.391	vs.	2.646	(*)

ORIGINAL VALUES:

RMS	= 905.858579	vs.	962.999015	(*)
MINIMUM	= -2340.000000	vs.	-1820.000000	(*)
MAXIMUM	= 2340.000000	vs.	2080.000000	(*)
MEAN	= 208.023313	vs.	673.758621	(*)
STANDARD DEVIATION	= 881.650	vs.	688.053	(*)

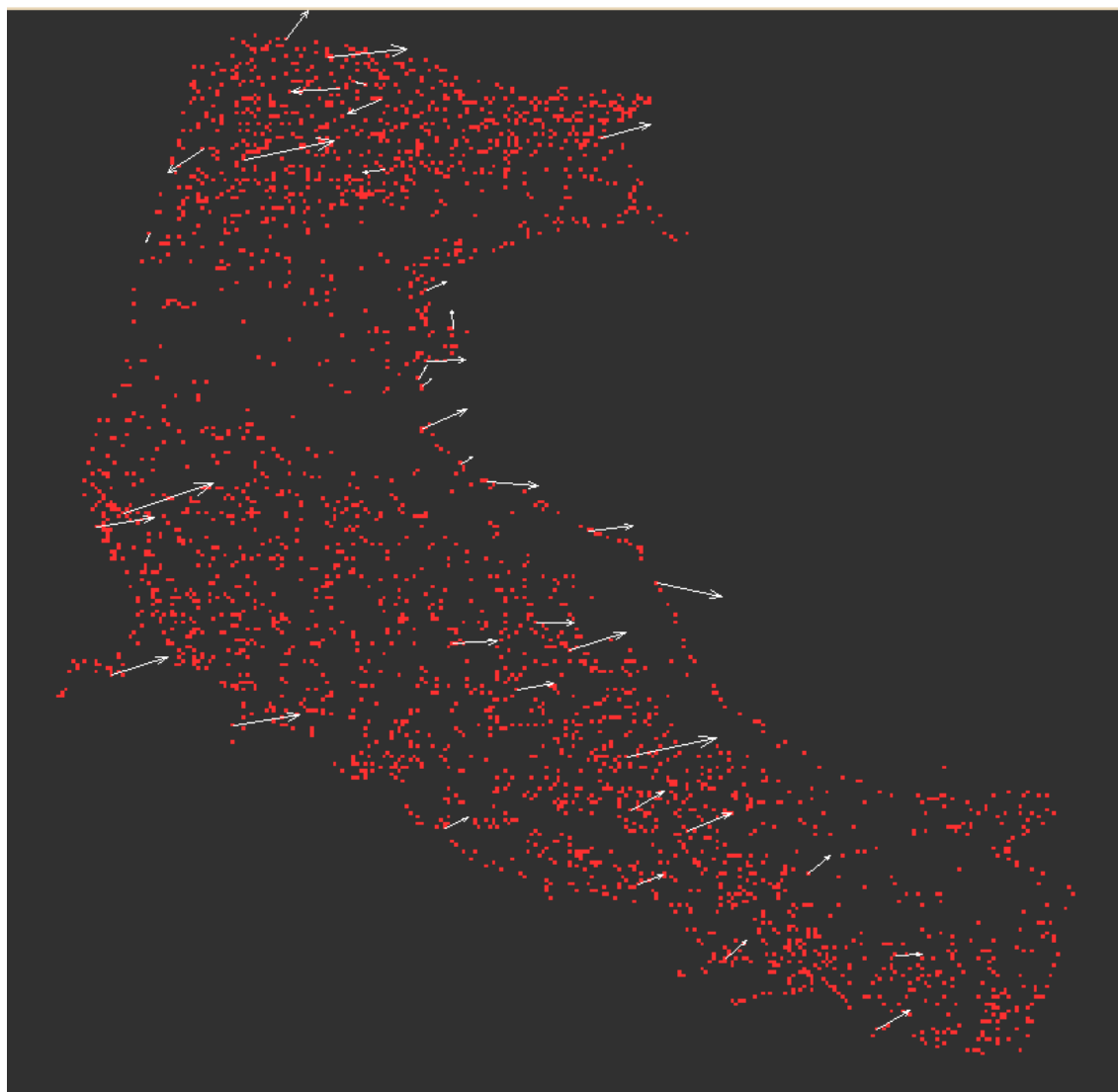
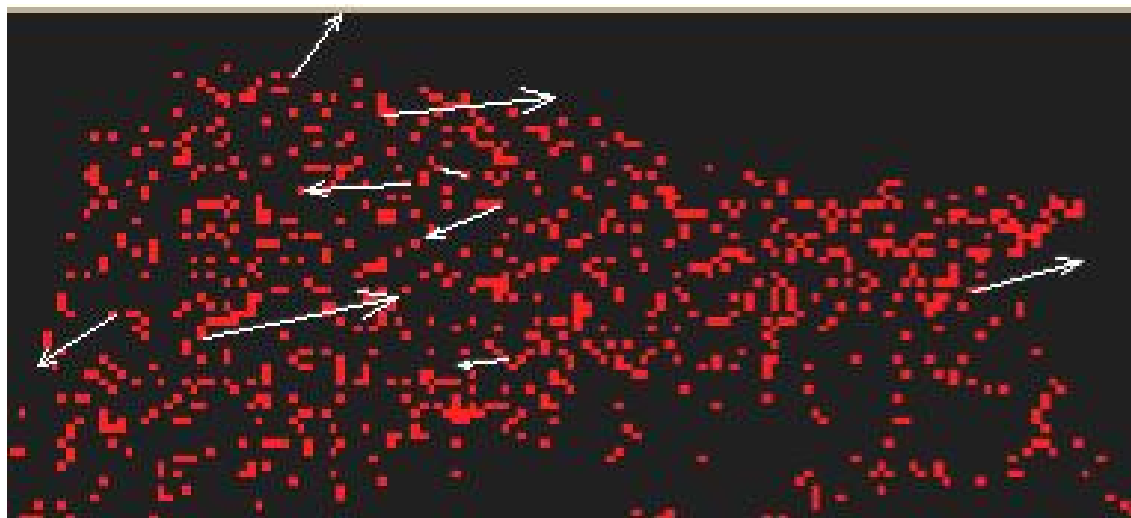


fig. 38 - No-orthorectification – Highest confidence (red) and 95% tie-points



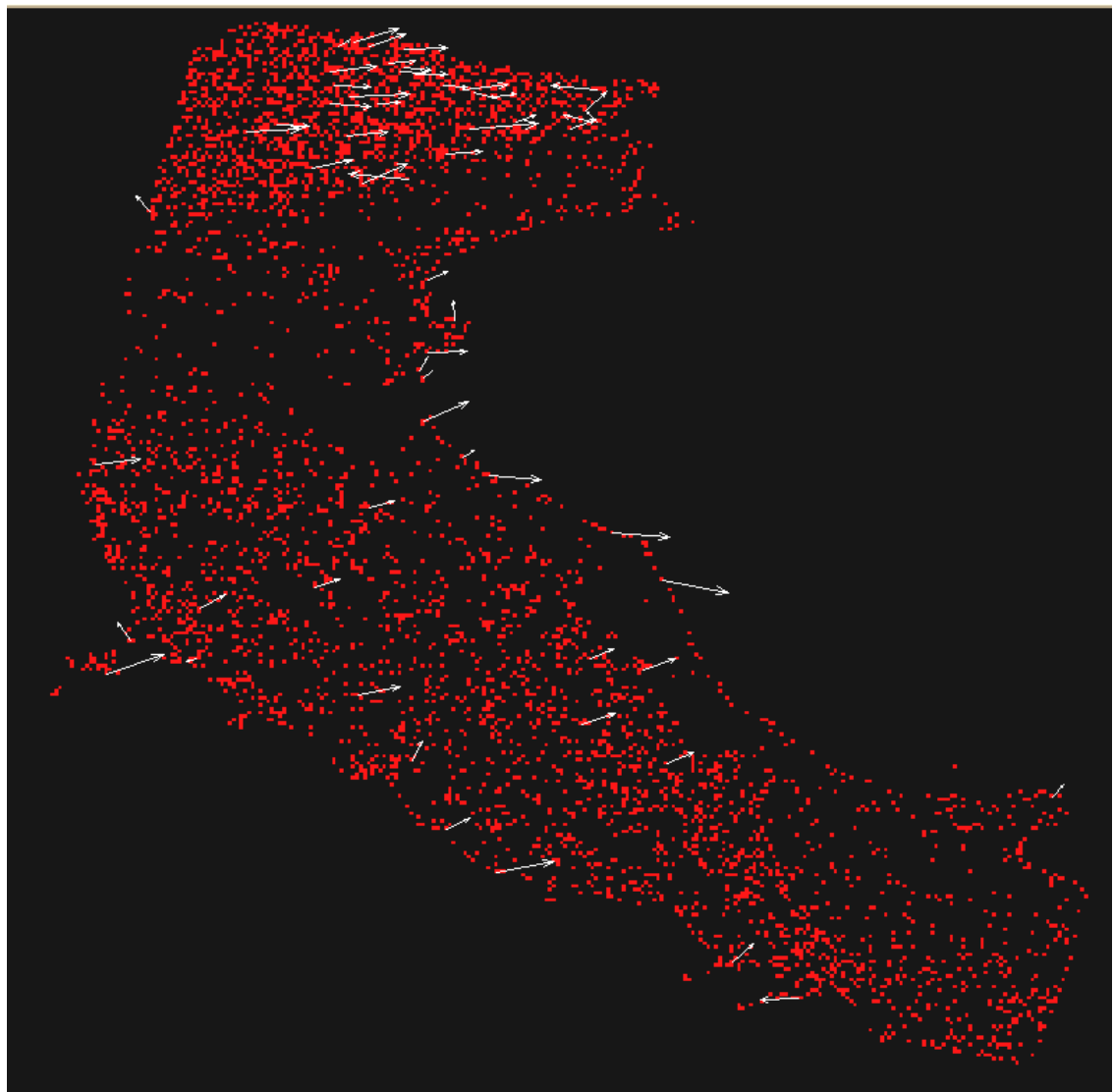
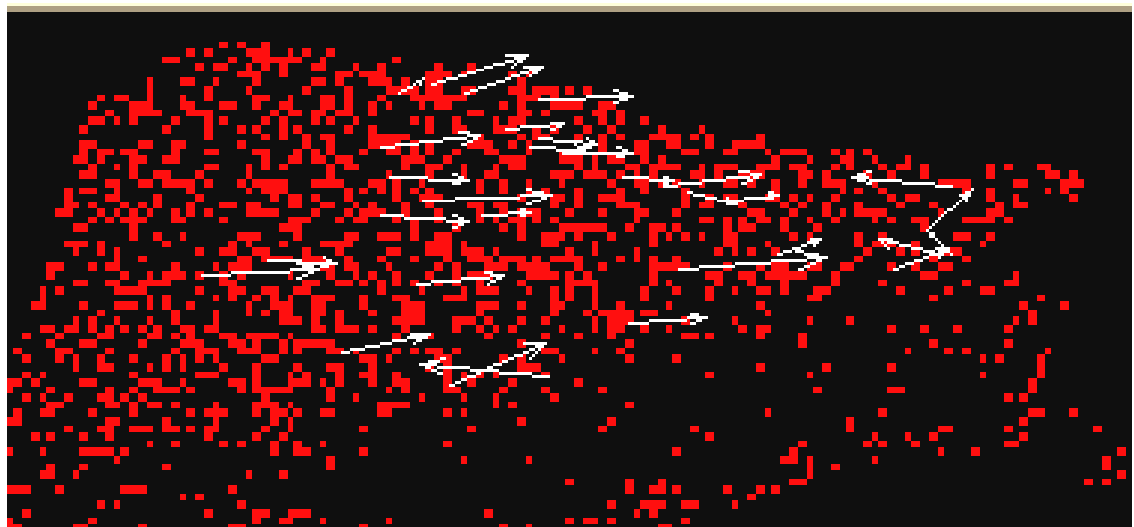


fig. 39 – Orthorectification from SRTM DEM – Highest confidence (red) and 95% tie-points



4.7 Comparison with BEAM / VISAT

Scope of this section is to compare the geometry of the images produced by the BEAM software (downloaded from <http://scipc3.scicon.gkss.de/services/beam2/software> on 20/08/2004) with the image produced by MERSYN.

In its version 2.3, BEAM / VISAT does not process orthorectification and therefore the image produced by MERSYN is also not orthorectified (parameter “-ort” set to NO).

Both images have been geocoded in the “UTM 31, ellipsoid WGS-84 and Datum WGS-84”. Figure here below shows the BEAM image (left) and the MERSYN image (right) with a resolution of 260 metres each one.

An accurate superimposability has been verified setting the Flicker tool with a x4 zoom within the four zones illustrated on the MERSYN image. Behaviour of the REGIST application is described in section **Erreur ! Source du renvoi introuvable.**).

Four animations are available on demand that clearly show a perfect superimposability of BEAM and MERSYN images. The few points that are not exactly superimposed are probably due to the different (nearest neighbour) interpolation methods.

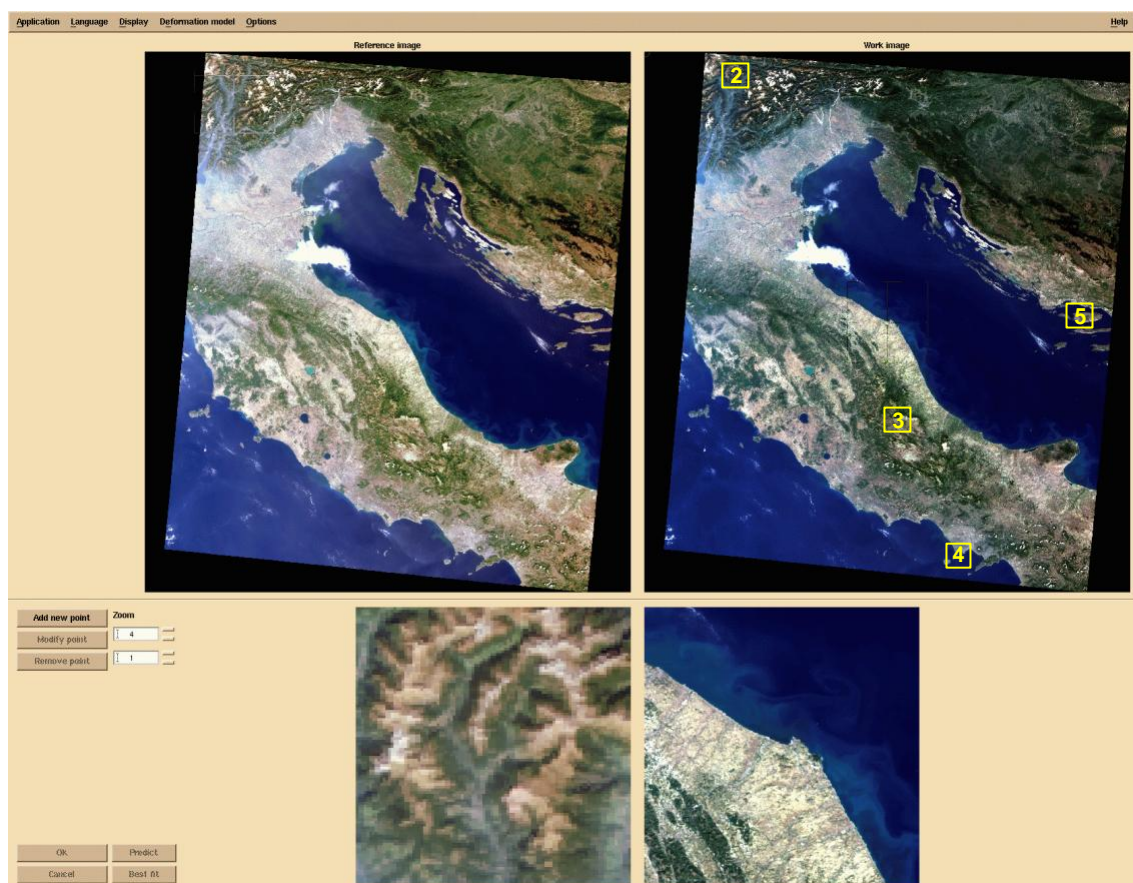


fig. 40 - REGIST application (snap11_REGIST.gif)

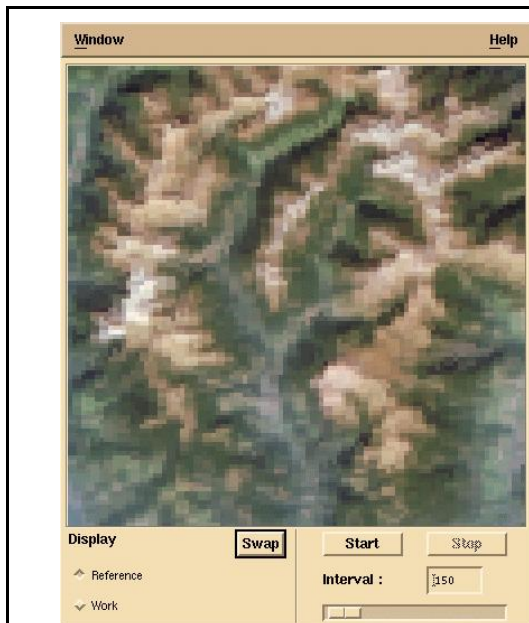


fig. 41 - BEAM
(snap12_REGIST_Flicker_x4_beams.gif)



fig. 42 - MERSYN
(snap12_REGIST_Flicker_x4_mersyns.gif)

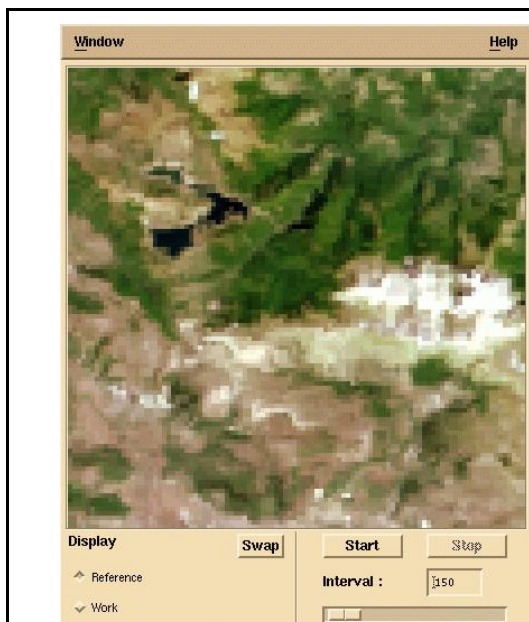
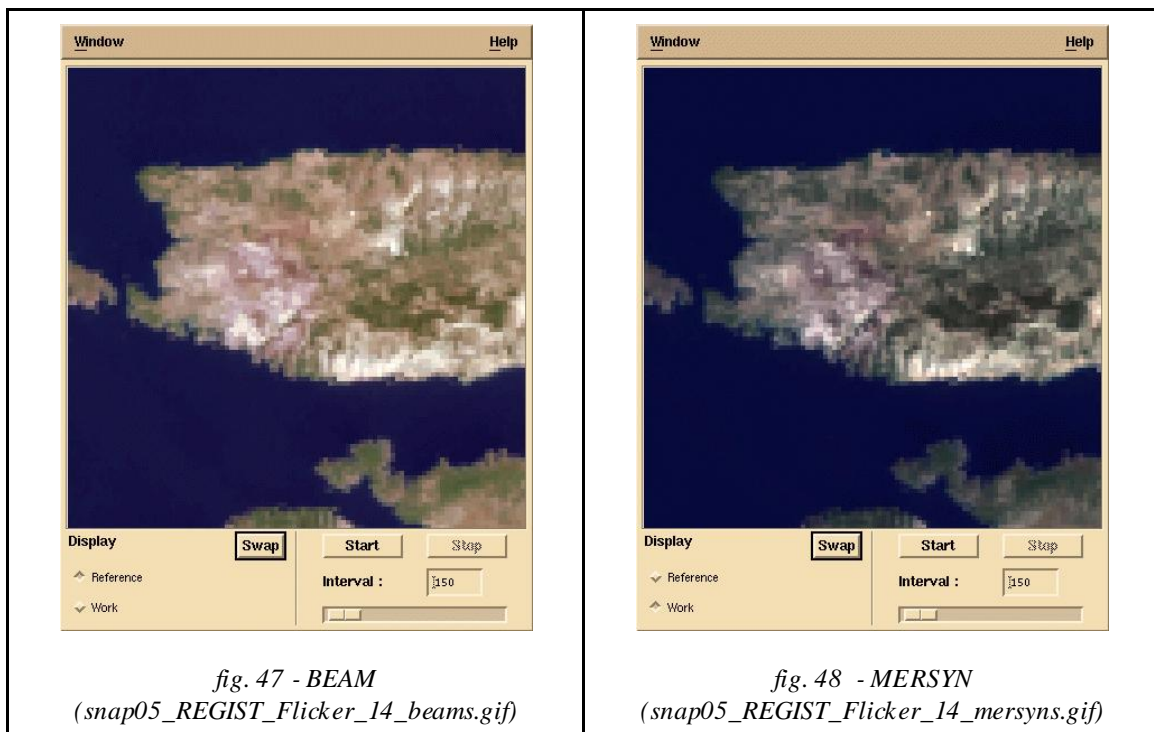
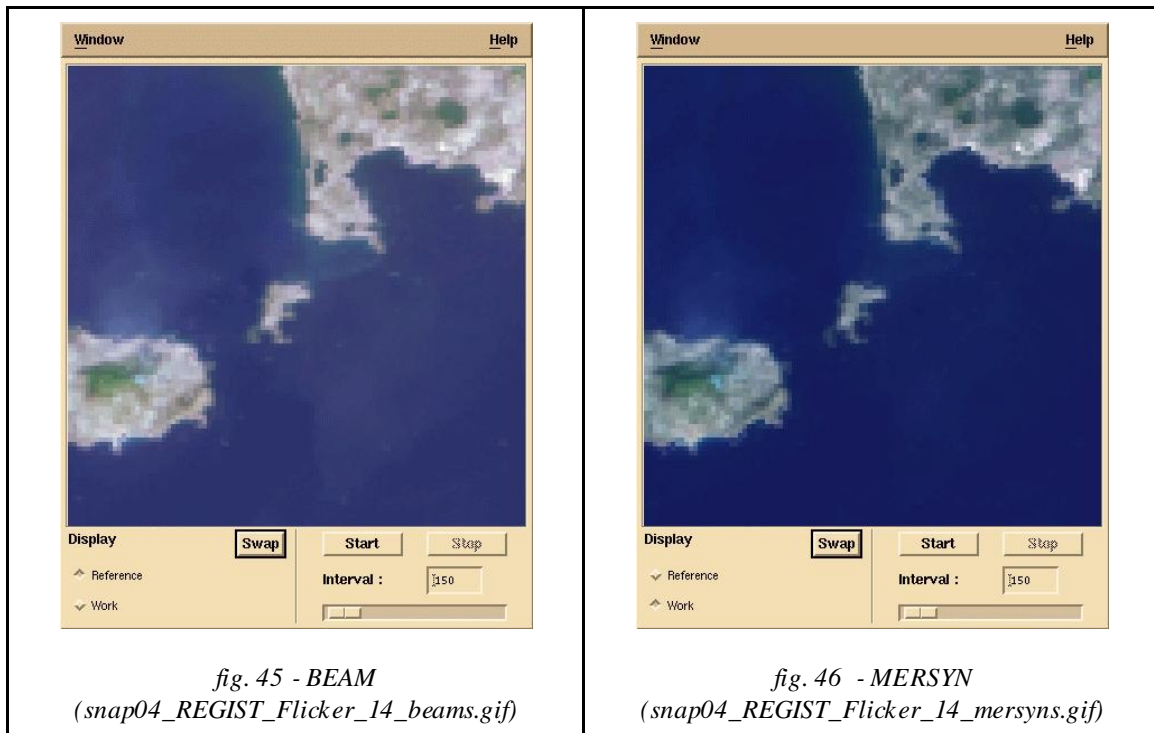


fig. 43 - BEAM
(snap13_REGIST_Flicker_x4_beams.gif)



fig. 44 - MERSYN
(snap13_REGIST_Flicker_x4_mersyns.gif)



4.8 Benchmark

A benchmark of 25 points is provided in APPENDIX D. Points are dispatched within the MERIS synthesis image orthorectified from the GETASSE30 DEM.

" This document discloses subject matter in which VisioTerra has proprietary rights. Recipient of this document shall not duplicate, use or disclose in whole or in part, information disclosed hereon except for or on behalf of VisioTerra to fulfil the purpose for which the document was delivered to him. "

5 GETASSE30 QUALITY CONTROL

GETASSE30 has been produced by Marc BOUVET (ESA/ESTEC) after an analysis of the ACE data (see R-5).

"GETASSE30 is a composite dataset. It is using the SRTM30 dataset, ACE dataset, Mean Sea Surface (MSS) data and the EGM96 ellipsoid as sources. The resulting GETASSE30 dataset represents the Earth Topography And Sea Surface Elevation with respect to the WGS84 ellipsoid at 30 arc second resolution." (R-6).

Figure here below (fig. 49 extracted from R-6) shows the flags associated to the origin of GETASSE30 data.



fig. 49 - Origin of GETASSE30 data.

From an e-mail of Steven DELWART dated on 21/10/2004, GETASSE30 data have been extracted from the ESTEC FTP site <ftp://estec.esa.int/pub/wipsftp/steven/getasse30/>.

GETASSE30 data are organised in the following way:

- Tiles of $15^\circ \times 15^\circ$ with a resolution of 30" arc leading to images of 1800x1800 pixels.
- Tile name **nnVeeeH** is based on the coordinates (nn,eee) of the lower-left corner where:
 - nn is the latitude expressed in degrees within $[-90^\circ, +90^\circ]$
 - V is the hemisphere: N for North or S for South
 - nn is the longitude expressed in degrees within $[-180^\circ, +180^\circ]$
 - H is the West demi-sphere (W) or East demi-sphere (E).
- Elevation values are given in metres above the WGS84 ellipsoid and are stored in 4-bytes ANSI-IEEE floating values.
- Elevations are arranged lines per lines from South to North, and along each line from West to East.
- For each tile, two files are given:
 - nnVeeeH containing the elevation data (1800x1800x4 bytes = 12960000),
 - nnVeeeH_flag giving the origin of the data (1800x1800x2 unsigned bytes = 6480000).

To cover Europe, the following six tiles have been downloaded:

```
-rw-r--r-- 1 telimago telimago 12960000 Oct 21 14:06 30N000E.GETASSE30
-rw-r--r-- 1 telimago telimago 6480000 Oct 21 13:40 30N000E.GETASSE30_flag
-rw-r--r-- 1 telimago telimago 12960000 Nov 1 11:11 30N015E.GETASSE30
-rw-r--r-- 1 telimago telimago 6480000 Nov 1 11:11 30N015E.GETASSE30_flag
-rw-r--r-- 1 telimago telimago 12960000 Oct 21 13:46 30N015W.GETASSE30
-rw-r--r-- 1 telimago telimago 6480000 Oct 21 13:49 30N015W.GETASSE30_flag
-rw-r--r-- 1 telimago telimago 12960000 Oct 20 09:42 45N000E.GETASSE30
-rw-r--r-- 1 telimago telimago 6480000 Oct 20 09:42 45N000E.GETASSE30_flag
-rw-r--r-- 1 telimago telimago 12960000 Nov 1 11:11 45N015E.GETASSE30
-rw-r--r-- 1 telimago telimago 6480000 Nov 1 11:11 45N015E.GETASSE30_flag
-rw-r--r-- 1 telimago telimago 12960000 Oct 21 13:56 45N015W.GETASSE30
-rw-r--r-- 1 telimago telimago 6480000 Oct 21 13:59 45N015W.GETASSE30_flag
```

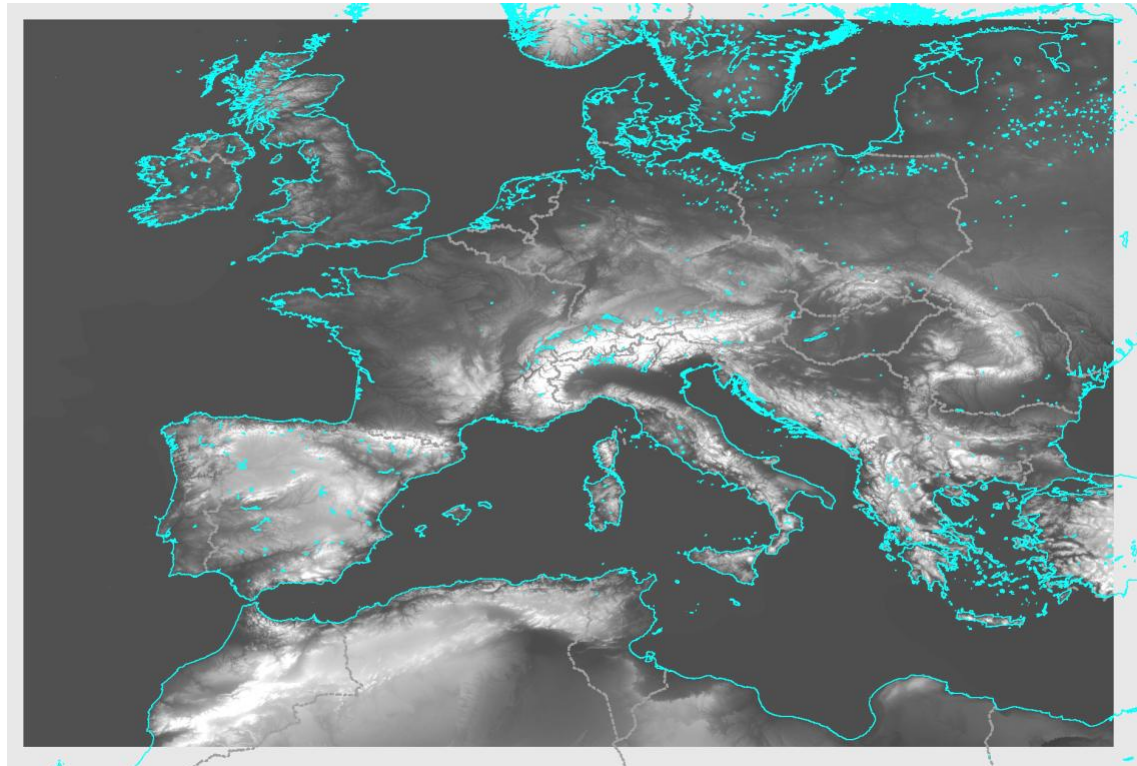


fig. 50 - GETASSE30 over Europe.

In the next sections, GETASSE30 data are compared with:

- EUROPE09, a DEM with a resolution of 9'' arc, and
- a collection of 216 GPS points.

5.1 Comparison with EUROPE09

The 9-seconds Digital Elevation Model of Europe has been one of the most precise and the most used by various organizations of Europe. It is also known as the 250 metres DEM of Europe.

Using the mean Earth radius, the spatial resolution linking the angular resolution and the vertical geodetic distances (or the horizontal ones at equator) is given by the following formula:

$$9'' \text{ arc} \times 6\,370\,997 \text{ m} \approx \underline{278 \text{ m}}$$

Eq. 6

" This document discloses subject matter in which VisioTerra has proprietary rights. Recipient of this document shall not duplicate, use or disclose in whole or in part, information disclosed here on except for or on behalf of VisioTerra to fulfil the purpose for which the document was delivered to him. "

EUROPE09 has been resampled to achieve the 30'' arc resolution of GETASSE30 and using the WGS84 planimetric reference system (ellipsoid and datum).

Unfortunately, few annotation data are given with EUROPE09 and, in particular, the vertical reference system (WGS84, EGM96 or an other one) is unknown. One of the objectives of this section is to determine the closest vertical reference system of EUROPE09 from the one of GETASSE30.

Visual inspection

Shading effect (see fig. 51 and fig. 52) is computed from the first derivative (gain 70 and offset 32768) simulating two illuminations:

- illumination North-West to South-East with a factor 2, and
- illumination North to South with a factor 1.

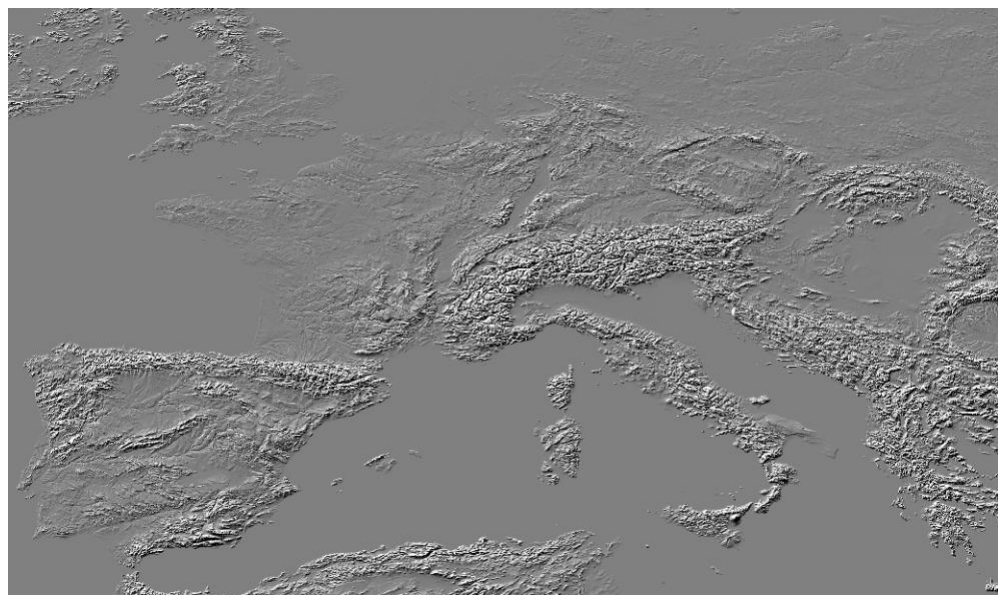


fig. 51 - Shading of GETASSE30 – Full image.

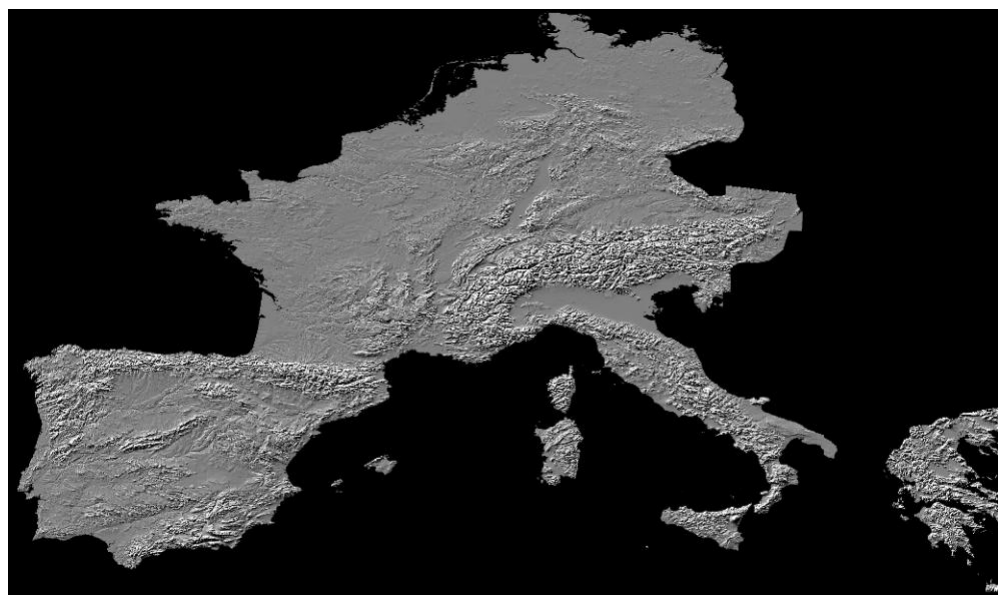


fig. 52 - Shading of EUROPE09 – Full image.

Sea areas of EUROPE09 are set to 0 and are considered as background (represented in black in fig. 52).

At small scale, the morphological structures look exactly the same in both DEMs. On the other hand a full resolution inspection enables identifying small differences when images are alternately displayed (see the animation process as explained in section 4.4).

The two animations “snap32_anim01_switzerland.gif” and “snap33_anim02_spain.gif” are available on demand.

Some of the collected differences are given here below:

1. Two small structures are present only in EUROPE09 (see yellow area of fig. 53).
2. EUROPE09 is moved southward of about 1 pixel (see orange arrow of fig. 53).
3. Roughness of EUROPE09 is higher than GETASSE30 (see in particular in green area of fig. 53).

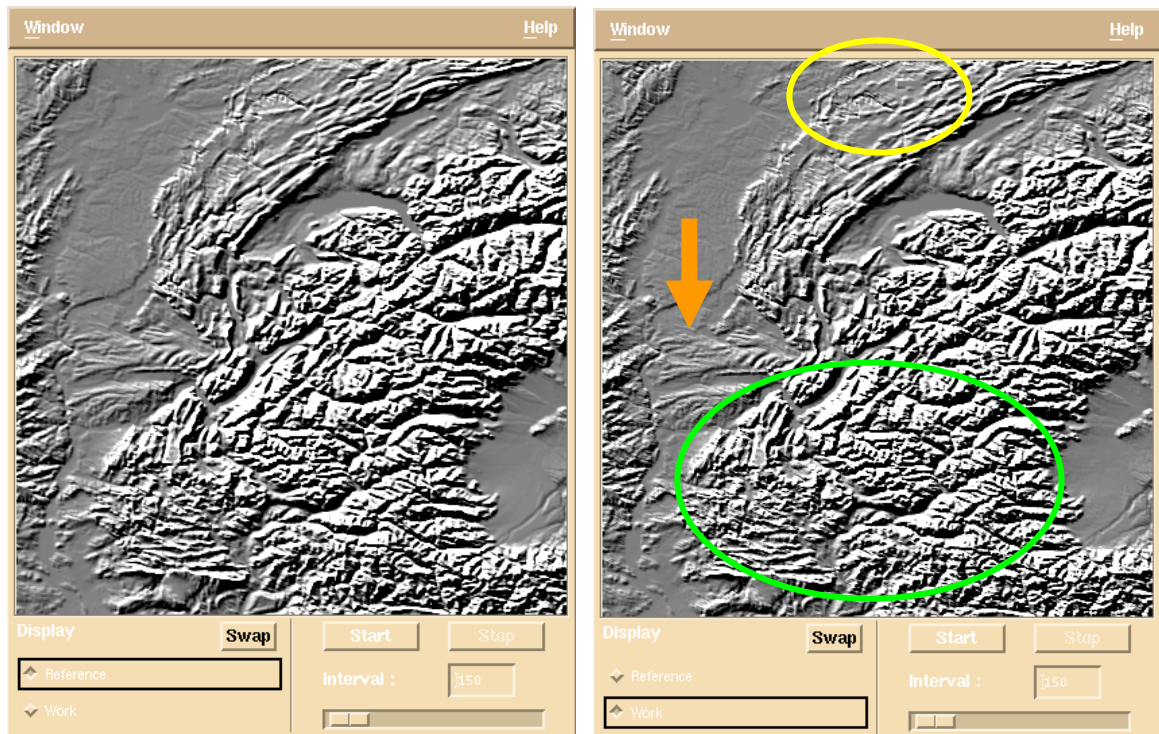
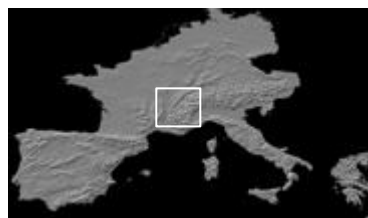


fig. 53 - Switzerland animation 01. GETASSE30 (left) and EUROPE09 (right).

On an other region of South of Spain (see fig. 54) processing an animation underlines the following defects:

4. Stitches between probable tiles within EUROPE09 (see blue area of fig. 54).

" This document discloses subject matter in which VisioTerra has proprietary rights. Recipient of this document shall not duplicate, use or disclose in whole or in part, information disclosed here on except for or on behalf of VisioTerra to fulfil the purpose for which the document was delivered to him. "

5. EUROPE09 is moved southward of about 1 pixel (see orange arrow of fig. 54).
6. Roughness of EUROPE09 is higher than GETASSE30.

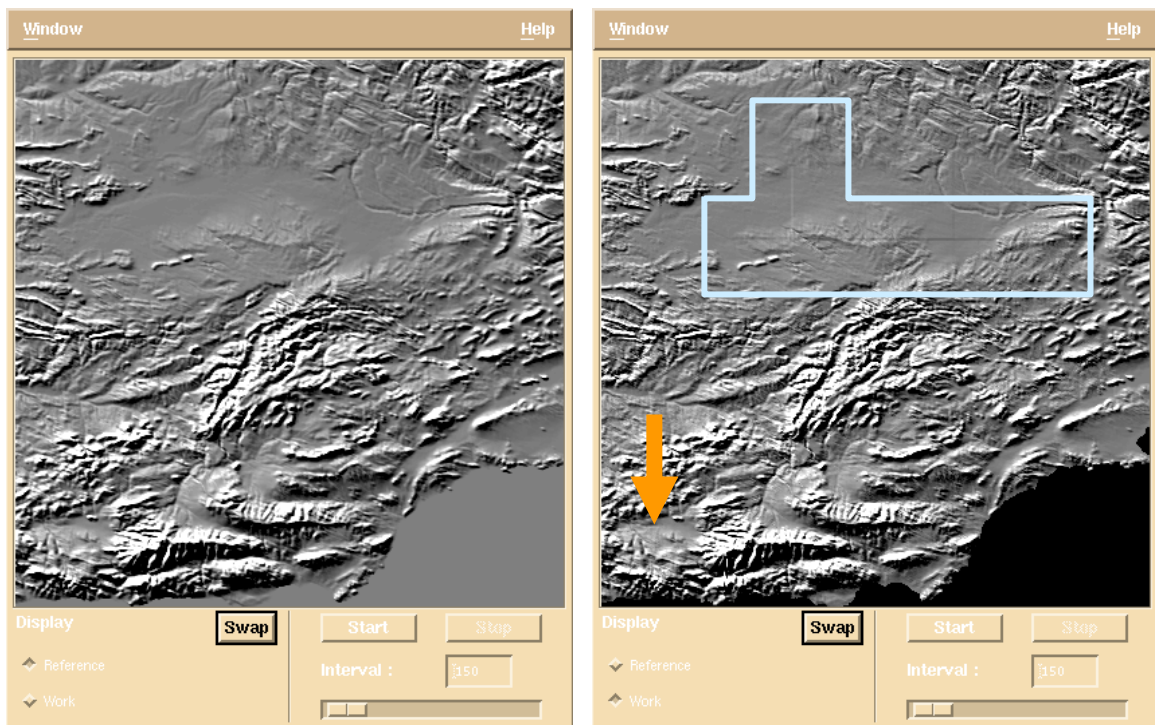
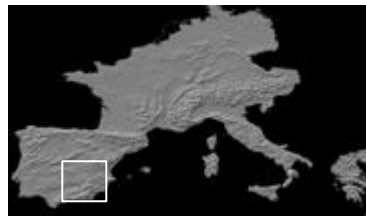


fig. 54 - Spain animation 02. GETASSE30 (left) and EUROPE09 (right).

Statistics of image difference

GETASSE30 elevations are given above the WGS84 ellipsoid (R-6).

In order to determine the most probable vertical reference system in which EUROPE09 elevations are given, GETASSE30 has been also computed above EGM96 geoid, subtracting the EGM96 image downloaded from:

<http://cdssda.gsfc.nasa.gov/926/egm96/egm96.html>
 -> <http://earth-info.nga.mil/GandG/wgsegm/>
 -> <http://earth-info.nima.mil/GandG/wgsegm/egm96.html>

This section shows result images and statistics when computing the differences:

1. GETOPO30_EGM96 – EUROPE09, and
2. GETOPO30_WGS84 – EUROPE09.

" This document discloses subject matter in which VisioTerra has proprietary rights. Recipient of this document shall not duplicate, use or disclose in whole or in part, information disclosed here on except for or on behalf of VisioTerra to fulfil the purpose for which the document was delivered to him. "

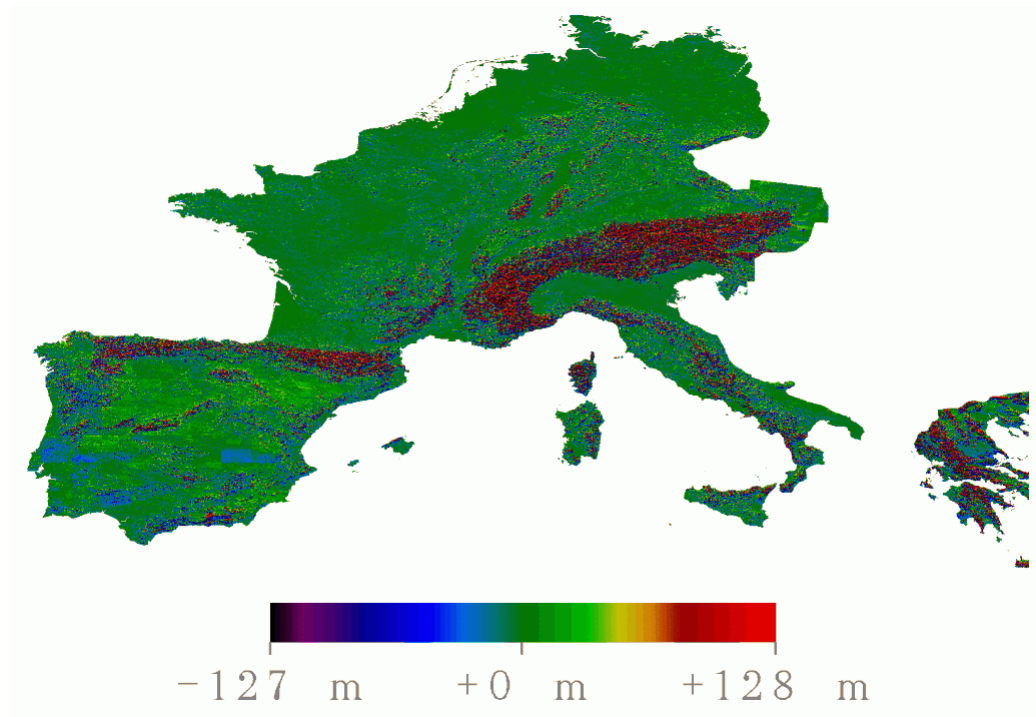
GETOP030_EGM96 – EUROPE09

fig. 55 - EUROPE09 subtracted to GETASSE30 above EGM96 – Image of differences.

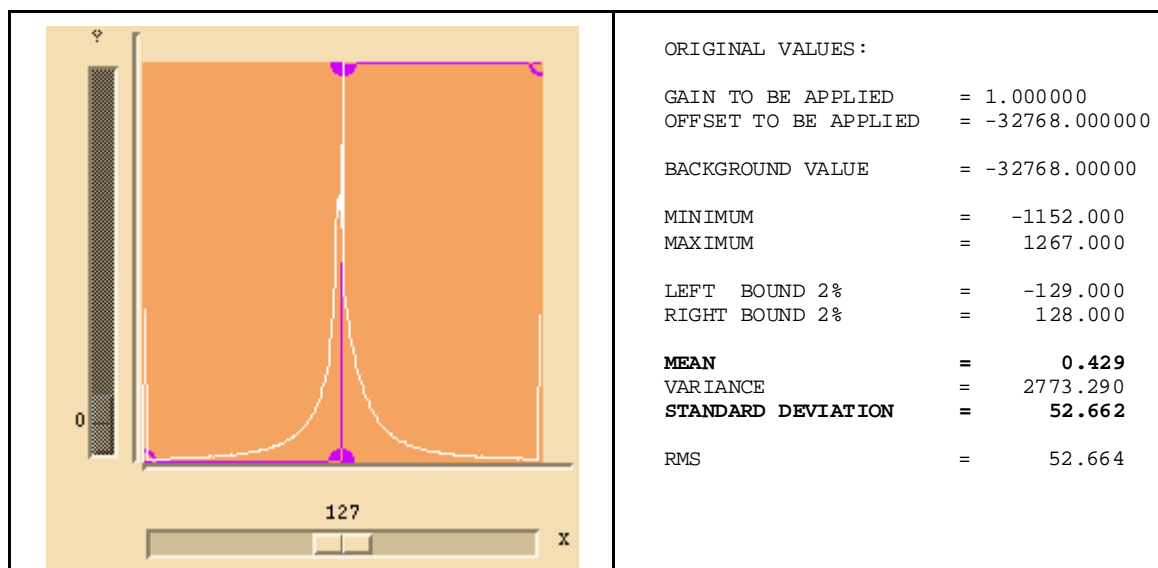


fig. 56 - EUROPE09 subtracted to GETASSE30 above EGM96 – Statistics.

GETOP030_WGS84 – EUROPE09

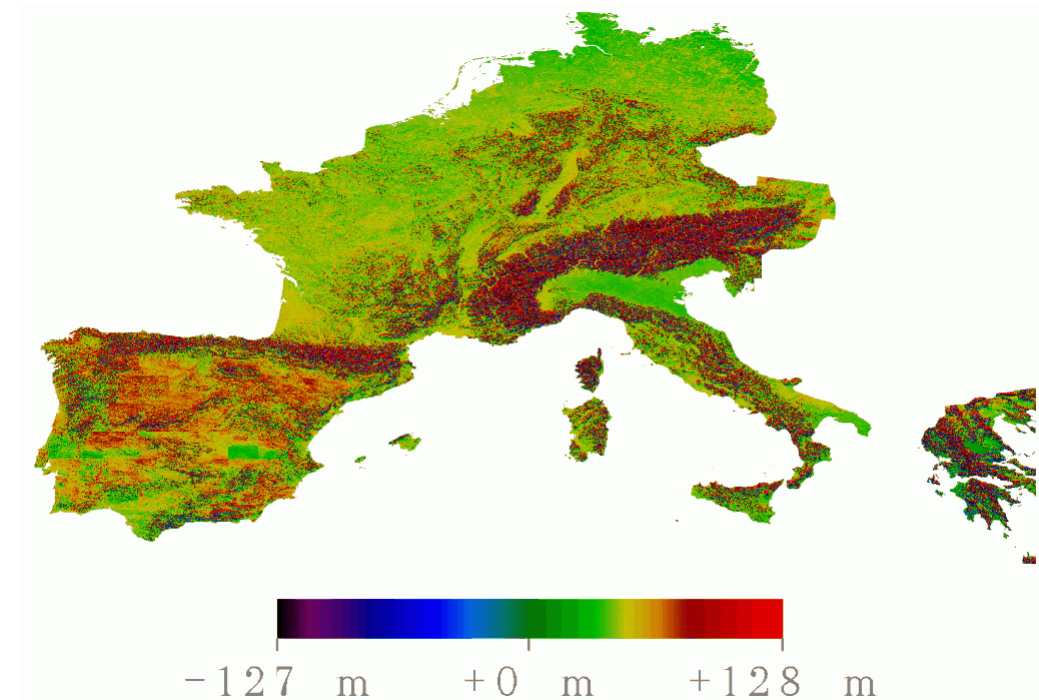


fig. 57 - EUROPE09 subtracted to GETASSE30 above WGS84 – Image of differences.

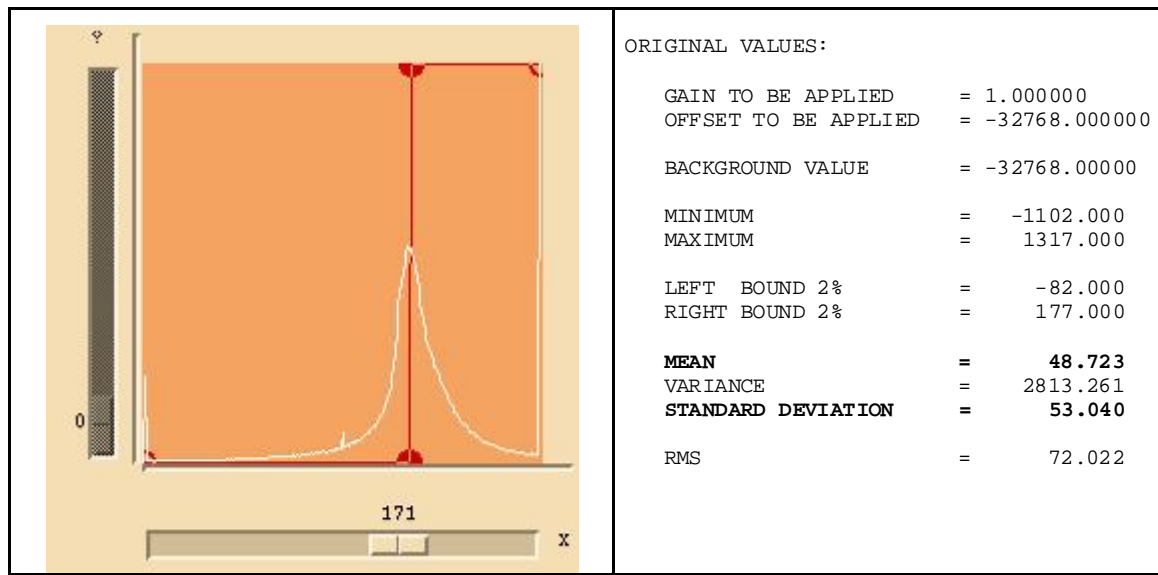


fig. 58 - EUROPE09 subtracted to GETASSE30 above WGS84 – Statistics.

EUROPE09 vertical reference system

EUROPE09 is much closer to GETASSE30 above EGM96 (difference mean of 0.429 metres) than to GETASSE30 above WGS84 (difference mean of 48.723 metres). This means that EUROPE09 shall have been expressed above a geoid (for example EGM96) or above national geoids for each country.

" This document discloses subject matter in which VisioTerra has proprietary rights. Recipient of this document shall not duplicate, use or disclose in whole or in part, information disclosed hereon except for or on behalf of VisioTerra to fulfil the purpose for which the document was delivered to him. "

Distribution of differences

Distribution of differences seems to obey a normal distribution leading to a Gaussian histogram with a standard deviation of +/-53 metres.

Defect identification

Stretching the difference between the two DEMs magnifies the defect identification. For example, fig. 59 clearly underlines the tile defect observed in the DEM of Spain. More subtle defects may also be accounted like punctual anomalies illustrated in fig. 60.

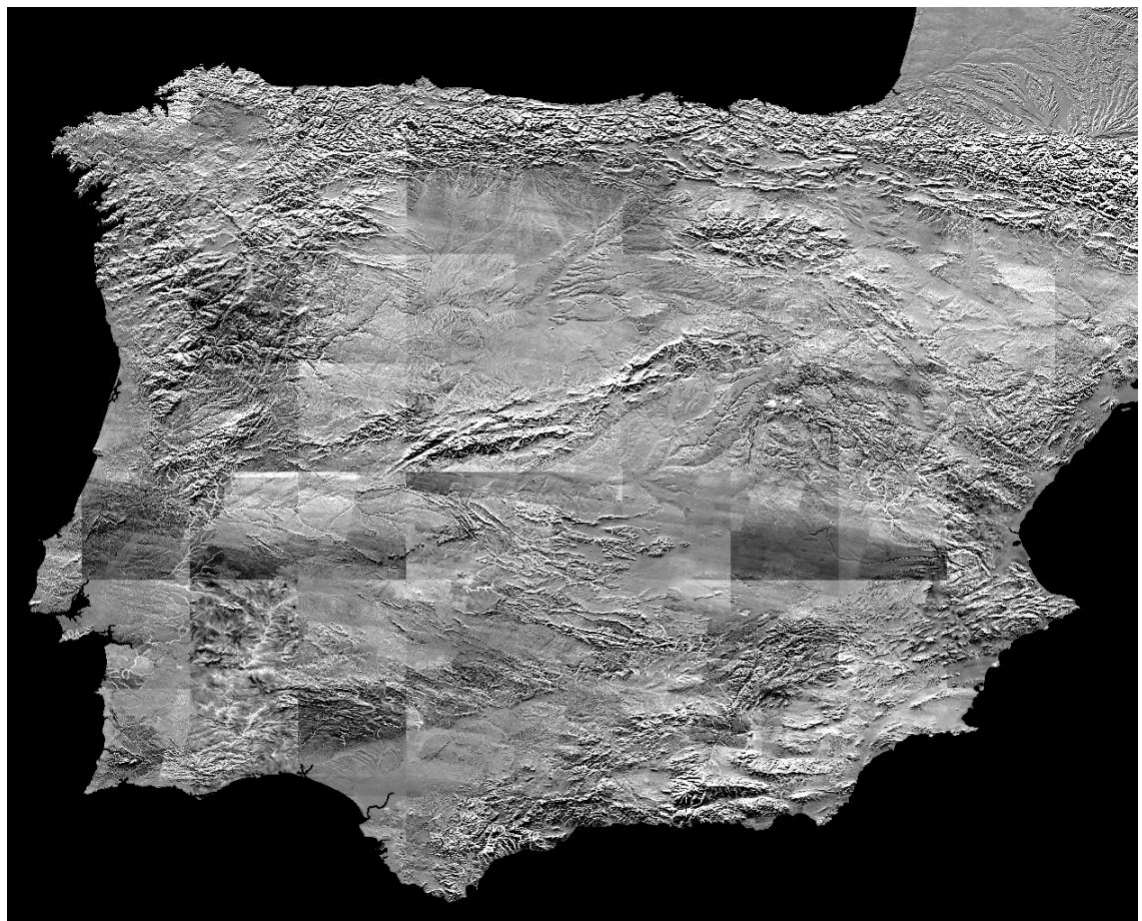


fig. 59 - GETOP030_EGM96-EUROPE09 – Tile defect.

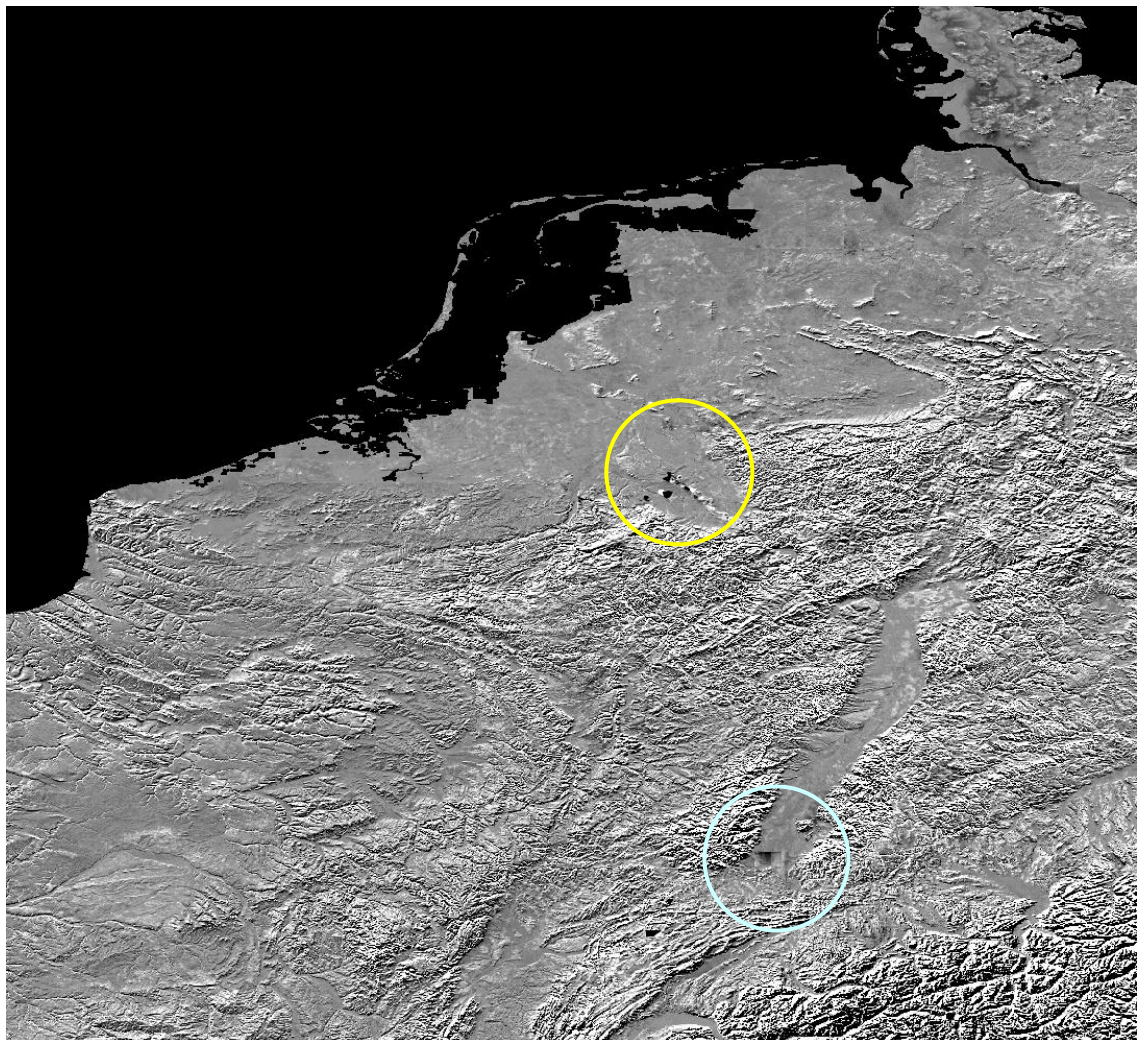


fig. 60 - GETOP030_EGM96-EUROPE09 – Punctual defects.

5.2 Comparison with EUVN geodesic points

Description of reference data

Geodesic points

Geodesic points are available at the address <http://crs.bkg.bund.de/evrs/Results.html> of the European Vertical Reference System (EVRS) page shown in figure here below.

This site is maintained by the EUREF (see <http://www.euref-iag.net/>).


European Vertical Reference System (EVRS)


EUVN Results

EUVN - GPS Solution
Results of GPS measurements for the determination of the ellipsoidal heights of all defined EUVN points

The following final products were generated: coordinate files containing geocentric coordinates and ellipsoidal coordinates in system ITRF96 epoch 1997.4 and ETRS89 (ETRF96, epoch 1997.4) and a file in the **Solution INdependent EXchange (SINEX)** format, containing in addition to the coordinates the variance-covariance information of the EUVN97 GPS network.

For detailed information see paper [EUVN97 Combined GPS Solution](#)

EUVN_ITRF.CRD	EUVN_ITRF.BLH	geocentric coordinates ellipsoidal coordinates
EUVN_ITRF.CRD	EUVN_ITRF.BLH	geocentric coordinates ellipsoidal coordinates
EUVN_ITRF.SNX.Z		Solution in SINEX format (Unix-Compressed)

EUVN - Height Solution

For detailed information see paper [The EUVN Height Solution - Report of the EUVN Working Group](#)

EUVN Tide Gauge Data

For detailed information see paper [Status Report on sea-level data collection and analysis within the EUVN Project](#)

Compilation of the Numerical Results

Find a table with the

- Ellipsoidal coordinates in ITRF96 Epoch 1997.4
- Normal heights H in UELN 95/98
- Difference ellipsoidal height h - normal height H
- EGG97 Geoid
- Difference EGG97 - (h-H)
- Ellipsoidal height of the mean sea level 1997 above the EUVN tide gauge stations
- Normal height of the mean sea level 1997 above the EUVN tide gauge stations

fig. 61 - Site providing a collections of geodesic points.

File [EUVN_ETRF.BLH](#) contains 217 points that are distributed over Europe as shown by fig. 62.



fig. 62 - Distribution of GPS points over Europe.

ITRS and WGS84

ITRS (International Terrestrial Reference System) and WGS84 (World Geodetic System 1984) are almost equivalent (see <http://www.ensg.ign.fr/ITRF/trans para.php> here below).

In general the ITRS (and its realizations ITRFyy) are identical to WGS84 at one meter level.

Meanwhile there are two types of WGS84 realization:

- old realization based on U.S. Navy Navigation Satellite System, commonly known as DOPPLER Transit, and provided station coordinates with accuracies of about one meter. With respect to this realization we published, some years ago, transformation parameters between ITRF90 and this Doppler realized system:

Parameters from ITRF90 to WGS84-Doppler realized system

UNITS	T1 -----> (m)	T2 (m)	T3 (m)	D (ppm)	R1 ("")	R2 ("")	R3 ("")
	0.060	-0.517	-0.223	-0.011	0.0183	-0.0003	0.0070

- New realizations of WGS84 based on GPS data, such as WGS84(G730 or G873).

These new WGS84 realizations are coincident with ITRF at about 10-centimeter level. For these realizations there are no official

transformation parameters. This means that one can consider that ITRF coordinates are also expressed in WGS84 at 10 cm level.

A French explanation of ITRS is provided in a document of IGN at URL address <http://www.ign.fr/telechargement/education/fiches/geodesie/systèmes.pdf>.

L'ITRS, système de référence terrestre de l'International Earth Rotation Service (IERS), est matérialisé par un réseau mondial de près de 300 points. Avec une exactitude au niveau centimétrique, il s'agit du plus précis des systèmes géodésiques mondiaux. Depuis 1988, l'IERS fournit chaque année une réalisation appelée ITRFyy, avec yy comme derniers chiffre du millésime. La dernière en date est l'ITRF97.

Du fait de la précision de ce système, l'époque de référence des coordonnées qui sont publiées doit être précisée (par exemple : 1997.0 pour l'ITRF97). De plus, les réalisations ITRFnn donnent pour chaque point une vitesse de déplacement, qui est une mesure du mouvement de ce point résultant de phénomènes géophysiques comme les mouvements tectoniques et le rebond post-glaciaire. D'autre part, on applique lors du calcul de ces coordonnées des corrections diverses : marées terrestres, pression atmosphérique, etc...

Les réalisations ITRFnn sont obtenues par combinaison de jeux de coordonnées issues de différentes techniques de géodésie spatiale très précises :

VLBI : Very Long Base Interferometry (interférométrie à très longue base) LLR : Lunar Laser Ranging (télémétrie laser sur la lune) SLR : Satellite Laser Ranging (télémétrie laser sur satellite) GPS : Global positioning System DORIS : Doppler Orbitography Radiopositionning Integrated by Satellite

Le système ETRS89 (European Terrestrial Reference System 1989)

Le système ETRS89 est défini à partir de l'ITRS et coïncide avec ITRS à l'époque 1989.0.

Il est attaché à la partie stable de la plaque eurasienne. A une époque quelconque on applique une vitesse théorique de la plaque Eurasie sur les coordonnées.

L'ETRFyy, réalisation de ETRS utilise des points ITRFyy européens et des points de densification par GPS. Successeur de ED87, initialement localisé sur l'Europe occidentale, ETRS89 s'étend à présent sur l'Europe de l'Est.

More information can be found on the following sites:

- ITRF <http://www.ensg.ign.fr/ITRF/>
- Geodesy tutorial http://www.qsl.com/geodesy_tutorial/intro.php

GTASSE30 Vertical Reference System

As indicated in the “**Readme_with_images.doc**” file of the GETASSE30 distribution, this DEM contains elevation expressed above the WGS84 ellipsoid.

...
=====

GETASSE30

Global Earth Topography and Sea Surface Elevation at 30 arc second resolution

=====

Data set:

GETASSE30 is a composite dataset. It is using the SRTM30 dataset, ACE dataset, Mean Sea Surface (MSS) data and the EGM96 ellipsoid as sources.

The resulting GETASSE30 dataset represents the Earth Topography And Sea Surface Elevation with respect to the WGS84 ellipsoid at 30 arc second resolution.

...

EUVN ground control points are GPS measurements expressed in reference to the ETRS89 or ITRF96 reference systems that are, as shown in the previous section, very close the WGS84 reference system.

As a consequence, elevations of EUVN geodesic points and those found in GETASSE30 are expressed with respect to very close vertical reference systems, and may be immediately compared without performing a reference system conversion (see for example the HEIGHT process to add/subtract geoid elevations above the WGS84 ellipsoid).

Quality control results

The full logs of quality controls are stored in APPENDIX F.

For each one of the 217 geodesic point (X_i, Y_i, h_i) , DEMCHK process checks if the point (X_i, Y_i) is inside the DEM or not. In the positive case, the corresponding elevation h_i is interpolated from the DEM to be controlled.

Statistics are computed according to the following formulae:

$$\begin{aligned}
 \text{ARITHMETIC MEAN} &= \frac{1}{N} \times \sum_{i=1}^N (H_i - h_i) \\
 \text{QUADRATIC MEAN} &= \sqrt{\frac{1}{N} \times \sum_{i=1}^N (h_i - H_i)^2} \\
 \text{STANDARD DEVIATION} &= \sqrt{\frac{1}{N} \times \sum_{i=1}^N (h_i - H_i)^2 - \left[\frac{1}{N} \times \sum_{i=1}^N (h_i - H_i) \right]^2} \\
 \text{MINIMUM} &= \min_{i=1..N} (H_i - h_i) \\
 \text{MAXIMUM} &= \max_{i=1..N} (H_i - h_i)
 \end{aligned}$$

Interpolated value h_i depends on the interpolation method being used. The three classical methods (*Nearest neighbour*, *Bi-linear* and *Bi-cubic*) have been tested.

Checking has been applied to the GTASSE30 DEM over Europe (see fig. 50). On this area **169 EUVN control points** among the 217 available ones fail inside the DEM (77.9% of the points).

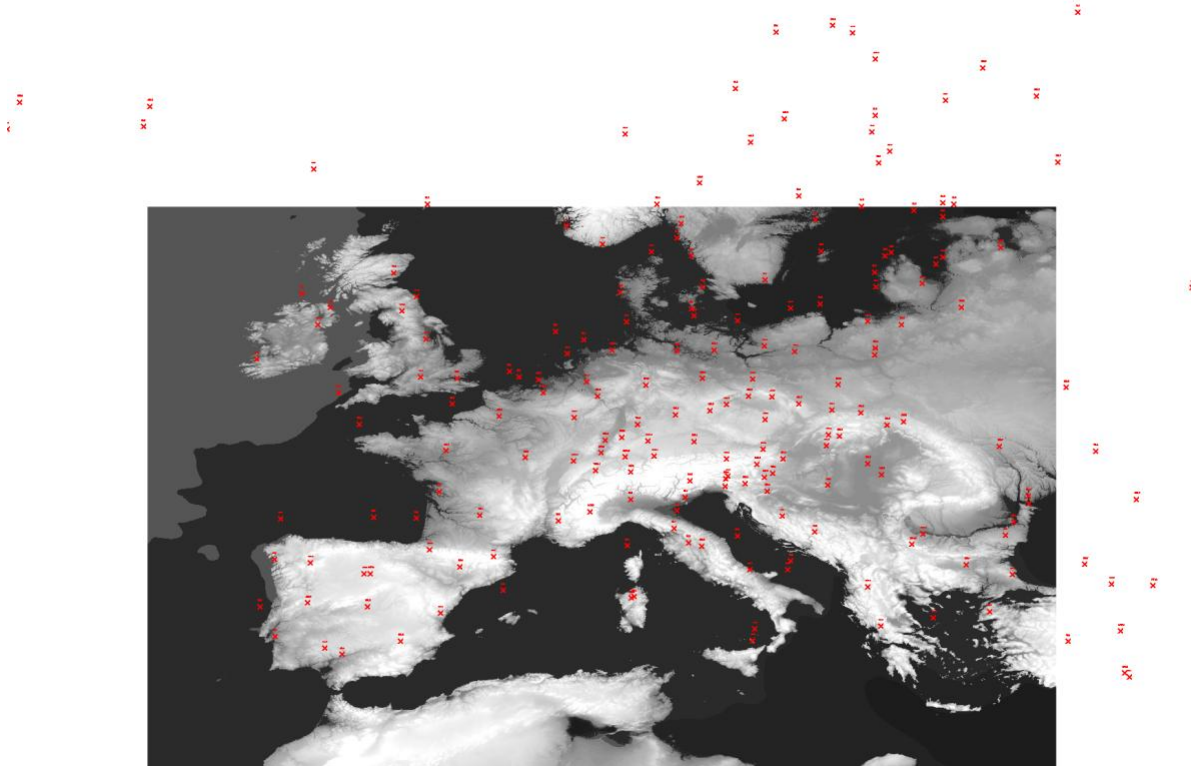


fig. 63 - Distribution of the geodesic control points relatively to GTASSE30 DEM over Europe.

Table here below gives results of the controls performed on GTASSE30 Europe DEM for the three interpolation methods (“Nearest neighbour”, “Bi-linear”, and “Bi-cubic”) and a control performed on ACE DEM using the “Nearest neighbour” interpolation method.

	GTASSE30 Nearest neighbour	GTASSE30 Bi-linear	GTASSE30 Bi-cubic	ACE Nearest neighbour
ARITHMETIC MEAN	+10.828	+11.304	+12.008	-2201.149
QUADRATIC MEAN	32.368	34.017	32.915	12109.911
STANDARD DEVIATION	30.503	32.083	30.646	11908.186
MINIMUM	-127.560	-181.091	-172.570	-65001.139
MAXIMUM	+100.931	+125.763	127.387	+325.560

table 4 - Statistics of elevation differences (expressed in metres).

Surprisingly, the “Nearest neighbour” interpolation leads to the lowest error estimation. Such an observation may be due to the error introduced by whatever interpolation when considering the surrounding pixels. These classical interpolation methods are not relevant to topographic surfaces that may be complex.

" This document discloses subject matter in which VisioTerra has proprietary rights. Recipient of this document shall not duplicate, use or disclose in whole or in part, information disclosed here on except for or on behalf of VisioTerra to fulfil the purpose for which the document was delivered to him. "

Controls performed on ACE lead to signifi errors. These statistical results for ACE are not significant because of specific values found within the ACE DEM file and that are not elevations (see appendix F.1). A full analysis of ACE would require to check the ACE image of flags indicating if the elevation is relevant or not and the origin of this elevation.

Figures below show the distribution of elevation errors for the various interpolation methods. We may note that the distribution is almost symmetrical towards a vertical axis located at abscise almost given by the arithmetic mean. ($\approx +11$).

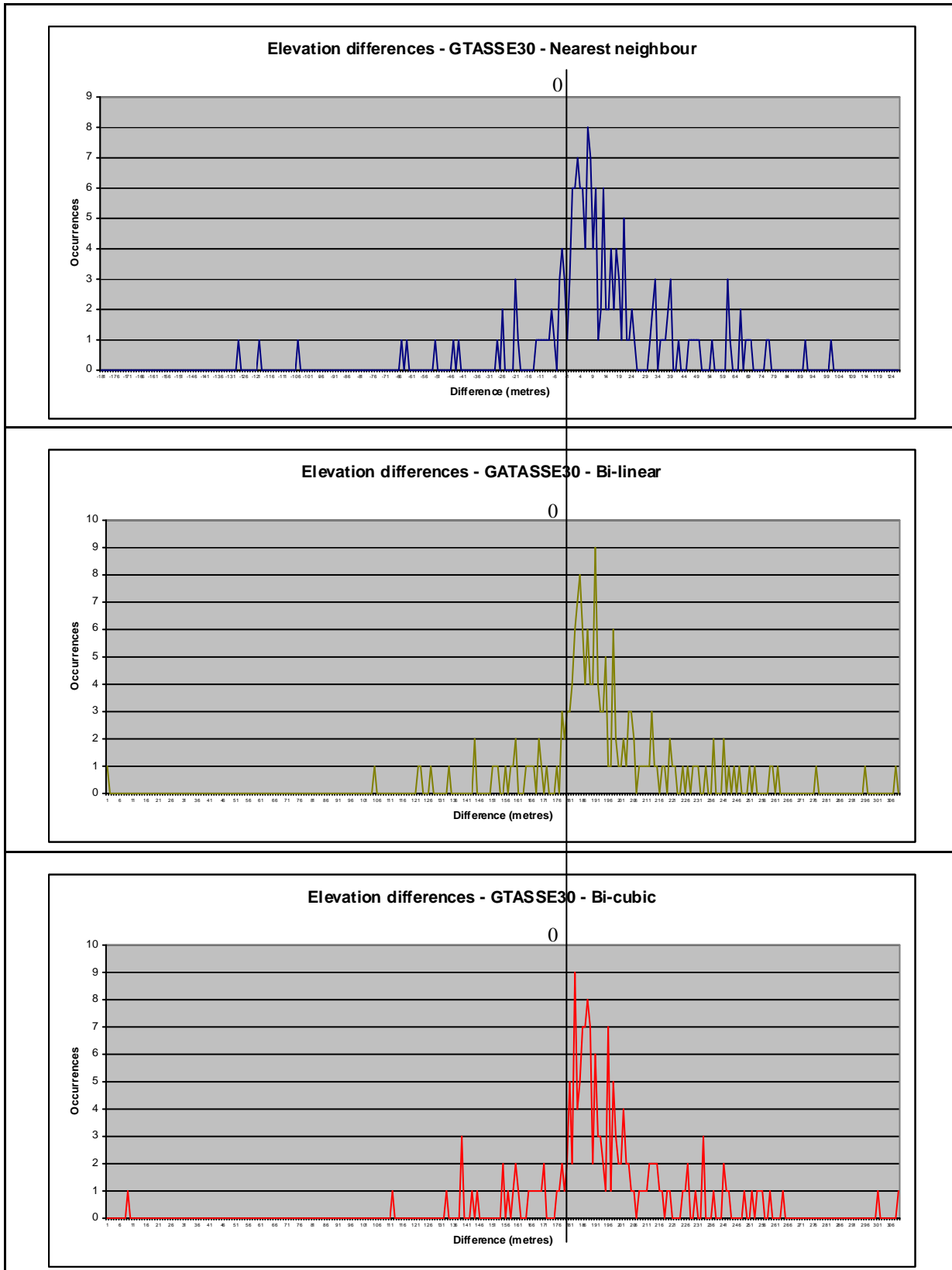


fig. 64 - Elevation errors distribution for various interpolation methods.

" This document discloses subject matter in which VisioTerra has proprietary rights. Recipient of this document shall not duplicate, use or disclose in whole or in part, information disclosed here on except for or on behalf of VisioTerra to fulfil the purpose for which the document was delivered to him. "

APPENDIX A MERIS SCENE FR ITALY

A.1 Decoding log

MAIN PRODUCT HEADER:

```

Product File Name : MER_FR__1PNUPA20030921_092341_000000982020_00079_08149_0534.N1
Processing Stage Flag : N
Reference Document Describing Product : PO-RS-MDA-GS2009_11_3J
Acquisition Station ID : PDHS-E
Processing Center ID : UK-PAC
UTC Time of Processing : 26/01/2004 13:24:19.434677
Software Version Number of Processing SW : MERIS/4.07
UTC Start Time of Data Sensing : 21/09/2003 09:22:17.265770
UTC Stop Time of Data Sensing : 21/09/2003 09:26:36.187634
Phase : 2
Cycle : 20
Start Relative Orbit Number : 79
Start Absolute Orbit Number : 8149
State vector at ascending node:
    Date Time : 21/09/2003 09:23:00.000000
    Position : 4513681.740000 1552817.947000 5333228.142000
    Velocity : 5786.205174 -136.373816 -4845.448794
    DUT1=UT1-UTC : -0.352582
    Source of Orbit Vectors : FR (FOS restituted)
    UTC time corresponding to SBT below : 21/09/2003 09:10:16.414244
    Satellite Binary Time (SBT) : 4008373760
    Clock Step Size (in picoseconds) : 0.003906249810
    UTC time of occurrence of Leap Second : 17/10/2001 00:00:00.000000
    Leap second sign : 1
    Leap second error : 0
    Product error : 0
    Total Size of Product : 166271715
    Length of SPH : 9942
    Number of DSDs : 30
    Length of each DSD : 280
    Number of DSs attached : 19

```

SPECIFIC PRODUCT HEADER:

```

SPH Descriptor : MER_FR__1P SPECIFIC HEADER
Stripline Continuity Indicator : 0
Slice Position : 1
Number of Slices in this Stripline : 1
Azimuth time first line of product : 21/09/2003 09:23:41.714409
Azimuth time last line of product : 21/09/2003 09:25:20.267689
Geo. Lat. of first sample of first line : 45.90986300
Geo. Long. of first sample of first line : 18.01469200
Geo. Lat. of middle sample of first line : 46.52906400
Geo. Long. of middle sample of first line : 14.34706300
Geo. Lat. of last sample of first line : 47.02819600
Geo. Long. of last sample of first line : 10.60349600
Geo. Lat. of first sample of last line : 40.14283200
Geo. Long. of first sample of last line : 15.96981400
Geo. Lat. of middle sample of last line : 40.73596700
Geo. Long. of middle sample of last line : 12.62631800
Geo. Lat. of last sample of last line : 41.23065400
Geo. Long. of last sample of last line : 9.22799100
Transmission error flag : 0
Format error flag : 0
Database error flag : 0
Coarse error flag : 0
Forecast (0) / Analysis (1) ECMWF data : 1
Number of transmission errors in product : 0
Number of format errors in the product : 0
Threshold for setting TRANS_ERR_FLAG : 0.000000 %
Threshold for setting FORMAT_ERR_FLAG : 0.000000 %

```

Number of bands in the product	: 15
Central wavelength of the bands:	
Band 1	: 412.545 nm
Band 2	: 442.401 nm
Band 3	: 489.744 nm
Band 4	: 509.700 nm
Band 5	: 559.634 nm
Band 6	: 619.620 nm
Band 7	: 664.640 nm
Band 8	: 680.902 nm
Band 9	: 708.426 nm
Band 10	: 753.472 nm
Band 11	: 761.606 nm
Band 12	: 778.498 nm
Band 13	: 864.833 nm
Band 14	: 884.849 nm
Band 15	: 899.860 nm
Bandwidth of the bands:	
Band 1	: 9.930 nm
Band 2	: 9.946 nm
Band 3	: 9.965 nm
Band 4	: 9.971 nm
Band 5	: 9.983 nm
Band 6	: 9.991 nm
Band 7	: 9.994 nm
Band 8	: 7.493 nm
Band 9	: 9.996 nm
Band 10	: 7.493 nm
Band 11	: 3.742 nm
Band 12	: 15.000 nm
Band 13	: 19.999 nm
Band 14	: 9.990 nm
Band 15	: 9.989 nm
Instantaneous Field of View	: 0.019159 deg.
Processor mode of oper. (1:Raw, 0:Full)	: 1
Offset compensation flag (1:Yes, 0:No)	: 1
Line spacing in time	: 0.043997 s.
Number of samples per output line	: 2241
Nb. of lines between along track tie pts	: 64
Nb. samples between across track tie pts	: 64
On ground spacing between columns	: 260.000 m.

DATA SET DESCRIPTOR #1:

Data Set Name	: Quality ADS
Data Set Type	: A
External Product Reference	:
DS Offset in bytes	: 11189
Total Size of DS in bytes	: 165
Number of DSRs within the DS	: 5
Length of the DSRs in bytes	: 33

DATA SET DESCRIPTOR #2:

Data Set Name	: Scaling Factor GADS
Data Set Type	: G
External Product Reference	:
DS Offset in bytes	: 11354
Total Size of DS in bytes	: 292
Number of DSRs within the DS	: 1
Length of the DSRs in bytes	: 292

DATA SET DESCRIPTOR #3:

Data Set Name	: Tie points ADS
Data Set Type	: A
External Product Reference	:
DS Offset in bytes	: 11646
Total Size of DS in bytes	: 65268
Number of DSRs within the DS	: 36
Length of the DSRs in bytes	: 1813

DATA SET DESCRIPTOR #4:

Data Set Name	:	Radiance MDS(1)
Data Set Type	:	M
External Product Reference	:	
DS Offset in bytes	:	76914
Total Size of DS in bytes	:	10073295
Number of DSRs within the DS	:	2241
Length of the DSRs in bytes	:	4495

DATA SET DESCRIPTOR #5:

Data Set Name	:	Radiance MDS(2)
Data Set Type	:	M
External Product Reference	:	
DS Offset in bytes	:	10150209
Total Size of DS in bytes	:	10073295
Number of DSRs within the DS	:	2241
Length of the DSRs in bytes	:	4495

DATA SET DESCRIPTOR #6:

Data Set Name	:	Radiance MDS(3)
Data Set Type	:	M
External Product Reference	:	
DS Offset in bytes	:	20223504
Total Size of DS in bytes	:	10073295
Number of DSRs within the DS	:	2241
Length of the DSRs in bytes	:	4495

DATA SET DESCRIPTOR #7:

Data Set Name	:	Radiance MDS(4)
Data Set Type	:	M
External Product Reference	:	
DS Offset in bytes	:	30296799
Total Size of DS in bytes	:	10073295
Number of DSRs within the DS	:	2241
Length of the DSRs in bytes	:	4495

DATA SET DESCRIPTOR #8:

Data Set Name	:	Radiance MDS(5)
Data Set Type	:	M
External Product Reference	:	
DS Offset in bytes	:	40370094
Total Size of DS in bytes	:	10073295
Number of DSRs within the DS	:	2241
Length of the DSRs in bytes	:	4495

DATA SET DESCRIPTOR #9:

Data Set Name	:	Radiance MDS(6)
Data Set Type	:	M
External Product Reference	:	
DS Offset in bytes	:	50443389
Total Size of DS in bytes	:	10073295
Number of DSRs within the DS	:	2241
Length of the DSRs in bytes	:	4495

DATA SET DESCRIPTOR #10:

Data Set Name	:	Radiance MDS(7)
Data Set Type	:	M
External Product Reference	:	
DS Offset in bytes	:	60516684
Total Size of DS in bytes	:	10073295
Number of DSRs within the DS	:	2241
Length of the DSRs in bytes	:	4495

DATA SET DESCRIPTOR #11:

Data Set Name	:	Radiance MDS(8)
Data Set Type	:	M

External Product Reference	:
DS Offset in bytes	: 70589979
Total Size of DS in bytes	: 10073295
Number of DSRs within the DS	: 2241
Length of the DSRs in bytes	: 4495

DATA SET DESCRIPTOR #12:	
Data Set Name	: Radiance MDS(9)
Data Set Type	: M
External Product Reference	:
DS Offset in bytes	: 80663274
Total Size of DS in bytes	: 10073295
Number of DSRs within the DS	: 2241
Length of the DSRs in bytes	: 4495

DATA SET DESCRIPTOR #13:	
Data Set Name	: Radiance MDS(10)
Data Set Type	: M
External Product Reference	:
DS Offset in bytes	: 90736569
Total Size of DS in bytes	: 10073295
Number of DSRs within the DS	: 2241
Length of the DSRs in bytes	: 4495

DATA SET DESCRIPTOR #14:	
Data Set Name	: Radiance MDS(11)
Data Set Type	: M
External Product Reference	:
DS Offset in bytes	: 100809864
Total Size of DS in bytes	: 10073295
Number of DSRs within the DS	: 2241
Length of the DSRs in bytes	: 4495

DATA SET DESCRIPTOR #15:	
Data Set Name	: Radiance MDS(12)
Data Set Type	: M
External Product Reference	:
DS Offset in bytes	: 110883159
Total Size of DS in bytes	: 10073295
Number of DSRs within the DS	: 2241
Length of the DSRs in bytes	: 4495

DATA SET DESCRIPTOR #16:	
Data Set Name	: Radiance MDS(13)
Data Set Type	: M
External Product Reference	:
DS Offset in bytes	: 120956454
Total Size of DS in bytes	: 10073295
Number of DSRs within the DS	: 2241
Length of the DSRs in bytes	: 4495

DATA SET DESCRIPTOR #17:	
Data Set Name	: Radiance MDS(14)
Data Set Type	: M
External Product Reference	:
DS Offset in bytes	: 131029749
Total Size of DS in bytes	: 10073295
Number of DSRs within the DS	: 2241
Length of the DSRs in bytes	: 4495

DATA SET DESCRIPTOR #18:	
Data Set Name	: Radiance MDS(15)
Data Set Type	: M
External Product Reference	:
DS Offset in bytes	: 141103044
Total Size of DS in bytes	: 10073295

Number of DSRs within the DS	:	2241
Length of the DSRs in bytes	:	4495

DATA SET DESCRIPTOR #19:

Data Set Name	:	Flags MDS(16)
Data Set Type	:	M
External Product Reference	:	
DS Offset in bytes	:	151176339
Total Size of DS in bytes	:	15095376
Number of DSRs within the DS	:	2241
Length of the DSRs in bytes	:	6736

DATA SET DESCRIPTOR #20:

Data Set Name	:	MERIS_SOURCE_PACKETS
Data Set Type	:	R
External Product Reference	:	
MER_FR_OPNPDE20030921_092217_000002582020_00079_08149_1418.N1	:	
DS Offset in bytes	:	0
Total Size of DS in bytes	:	0
Number of DSRs within the DS	:	0
Length of the DSRs in bytes	:	0

DATA SET DESCRIPTOR #21:

Data Set Name	:	INSTRUMENT_DATA_FILE
Data Set Type	:	R
External Product Reference	:	
MER_INS_AXVIEC20030620_120000_20020321_193100_20121008_190821	:	
DS Offset in bytes	:	0
Total Size of DS in bytes	:	0
Number of DSRs within the DS	:	0
Length of the DSRs in bytes	:	0

DATA SET DESCRIPTOR #22:

Data Set Name	:	PROCESSING_PARAMS_L1B_FILE
Data Set Type	:	R
External Product Reference	:	
MER_CP1_AXVIEC20030620_120000_20020429_040000_20120920_173421	:	
DS Offset in bytes	:	0
Total Size of DS in bytes	:	0
Number of DSRs within the DS	:	0
Length of the DSRs in bytes	:	0

DATA SET DESCRIPTOR #23:

Data Set Name	:	RADIOMETRIC_CALIBRATION_FILE
Data Set Type	:	R
External Product Reference	:	
MER_RAC_AXVIEC20030620_120000_20021224_121445_20121224_121445	:	
DS Offset in bytes	:	0
Total Size of DS in bytes	:	0
Number of DSRs within the DS	:	0
Length of the DSRs in bytes	:	0

DATA SET DESCRIPTOR #24:

Data Set Name	:	DIGITAL_ELEVATION_MODEL_FILE
Data Set Type	:	R
External Product Reference	:	
AUX_DEM_AXVIEC20020123_121901_20020101_000000_20200101_000000	:	
DS Offset in bytes	:	0
Total Size of DS in bytes	:	0
Number of DSRs within the DS	:	0
Length of the DSRs in bytes	:	0

DATA SET DESCRIPTOR #25:

Data Set Name	:	DIGITAL_ROUGHNESS_MODEL_FILE
Data Set Type	:	R

External Product Reference	:
MER_DRM_AXVIEC20020122_083343_20020101_000000_20200101_000000	
DS Offset in bytes	: 0
Total Size of DS in bytes	: 0
Number of DSRs within the DS	: 0
Length of the DSRs in bytes	: 0

DATA SET DESCRIPTOR #26:	:
Data Set Name	: LAND_SEA_MASK_DATA_FILE
Data Set Type	: R
External Product Reference	:
AUX_LSM_AXVIEC20020123_141228_20020101_000000_20200101_000000	
DS Offset in bytes	: 0
Total Size of DS in bytes	: 0
Number of DSRs within the DS	: 0
Length of the DSRs in bytes	: 0

DATA SET DESCRIPTOR #27:	:
Data Set Name	: ECMWF_DATA_FILE
Data Set Type	: R
External Product Reference	:
AUX_ECA_AXNECM20030921_233653_20030921_090000_20030921_210000	
DS Offset in bytes	: 0
Total Size of DS in bytes	: 0
Number of DSRs within the DS	: 0
Length of the DSRs in bytes	: 0

DATA SET DESCRIPTOR #28:	:
Data Set Name	: ORBIT_STATE_VECTOR_FILE
Data Set Type	: R
External Product Reference	:
AUX_FRO_AXVPDS20030924_101146_20030920_221000_20030923_005000	
DS Offset in bytes	: 0
Total Size of DS in bytes	: 0
Number of DSRs within the DS	: 0
Length of the DSRs in bytes	: 0

DATA SET DESCRIPTOR #29:	:
Data Set Name	: ATTITUDE_DATA_FILE
Data Set Type	: R
External Product Reference	:
AUX_ATT_AXVIEC20020924_131534_20020703_120000_20781231_235959	
DS Offset in bytes	: 0
Total Size of DS in bytes	: 0
Number of DSRs within the DS	: 0
Length of the DSRs in bytes	: 0

DATA SET #1 - "Quality ADS":	:											
No.	Date	Blank	Out of Range 1	Out of Range 2	Out of Range 3	Out of Range 4	Out of Range 5	Out R. blank 1	Out R. blank 2	Out R. blank 3	Out R. blank 4	Out R. blank 5
1	117451446.74469	0
2	117451444.240873	0
3	117451466.767337	0	1.....
4	117451489.298801	0	1.....
5	117451511.820265	0	1.....

DATA SET #2 - "Scaling Factor GADS":	:
Scaling factor - altitude	: 1.000000
Scaling factor - roughness	: 1.000000
Scaling factor - zonal wind	: 0.100000
Scaling factor - meridional wind	: 0.100000
Scaling factor - atmospheric pressure	: 0.100000
Scaling factor - ozone	: 0.010000
Scaling factor - relative humidity	: 0.100000
Radiances:	
Band 1	: 0.009333
Band 2	: 0.010466
Band 3	: 0.011501
Band 4	: 0.010642
Band 5	: 0.009280
Band 6	: 0.008147

Band 7	:	0.006815
Band 8	:	0.006899
Band 9	:	0.006270
Band 10	:	0.008617
Band 11	:	0.008811
Band 12	:	0.003613
Band 13	:	0.003546
Band 14	:	0.006090
Band 15	:	0.005418
Gain setting:		
Module #1 - Band 1	:	9
Module #1 - Band 2	:	10
Module #1 - Band 3	:	11
Module #1 - Band 4	:	11
Module #1 - Band 5	:	11
Module #1 - Band 6	:	11
Module #1 - Band 7	:	11
Module #1 - Band 8	:	10
Module #1 - Band 9	:	11
Module #1 - Band 10	:	11
Module #1 - Band 11	:	11
Module #1 - Band 12	:	10
Module #1 - Band 13	:	9
Module #1 - Band 14	:	11
Module #1 - Band 15	:	10
Module #1 - Band 16	:	0
Module #2 - Band 1	:	9
Module #2 - Band 2	:	10
Module #2 - Band 3	:	11
Module #2 - Band 4	:	11
Module #2 - Band 5	:	11
Module #2 - Band 6	:	11
Module #2 - Band 7	:	11
Module #2 - Band 8	:	10
Module #2 - Band 9	:	11
Module #2 - Band 10	:	11
Module #2 - Band 11	:	11
Module #2 - Band 12	:	10
Module #2 - Band 13	:	9
Module #2 - Band 14	:	11
Module #2 - Band 15	:	10
Module #2 - Band 16	:	0
Module #3 - Band 1	:	9
Module #3 - Band 2	:	10
Module #3 - Band 3	:	11
Module #3 - Band 4	:	11
Module #3 - Band 5	:	11
Module #3 - Band 6	:	11
Module #3 - Band 7	:	11
Module #3 - Band 8	:	10
Module #3 - Band 9	:	11
Module #3 - Band 10	:	11
Module #3 - Band 11	:	11
Module #3 - Band 12	:	10
Module #3 - Band 13	:	9
Module #3 - Band 14	:	11
Module #3 - Band 15	:	10
Module #3 - Band 16	:	0
Module #4 - Band 1	:	9
Module #4 - Band 2	:	10
Module #4 - Band 3	:	11
Module #4 - Band 4	:	11
Module #4 - Band 5	:	11
Module #4 - Band 6	:	11
Module #4 - Band 7	:	11
Module #4 - Band 8	:	10
Module #4 - Band 9	:	11
Module #4 - Band 10	:	11
Module #4 - Band 11	:	11
Module #4 - Band 12	:	10
Module #4 - Band 13	:	9
Module #4 - Band 14	:	11
Module #4 - Band 15	:	10

Module #4 - Band 16	:	0
Module #5 - Band 1	:	9
Module #5 - Band 2	:	10
Module #5 - Band 3	:	11
Module #5 - Band 4	:	11
Module #5 - Band 5	:	11
Module #5 - Band 6	:	11
Module #5 - Band 7	:	11
Module #5 - Band 8	:	10
Module #5 - Band 9	:	11
Module #5 - Band 10	:	11
Module #5 - Band 11	:	11
Module #5 - Band 12	:	10
Module #5 - Band 13	:	9
Module #5 - Band 14	:	11
Module #5 - Band 15	:	10
Module #5 - Band 16	:	0
Sampling rate	:	43997 (1.e-6 s)
Sun spectral flux:		
Band 1	:	1703.201782
Band 2	:	1859.746582
Band 3	:	1911.582886
Band 4	:	1914.315063
Band 5	:	1789.023315
Band 6	:	1637.997314
Band 7	:	1519.083252
Band 8	:	1459.818726
Band 9	:	1395.926514
Band 10	:	1255.756104
Band 11	:	1243.889160
Band 12	:	1167.314209
Band 13	:	950.546509
Band 14	:	922.478821
Band 15	:	888.092041

DATA SET #3 - "Tie points ADS":

No.	Date	FIRST (Lat., Lon.)	Alt. Rough.	Corr. Lat. Lon.	Sun (Zen., Azi.)	View (Zen., Azi.)	LAST (Lat., Lon.)	Alt. Rough.	Corr. Lat. Lon.	Sun (Zen., Azi.)	View (Zen., Azi.)		
1	117451421.714409	(45.909863, 18.014693)	98	3	0 le-6	0 le-6 (46.2, 153.6)	(0.0, 182.0)	(47.028196, 10.603496)	1476	382	-1907 le-6	-16512 le-6 (51.8, 145.0)	(40.7, 99.6)
9	117451444.240873	(44.594348, 17.519381)	591	159	0 le-6	0 le-6 (47.2, 152.5)	(0.0, 181.9)	(45.703992, 10.28711)	850	227	-1101 le-6	-9284 le-6 (50.8, 144.1)	(40.7, 99.6)
10	117451444.240873	(44.594348, 17.519381)	591	159	0 le-6	0 le-6 (47.2, 152.5)	(0.0, 181.9)	(45.703992, 10.28711)	850	227	-1101 le-6	-9284 le-6 (50.8, 144.1)	(40.7, 99.6)
25	117451489.293801	(43.958432, 16.580328)	-110	0	0 le-6	0 le-6 (46.1, 150.3)	(0.0, 181.9)	(43.053669, 9.684878)	-366	0	0 le-6	0 le-6 (48.9, 142.3)	(40.7, 99.7)
33	117451511.820265	(40.638252, 16.133722)	540	177	0 le-6	0 le-6 (44.1, 149.2)	(0.0, 181.8)	(41.727992, 9.341743)	116	23	-152 le-6	-1186 le-6 (47.9, 141.3)	(40.7, 99.7)
36	117451520.267689	(40.142832, 15.969815)	1053	209	0 le-6	0 le-6 (43.7, 148.8)	(0.0, 181.8)	(41.230654, 9.227991)	79	54	-103 le-6	-801 le-6 (47.6, 140.9)	(40.7, 99.8)

APPENDIX B - ORTHORECTIFICATION LOGS

This section contains the log of MERSYN execution when applied to MERIS FR scene MER_FR_1PNUPA20030921_092341_000000982020_00079_08149_0534.N1 of Italy.

These logs contain in particular information regarding:

- Automatic settings – Size, origin and ground sampling automatically computed by MERSYN.
- Prediction/correction loop performances – Loop convergence tracing for point (117,872) and convergence statistics,
- Runtime performances,
- Statistics on the number of processed points.

B.1 No orthorectification

```

SETTING PIXEL SIZE DEFAULT VALUES
PIXEL HEIGHT = 260.000000
PIXEL WIDTH = 260.000000

COMPUTING IMAGE SIZE AND ORIGIN
UL: X = 1025533.187500 Y = 5226455.019000
LR: X = 2002024.500000 Y = 4461188.500000
IMAGE HEIGHT = 765267.519000 metres
IMAGE WIDTH = 976491.312500 metres
LINE NUMBER = 2943
PIXEL NUMBER = 3755
LINE= 106 elapsed/line= 0 facet search: -same= 98.8% -neighbour= 1.0% -all= 0.2%
INITIALISATION: INVERSE: lonlat_origin=(0.196665,0.816031) -->
mer_xy_origin(72.692636,2028.052061) facet=(1,31) delta=(0.135822,0.688313)
LINE= 2942 elapsed/line= 0 facet search: -same= 98.7% -neighbour= 1.3% -all= 0.0%
Total elapsed time=27.700 seconds elapsed time/facet=15.630 seconds ( 56.4%)

PREDICTION/CORRECTION LOOP STATISTICS (total processed points = 7818186)
. ITERATION [ 0] = 7818186 (100.0 %)
. ITERATION [ 1] = 0 ( 0.0 %)
. ITERATION [ 2] = 0 ( 0.0 %)
. ITERATION [ 3] = 0 ( 0.0 %)
. ITERATION [ 4] = 0 ( 0.0 %)
. ITERATION [ 5] = 0 ( 0.0 %)
. ITERATION [ 6] = 0 ( 0.0 %)
. ITERATION [ 7] = 0 ( 0.0 %)
. ITERATION [ 8] = 0 ( 0.0 %)
. ITERATION [ 9] = 0 ( 0.0 %)
. ITERATION [10] = 0 ( 0.0 %)

ORTHORECTIFICATION PROCESSING = NO
NUMBER OF PROCESSED POINTS IN SEGMENT = 7815250 (70.7% of synthesis)
NUMBER OF VALIDATED POINTS IN SEGMENT = 7815250 (100.0% of segment) (70.7% of synthesis)

```

B.2 Altitudes from tie-point grid

```

SETTING PIXEL SIZE DEFAULT VALUES
PIXEL HEIGHT = 260.000000
PIXEL WIDTH = 260.000000

COMPUTING IMAGE SIZE AND ORIGIN
UL: X = 1025533.187500 Y = 5226455.019000

```

" This document discloses subject matter in which VisioTerra has proprietary rights. Recipient of this document shall not duplicate, use or disclose in whole or in part, information disclosed hereon except for or on behalf of VisioTerra to fulfil the purpose for which the document was delivered to him."

```

LR: X = 2002024.500000    Y = 4461188.500000
IMAGE HEIGHT = 765267.519000 metres
IMAGE WIDTH = 976491.312500 metres
LINE NUMBER = 2943
PIXEL NUMBER = 3755
LINE= 106 elapsed/line= 20000 facet search: -same= 88.8% -neighbour= 10.0% -all=
1.2%
INITIALISATION:           INVERSE: lonlat_origin=(0.196665,0.816031)      -->
mer_xy_origin(72.692636,2028.052061) facet=(1,31) delta=(0.135822,0.688313)

PREDICTION_CORRECTION_NUMBER=0
dem_altitude=1406.003360
    Interpolated lonlat=(0.196665,0.816031)
    Viewing zenith=0.657754 Viewing azimuth=1.747770
    dlon=-0.000245 dlat=-0.000030 meters=(-1560.593089,-191.218894)
    DIRECT: mer_xy0=(72.692636,2028.052061) --> lonlat1=(0.196910,0.816061) dlonlat=(-
0.000245,-0.000030) = (-1560.591599,-191.216959)
    INVERSE: lonlat1=(0.196910,0.816061) --> mer_xy1=(71.400363,2024.121496)
facet=(1,31) delta=(0.115631,0.626898)
    NEW FACET for corrected point (73.984910,2031.982627): iline/ipmapel_facet=(1,31)
delta_facet_xy=(0.156014,0.749729)

PREDICTION_CORRECTION_NUMBER=1
dem_altitude=1347.322220
    Interpolated lonlat=(0.196420,0.816001)
    Viewing zenith=0.658753 Viewing azimuth=1.747602
    dlon=-0.000235 dlat=-0.000029 meters=(-1498.548552,-183.444896)
    DIRECT: mer_xy0=(73.984910,2031.982627) --> lonlat1=(0.196655,0.816030)
dlonlat=(0.000010,0.000001) = (61.864355,7.774689)
    INVERSE: lonlat1=(0.196655,0.816030) --> mer_xy1=(72.744521,2028.207753)
facet=(1,31) delta=(0.136633,0.690746)
    NEW FACET for corrected point (73.933025,2031.826935): iline/ipmapel_facet=(1,31)
delta_facet_xy=(0.155204,0.747296)

PREDICTION_CORRECTION_NUMBER=2
dem_altitude=1349.637452
    Interpolated lonlat=(0.196430,0.816003)
    Viewing zenith=0.658713 Viewing azimuth=1.747609
    dlon=-0.000236 dlat=-0.000029 meters=(-1501.001059,-183.751925)
    DIRECT: mer_xy0=(73.933025,2031.826935) --> lonlat1=(0.196665,0.816031) dlonlat=(-
0.000000,-0.000000) = (-2.445607,-0.307057)
    INVERSE: lonlat1=(0.196665,0.816031) --> mer_xy1=(72.690586,2028.045906)
facet=(1,31) delta=(0.135790,0.688217)
    NEW FACET for corrected point (73.935075,2031.833090): iline/ipmapel_facet=(1,31)
delta_facet_xy=(0.155236,0.747392)
LINE= 2942 elapsed/line= 0 facet search: -same= 97.9% -neighbour= 2.1% -all=
0.0%

Total elapsed time=68.760 seconds elapsed time/facet=41.250 seconds ( 60.0%)

PREDICTION/CORRECTION LOOP STATISTICS (total processed points = 7818186)
. ITERATION [ 0 ] = 2936 ( 0.0 %)
. ITERATION [ 1 ] = 2852732 (36.5 %)
. ITERATION [ 2 ] = 4833499 (61.8 %)
. ITERATION [ 3 ] = 129019 ( 1.7 %)
. ITERATION [ 4 ] = 0 ( 0.0 %)
. ITERATION [ 5 ] = 0 ( 0.0 %)
. ITERATION [ 6 ] = 0 ( 0.0 %)
. ITERATION [ 7 ] = 0 ( 0.0 %)
. ITERATION [ 8 ] = 0 ( 0.0 %)
. ITERATION [ 9 ] = 0 ( 0.0 %)
. ITERATION [ 10 ] = 0 ( 0.0 %)

ORTHORECTIFICATION PROCESSING = YES
NUMBER OF PROCESSED POINTS IN SEGMENT = 7806229 (70.6% of synthesis)
NUMBER OF VALIDATED POINTS IN SEGMENT = 7806229 (100.0% of segment) (70.6% of
synthesis)

```

B.3 DEM Italy

```

SETTING PIXEL SIZE DEFAULT VALUES
    PIXEL HEIGHT = 260.000000
    PIXEL WIDTH   = 260.000000

COMPUTING IMAGE SIZE AND ORIGIN
    UL: X = 1025533.187500    Y = 5226455.019000
    LR: X = 2002024.500000    Y = 4461188.500000
    IMAGE HEIGHT = 765267.519000 metres
    IMAGE WIDTH  = 976491.312500 metres
    LINE NUMBER  = 2943
    PIXEL NUMBER = 3755
LINE= 106 elapsed/line= 50000 facet search: -same= 88.7% -neighbour= 10.0% -all= 1.3%
INITIALISATION:           INVERSE:          lonlat_origin=(0.196665,0.816031)      -->
mer_xy_origin(72.692636,2028.052061) facet=(1,31) delta=(0.135822,0.688313)

PREDICTION_CORRECTION_NUMBER=0
    dem_altitude=2230.704269
        Interpolated lonlat=(0.196665,0.816031)
        Viewing zenith=0.657754 Viewing azimuth=1.747770
        dlon=-0.000389 dlat=-0.000048 meters=(-2475.969664,-303.379646)
        DIRECT: mer_xy0=(72.692636,2028.052061) --> lonlat1=(0.197054,0.816079) dlonlat=(-0.000389,-0.000048) = (-2475.968174,-303.377712)
        INVERSE: lonlat1=(0.197054,0.816079) --> mer_xy1=(70.642402,2021.816213)
facet=(1,31) delta=(0.103788,0.590878)
    NEW FACET for corrected point (74.742871,2034.287910):  iline/ipmapel_facet=(1,31)
delta_facet_xy=(0.167857,0.785749)

PREDICTION_CORRECTION_NUMBER=1
    dem_altitude=2230.704269
        Interpolated lonlat=(0.196276,0.815984)
        Viewing zenith=0.659339 Viewing azimuth=1.747504
        dlon=-0.000390 dlat=-0.000048 meters=(-2484.086078,-303.922619)
        DIRECT: mer_xy0=(74.742871,2034.287910) --> lonlat1=(0.196666,0.816032) dlonlat=(-0.000001,-0.000000) = (-8.570086,-0.541638)
        INVERSE: lonlat1=(0.196666,0.816032) --> mer_xy1=(72.687253,2028.030131)
facet=(1,31) delta=(0.135738,0.687971)
    NEW FACET for corrected point (74.748255,2034.309840):  iline/ipmapel_facet=(1,31)
delta_facet_xy=(0.167941,0.786091)
LINE= 2942 elapsed/line= 0 facet search: -same= 97.9% -neighbour= 2.0% -all= 0.0%

Total elapsed time=325.960 seconds elapsed time/facet=44.140 seconds ( 13.5%)

PREDICTION/CORRECTION LOOP STATISTICS (total processed points = 7818186)
. ITERATION [ 0] = 2936 ( 0.0 %)
. ITERATION [ 1] = 3008252 (38.5 %)
. ITERATION [ 2] = 4798944 (61.4 %)
. ITERATION [ 3] = 8054 ( 0.1 %)
. ITERATION [ 4] = 0 ( 0.0 %)
. ITERATION [ 5] = 0 ( 0.0 %)
. ITERATION [ 6] = 0 ( 0.0 %)
. ITERATION [ 7] = 0 ( 0.0 %)
. ITERATION [ 8] = 0 ( 0.0 %)
. ITERATION [ 9] = 0 ( 0.0 %)
. ITERATION [10] = 0 ( 0.0 %)

ORTHORECTIFICATION PROCESSING = YES
NUMBER OF PROCESSED POINTS IN SEGMENT = 7806166 (70.6% of synthesis)
NUMBER OF VALIDATED POINTS IN SEGMENT = 7806166 (100.0% of segment) (70.6% of synthesis)

```

B.4 DEM SRTM

```

SETTING PIXEL SIZE DEFAULT VALUES
    PIXEL HEIGHT = 260.000000
    PIXEL WIDTH   = 260.000000

COMPUTING IMAGE SIZE AND ORIGIN
    UL: X = 1025533.187500      Y = 5226455.019000
    LR: X = 2002024.500000      Y = 4461188.500000
    IMAGE HEIGHT = 765267.519000 metres
    IMAGE WIDTH  = 976491.312500 metres
    LINE NUMBER  = 2943
    PIXEL NUMBER = 3755
    LINE= 106 elapsed/line= 40000 facet search: -same= 88.8% -neighbour= 9.8% -all= 1.4%
INITIALISATION:           INVERSE:          lonlat_origin=(0.196665,0.816031)      -->
mer_xy_origin(72.692636,2028.052061) facet=(1,31) delta=(0.135822,0.688313)

PREDICTION_CORRECTION_NUMBER=0
    dem_altitude=2106.815331
        Interpolated lonlat=(0.196665,0.816031)
        Viewing zenith=0.657754 Viewing azimuth=1.747770
        dlon=-0.000367 dlat=-0.000045 meters=(-2338.459168,-286.530536)
        DIRECT: mer_xy0=(72.692636,2028.052061) --> lonlat1=(0.197032,0.816076) dlonlat=(-0.000367,-0.000045) = (-2338.457677,-286.528601)
        INVERSE: lonlat1=(0.197032,0.816076) --> mer_xy1=(70.756263,2022.162509)
facet=(1,31) delta=(0.105567,0.596289)
        NEW FACET for corrected point (74.629009,2033.941614): iline/ipmapel_facet=(1,31)
delta_facet_xy=(0.166078,0.780338)

PREDICTION_CORRECTION_NUMBER=1
    dem_altitude=2106.815331
        Interpolated lonlat=(0.196298,0.815986)
        Viewing zenith=0.659251 Viewing azimuth=1.747519
        dlon=-0.000368 dlat=-0.000045 meters=(-2345.698628,-287.014884)
        DIRECT: mer_xy0=(74.629009,2033.941614) --> lonlat1=(0.196666,0.816032) dlonlat=(-0.000001,-0.000000) = (-7.644129,-0.483121)
        INVERSE: lonlat1=(0.196666,0.816032) --> mer_xy1=(72.687834,2028.032501)
facet=(1,31) delta=(0.135747,0.688008)
        NEW FACET for corrected point (74.633811,2033.961175): iline/ipmapel_facet=(1,31)
delta_facet_xy=(0.166153,0.780643)
    LINE= 2942 elapsed/line= 0 facet search: -same= 97.9% -neighbour= 2.0% -all= 0.0%

Total elapsed time=304.440 seconds elapsed time/facet=43.130 seconds ( 14.2%)

PREDICTION/CORRECTION LOOP STATISTICS (total processed points = 7818186)
. ITERATION [ 0] = 2936 ( 0.0 %)
. ITERATION [ 1] = 3034335 (38.8 %)
. ITERATION [ 2] = 4777361 (61.1 %)
. ITERATION [ 3] = 3554 ( 0.0 %)
. ITERATION [ 4] = 0 ( 0.0 %)
. ITERATION [ 5] = 0 ( 0.0 %)
. ITERATION [ 6] = 0 ( 0.0 %)
. ITERATION [ 7] = 0 ( 0.0 %)
. ITERATION [ 8] = 0 ( 0.0 %)
. ITERATION [ 9] = 0 ( 0.0 %)
. ITERATION [10] = 0 ( 0.0 %)

ORTHORECTIFICATION PROCESSING = YES
NUMBER OF PROCESSED POINTS IN SEGMENT = 7806080 (70.6% of synthesis)
NUMBER OF VALIDATED POINTS IN SEGMENT = 7806080 (100.0% of segment) (70.6% of synthesis)

```

B.5 DEM GETASSE30

```

MERSYN -mer ../scene01-04/MER_FR_1PNUPA20030921_092341_000000982020_00079_08149_0534.N1
-osy synthesis_dem-getasse.{3,5,7} -dem ../DEM_GETASSE30/EUROPA_WGS84 -sam "Nearest
neighbour" -prj "projection=Plate_carree ellipsoid=WGS_1984 datum=WGS_84" -cha 3 5 7

SETTING PIXEL SIZE DEFAULT VALUES
PIXEL HEIGHT = 260.000000
PIXEL WIDTH = 260.000000

COMPUTING IMAGE SIZE AND ORIGIN
UL: X = 1025533.187500 Y = 5226455.019000
LR: X = 2002024.500000 Y = 4461188.500000
IMAGE HEIGHT = 765267.519000 metres
IMAGE WIDTH = 976491.312500 metres
LINE NUMBER = 2943
PIXEL NUMBER = 3755
LINE= 2942 elapsed/line= 0 facet search: -same= 98.4% -neighbour= 1.5% -all= 0.0%

Total elapsed time=317.750 seconds elapsed time/facet=42.450 seconds ( 13.4%)

PREDICTION/CORRECTION LOOP STATISTICS (total processed points = 7818186)
. ITERATION [ 0] = 2936 ( 0.0 %)
. ITERATION [ 1] = 2811159 (36.0 %)
. ITERATION [ 2] = 5004091 (64.0 %)
. ITERATION [ 3] = 0 ( 0.0 %)
. ITERATION [ 4] = 0 ( 0.0 %)
. ITERATION [ 5] = 0 ( 0.0 %)
. ITERATION [ 6] = 0 ( 0.0 %)
. ITERATION [ 7] = 0 ( 0.0 %)
. ITERATION [ 8] = 0 ( 0.0 %)
. ITERATION [ 9] = 0 ( 0.0 %)
. ITERATION [10] = 0 ( 0.0 %)

ORTHORECTIFICATION PROCESSING = YES
NUMBER OF PROCESSED POINTS IN SEGMENT = 7810559 (70.7% of synthesis)
NUMBER OF VALIDATED POINTS IN SEGMENT = 7810559 (100.0% of segment) (70.7% of synthesis)

BENCHMAK POINTS
## LINE PIXEL GCP LON. GCP LAT. GCP ALT. EASTING NORTHING LONGITUDE
LATITUDE ALTITUDE VIEW.ZENITH VIEW.AZIMUTH LON.CORR. LAT.CORR. ORIGIN: LINE PIXEL
MERIS: LINE PIXEL
0 38 788 11.071550 46.939982 2864 1230413.2 5216575.0 11.071550
46.939981 2841 38.825 99.946 0.029666 -0.003551 12.362 2098.622
12.375 2107.442
1 149 968 11.492668 46.680293 2054 1277213.2 5187715.0 11.492668
46.680292 2036 36.737 100.298 0.019604 -0.002443 90.297 1957.374
90.302 1963.237
2 204 1431 12.575876 46.551618 1229 1397593.2 5173415.0 12.575875
46.551617 1424 31.672 101.089 0.011273 -0.001519 85.682 1633.586
85.684 1636.974
3 231 1792 13.420450 46.488450 1265 1491453.2 5166395.0 13.420450
46.488449 1436 27.462 101.695 0.009548 -0.001361 65.485 1383.903
65.488 1386.782
4 728 1972 13.841567 45.325698 112 1538253.2 5037175.0 13.841568
45.325697 164 23.385 102.166 0.000884 -0.000134 473.198 1158.107
473.198 1158.380
5 397 2487 15.046431 46.100086 944 1672153.2 5123235.0 15.046432
46.100085 985 18.091 102.895 0.004068 -0.000646 118.239 877.737
118.240 878.979
6 784 2745 15.650033 45.194683 230 1739233.2 5022615.0 15.650033
45.194683 252 12.812 103.431 0.000710 -0.000119 414.628 613.340
414.628 613.561
7 507 3234 16.794069 45.842737 158 1866373.2 5094635.0 16.794069
45.842736 158 7.285 104.152 0.000252 -0.000044 105.166 345.520
105.166 345.598
8 1308 2745 15.650033 43.968764 210 1739233.2 4886375.0 15.650033
43.968763 215 10.309 103.573 0.000474 -0.000082 864.013 490.957
864.013 491.107

```

9	916	3260	16.854897	44.885864	194	1873133.2	4988295.0	16.854897
44.	885863	196	4.804	104.297	0.000203	-0.000037	450.513	227.214
450.	513	227.278						
10	1303	3312	16.976553	43.980461	1551	1886653.2	4887675.0	16.976554
43.	980461	1516	2.016	104.478	0.000646	-0.000120	772.409	94.983
772.	409	95.189						
11	419	942	11.431840	46.048616	460	1270453.2	5117515.0	11.431840
46.	048616	522	36.219	100.377	0.004872	-0.000619	329.537	1926.552
329.	536	1928.026						
12	806	994	11.553496	45.143214	46	1283973.2	5016895.0	11.553496
45.	143213	47	34.585	100.619	0.000402	-0.000053	661.958	1820.076
661.	958	1820.200						
13	1247	525	10.456251	44.111476	359	1162033.2	4902235.0	10.456251
44.	111475	459	38.335	100.049	0.004474	-0.000569	1101.176	2070.374
1101.	176	2071.773						
14	1827	473	10.334595	42.754542	48	1148513.2	4751435.0	10.334594
42.	754541	48	37.390	100.208	0.000442	-0.000058	1614.970	2005.610
1614.	970	2005.751						
15	1275	1014	11.600287	44.045968	502	1289173.2	4894955.0	11.600287
44.	045968	559	33.026	100.830	0.004465	-0.000614	1068.898	1718.696
1068.	900	1720.097						
16	1827	937	11.420142	42.754541	582	1269153.2	4751435.0	11.420142
42.	754541	588	32.249	100.918	0.004465	-0.000632	1559.338	1669.616
1559.	338	1671.048						
17	1523	1529	12.805151	43.465762	510	1423073.2	4830475.0	12.805151
43.	465761	473	26.044	101.727	0.002805	-0.000423	1219.772	1304.177
1219.	772	1305.069						
18	1993	1478	12.685834	42.366178	544	1409813.2	4708275.0	12.685834
42.	366177	583	24.994	101.805	0.003241	-0.000500	1633.713	1244.989
1633.	714	1246.038						
19	2407	1761	13.347924	41.397607	646	1483393.2	4600635.0	13.347924
41.	397607	637	19.533	102.362	0.002647	-0.000435	1952.375	951.629
1952.	377	952.501						
20	2158	2096	14.131670	41.980153	919	1570493.2	4665375.0	14.131671
41.	980152	919	15.805	102.796	0.003069	-0.000518	1689.644	760.930
1689.	646	761.933						
21	2241	2869	15.940136	41.785971	617	1771473.2	4643795.0	15.940137
41.	785970	662	3.816	103.997	0.000517	-0.000096	1642.937	180.101
1642.	937	180.271						
22	2517	2328	14.674444	41.140258	243	1630813.2	4572035.0	14.674444
41.	140257	304	10.719	103.244	0.000669	-0.000119	1963.413	510.395
1963.	413	510.617						
23	2683	2843	15.879308	40.751894	756	1764713.2	4528875.0	15.879308
40.	751893	780	1.953	104.063	0.000306	-0.000058	2024.333	92.061
2024.	333	92.164						
24	944	654	10.758052	44.820357	64	1195573.2	4981015.0	10.758052
44.	820356	66	37.769	100.131	0.000634	-0.000080	821.305	2032.557
821.	305	2032.753						

APPENDIX C – MERSYN SOURCE CODE

```
/*
***** MERSYN SOURCE CODE *****

/* NAME
/* MERSYN (abbreviation "syn") adds the MERIS segment to the synthesis.
/* **** Synopsis ****
/* MERSYN [<sequence_name>] [-mer <MERIS_segment_in_input>]
/*   [-isy <input_synthesis_channel_list>]
/*   [-ivi <input_NDVI_maximum_image>]
/*   [-cav <output_synthesis_channel_list>]
/*   [-cvi <output_NDVI_maximum_image>]
/*   [-dem <input_DEM_list>]
/*   [-dm <sampling_method>]
/*   [-prj <projection>]
/*   [-cha <channel_identification>]
/*   [-ul <upper-left corner coordinates>]
/*   [-lr <lower-right corner coordinates>]
/*   [-pxh <pixel_height>]
/*   [-txw <pixel_width>]
/*   [-ort <process_orthorectification>]
/* **** Description ****
/* MERSYN merges radiances found within the MERIS segment into the various
/* bands of the synthesis provided in input. Merging is performed according to
/* an algorithm to avoid clouds and invalid values.
/* MERIS products in input of MERSYN may be any scene or segments 1B with the
/* full or reduced resolution.
/* Products in output of MERSYN are orthorectified. I.e., the parallax defect
/* due to the relief and the view angle are corrected. At each point of the
/* output synthesis, the elevation value may be interpolated from the
/* elevation data found within the "tie-point grid" or retrieved from one or
/* more DEMs given as "dem" parameter.
/* At each point of the output synthesis, the viewing angle is interpolated
/* from the values found in the "tie-point grid".
/* MERSYN may be used in three different contexts. In each one of these cases
/* the set of files in input and output differ according to different
/* parameter values.

/* USE CASE 1 - Minimum-radiance synthesis
/*
/*      lx -mer      Nx -isy      Dx -dem
/*      MERIS      input      synthesis      DEM
/*      segment      synthesis      required parameters
/*                  -sal = "Radiance minimum"
/*
/*      MERSYN
/*
/*      Nx -osy      output
/*      synthesis
/*
/* In this use case 1, the selection algorithm (parameter "-sal") has the
/* value "Radiance minimum". The N bands of the output synthesis are computed
/* from the N bands of the input synthesis in which the corresponding pixels
/* of the MERIS segment replaces the "synthesis pixel" if its radiance is
/* inferior and if the "MERIS pixel" is not flagged as corrupted.
/*
/* USE CASE 2 - Maximum-NDVI synthesis
/*
/*      lx -mer      Nx -isy      lx -ivi      Dx -dem
/*      MERIS      input      input      DEM
/*      segment      synthesis      NDVI      list
/*
/*      MERSYN
/*
/*      Nx -osy      lx -ovi      output
/*      synthesis      NDVI
/*
/* In this use case 2, the selection algorithm (parameter "-sal") has the
/* value "NDVI maximum". The N bands of the output synthesis are computed
/* from the N bands of the input synthesis in which the corresponding pixels
/* of all the N bands of the MERIS segment replaces the "synthesis pixels" of
/* the N bands if the NDVI computed from the red and NIR bands is greater
/* than the one found in the "input NDVI image".
/*
/* USE CASE 3 - Mapping
/*
/*      lx -mer      Dx -dem
/*      MERIS      DEM
/*      segment      list
/*
/*      MERSYN
/*
/*      required parameters
/*      -cha selected bands
/*      -proj output projection
/*      -ul upper-left coordinates
/*      -lr lower-right coordinates
/*      -pxh pixel height
/*      -pxw pixel width
/*
/* In this use case 3, MERSYN acts as a simple orthorectification process
/* (like MAPPER) producing N bands (parameter "-cha") of geocoded images which
/* projection ("proj"), bounding box ("ul", "lr") and pixel size ("pxh",
/* "pxw") are defined by the user and not implicitly deduced from the input
/* synthesis like in the other cases.
/*
/* The selection algorithm is assumed to have the "Radiance minimum" value.
/* This use case 3, may be used as the first step to produce a first synthesis
/* which will be iteratively upgraded like in the use cases 1 and 2.
/* Parameters "-ul" and "-lr" enables clipping a particular area of interest.

/*
***** Parameters *****
/* When no values are given by user for these parameters, the bounding box
/* will be automatically computed by MERSYN as the smallest rectangle that
/* includes the entire MERIS segment in input.
/*
/* When no values are given by user for pixel size parameters ("pxh" and
/* "pxw"), MERSYN will set these parameters to the nominal value of the FR or
/* RR products.
/*
/* Unlike the other use cases, when no synthesis is provided in input, MERSYN
/* will no check if the pixel is corrupted looking for the values found in
/* MDS(16). All the pixels of the image will be mapped.
/*
/* ----- */
/* PARAMETERS
/*
/* Input segment (<MERIS_segment_in_input>) is a Foreign file formatted in
/* Earth Explorer (ENVISAT) format. Its name should normally start with
/* "MER_RR_1P..." prefix and should have ".NI" as suffix. Decoding of its
/* Main Product Header (MHS) and Specific Product Header (SPH) will lead to
/* a long listing printed on the standard output.
/*
/* Synthesis in input includes a list of 16-bits 2D-Raster files matching the
/* various bands of the MERIS data to be processed. MERIS instrument has 15
/* bands in visible and near infrared spectra. The "channel" resource of the
/* provided channels shall be distinct and within the range [1,15].
/*
/* Synthesis images includes a background to indicate that no valid value has
/* been yet found for this pixel location.
/*
/* When the "NDVI maximum" algorithm is selected, the max. NDVI matching the
/* initialised values shall be kept and provided as <input_NDVI_maximum_image>.
/*
/* parameter. For the first time (i.e. if the synthesis does not yet include
/* any segment), this "-ivi" parameter may not be given.
/*
/* NDVI values are in the range [-1,+1] and are represented within a 16-bits
/* image within the range [1,65535] (value 0 being to represent the
/* background).
/*
/* Synthesis in output (<output_synthesis_channel_list>) contains a file list
/* matching the synthesis provided in input (same number of bands and channel
/* list). For each pixel, if the pixel is declared as valid, pixels of all the
/* bands will be updated according to the algorithm.
/*
/* The NDVI maximum image (<output_NDVI_maximum_image>) is an updated version
/* of the <input_NDVI_maximum_image> in which the pixels having a NDVI greater
/* than the one found in input (if any) will be set to the value of this
/* maximum.
/*
/* When no NDVI maximum image is provided in input, all the pixels of the
/* output NDVI image will be initialised with a background value.
/*
/* DOCUMENT
/*
/* DO-BS-MDA-GS-2009 - ENVISAT PAYLOAD DATA SEGMENT - ENVISAT-1 PRODUCTS
/*
/* SPECIFICATIONS - VOLUME 11: MERIS PRODUCTS SPECIFICATIONS - Issue 3
/*
/* Revision F - 20/11/2000 - ESA, ALCATEL SPACE
/*
/* COPYRIGHTS
/*
/* Copyrights 2003 by GREL Consultant - All rights Reserved.
/*
/* GREL Consultant Proprietary - Delivered under License Agreement.
/*
/* Copying and Disclosure Prohibited Without Express Written Permission From
/*
/* GREL Consultant.
/*
/* ADMINISTRATION
/*
/* Serge RIAZANOFF | 11.05.03 | v00.01 | Creation of the SW component
/*
/* Serge RIAZANOFF | 15.05.03 | v00.02 | Maximum NDVI option
/*
/* Serge RIAZANOFF | 29.05.03 | v00.03 | Flag is_replaced -> added_point_nu.
/*
/* Stephane MBEY | 09.08.03 | v00.04 | Checked/Adapted for FR mode
/*
/* Serge RIAZANOFF | 04.11.03 | v01.01 | Case of MAPPER behaviour
/*
/* Serge RIAZANOFF | 25.12.03 | v01.02 | Management of large files (> 2GB)
/*
/* Serge RIAZANOFF | 12.07.08 | v02.01 | Full new release
/*
/* Serge RIAZANOFF | 09.08.04 | v02.02 | Fixing of prediction/correction bugs
/*
/* Serge RIAZANOFF | 15.08.04 | v02.03 | "-ort" option added
/*
/* Serge RIAZANOFF | 07.11.04 | v02.04 | #ifdef TIM_BENCH (Generate_bench_pt)
/*
/* Serge RIAZANOFF | 03.01.05 | v02.05 | Change in dial_dion corrections
/*
/* ANSI C inclusion files
/*
/* #include <stdio.h>
/*
/* #include <stdlib.h>
/*
/* #include <string.h>
/*
/* #include <math.h>
/*
/* #include <memory.h>
/*
/* #include <errno.h>
/*
/* #ifdef TIM_PERF
/*
/* #include <time.h>
/*
/* X inclusion files are required while using TimFmt (progress bar)
/*
/* #include <X11/XIntrinsic.h>
/*
/* #include <Xm/Xm.h>
/*
/* TELMAGO inclusion files
/*
/* #define _TimNeedProcess
/*
/* #define _TimNeedFile
/*
/* #define _TimNeedFormat
/*
/* #define _TimNeedDrj
/*
/* #include <Tim.h>
/*
/* #include <TimX.h>
/*
/* Global constants (maximum 31 characters)
/*
/* Define MODULE_NAME "STATION" /* module including this process*/
/*
/* TIM_MERSYN_BREAK_DETECTION is a large maximum of the possible X-difference
/* between adjacent vertices of the segment boundary. When two successive
/* points have a difference greater than this value, a -180/+180 break is
/* assumed.
/*
/* Define TIM_MERSYN_BREAK_DETECTION (90 / 180. * TIM_PI)
/*
/* Define TIM_MERSYN_PREDICTION_CORRECTION_MAX_ITERATION 10
/*
/* Define TIM_MERSYN_SELECTION_ALGORITHM_RADIANCE_MINIMUM 0
*/


```

```

#define TIM_MERSYN_SELECTION_ALGORITHM_NDVI_MAXIMUM 1
#define TIM_MERSYN_MERIS_TYPE_FR 0
#define TIM_MERSYN_MERIS_TYPE_RR 1
#define TIM_MERSYN_PARALLELISM_THRESHOLD ((double)1.e-12)
#define TIM_MERSYN_HOT_AREA (TIM_PI-.01)
#define TIM_MERSYN_MEAN_EARTH_RADIUS 6370997.0
/* Precision expressed in part of output pixel size */
#define TIM_MERSYN_MAX_ERROR 0.1
/* Number of lines per channels (selected channels + NDVI(if any) + MDS(16)) */
/* To optimize access, many lines are kept within the buffer that is */
/* permuted modulo the number of the line to access. */
#define TIM_MERIS_BUFFER_MAX_LINE_NUMBER 1000
/* Type definitions */
/* Input parameters structure */
typedef struct {
    TimForeign mer; /* MERIS segment in input */
    Tim2DRasterList isy; /* Input synthesis channel list */
    TimRasterList ivi; /* Input NDVI maximum image */
    TimRasterList osy; /* Output synthesis channel list */
    TimRasterList ovi; /* Output NDVI maximum image */
    TimString szi; /* Selected algorithm */
    TimDEMList dem; /* Input dem list */
    TimString sams; /* Sampling method */
    TimString prj; /* Projection */
    TimIntegerList chs; /* Channel identification */
    TimVector ul; /* Output image upper left corner */
    TimVector lr; /* Output image lower right corner */
    TimFloat pxch; /* Output image pixel height */
    TimFloat pxwi; /* Output image pixel width */
    TimBoolean ort; /* Process orthorectification */
} TimMersynIp;
TimMersynIp; /* PROCESS PARAMETERS */

/* Buffer used to access and keep MERIS data */
typedef struct {
    unsigned short lineIndex [TIM_MERIS_BUFFER_MAX_LINE_NUMBER];
    unsigned short *line [TIM_MERIS_BUFFER_MAX_LINE_NUMBER];
} TimMerisBuffer;
TimMerisBuffer; /* PROCESS PARAMETERS */

/* Forward declarations */
int TimMersynComputeBoundary TIM_PROTO(
    TimForeign meris_file, /* MERIS segment in input */
    TimPrJProjection *geographic_projection, /* projection of tie-points */
    TimPrJProjection *synthesis_projection, /* output image projection */
    TimPolyVectorList *boundary_p /* envelope to be computed */
);
int TimMersynComputeLineIntersection TIM_PROTO(
    double point_0_x, /* X-coordinate of point 1 of D1 */
    double point_0_y, /* Y-coordinate of point 1 of D1 */
    double point_1_x, /* X-coordinate of point 2 of D1 */
    double point_1_y, /* Y-coordinate of point 2 of D1 */
    double point_2_x, /* X-coordinate of point 1 of D2 */
    double point_2_y, /* Y-coordinate of point 1 of D2 */
    double point_3_x, /* X-coordinate of point 2 of D2 */
    double point_3_y, /* Y-coordinate of point 2 of D2 */
    double *point_x_p, /* X-coordinate of concurrence point */
    double *point_y_p, /* Y-coordinate of concurrence point */
);
int TimMersynComputeIntersectionsWithBoundary TIM_PROTO(
    TimPolVectorList *boundary_p, /* envelope of MERIS segment */
    TimFloatList *intersection_p, /* list of intersect. segment $ line */
    int *is_inside_p, /* point is inside segment? flag */
    int *current_intersection_p /* intersection to be reached */
);
int TimMersynGetAltitudeFromPn TIM_PROTO(
    double longitude, /* X-coord of point to be processed */
    double latitude, /* Y-coord of point to be processed */
    TimPrJProjection *geographic_projection, /* projection structure */
    TimDEMList *dem_p, /* DEMs in order they have to be read */
    double *altitude_p /* altitude to be initialized */
);
int TimMersynIsInFacet TIM_PROTO(
    int iline_facet, /* line index of the UL tie-pt corner */
    int ipixel_facet, /* pixel index of the UL tie-pt corner */
    double syn_lon, /* X-coord. point in synthesis */
    double syn_lat, /* Y-coord. point in synthesis */
    double *delta_facet_x, /* line-position to compute */
    double *delta_facet_y, /* pixel-position to compute */
);
int TimMersynLocationDirect TIM_PROTO(
    double mer_x, /* X-coordinates in MERIS segment */
    double mer_y, /* Y-coordinates in MERIS segment */
    double altitude, /* Z-coordinates in MERIS segment */
    int iline_facet, /* number of the tie-point frame */
    int ipixel_facet, /* number of the tie-point column */
    double delta_facet_x, /* X-coordinates within facet [0,1] */
    double delta_facet_y, /* Y-coordinates within facet [0,1] */
    double *longitude_p, /* longitude to be computed */
    double *latitude_p /* latitude to be computed */
);
int TimMersynLocationInverse TIM_PROTO(
    double longitude, /* X-coord of point to be processed */
    double latitude, /* Y-coord of point to be processed */
    int *iline_facet_p, /* number of the tie-point frame */
    int *ipixel_facet_p, /* number of the tie-point column */
    double *delta_facet_x_p, /* X-coordinates within facet [0,1] */
    double *delta_facet_y_p, /* Y-coordinates within facet [0,1] */
    double *mer_x_p, /* X-coordinates in MERIS segment */
    double *mer_y_p, /* Y-coordinates in MERIS segment */
);

int TimMersynReadLine TIM_PROTO(
    TimForeign mer, /* MERIS segment in input */
    int iband, /* spectral band to be processed */
    int iline, /* line to be read */
    TimMerisBuffer *meris_buffer_p /* MERIS buffer to initialize */
);
/* Global variables */
int process_MERIS_flag = TIM_TRUE;
int channel_index_red = 6; /* BAND 7 in MERIS buffer list */
int channel_index_NIR = 12; /* BAND 13 in MERIS buffer list */
/* Used to monitor performance */
#ifndef TIM_PERF
clock_t current_clock; /* current clock value */
long time_line0; /* clock value of the 1st line */
long time_line; /* current clock value of the line */
long time_facet; /* clock value of facet research start */
long elapsed_time_facet; /* elapsed time of facet search / line */
int facet_search_same = 0; /* found within current */
int facet_search_neighbour = 0; /* found around current */
int facet_search_all = 0; /* search within all facets */
#endif
/* Used to print out bench points */
#ifndef TIM_BENCH
struct Tim2DCoordinates gcp; /* GCP collected in GEOREF application */
    double easting; /* synthesis horizontal coordinate */
    double northings; /* synthesis vertical coordinate */
    double longitude; /* geodetic longitude */
    double latitude; /* geodetic latitude */
    double altitude; /* interpolated altitude */
    double viewingZenith; /* latest viewing zenith */
    double viewingAzimuth; /* latest viewing azimuth */
    double longitudeCorrection; /* latest longitude correction */
    double latitudeCorrection; /* latest latitude correction */
    double meri_x0; /* X-coord in MERIS segment, 1st iter */
    double meri_y0; /* Y-coord in MERIS segment, 1st iter */
    double meri_xk; /* X-coord in MERIS segment, last iter */
    double meri_sk; /* Y-coord in MERIS segment, last iter */
} TIM_MERSYN_BENCH;
TIM_MERSYN_BENCH[] = {
{{ 38, 788, 8.19257421855421148e-01, 1.9323500789379031e-01, 2.8640e+03 }},
{{ 149, 968, 8.1472480475713269e-01, 2.00584894386977269e-01, 2.0540e+03 }},
{{ 204, 1431, 8.12479007693401e-01, 2.19490434571149489e-01, 1.2290e+03 }},
{{ 231, 1792, 8.1137652385225703e-01, 2.34213039082843873e-01, 1.2650e+03 }},
{{ 728, 1972, 7.910826620966137e-01, 2.41580924142774267e-01, 1.1200e+02 }},
{{ 397, 2487, 8.04598392212329973e-01, 2.6260976892887175e-01, 9.4400e+02 }},
{{ 784, 2745, 8.878963013428918e-01, 2.73144604332492325e-01, 2.3000e+02 }},
{{ 507, 3234, 8.001069481550877e-01, 2.9311180299720723e-01, 1.5800e+02 }},
{{ 1308, 3745, 7.6739969434324635e-01, 2.73144603481369597e-01, 2.1000e+02 }},
{{ 916, 3260, 7.8340611450320476e-01, 2.94173452210109931e-01, 1.9400e+02 }},
{{ 1303, 3312, 7.6760365932452452e-01, 2.96296753023537141e-01, 1.5510e+03 }},
{{ 419, 942, 8.036997928737817e-01, 1.99523244202737482e-01, 4.6000e+02 }},
{{ 806, 994, 7.878977113954668149574e-01, 2.01646544668149574e-01, 4.6000e+01 }},
{{ 1247, 525, 7.69890487863912787e-01, 2.82496007596055609e-01, 3.5900e+01 }},
{{ 1827, 473, 7.4620752406383874e-01, 1.803727067090750301e-01, 4.8000e+01 }},
{{ 1275, 1014, 7.6874717070871125e-01, 2.02466319669263030e-01, 5.0200e+02 }},
{{ 1827, 337, 7.4620751972464e-01, 1.9931908792183273e-01, 5.8200e+02 }},
{{ 1516, 1392, 7.586206592567303e-01, 2.2349203861500000e-01, 5.4000e+02 }},
{{ 1993, 1474, 7.39429394943063561e-01, 2.2140957072334397e-01, 5.4400e+02 }},
{{ 2007, 1761, 7.22525552646203966e-01, 2.32966784840718077e-01, 6.4000e+02 }},
{{ 2159, 2094, 7.22525552646203966e-01, 2.4471789527881e-01, 9.1900e+02 }},
{{ 2241, 2869, 7.29302781575709395e-01, 2.782078673241208e-01, 6.1700e+02 }},
{{ 2517, 2328, 7.18032956127631738e-01, 2.5611736684067871e-01, 2.4300e+02 }},
{{ 2683, 2843, 7.1125472921615366e-01, 2.77146211985425106e-01, 7.5600e+02 }},
{{ 944, 654, 7.822679806772791e-01, 1.87763426261147615e-01, 6.4000e+01 }}
};

int main()
{
    argc, argv; /* argument count */
    argc, argv; /* argument values */
    #else
    argc, argv; /* argument count */
    argc, argv; /* argument values */
    #endif
}

/* Local variables (maximum 31 characters) */
TimersynIp ip; /* input parameters structure */
TimProcess process; /* standard process structure */
TimInteger sampling_method; /* integer value of sampling method */
int selection_algorithm; /* numerical value of ip.sel */
int process_ortho; /* process orthorectification */
int meris_type; /* numerical product type (FR or RR) */
TimSensor header; /* MERIS segment header */
TimMerisBuffer *i_buf_meris[16]; /* MERIS buffer (radiances+ndvi-flag) */
TimBufferInt **i_buf_synthesisNULL; /* input buffer list for synthesis */
TimBufferInt **o_buf_synthesisNULL; /* output buffer list for synthesis */
TimBufferFloat *i_buf_ndviNULL; /* input buffer for NDVI maximum */
TimBufferFloat *o_buf_ndviNULL; /* output buffer for NDVI maximum */
TimBufferList fnt_buffer; /* list of buffers to access TimFnt */
TimFileList input_file; /* struct used to pass ip.mer */
TimPrJProjection *geographic_projectionNULL; /* projections of tie-points */
TimPrJProjection *synthesis_projectionNULL; /* output image projection */
TimPrJCoordinate pri_coordinate; /* conversion pri coordinate struct */
TimPolyVectorList boundary; /* coord. of the segment envelope(s) */
#ifndef TIM_PERF
    int prediction_correction_histol;
    TIM_MERSYN_PREDICTION_CORRECTION_MAX_ITERATION+1;
    histo; /* prediction/correction histogram */
    int point_number; /* total number of samples in histo. */
    double syn_lon_origin; /* longitude of current point in synth*/
    double syn_lat_origin; /* latitude of current point in synth*/
    double syn_lon1; /* longitude of (mer_x0,mer_y0) image */
    double syn_lat1; /* latitude of (mer_x0,mer_y0) image */
#endif
}

```

This document discloses subject matter in which VisioTerra has proprietary rights. Recipient of this document shall not duplicate, use or disclose in whole or in part, information disclosed here on except for or on behalf of VisioTerra to fulfil the purpose for which the document was delivered to him.

```

double    mer_x_origin; /* 1st antecedent X-coord */
double    mer_y_origin; /* 1st antecedent Y-coord */
double    mer_x0;      /* previous antecedent X-coord */
double    mer_y0;      /* previous antecedent Y-coord */
double    mer_x1;      /* current antecedent X-coord */
double    mer_y1;      /* current antecedent Y-coord */

int      band_number; /* number of bands in the synthesis */
int      iband;       /* index among bands in list */
int      iline;       /* index among lines in image */
int      ipixel;     /* index among columns in image */
int      iline_facet; /* line index of current tie-pt facet */
int      ipixel_facet; /* pixel index of current tie-pt facet */
int      iboundary;  /* index among boundaries in list */
int      ipoint;     /* index among points in list */
int      iline_facet_first; /* memory of last full search: line */
int      ipixel_facet_first; /* memory of last full search: pixel */
int      iline_in_buffer; /* nb of the line within MERIS buffer */
int      i;           /* convenient index */
int      iline_segment; /* NN int. of origin pixel in segment */
int      ipixel_segment; /* NN int. of origin pixel in segment */
TimFloatList intersection; /* list of intersect. segment * line */
current_intersection; /* intersection to be reached */
double   delta_facet_x; /* line-position within facet */
double   delta_facet_y; /* pixel-position within facet */
int      prediction_correction_number; /* number of iterations */
int      dem_altitude; /* local altitude of DEM from facet */
int      processed_point_number; /* stat. checked pts in segment */
TimDouble image_height; /* height of output image */
TimDouble image_width; /* height of output image */
double   x_min;       /* used to compute bounding box */
double   x_max;       /* used to compute bounding box */
double   y_min;       /* used to compute bounding box */
double   y_max;       /* used to compute bounding box */
double   x_current;  /* curr point X-coord in output proj */
double   y_current;  /* curr point Y-coord in output proj */
unsigned short flag_value; /* value of current pixel flags */
int      channel_index; /* absolute channel index: 0->15 */
int      radience_old; /* previous value of syntheses.radiance */
int      radience_new; /* new value of synthesis radiance */
int      radience_new_red; /* new value of syntheses. red radiance */
int      radience_new_NIR; /* new value of syntheses. NIR radiance */
double   ndvi_old;   /* previous value of NDVI */
double   ndvi_new;   /* new value of NDVI */
int      ndvi_min_pixel; /* min. value in NDVI file represent. */
int      ndvi_max_pixel; /* max. value in NDVI file represent. */
int      ndvi_min_value; /* min. value in external NDVI repres. */
int      ndvi_max_value; /* max. value in external NDVI repres. */
int      pixel_value; /* auxiliary variable for int. value */

int      status;        /* status returned by I/O functions */
int      is_inside;     /* point is inside segment* flag */
int      is_found;      /* facet has been found* flag */
int      done;          /* loop is completed* flag */
int      altitude_found; /* altitude has been found* flag */
int      process_pixel; /* pixel may be processed* flag */
int      is_background; /* current pixel is background* flag */
int      is_replaced;   /* at least one band replaced* flag */
int      is_first_of_line; /* Is the 1st pixel processed* flag */

/* Initialize application */
if (TimInit(&process, argc, argv, MODULE_NAME, &ip) != TIM_OK)
    TimExit (&process, TIM_PRS_ERROR);
/* Initialize files */
if (TimInitProcessing(&process, TIM_FILE_ALL) != TIM_OK)
    TimExit (&process, TIM_PRS_ERROR);
if (ip.isy.num > 0)
    band_number = ip.isy.num;
else
    band_number = ip.cha.num;
/* Check parameters */
/* Check algorithm options */
/* If (strcmp(ip.sal,"Radiance minimum") == 0)
    selection_algorithm = TIM_MERSYN_SELECTION_ALGORITHM_RADIANCE_MINIMUM;
else if (strcmp(ip.sal,"NDVI maximum") == 0)
    selection_algorithm = TIM_MERSYN_SELECTION_ALGORITHM_NDVI_MAXIMUM;
else
{
    fprintf(TimStderr, "MERSYN: Invalid \"-sal\" parameter.\n");
    TimExit (&process, TIM_PRS_PARAM);
}
/* Check synthesis files */
if (ip.isy.num > 0)
{
/* Check that all the channels have the same required resources */
for (iband=0; iband<band_number; iband++)
{
    if ((ip.isy.list[iband] > lineNumber != ip.isy.list[0] > lineNumber) ||
        (ip.isy.list[iband] > pixelNumber != ip.isy.list[0] > pixelNumber) ||
        (ip.isy.list[iband] > dataDepth != 16) ||
        (ip.isy.list[iband] > backgroundFlag != TIM_TRUE) ||
        (ip.isy.list[iband] > background != 0))
    {
        fprintf(TimStderr,
            "MERSYN: Resources of input synthesis images are not valid.\n");
        TimExit (&process, TIM_PRS_PARAM);
    }
}
for (iband=0; iband<band_number; iband++)
{
    if ((ip.osy.list[iband] > lineNumber != ip.osy.list[0] > lineNumber) ||
        (ip.osy.list[iband] > pixelNumber != ip.osy.list[0] > pixelNumber) ||
        (ip.osy.list[iband] > dataDepth != 16) ||
        (ip.osy.list[iband] > backgroundFlag != TIM_TRUE) ||
        (ip.osy.list[iband] > background != 0))
    {
        fprintf(TimStderr,
            "MERSYN: Resources of output synthesis images are not valid.\n");
        TimExit (&process, TIM_PRS_PARAM);
    }
}
/* Check that all the channels are geocoded with the same projection */
/* resources */
for (iband=0; iband<band_number; iband++)
{
    if ((ip.isy.list[iband] > projection == NULL)
        || (strncpy(ip.isy.list[iband] > projection,
                    ip.isy.list[0] > projection, ip.isy.list[0] > pixelWidth) != 0)
        || (ip.isy.list[iband] > origin.x != ip.isy.list[0] > origin.x)
        || (ip.isy.list[iband] > origin.y != ip.isy.list[0] > origin.y)
        || (ip.isy.list[iband] > pixelHeight != 0.0)
        || (ip.isy.list[iband] > pixelHeight != ip.isy.list[0] > pixelHeight)
        || (ip.isy.list[iband] > pixelWidth != 0.0)
        || (ip.isy.list[iband] > pixelWidth != ip.isy.list[0] > pixelWidth))
    {
        fprintf(TimStderr, "MERSYN: Invalid projection resources.\n");
        TimExit (&process, TIM_PRS_PARAM);
    }
}
/* Check the presence of NDVI file */
/* If (selection_algorithm == TIM_MERSYN_SELECTION_ALGORITHM_NDVI_MAXIMUM)
{
    if (ip.ovf == NULL)
    {
        fprintf(TimStderr, "MERSYN: Algorithm based on NDVI analysis => "
                "Output NDVI file is required.\n");
        TimExit (&process, TIM_PRS_PARAM);
    }
}
else
{
    if (ip.ovf != NULL)
    {
        fprintf(TimStderr,
            "MERSYN: Warning: Algorithm not based on NDVI analysis => "
            "Output NDVI file is not required.\n");
    }
}
/* Analyze the sampling method */
/* Sampling method */
if ((strcmp(ip.sam.TIM_SAMPLING_NEAREST_NEIGHOUR) == 0)
    || (strcmp(ip.sam.TIM_SAMPLING_METHOD_NEAREST_NEIGHOUR) == 0))
    sampling_method = TIM_SAMPLING_METHOD_NEAREST_NEIGHOUR;
else if ((strcmp(ip.sam.TIM_SAMPLING_BL_LINEAR) == 0)
    || (strcmp(ip.sam.TIM_SAMPLING_METHOD_BL_LINEAR) == 0))
    sampling_method = TIM_SAMPLING_METHOD_BL_LINEAR;
else if ((strcmp(ip.sam.TIM_SAMPLING_BL_CUBIC) == 0)
    || (strcmp(ip.sam.TIM_SAMPLING_METHOD_BL_CUBIC) == 0))
    sampling_method = TIM_SAMPLING_METHOD_BL_CUBIC;
else if ((strcmp(ip.sam.TIM_SAMPLING_SINC) == 0)
    || (strcmp(ip.sam.TIM_SAMPLING_METHOD_SINC) == 0))
    sampling_method = TIM_SAMPLING_METHOD_SINC;
else if ((strcmp(ip.sam.TIM_SAMPLING_MEAN) == 0)
    || (strcmp(ip.sam.TIM_SAMPLING_METHOD_MEAN) == 0))
    sampling_method = TIM_SAMPLING_METHOD_MEAN;
else
{
    fprintf (TimStderr,
        "MERSYN: Warning: Unrecognized sampling method \"%s\". "
        "Setting default one: \"Nearest neighbour\"\n", ip.sam);
    sampling_method = TIM_SAMPLING_METHOD_NEAREST_NEIGHOUR;
}
/* When input synthesis is provided, the "-prj", "-cha", "-ul", "-lr", "-pxh" */
/* nor "-pxw" parameters shall not be provided by user */
if (ip.isy.num != 0)
{
    if ((ip.prj != NULL)
        || (ip.cha.num != 0)
        || ((ip.ul.x != 0.0) || (ip.ul.y != 0.0))
        || ((ip.lr.x != 0.0) || (ip.lr.y != 0.0))
        || (ip.pch != 0.0)
        || (ip.pw != 0.0))
    {
        fprintf(TimStderr,
            "MERSYN: When the input synthesis is provided, \"-prj\", \"-cha\", "
            "-ul", "-lr", "-pxh" nor "-pxw" parameters shall be "
            "provided.\n");
        TimExit (&process, TIM_PRS_PARAM);
    }
}
/* When input synthesis is not provided, the "-prj", "-cha", "-ul", "-pxh" and */
/* "-pxw" parameters shall all be provided by user */
else
{
    /* Check that this parameters have been initialised */
    if ((ip.prj == NULL)
        || (ip.cha.num == 0))
    {
        /* Automatic setting of default values. See here after */
        ((ip.ul.x == 0.0) && (ip.ul.y == 0.0))
        || ((ip.lr.x == 0.0) && (ip.lr.y == 0.0))
        || (ip.pch == 0.0)
        || (ip.pw == 0.0)
    }
    {
        fprintf(TimStderr,
            "MERSYN: When the input synthesis is not provided, "
            "-prj", "-cha", "
            "-ul", "-lr", "-pxh" and "-pxw" "
            "parameters shall all be provided.\n");
        TimExit (&process, TIM_PRS_PARAM);
    }
}
/* Channel number must match the number of channels in output synthesis */
if (ip.cha.num != ip.osy.num)
{
    fprintf(TimStderr,
        "MERSYN: When the channel identification list is provided, "
        "its number of items (%d) shall exactly match the number of bands "
        "%(d) of the output synthesis \"-osy\".\n", ip.cha.num, ip.osy.num);
    TimExit (&process, TIM_PRS_PARAM);
}
/* Check the UL / LR coordinates */
if ((ip.ul.x > ip.lr.x)
    || (ip.ul.y < ip.lr.y))
{
    fprintf(TimStderr, "MERSYN: Inconsistent UL / LR values.\n");
    TimExit (&process, TIM_PRS_PARAM);
}
/* Check the pixel size */
if ((ip.pch < 0.0)
    || (ip.pw < 0.0))
{
    fprintf(TimStderr, "MERSYN: Invalid pixel height or width.\n");
    TimExit (&process, TIM_PRS_PARAM);
}

```

This document discloses subject matter in which VisioTerra has proprietary rights. Recipient of this document shall not duplicate, use or disclose in whole or in part, information disclosed here on except for or on behalf of VisioTerra to fulfil the purpose for which the document was delivered to him.



```

}
/* When input synthesis is not provided, the "-ivi" parameter shall not be */
/* provided */
/*
if (ip.isy.num == 0)
{
    if (ip.iv != NULL)
        fprintf(TimStderr,
            "MERSYN: When the input synthesis is not provided, \\"-ivi\\" "
            "parameter shall not be provided.\n");
    TimExit (&process,TIM_PRS_PARAM);
}
/* When input synthesis is not provided, the MDS(16) flags will not be */
/* processed */
/*
if (ip.isy.num == 0)
{
    process_MERIS_flag = TIM_FALSE;
}
/* When no orthorectification is required, no DEM shall be provided in input */
/*
if (!ip.ort)
{
    if (ip.dem.num != 0)
        fprintf(TimStderr,"MERSYN: When no orthorectification is required, "
            "no DEM shall be provided in input.\n");
    TimExit (&process,TIM_PRS_PARAM);
}
process_ortho = ip.ort;
*/
/* Read MERIS segment header */
/*
header = NULL;
fmt_buffer.num = 0;
fmt_buffer.list = NULL;
input_file.num = 1;
input_file.list = (TimRFile*)TimAlloc(NULL,1,sizeof(TimRFile));
input_file.list[0] = (TimRFile*)(ip.mer);
if ((status=TimMEnvReadHeader(&input_file,TIM_FMT_LEVEL_STANDARD,
    &fmt_buffer,TIM_FALSE,(TimRFile*)(&header))) == TIM_FMT_ERROR)
{
    fprintf(TimStderr,"MERSYN: Error while decoding \'%s\'.\n",
        ip.mer->name);
    TimExit (&process,TIM_PRS_ERROR);
}
if (status != TIM_FMT_VALID)
{
    fprintf(TimStderr,
        "MERSYN: MERIS format has not been recognized in \'%s\'.\n",
        ip.mer->name);
    TimExit (&process,TIM_PRS_ERROR);
}
*/
/* Determine the type of MERIS segment to be processed */
/*
if (strncmp(&(TIM_FMT_ENVISAT_MERIS_SPECIAL.SphDescriptor[4]),"FR",2) == 0)
    meris_type = TIM_MERSYN_MERIS_TYPE_FR;
else if (strncmp(&(TIM_FMT_ENVISAT_MERIS_SPECIAL.SphDescriptor[4]),"RR",2) == 0)
    meris_type = TIM_MERSYN_MERIS_TYPE_RR;
else
{
    fprintf(TimStderr,
        "MERSYN: Unknown MERIS type. SPH descriptor=%s.\n",
        TIM_FMT_ENVISAT_MERIS_SPECIAL.SphDescriptor);
    TimExit (&process,TIM_PRS_PARAM);
}
*/
/* Set output file resources */
/*
/* When the input synthesis is not provided, all the resources shall be set */
/* here (no heritage from "isy") */
/*
if (ip.isy.num == 0)
{
    for (iband=0; iband<ip.osy.num; iband++)
    {
        ip.osy.list[iband]->dataDepth = 16;
        ip.osy.list[iband]->backgroundFlag = TIM_TRUE;
        ip.osy.list[iband]->background = TIM_BACKGROUND;
        ip.osy.list[iband]->projection = TimStrDup(ip.prj);
    }
}
/* Pixel height */
/*
if (ip.pxh != 0.0)
{
    ip.osy.list[iband]->pixelHeight = ip.pxh;
}
else
{
    if (strstr(ip.osy.list[iband]->projection, "projection=Geographic") != NULL)
    {
        if (meris_type == TIM_MERSYN_MERIS_TYPE_RR)
        {
            ip.osy.list[iband]->pixelHeight =
                TIM_FMT_ENVISAT_MERIS_RR_PIXEL_SIZE /
                TIM_MERSYN_MEAN_EARTH_RADIUS;
        }
        else if (meris_type == TIM_MERSYN_MERIS_TYPE_FR)
        {
            ip.osy.list[iband]->pixelHeight =
                TIM_FMT_ENVISAT_MERIS_FR_PIXEL_SIZE /
                TIM_MERSYN_MEAN_EARTH_RADIUS;
        }
    }
}
*/
/* Pixel width */
/*
if (ip.pwx != 0.0)
{
    ip.osy.list[iband]->pixelWidth = ip.pwx;
}
else
{
    if (strstr(ip.osy.list[iband]->projection, "projection=Geographic") != NULL)
    {
        if (meris_type == TIM_MERSYN_MERIS_TYPE_RR)
        {
            ip.osy.list[iband]->pixelWidth =
                TIM_FMT_ENVISAT_MERIS_RR_PIXEL_SIZE /
                TIM_MERSYN_MEAN_EARTH_RADIUS;
        }
        else if (meris_type == TIM_MERSYN_MERIS_TYPE_FR)
        {
            ip.osy.list[iband]->pixelWidth =
                TIM_FMT_ENVISAT_MERIS_FR_PIXEL_SIZE /
                TIM_MERSYN_MEAN_EARTH_RADIUS;
        }
    }
}
*/
/* Loop on bands */
#endif /* TIM_DEBUG */
fprintf (TimStdout, "\nSETTING PIXEL SIZE DEFAULT VALUES\n");
fprintf (TimStdout, "    PIXEL HEIGHT = %f\n",
    ip.osy.list[0]->pixelHeight);
fprintf (TimStdout, "    PIXEL WIDTH = %f\n",
    ip.osy.list[0]->pixelWidth);
#endif /* When the input synthesis is not provided ... */
/*
/* NDVI output image */
/*
if (selection_algorithm == TIM_MERSYN_SELECTION_ALGORITHM_NDVI_MAXIMUM)
{
    ip.ovi->dataDepth = 16;
    ip.ovi->backgroundFlag = TIM_TRUE;
    ip.ovi->background = 0;
    ndvi_min_pixel = 1;
    ndvi_max_pixel = pow((double)2, (double)ip.ovi->dataDepth) - 1;
    ndvi_max_value = -1.0;
    ndvi_min_value = 1.0;
    ip.ovi->radioShift = (ndvi_min_value * ndvi_max_pixel -
        ndvi_max_value * ndvi_min_pixel) /
        (ndvi_max_pixel - ndvi_min_pixel);
    ip.ovi->radioFactor = (ndvi_max_value - ndvi_min_value) /
        (ndvi_max_pixel - ndvi_min_pixel);
}
*/
/* Allocate the geographic and output projections to process conversion */
/*
geographic_projection = NULL;
synthesis_projection = NULL;
if (TimPrjAllocProjection("projection=Geographic ellipsoid=WGS_1984 "
    "datum=WGS_84 unit=radian central_meridian=Greenwich",
    NULL,&geographic_projection) != TIM_OK)
{
    fprintf(TimStderr,"MERSYN: Cannot allocate geographic projection.\n");
    TimExit (&process,TIM_PRS_ERROR);
}
if (TimPrjAllocProjection(ip.osy.list[0]->projection,NULL,
    &synthesis_projection) != TIM_OK)
{
    fprintf(TimStderr,
        "MERSYN: Cannot allocate output synthesis projection.\n");
    TimExit (&process,TIM_PRS_ERROR);
}
*/
/* Build the segment boundary (footprint frontiers) within the projection of */
/* the synthesis image. This envelope will enable to compute the intersection */
/* of each line of the synthesis with the segment speeding up the processing. */
/*
boundary_num = 0;
boundary_list = NULL;
if (TimMersynCmpntBoundary(
    ip.mer,
    geographic_projection,
    synthesis_projection,
    &boundary) != TIM_OK)
{
    fprintf(TimStderr,
        "MERSYN: Cannot compute the segment boundary.\n");
    TimExit (&process,TIM_PRS_ERROR);
}
*/
/* When the input synthesis is not provided, the output synthesis size and */
/* origin shall be retrieved from the segment boundary list */
/*
if (ip.isy.num == 0)
{
    /*
    /* Get the minimum and maximum coordinates from all the boundary segments */
    /*
    x_min = TIM_FLT_MAX;
    x_max = -TIM_FLT_MAX;
    y_min = TIM_FLT_MAX;
    y_max = -TIM_FLT_MAX;
    for (lboundary=0; lboundary<boundary.num; lboundary++)
    {
        for (ipoint=0; ipoint<boundary.list[lboundary].num; ipoint++)
        {
            if (boundary.list[lboundary].list[ipoint].x < x_min)
                x_min = boundary.list[lboundary].list[ipoint].x;
            if (boundary.list[lboundary].list[ipoint].x > x_max)
                x_max = boundary.list[lboundary].list[ipoint].x;
            if (boundary.list[lboundary].list[ipoint].y < y_min)
                y_min = boundary.list[lboundary].list[ipoint].y;
            if (boundary.list[lboundary].list[ipoint].y > y_max)
                y_max = boundary.list[lboundary].list[ipoint].y;
        }
    }
}
*/

```

```

        y_min = boundary.list[iboundary].list[ipoint].y;
        if (boundary.list[iboundary].list[ipoint].y > y_max)
            y_max = boundary.list[iboundary].list[ipoint].y;
    }

/*-----*
 * Add a small quantity to y_max in order not to cross single upper corner */
/*-----*/
y_max = y_max + (y_max - y_min) / 10000.;

#ifndef TIM_DEBUG
    fprintf (TimStdout, "\nCOMPUTING IMAGE SIZE AND ORIGIN\n");
    fprintf (TimStdout, " UL: X = %lf Y = %lf\n", x_min,y_max);
    fprintf (TimStdout, " LR: X = %lf Y = %lf\n", x_max,y_min);
#endif

/*-----*
 * Compute the image height
 */
image_height = y_max - y_min + 1;

#ifdef TIM_DEBUG
    fprintf (TimStdout, " IMAGE HEIGHT = %lf %s\n", image_height,
            ((strchr(ip.osy.list[0])>projection,"projection=Geographic")!=NULL)?
                "metres": "degrees"));
#endif

/*-----*
 * Compute the image width
 */
image_width = x_max - x_min;

#ifndef TIM_DEBUG
    fprintf (TimStdout, " IMAGE WIDTH = %lf %s\n", image_width,
            ((strchr(ip.osy.list[0])>projection,"projection=Geographic")!=NULL)?
                "metres": "degrees"));
#endif

/*-----*
 * Set output synthesis resources
 */
for (iband=0; iband<ip.osy.num; iband++)
{
    ip.osy.list[iband]->lineNumber = image_height /
        ip.osy.list[iband]->pixelHeight;
    ip.osy.list[iband]->pixelNumber = image_width /
        ip.osy.list[iband]->pixelWidth;
    ip.osy.list[iband]->origin_x = x_min;
    ip.osy.list[iband]->origin_y = y_max;
    ip.osy.list[iband]->recordlength =
        TimComputeRecordLength((TimRFile)(ip.osy.list[iband]));
}

#ifndef TIM_DEBUG
    fprintf (TimStdout, " LINE NUMBER = %d\n", ip.osy.list[0]->lineNumber);
    fprintf (TimStdout, " PIXEL NUMBER = %d\n", ip.osy.list[0]->pixelNumber);
#endif

/*-----*
 * When the input synthesis is not provided ...
 */
/*-----*
 * Allocated buffers
 */
/*-----*
 * List of input and output synthesis buffers
 */
/*-----*
 * If (((ip.isy.num > 0) &&
 *      (i_buf_synthesis=(TimBufferInt**)TimAlloc(NULL,band_number,
 *          sizeof(TimBufferInt*)) == NULL)) ||
 *      ((o_buf_synthesis=(TimBufferInt**)TimAlloc(NULL,band_number,
 *          sizeof(TimBufferInt*)) == NULL))
 * {
    fprintf(TimStderr,
            "MERSYN: Cannot allocate input and output synthesis buffers lists.\n");
    TimExit (&process,TIM_PRS_ERROR);
}
/*-----*
 * Allocate input and output buffers for each band of the synthesis
 */
/*-----*
 * for (iband=0; iband<band_number; iband++)
 * {
    if (ip.isy.num > 0)
    {
        if ((i_buf_synthesis[iband]=(TimBufferInt*)TimAllocBufferSequential(
                (TimRFile)(ip.isy.list[iband]),TIM_DATA_TYPE_INT,1,
                TIM_EDGE_INIT_METHOD_NONE)) == NULL)
        {
            fprintf(TimStderr,
                    "MERSYN: Cannot allocate buffers of bands.\n");
            TimExit (&process,TIM_PRS_ERROR);
        }
        if ((o_buf_synthesis[iband]=(TimBufferInt*)TimAllocBufferSequential(
                (TimRFile)(ip.osy.list[iband]),TIM_DATA_TYPE_INT,1,
                TIM_EDGE_INIT_METHOD_NONE)) == NULL)
        {
            fprintf(TimStderr,
                    "MERSYN: Cannot allocate output buffer of synthesis.\n");
            TimExit (&process,TIM_PRS_ERROR);
        }
    }
/*-----*
 * Allocate buffers for each one of the 16 possible channels
 */
/*-----*
 * Buffer lines will be dynamically allocated while reading the line
 */
/*-----*
 * for (iband=0; iband<16; iband++)
 * {
    if ((i_buf_meris[iband]=(TimMerisBuffer*)TimAlloc (NULL,1,
        sizeof(TimMerisBuffer))) == NULL)
    {
        fprintf(TimStderr,
                "MERSYN: Cannot allocate input buffers for MERIS.\n");
        TimExit (&process,TIM_PRS_ERROR);
    }
    for (i=0; i<TIM_MERIS_BUFFER_MAX_LINE_NUMBER; i++)
    {
        i_buf_meris[iband]->lineIndex[i] = -1;
        i_buf_meris[iband]->line[i] = NULL;
    }
}
/*-----*
 * Input and output NDVI buffers
 */
/*-----*
 * If (((ip.ivy != NULL) &&
 *      ((i_buf_ndvi=(TimBufferFloat*)TimAllocBufferSequential(
 *          (TimRFile)(ip.ivy),TIM_DATA_TYPE_FLOAT,1,
 *          TIM_EDGE_INIT_METHOD_NONE)) == NULL)) ||
 *      ((ip.ovl != NULL) &&
 *      ((o_buf_ndvi=(TimBufferFloat*)TimAllocBufferSequential(
 *          (TimRFile)(ip.ovl),TIM_DATA_TYPE_FLOAT,1,
 *          TIM_EDGE_INIT_METHOD_NONE)) == NULL)))
{
    fprintf(TimStderr,
            "MERSYN: Cannot allocate input and/or output NDVI buffers.\n");
    TimExit (&process,TIM_PRS_ERROR);
}
/*-----*
 * Initialise the prediction/correction histogram
 */
#endif
#endif

```

This document discloses subject matter in which VisioTerra has proprietary rights. Recipient of this document shall not duplicate, use or disclose in whole or in part, information disclosed here on except for or on behalf of VisioTerra to fulfil the purpose for which the document was delivered to him.

```

        (ibench<TimNumber(TIM_MERSYN_BENCH)) ; ibench++)
    {
        if ((TIM_MERSYN_BENCH[ibench].gpx.x == iline)
            && (TIM_MERSYN_BENCH[ibench].gpx.y == ipixel))
            bench_index = ibench;
    }
#endif
    x_current = ip.osy.list[0]>origin.x +
        ipixel * ip.osy.list[0].pixelWidth;
/*=====
     Case of point inside the segment
=====*/
/*=====
 Check that geographic coordinates are valid
=====*/
prj_coordinate.x = x_current;
prj_coordinate.y = y_current;
prj_coordinate.z = 0.0;
if (TimPrjConvertCoordinate(&prj_coordinate,synthesis_projection,
    &prj_coordinate,geographic_projection) != TIM_OK)
{
    fprintf(TimStderr,
        "MERSYN: Cannot convert coordinates of current synthesis "
        "point (%lf,%lf,%lf).\n",x_current,y_current);
    TimExit (&process,TIM_PRS_ERROR);
}
syn_lon_origin = prj_coordinate.x;
syn_lat_origin = prj_coordinate.y;
#endifif TIM_BENCHH
    if (bench_index != -1)
    {
        TIM_MERSYN_BENCH[bench_index].easting = x_current;
        TIM_MERSYN_BENCH[bench_index].northing = y_current;
        TIM_MERSYN_BENCH[bench_index].longitude = syn_lon_origin;
        TIM_MERSYN_BENCH[bench_index].latitude = syn_lat_origin;
    }
#endif
    if (prj_coordinate.x != TIM_FLQAT_UNKNOWN)
{
/*=====
 PREDICTION / CORRECTION ALGORITHM - INITIALISATION
=====*/
/*=====
 For the first pixel to be processed per line, start the search
 around the facet matching the first pixel of the previous line
=====*/
/*=====
 if (is_first_of_line)
{
    iline_facet = iline_facet_first;
    ipixel_facet = ipixel_facet_first;
}
*/
/*=====
 Process the inverse location model
 Retrieve the antecedent of the point being processed
=====*/
/*=====
 if ((is_found=TimMersynLocationInverse(
    syn_lon_origin,
    syn_lat_origin,
    &line_facet,
    &ipixel_facet,
    &delta_facet_x,
    &delta_facet_y,
    &mer_x_origin,
    &mer_y_origin)) == TIM_ERROR)
{
    fprintf(TimStderr,
        "MERSYN: Cannot retrieve antecedent of (%lf,%lf).\n",
        syn_lon_origin,syn_lat_origin);
    TimExit (&process,TIM_PRS_ERROR);
}
mer_x0 = mer_x_origin;
mer_y0 = mer_y_origin;
#endifif TIM_BENCHH
    if (bench_index != -1)
    {
        TIM_MERSYN_BENCH[bench_index].merisX0 = mer_x_origin;
        TIM_MERSYN_BENCH[bench_index].merisY0 = mer_y_origin;
    }
*/
/*=====
 For the first pixel to be processed per line, keep the facet
 that has been found to prepare the processing of the first
 pixel of the next line
=====*/
/*=====
 if ((is_first_of_line) && (is_found))
{
    iline_facet_first = iline_facet;
    ipixel_facet_first = ipixel_facet;
    is_first_of_line = TIM_FALSE;
}
*/
/*=====
 PREDICTION / CORRECTION ALGORITHM - LOOP
 Scope is here to refine the inverse localisation in order to
 correct parallax effects
=====*/
/*=====
 prediction_correction_number = 0;
mer_x0 = mer_x_origin;
mer_y0 = mer_y_origin;
done = TIM_FALSE;
while ((process_ortho)
    && (is_found)
    && (!done))
{
    /*
        Increment the number of iterations
    */
    prediction_correction_number =
        prediction_correction_number + 1;
/*=====
 Get altitude at (mer_x0,mer_y0) point
=====*/
/*=====
 Get altitude from DBMs (if any)
=====*/
altitude_found = TIM_FALSE;
dem_altitude = 0.0;
if (ip.dem.num > 0)
{
    if ((altitude_found=TimMersynGetAltitudeFromDem(
        syn_lon_origin,
        syn_lat_origin,
        geographic_projection,
        &(ip.dem),
        &dem_altitude)) == TIM_ERROR)
    {
        fprintf(TimStderr,
            "MERSYN: Cannot get altitude from DEMs.\n");
        TimExit (&process,TIM_PRS_ERROR);
    }
}
*/
/*=====
 If not found, interpolate altitude from tie-points grid
=====*/
/*=====
 if (!altitude_found)
{
    dem_altitude =
        (1 - delta_facet_x) * (1 - delta_facet_y) *
        TIM_FMT_ENVISAT_MERIS_SPECIAL.tiePointLine.list[
            iline_facet].DemAltitude[ipixel_facet] +
        (1 - delta_facet_x) * delta_facet_y *
        TIM_FMT_ENVISAT_MERIS_SPECIAL.tiePointLine.list[
            iline_facet].DemAltitude[ipixel_facet+1] +
        delta_facet_x * (1 - delta_facet_y) *
        TIM_FMT_ENVISAT_MERIS_SPECIAL.tiePointLine.list[
            iline_facet+1].DemAltitude[ipixel_facet] +
        delta_facet_x * delta_facet_y *
        TIM_FMT_ENVISAT_MERIS_SPECIAL.tiePointLine.list[
            iline_facet+1].DemAltitude[ipixel_facet+1];
    dem_altitude = dem_altitude *
        TIM_FMT_ENVISAT_MERIS_SPECIAL.scalingFactorAltitude;
    altitude_found = TIM_TRUE;
}
#endifif TIM_BENCHH
    if (bench_index != -1)
    {
        TIM_MERSYN_BENCH[bench_index].altitude = dem_altitude;
    }
#endifif
/*=====
 Process the direct location applying the parallax correction
=====*/
/*=====
 if (TimMersynLocationDirect(
    mer_x0,
    mer_y0,
    dem_altitude,
    iline_facet,
    ipixel_facet,
    delta_facet_x,
    delta_facet_y,
    &syn_lon1,
    &syn_lat1) != TIM_OK)
{
    fprintf(TimStderr,
        "MERSYN: Cannot get direct image of (%lf,%lf,%lf).\n",
        mer_x0,mer_y0,dem_altitude);
    TimExit (&process,TIM_PRS_ERROR);
}
*/
/*=====
 Process the inverse location model
 Retrieve the antecedent of the point being processed
=====*/
/*=====
 if ((is_found=TimMersynLocationInverse(
    syn_lon1,
    syn_lat1,
    &iline_facet,
    &ipixel_facet,
    &delta_facet_x,
    &delta_facet_y,
    &mer_x1,
    &mer_y1)) == TIM_ERROR)
{
    fprintf(TimStderr,
        "MERSYN: Cannot retrieve antecedent for correction of (%lf,%lf).\n",
        syn_lon1,syn_lat1);
    TimExit (&process,TIM_PRS_ERROR);
}
*/
/*=====
 Process refinement of the MERIS point
=====*/
/*=====
 if ((is_found))
{
    done = TIM_TRUE;
}
else
{
    /*
        Process correction
    */
    mer_x0 = mer_x0 + (mer_x_origin - mer_x1);
    mer_y0 = mer_y0 + (mer_y_origin - mer_y1);
    /*
        Check that the corrected position stays within segment
    */
    if ((mer_x0 < 0) ||
        (mer_x0 > header->lineNumber - 1) ||
        (mer_y0 < 0) ||
        (mer_y0 > header->pixelNumber - 1))
    {
        done = TIM_TRUE;
    }
    /*
        Compute the facet coordinates matching the new point
    */
    else
    {
        iline_facet =
            (int)(mer_x0 /
                TIM_FMT_ENVISAT_MERIS_SPECIAL.linesPerTiePt);
        delta_facet_x = (mer_x0 -
            iline_facet) *
            TIM_FMT_ENVISAT_MERIS_SPECIAL.linesPerTiePt) /
            (double)(TIM_FMT_ENVISAT_MERIS_SPECIAL.linesPerTiePt);
        ipixel_facet =
            (int)(mer_y0 /
                TIM_FMT_ENVISAT_MERIS_SPECIAL.samplesPerTiePt);
        delta_facet_y = (mer_y0 -
            ipixel_facet) *
            TIM_FMT_ENVISAT_MERIS_SPECIAL.samplesPerTiePt) /
            (double)(TIM_FMT_ENVISAT_MERIS_SPECIAL.samplesPerTiePt);
    }
}
*/
/*=====
 Check prediction / correction loop termination
=====*/
/*=====
 Case of precision reached
=====*/
/*=====
 if ((fabs(mer_x_origin - mer_x1) <= TIM_MERSYN_MAX_ERROR) &&
    (fabs(mer_y_origin - mer_y1) <= TIM_MERSYN_MAX_ERROR))
{
    done = TIM_TRUE;
}
*/
/*=====
 Case of maximum iteration
=====*/
/*=====
 if (prediction_correction_number >=
    TIM_MERSYN_PREDICTION_CORRECTION_MAX_ITERATION)
{
    done = TIM_TRUE;
}
*/

```

```

        }
    } /* PREDICTION / CORRECTION ALGORITHM - LOOP */

#ifndef TIM_PERF
    prediction_correction_hist[prediction_correction_number] =
        prediction_correction_hist[prediction_correction_number] + 1;
#endif
    iline_segment = TimRound((float)mer_x0);
    ipixel_segment = TimRound((float)mer_y0);

#ifndef TIM_BENCH
    if (bench_index != -1)
    {
        TIM_MERSYN_BENCH[bench_index].merisX = mer_x0;
        TIM_MERSYN_BENCH[bench_index].merisY = mer_y0;

        /*----- Compute the (lon,lat) correction at the new MERIS location -----*/
        /*----- (mer_x0,mer_y0) assuming a null elevation -----*/
        if (TimMersynLocationDirect(
            mer_x0,
            mer_y0,
            (double)0.0,
            iline_facet,
            ipixel_facet,
            delta_facet_x,
            delta_facet_y,
            &null_elevation_longitude,
            &null_elevation_latitude) != TIM_OK)
        {
            fprintf(TimStderr,
                "MERSYN: Cannot get null elevation direct image of "
                "(%f,%f).\n",
                mer_x0,mer_y0);
            TimExit (&process,TIM_PRS_ERROR);
        }
        TIM_MERSYN_BENCH[bench_index].longitudeCorrection =
            TIM_MERSYN_BENCH[bench_index].longitude -
            null_elevation_longitude;
        TIM_MERSYN_BENCH[bench_index].latitudeCorrection =
            TIM_MERSYN_BENCH[bench_index].latitude -
            null_elevation_latitude;
    }
#endif
/*----- Check that facet has been found and that the coordinates found -----*/
/*----- are within the segment -----*/
/*----- */
if ((is_found)
    (iline_segment == 0)                                     &&
    (iline_segment < header->lineNumber)                   &&
    (ipixel_segment > 0)                                    &&
    (ipixel_segment < header->pixelNumber))
{
    process_pixel = TIM_TRUE;
    processed_point_number = processed_point_number + 1;
    iline_in_buffer = iline_segment &
        TIM_MERIS_BUFFER_MAX_LINE_NUMBER;
}

/*----- Process MERIS flag getting the measurement from the MDS(16) -----*/
/*----- */
if (process_MERIS_flag)
{
    /*----- Read value of this pixel -----*/
    if (i_buf_meris[15]->lineIndex[iline_in_buffer] != iline_segment)
    {
        if (TimMersynReadLine(ip.mer,15,iline_segment,
            i_buf_meris[15]) != TIM_OK)
        {
            fprintf (TimStderr,
                "MERSYN: Unable to get pixel flag.\n");
            TimExit (&process,TIM_PRS_ERROR);
        }
        flag_value =
            i_buf_meris[15]->line[iline_in_buffer][ipixel_segment];
        flag_value = flag_value >> 8;
    }
    /*----- Check that pixel is flagged as valid -----*/
    if (flag_value &
        (TIM_FMT_ENVISAT_QUALITY_FLAG_GLINT_RISK |
         TIM_FMT_ENVISAT_QUALITY_FLAG_BRIGHT |
         TIM_FMT_ENVISAT_QUALITY_FLAG_INVALID))
        process_pixel = TIM_FALSE;
} /* Process MERIS flags */

/*----- Case of "Maximum NDVI" algorithm -----*/
/*----- */
if ((process_pixel)
    (selection_algorithm ==
     TIM_MERSYN_SELECTION_ALGORITHM_NDVI_MAXIMUM))
{
    /*----- Get the Red value -----*/
    if (i_buf_meris[channel_index_red]->lineIndex[iline_in_buffer] != iline_segment)
    {
        if (TimMersynReadLine(ip.mer,channel_index_red,
            iline_segment,i_buf_meris[channel_index_red]) != TIM_OK)
        {
            fprintf (TimStderr,
                "MERSYN: Unable to get red pixel (%d,%d) from '%s'.\n",
                iline_segment,ipixel_segment,ip.mer->name);
            TimExit (&process,TIM_PRS_ERROR);
        }
        radiance_new_red = i_buf_meris[channel_index_red]->line[iline_in_buffer][ipixel_segment];
    }
    /*----- Get the NIR value -----*/
    if (i_buf_meris[channel_index_NIR]->lineIndex[iline_in_buffer] != iline_segment)
    {
        if (TimMersynReadLine(ip.mer,channel_index_NIR,
            iline_segment,i_buf_meris[channel_index_NIR]) != TIM_OK)
        {
            fprintf (TimStderr,
                "MERSYN: Unable to get NIR pixel (%d,%d) from '%s'.\n",
                iline_segment,ipixel_segment,ip.mer->name);
            TimExit (&process,TIM_PRS_ERROR);
        }
    }
}

radiance_new_NIR = i_buf_meris[channel_index_NIR]->line[iline_in_buffer][ipixel_segment];
/*----- Compute the new NDVI value -----*/
/*----- */
if (radiance_new_red + radiance_new_NIR == 0)
    ndvi_new = 0.0;
else
    ndvi_new = (float)(radiance_new_NIR - radiance_new_red)/
        (float)(radiance_new_NIR + radiance_new_red);

/*----- Compute the previous NDVI value checking for background -----*/
/*----- */
if (ip.ivy == NULL)
{
    is_background = TIM_TRUE;
}
else if (TimValueSequential(i_buf_ndvi,iline,ipixel) ==
        ip.ivy->background)
{
    is_background = TIM_TRUE;
}
else
{
    is_background = TIM_FALSE;
    ndvi_old = TimValueSequential(i_buf_ndvi,iline,ipixel);
}

/*----- Case of new NDVI greater than the previous one (if any) -----*/
/*----- */
if ((is_background)
    (ndvi_new > ndvi_old))
{
    /*----- Report the new values for all the bands -----*/
    for (iband=0; iband<band_number; iband++)
    {
        channel_index = ip.osy.list[iband]->channel - 1;

        /*----- When the line is not in buffer, read it -----*/
        if (i_buf_meris[channel_index]->lineIndex[iline_in_buffer] != iline_segment)
        {
            if (TimMersynReadLine(ip.mer,channel_index,
                iline_segment,i_buf_meris[channel_index]) != TIM_OK)
            {
                fprintf (TimStderr,
                    "MERSYN: Unable to get pixel (%d,%d) from '%s'.\n",
                    iline_segment,ipixel_segment,ip.mer->name);
                TimExit (&process,TIM_PRS_ERROR);
            }
        }

        /*----- Report value -----*/
        TimValueSequential(o_buf_synthetics[iband].iline,
            ipixel) = i_buf_meris[channel_index]->line[iline_in_buffer][ipixel_segment];
    } /* Report the new values for all the bands */
}

/*----- Keep this new value of the NDVI -----*/
/*----- */
TimValueSequential(o_buf_ndvi,iline,ipixel) =
    ndvi_new;
    added_point_number = added_point_number + 1;
} /* Case of new NDVI greater than the previous one */
/*----- Case of "Maximum NDVI" algorithm -----*/
/*----- */
else if ((process_pixel)
        (selection_algorithm ==
         TIM_MERSYN_SELECTION_ALGORITHM_RADIANCE_MINIMUM))
{
    /*----- Loop on radiance of each band -----*/
    /*----- */
    is_replaced = TIM_FALSE;
    for (iband=0; iband<band_number; iband++)
    {
        channel_index = ip.osy.list[iband]->channel - 1;

        /*----- When the line is not in buffer, read it -----*/
        if (i_buf_meris[channel_index]->lineIndex[iline_in_buffer] != iline_segment)
        {
            if (TimMersynReadLine(ip.mer,channel_index,
                iline_segment,i_buf_meris[channel_index]) != TIM_OK)
            {
                fprintf (TimStderr,
                    "MERSYN: Unable to get pixel (%d,%d) from '%s'.\n",
                    iline_segment,ipixel_segment,ip.mer->name);
                TimExit (&process,TIM_PRS_ERROR);
            }
        }

        /*----- Check that the new value is less than the previous one -----*/
        if (ip.osy.num > 0)
        {
            radiance_old = TimValueSequential(
                i_buf_synthetics[iband].iline,ipixel);
        }
        else
        {
            radiance_old = ip.osy.list[iband]->background;
        }
        radiance_new = i_buf_meris[channel_index]->line[iline_in_buffer][ipixel_segment];
        if ((radiance_old == ip.osy.list[iband]->background) ||
            (radiance_new < radiance_old))
        {
            /*----- Report value -----*/
            TimValueSequential(o_buf_synthetics[iband].iline,
                ipixel) = radiance_new;
            is_replaced = TIM_TRUE;
        } /* Chek that the new value is less ... */
    } /* Loop on radiance of each band */
}

/*----- When at least one band has been replaced, increment count -----*/
/*----- */
if (is_replaced)

```

```

        added_point_number = added_point_number + 1;
    } /* Case of "Minimum radiance" algorithm */
} /* Check that facet has been found */
} /* Check that geographic coordinates are valid */
} /* Case of point inside the segment */
/* When the next point is crossing the segment boundary -> invert the */
/* "is_inside" flag
while ((current_intersection < intersection.num) &&
       (intersection.list[current_intersection] <= x_current))
{
    is_inside = ! is_inside;
    current_intersection = current_intersection + 1;
}
/* LOOP ON PIXELS */
/* Write current line into output files
/* Synthesis image bands
for (iband=0; iband<band_number; iband++)
{
    if (TimWriteImageSequential((TimRFile)ip.osy.list[iband],
                               (TimBuffer*)o_buf_synthesis[iband]) != TIM_OK)
    {
        fprintf(TimStdout,
               "MERSYN: Cannot write line %d of band %d into \"%s\".\n",
               iline,iband,ip.osy.list[iband]->name);
        TimExit (&process,TIM_PRS_ERROR);
    }
}
/* NDVI maximum
if (selection_algorithm == TIM_MERSYN_SELECTION_ALGORITHM_NDVI_MAXIMUM)
{
    /* Transform scientific values into pixel values
    for (ipixel=0; ipixel<ip.osy.list[0]->pixelNumber; ipixel++)
    {
        if (TimValueSequential(o_buf_ndvi,iline,ipixel) != ip.ovi->background)
        {
            pixel_value = TimRound(
                (TimValueSequential(o_buf_ndvi,iline,ipixel) -
                 ip.ovi->radioShift) / ip.ovi->radioFactor);
            if (pixel_value < ndvi_min_pixel)
                pixel_value = ndvi_min_pixel;
            if (pixel_value > ndvi_max_pixel)
                pixel_value = ndvi_max_pixel;
            TimValueSequential(o_buf_ndvi,iline,ipixel) = pixel_value;
        }
    }
    /* Write line
    if (TimwriteImageSequential((TimRFile)ip.ovi,
                               (TimBuffer*)o_buf_ndvi) != TIM_OK)
    {
        fprintf(TimStdout,
               "MERSYN: Cannot write line %d into \"%s\".\n",
               iline,ip.ovi->name);
        TimExit (&process,TIM_PRS_ERROR);
    }
}
/* Release memory
if (intersection.list)
    TimFree(intersection.list);
intersection.list = NULL;
intersection.num = 0;
/* Print out line progress
/* */
#endifdef TIM_PRF
current_clock = clock();
fprintf(TimStdout,"LINE=%d elapsed/line=%8ld "
       "facet search: same=%5.1f% -neighbour=%5.1f% -all=%5.1f% \r",
       iline,current_clock-time_line,
       ((facet_search_same+facet_search_neighbour+facet_search_all)==0) ? 0.0 :
       facet_search_same * 100.0 /
       ((facet_search_same + facet_search_neighbour+facet_search_all)),
       ((facet_search_same+facet_search_neighbour+facet_search_all)==0) ? 0.0 :
       facet_search_neighbour * 100.0 /
       ((facet_search_same + facet_search_neighbour+facet_search_all)),
       ((facet_search_same+facet_search_neighbour+facet_search_all)==0) ? 0.0 :
       facet_search_all * 100.0 /
       ((facet_search_same + facet_search_neighbour+facet_search_all)));
time_line = current_clock;
#elseelse
    fprintf (TimStdout,"LINE=%d \r",iline);
#endif
} /* LOOP ON LINES */
/* Print out statistics
/* */
/* Retrieving of the facet from geographic coordinates
/* */
#endifdef TIM_PRF
fprintf (TimStdout,"n");
/* Convergence of the prediction/correction loop */
#endifdef TIM_PRF
fprintf (TimStdout,"n");
point_number = 0;
for (ihisto=0; ihisto<TIM_MERSYN_PREDICTION_CORRECTION_MAX_ITERATION;
     ihisto++)
{
    point_number = point_number + prediction_correction_hist[ihisto];
}

        fprintf (TimStdout,"PREDICTION/CORRECTION LOOP STATISTICS "
                  "(total processed points = %d)\n",
                  point_number,
                  for (ihisto=0; ihisto<TIM_MERSYN_PREDICTION_CORRECTION_MAX_ITERATION;
                       ihisto++)
{
    fprintf (TimStdout, " ITERATION [%2d] = %10d (%4.1f %%)\n",
            ihisto,prediction_correction_hist[ihisto],
            100.0 * prediction_correction_hist[ihisto] / (float)point_number);
}
#endifif
/* Number of processed and validated points
*/
/* */
fprintf (TimStdout,"n");
if (process_ortho)
    fprintf (TimStdout, "ORTHORECTIFICATION PROCESSING = YES \n");
else
    fprintf (TimStdout, "ORTHORECTIFICATION PROCESSING = NO \n");
fprintf (TimStdout, "NUMBER OF PROCESSED POINTS IN SEGMENT = %d "
        " (%.1f%% of synthesis)\n",
        processed_point_number,
        100.*processed_point_number/
        (ip.osy.list[0]->lineNumber*ip.osy.list[0]->pixelNumber));
fprintf (TimStdout, "NUMBER OF VALIDATED POINTS IN SEGMENT = %d "
        " (%.1f%% of segment) (%.1f%% of synthesis)\n",
        added_point_number,
        (processed_point_number==0)?100.*added_point_number/
        processed_point_number,
        100.*added_point_number/
        (ip.osy.list[0]->lineNumber*ip.osy.list[0]->pixelNumber));
/* */
/* Benchmark points
*/
#endifdef TIM_BENCH
fprintf (TimStdout, "\nBENCHMARK POINTS\n");
fprintf (TimStdout, "# LINE PIXEL GCP LON. GCP LAT. GCP ALT. "
        "EASTING NORTING LONGITUDE LATITUDE ALTITUDE "
        "VIEW_ZENITH VIEW_AZIMUTH LON_CORR. LAT_CORR. "
        "ORIGIN LINE_PIXEL MERIS LINE_PIXEL\n");
for (ibench=0; ibench<TimNumber(TIM_MERSYN_BENCH); ibench++)
{
    fprintf (TimStdout, "$2.4f $4.0f $12.6lf $12.6lf $4.0lf "
            "$11.1lf $11.1lf $12.6lf $12.6lf $4.0lf "
            "$8.3lf $8.3lf $9.6lf $9.6lf "
            "$8.3lf $8.3lf $8.3lf $8.3lf\n",
            ibench,
            TIM_MERSYN_BENCH[ibench].gcp_x,
            TIM_MERSYN_BENCH[ibench].gcp_y,
            TIM_MERSYN_BENCH[ibench].gcp_longitude*180/TIM_PI,
            TIM_MERSYN_BENCH[ibench].gcp_latitude*180/TIM_PI,
            TIM_MERSYN_BENCH[ibench].gcp_altitude,
            TIM_MERSYN_BENCH[ibench].eastng,
            TIM_MERSYN_BENCH[ibench].nortng,
            TIM_MERSYN_BENCH[ibench].longitude*180/TIM_PI,
            TIM_MERSYN_BENCH[ibench].latitude*180/TIM_PI,
            TIM_MERSYN_BENCH[ibench].altitude,
            TIM_MERSYN_BENCH[ibench].viewingZenith*180/TIM_PI,
            TIM_MERSYN_BENCH[ibench].viewingAzimuth*180/TIM_PI,
            TIM_MERSYN_BENCH[ibench].longitudeCorrection*180/TIM_PI,
            TIM_MERSYN_BENCH[ibench].latitudeCorrection*180/TIM_PI,
            TIM_MERSYN_BENCH[ibench].merisX0,
            TIM_MERSYN_BENCH[ibench].merisY0,
            TIM_MERSYN_BENCH[ibench].merisX,
            TIM_MERSYN_BENCH[ibench].merisY);
}
#endifif
/* */
/* Release projection structures
*/
/* */
if (geographic_projection)
    TimPrjFreeProjection (geographic_projection);
geographic_projection = NULL;
if (synthesis_projection)
    TimPrjFreeProjection (synthesis_projection);
synthesis_projection = NULL;
/* */
/* Close files
*/
buf[0] = '\0';
sprintf (buf, "%f,ORTHORECTIFICATION: %s SEGMENT POINTS: PROCESSED=%d ADDED=%d",
         (process_ortho)?YES:"NO",processed_point_number,added_point_number);
if (TimExitProcessing (&process,TIM_FILE_ALL,buf) != TIM_OK)
    TimExit (&process,TIM_PRS_ERROR);
/* */
/* Return
*/
TimExit (&process,TIM_PRS_OK);
} /* end of MERSYN process */

/*
* TimMersynIsInFacet retrieves the coordinates of the synthesis point inside
* the facet specified in input. These coordinates are relative to the facet
* and are in the range [0,1] each one. These values will be used as weight
* for further interpolation within the facet (parameters p and q in MERIS
* documentation volume II).
*/
/*
*          (iline_facet,ipixel_facet)
*          ^ O-----+
*          |           |
*          delta_facet_x | (syn_lon,syn_lat) |
*          |           |           |
*          v           +-----+
*          delta_facet_y
*/
/*
* TimMersynIsInFacet returns TIM_TRUE if the point falls inside the facet,
* TIM_FALSE if not and TIM_ERROR when an error occurs.
*/
int TimMersynIsInFacet
#endifdef TIM_ANSI_PROTOYPE
{
    int             iline_facet,           /* line index of the UL tie-pt corner */
                    ipixel_facet,          /* pixel index of the UL tie-pt corner */
                    double            syn_lon,           /* X-coord. point in synthesis */
                    double            syn_lat,           /* Y-coord. point in synthesis */
                    double            *delta_facet_x,      /* line-position to compute */
                    double            *delta_facet_y;      /* pixel-position to compute */
}
#endifelse
    (iline_facet,ipixel_facet,syn_lon,syn_lat,
     delta_facet_x,delta_facet_y)
    int             iline_facet;           /* line index of the UL tie-pt corner */
    int             ipixel_facet;          /* pixel index of the UL tie-pt corner */
    double            syn_lon;           /* X-coord. point in synthesis */
    double            syn_lat;           /* Y-coord. point in synthesis */
    double            *delta_facet_x,      /* line-position to compute */
    double            *delta_facet_y;      /* pixel-position to compute */
}
#endif

```

```

double      syn_lon;
double      syn_lat;
double      delta_facet_x;
double      delta_facet_y;
#endif
{
/* Local variables */
TimRDoubleVector facet[5]; /* list of facet vertices */
int         intersection_number; /* number of intersections found */
double      intersection_list[2]; /* list of intersection X-coordinates */
int         ivertex; /* current X-coord. of intersection */
int         inter_point1_x; /* intersection point X-coordinate */
double      inter_point1_y; /* intersection point Y-coordinate */
int         inter_point2_x; /* along edge intersect_point X-coord.*/
double      inter_point2_y; /* along edge intersect_point Y-coord.*/

/* Check that facet is included within the tie-point matrix */
if ((iline_facet < 0)
    || (iline_facet >= TIM_FMT_ENVISAT_MERIS_SPECIAL.tiePointLine.num - 1)
    || (ipixel_facet < 0)
    || (ipixel_facet >= TIM_FMT_ENVISAT_MERIS_SPECIAL.tiePointNumber - 1))
    return (TIM_FALSE);

/* Report coordinates found in the tie-point matrix */
facet[0].x = TIM_FMT_ENVISAT_MERIS_SPECIAL.tiePointLine.list[iline_facet].longitude[ipixel_facet];
facet[0].y = TIM_FMT_ENVISAT_MERIS_SPECIAL.tiePointLine.list[iline_facet].latitude[ipixel_facet];
facet[1].x = TIM_FMT_ENVISAT_MERIS_SPECIAL.tiePointLine.list[iline_facet].longitude[ipixel_facet+1];
facet[1].y = TIM_FMT_ENVISAT_MERIS_SPECIAL.tiePointLine.list[iline_facet].latitude[ipixel_facet+1];
facet[2].x = TIM_FMT_ENVISAT_MERIS_SPECIAL.tiePointLine.list[iline_facet+1].longitude[ipixel_facet+1];
facet[2].y = TIM_FMT_ENVISAT_MERIS_SPECIAL.tiePointLine.list[iline_facet+1].latitude[ipixel_facet+1];
facet[3].x = TIM_FMT_ENVISAT_MERIS_SPECIAL.tiePointLine.list[iline_facet+1].longitude[ipixel_facet];
facet[3].y = TIM_FMT_ENVISAT_MERIS_SPECIAL.tiePointLine.list[iline_facet+1].latitude[ipixel_facet];

/* Correct the possible overlap of the facet on the -180 / +180 frontier */
/* Case of at least one point located on the +180 degrees East frontier */
if( (facet[0].x > TIM_MERSYN_HOT_AREA)
    || (facet[1].x > TIM_MERSYN_HOT_AREA)
    || (facet[2].x > TIM_MERSYN_HOT_AREA)
    || (facet[3].x > TIM_MERSYN_HOT_AREA) )
{
    if( (facet[0].x<0)
        || (facet[1].x<0)
        || (facet[2].x<0)
        || (facet[3].x<0) )
    {
        if (syn_lon<0)
        {
            if (facet[0].x>0)
                facet[0].x-=2*TIM_PI;
            if (facet[1].x>0)
                facet[1].x-=2*TIM_PI;
            if (facet[2].x>0)
                facet[2].x-=2*TIM_PI;
            if (facet[3].x>0)
                facet[3].x-=2*TIM_PI;
        }
        else
        {
            if (facet[0].x<0)
                facet[0].x+=2*TIM_PI;
            if (facet[1].x<0)
                facet[1].x+=2*TIM_PI;
            if (facet[2].x<0)
                facet[2].x+=2*TIM_PI;
            if (facet[3].x<0)
                facet[3].x+=2*TIM_PI;
        }
    }
}
/* Case of at least one point located on the -180 degrees West frontier */
else
if( (facet[0].x < -TIM_MERSYN_HOT_AREA)
    || (facet[1].x < -TIM_MERSYN_HOT_AREA)
    || (facet[2].x < -TIM_MERSYN_HOT_AREA)
    || (facet[3].x < -TIM_MERSYN_HOT_AREA) )
{
    if( (facet[0].x>0)
        || (facet[1].x>0)
        || (facet[2].x>0)
        || (facet[3].x>0) )
    {
        if (syn_lon<0)
        {
            if (facet[0].x>0)
                facet[0].x-=2*TIM_PI;
            if (facet[1].x>0)
                facet[1].x-=2*TIM_PI;
            if (facet[2].x>0)
                facet[2].x-=2*TIM_PI;
            if (facet[3].x>0)
                facet[3].x-=2*TIM_PI;
        }
        else
        {
            if (facet[0].x<0)
                facet[0].x+=2*TIM_PI;
            if (facet[1].x<0)
                facet[1].x+=2*TIM_PI;
            if (facet[2].x<0)
                facet[2].x+=2*TIM_PI;
            if (facet[3].x<0)
                facet[3].x+=2*TIM_PI;
        }
    }
}

/* Close the polygon duplicating the first point append */
facet[4].x = facet[0].x;
facet[4].y = facet[0].y;

/* Compute the intersection of the horizontal passing through the synthesis */
/* point with each one of the four segments */
intersection_number = 0;
for (ivertex = 0; (intersection_number < 2) && (ivertex<4); ivertex++)
{
    if (!((TimDEqual(facet[ivertex].y,facet[ivertex+1].y,(double)1e-8)))
    {
        x_intersection = facet[ivertex].x +
                        (facet[ivertex+1].x - facet[ivertex].x) *
                        (syn_lat - facet[ivertex].y) /
                        (facet[ivertex+1].y - facet[ivertex].y);
    }
    /* Check that intersection point is within the vertex segment */
    if (facet[ivertex].x <= facet[ivertex+1].x)
    {
        if ((facet[ivertex].x <= x_intersection) &&
            (x_intersection < facet[ivertex+1].x))
        {
            intersection_list[intersection_number] = x_intersection;
            intersection_number = intersection_number + 1;
        }
    }
    else
    {
        if ((facet[ivertex].x >= x_intersection) &&
            (x_intersection > facet[ivertex+1].x))
        {
            intersection_list[intersection_number] = x_intersection;
            intersection_number = intersection_number + 1;
        }
    }
}

/* Check that the synthesis point is between the two intersections */
if (intersection_number != 2)
    return (TIM_FALSE);
if (intersection_list[0] <= intersection_list[1])
{
    if ((syn_lon < intersection_list[0])
        || (syn_lon > intersection_list[1]))
        return (TIM_FALSE);
}
else
{
    if ((syn_lon > intersection_list[0])
        || (syn_lon < intersection_list[1]))
        return (TIM_FALSE);
}

/* Compute the delta_facet_x delta_facet_y weights */
/* The solution solves the system:
   syn_lon = (1 - delta_facet_x).(1 - delta_facet_y).facet[0].x +
             + (1 - delta_facet_x). (1 - delta_facet_y).facet[3].x *
             + (1 - delta_facet_x).delta_facet_y .facet[1].x /
             + delta_facet_x .delta_facet_y .facet[2].x */

/* syn_lat = (1 - delta_facet_x).(1 - delta_facet_y).facet[0].y +
             + (1 - delta_facet_x). (1 - delta_facet_y).facet[3].y *
             + (1 - delta_facet_x).delta_facet_y .facet[1].y /
             + delta_facet_x .delta_facet_y .facet[2].y */

/* Compute delta_facet_y */
/* Check if (S0S3) and (S1S2) are not parallel */
if (fabs((facet[0].x - facet[3].x) * (facet[1].y - facet[2].y) -
          (facet[0].y - facet[3].y) * (facet[1].x - facet[2].x)) >
    TIM_MERSYN_PARALLELISM_THRESHOLD)
{
    /* Compute intersection II between (S0S3) and (S1S2) */
    TimMersynComputeLineIntersection (facet[0].x,facet[0].y,facet[3].x,
                                      facet[1].y,facet[1].x,facet[3].y,
                                      &inter_point1_x,&inter_point1_y);
    /* Compute intersection II between (S0S1) and (IIS) */
    TimMersynComputeLineIntersection (facet[0].x,facet[0].y,facet[1].x,
                                      facet[1].y,syn_lon,syn_lat,
                                      &inter_point2_x,&inter_point2_y);
}
/* Case of parallel edges */
else
{
    /* Compute intersection II between (S0S1) and the parallel to (S0S3) */
    TimMersynComputeLineIntersection (facet[0].x,facet[0].y,facet[1].x,
                                      facet[1].y,syn_lon,syn_lat,
                                      syn_lat + facet[0].y - facet[3].y,
                                      &inter_point2_x,&inter_point2_y);
}
/* Compute delta_facet_y */
delta_facet_y = TimEuclidianDistance(inter_point2_x,inter_point2_y,facet[0].x,facet[0].y) /
                TimEuclidianDistance(facet[0].x,facet[0].y,facet[1].x,facet[1].y);

/* Compute delta_facet_x */
/* Check if (S0S1) and (S2S3) are not parallel */
if (fabs((facet[0].x - facet[1].x) * (facet[2].y - facet[3].y) -
          (facet[0].y - facet[1].y) * (facet[2].x - facet[3].x)) >
    TIM_MERSYN_PARALLELISM_THRESHOLD)
{
    /* Compute intersection II between (S0S1) and (S2S3) */
    TimMersynComputeLineIntersection (facet[0].x,facet[0].y,facet[1].x,
                                      facet[1].y,facet[2].x,facet[3].y,
                                      &inter_point1_x,&inter_point1_y);
    /* Compute intersection II between (S0S3) and (IIS) */
    TimMersynComputeLineIntersection (facet[0].x,facet[0].y,facet[3].x,
                                      facet[1].y,syn_lon,syn_lat,
                                      &inter_point2_x,&inter_point2_y);
}

```

```

}

/* Case of parallel edges
*/
else
{
    /* Compute intersection II between (S0S3) and the parallel to (S0S1)
     * passing through S
    */
    /* TimMersynComputeLineIntersection(facet[0].x,facet[0].y,facet[3].x,
     * facet[3].y,
     * syn_lon,syn_lat,
     * syn_lat-facet[0].x-facet[1].x,
     * syn_lat-facet[0].y-facet[1].y,
     * &inter_point2_x,&inter_point2_y);
    */

    /* Compute delta_facet_x
    */
    *delta_facet_x =
        TimEuclideanDistance(inter_point2_x,inter_point2_y,facet[0].x,facet[0].y);
    TimEuclideanDistance(facet[0].x,facet[0].y,facet[3].x,facet[3].y);
    /* Return "Found" status
    */
    /* TimMersynIsInFacet */
    return (TIM_TRUE);
} /* TimMersynIsInFacet */

*****+
/* TimMersynComputeLineIntersection computes the location of the concurrence
 * point of two lines defined each one by a couple of points given as
 * parameters
*/
*****+
int TimMersynComputeLineIntersection
#ifndef TIM_ANSI_PROTOYPE
(
    double point0_x,           /* X-coordinate of point 1 of D1 */
    double point0_y,           /* Y-coordinate of point 1 of D1 */
    double point1_x,           /* X-coordinate of point 2 of D1 */
    double point1_y,           /* Y-coordinate of point 2 of D1 */
    double point2_x,           /* X-coordinate of point 1 of D2 */
    double point2_y,           /* Y-coordinate of point 1 of D2 */
    double point3_x,           /* X-coordinate of point 2 of D2 */
    double point3_y,           /* Y-coordinate of point 2 of D2 */
    double *point_x_p,          /* X-coordinate of concurrence point */
    double *point_y_p,          /* Y-coordinate of concurrence point */
)
#else
(point0_x,point0_y,point1_x,point1_y,point2_x,point2_y,point3_x,point3_y,
 point_x_p,point_y_p)
    double point0_x;           /* X-coordinate of point 1 of D1 */
    double point0_y;           /* Y-coordinate of point 1 of D1 */
    double point1_x;           /* X-coordinate of point 2 of D1 */
    double point1_y;           /* Y-coordinate of point 2 of D1 */
    double point2_x;           /* X-coordinate of point 1 of D2 */
    double point2_y;           /* Y-coordinate of point 1 of D2 */
    double point3_x;           /* X-coordinate of point 2 of D2 */
    double point3_y;           /* Y-coordinate of point 2 of D2 */
    double *point_x_p;          /* X-coordinate of concurrence point */
    double *point_y_p;          /* Y-coordinate of concurrence point */
#endif
{
    /* Local variables
    */
    double scalar_product;      /* (point0_x,point1_x) . (point2_x,point3_x) */

    /* Compute and check scalar product
    */
    scalar_product = (point0_x - point1_x) * (point3_y - point2_y) -
        (point2_x - point3_x) * (point1_y - point0_y);
    if (TimDEqual(scalar_product,(double)0.0,(double)1.e-12))
    {
        fprintf (TimStderr,"TimMersynComputeLineIntersection: "
            "'Lines [%lf,%lf] (%lf,%lf) (%lf,%lf) are parallel.\n",
            point0_x,point0_y,point1_x,point1_y,point2_x,point2_y,point3_x,point3_y);
        return (TIM_ERROR);
    }
    /* Compute coordinates
    */
    *point_y_p = ((point0_x * (point1_y - point0_y)) +
        point0_y * (point0_x - point1_x)) * (point3_y - point2_y) -
        (point2_x * (point3_y - point2_y)) +
        point2_y * (point2_x - point3_x)) * (point1_y - point0_y));
    scalar_product;

    *point_x_p = ((point0_x * (point1_y - point0_y)) +
        point0_y * (point0_x - point1_x)) / (point1_y - point0_y);

    /* Return "Ok" status
    */
    /* TimMersynReadLine */
    return (TIM_OK);
} /* TimMersynComputeLineIntersection */

*****+
/* TimMersynReadLine reads the specified line and store the result into the
 * provided buffer.
*/
*****+
int TimMersynReadLine
#ifndef TIM_ANSI_PROTOYPE
(
    TimForeign      mer,           /* MERIS segment in input */
    int             iband,         /* band to be processed (0:first) */
    int             iline,          /* line to be read */
    TimMerisBuffer *meris_buffer_p /* MERIS buffer to initialize */
)
#else
(mer,iband,iline,meris_buffer_p)
TimRForeign      mer;
int             iband;
int             iline;
TimMerisBuffer *meris_buffer_p;
#endif
{
    /* Local variables
    */
    int record_length;           /* input record length=2*pixelNumber */
    off64_t offset;              /* start of data in target file */
    int iline_in_buffer;          /* nb of the line within MERIS buffer */
    int ipixel;                  /* loop among pixels in line buffer */
    int status;                  /* status of I/O functions */
}

```

" This document discloses subject matter in which VisioTerra has proprietary rights. Recipient of this document shall not duplicate, use or disclose in whole or in part, information disclosed here on except for or on behalf of VisioTerra to fulfil the purpose for which the document was delivered to him."

```

{
    fprintf(TimStderr, "TimMersynComputeBoundary: "
           "Cannot allocate the boundary list of %d vertices.\n",
           boundary_p->list[0].num);
    return (TIM_ERROR);
}

/* Initialise the list of vertices of the segment boundary from the points */
/* around the tie-point matrix */
/*-----*/
for (ipoint=0; ipoint<boundary_p->list[0].num; ipoint++)
{
    /* Determine the edge being processed */
    /*-----*/
    /* Case of left vertical border (top to bottom) */
    /*-----*/
    if (ipoint < TIM_FMT_ENVISAT_MERIS_SPECIAL.tiePointLine.num - 1)
    {
        iline = ipoint;
        ipixel = 0;
    }
    /* Case of last line (left to right) */
    /*-----*/
    else if (ipoint < TIM_FMT_ENVISAT_MERIS_SPECIAL.tiePointLine.num - 1 +
             TIM_FMT_ENVISAT_MERIS_SPECIAL.tiePointNumber - 1)
    {
        iline = TIM_FMT_ENVISAT_MERIS_SPECIAL.tiePointLine.num - 1;
        ipixel = ipoint - TIM_FMT_ENVISAT_MERIS_SPECIAL.tiePointLine.num + 1;
    }
    /* Case of last vertical border (bottom to top) */
    /*-----*/
    else if (ipoint < TIM_FMT_ENVISAT_MERIS_SPECIAL.tiePointLine.num - 1 +
             TIM_FMT_ENVISAT_MERIS_SPECIAL.tiePointNumber - 1 +
             TIM_FMT_ENVISAT_MERIS_SPECIAL.tiePointLine.num - 1)
    {
        iline = TIM_FMT_ENVISAT_MERIS_SPECIAL.tiePointLine.num - 1 -
                (ipoint -
                 TIM_FMT_ENVISAT_MERIS_SPECIAL.tiePointLine.num + 1 -
                 TIM_FMT_ENVISAT_MERIS_SPECIAL.tiePointNumber + 1);
        ipixel = TIM_FMT_ENVISAT_MERIS_SPECIAL.tiePointNumber - 1;
    }
    /* Case of first line (right to left) */
    /*-----*/
    else
    {
        iline = 0;
        ipixel = TIM_FMT_ENVISAT_MERIS_SPECIAL.tiePointNumber - 1 -
                 (ipoint -
                  TIM_FMT_ENVISAT_MERIS_SPECIAL.tiePointLine.num + 1 -
                  TIM_FMT_ENVISAT_MERIS_SPECIAL.tiePointNumber + 1 -
                  TIM_FMT_ENVISAT_MERIS_SPECIAL.tiePointLine.num + 1);
    }
    /* Report tie-point values */
    /*-----*/
    boundary_p->list[0].list[ipoint].x =
        TIM_FMT_ENVISAT_MERIS_SPECIAL.tiePointLine.list[iline].longitude(ipixel);
    boundary_p->list[0].list[ipoint].y =
        TIM_FMT_ENVISAT_MERIS_SPECIAL.tiePointLine.list[iline].latitude(ipixel);
} /* Initialise the list of vertices of the segment boundary */

/* Detect the breaks -180 / +180 degrees */
/*-----*/
iboundary = 0;
ifoward = 0;
ibackward = boundary_p->list[iboundary].num - 1;
while (ifoward < ibackward)
{
    /* Case of -180 / +180 break */
    /*-----*/
    if (fabs((double)(boundary_p->list[iboundary].list[ifoward+1].x -
                      boundary_p->list[iboundary].list[ifoward].x)) >
        TIM_MERSYN_BREAK_DETECTION)
    {
        /* Look for the other break from the end of the current list */
        /*-----*/
        while (fabs((double)(boundary_p->list[iboundary].list[ibackward].x -
                           boundary_p->list[iboundary].list[ibackward-1].x)) <
               TIM_MERSYN_BREAK_DETECTION)
        {
            ibackward = ibackward - 1;
            if (ibackward <= ifoward)
            {
                fprintf(TimStderr, "TimMersynComputeBoundary: "
                       "Error in break detection algorithm.\n");
                return (TIM_ERROR);
            }
        } /* Look for the other break from the end of the current list */
        /*-----*/
        Split the current boundary reporting the [ifoward,ibackward]
        /* vertices within an extra list */
        /*-----*/
        boundary_p->num = boundary_p->num + 1;
        if ((boundary_p->list=(TimVectorList*)TimAlloc(boundary_p->list,
                                                       boundary_p->num, sizeof(TimVectorList))) == NULL)
        {
            fprintf(TimStderr, "TimMersynComputeBoundary: "
                   "Cannot allocate one more boundary envelope.\n");
            return (TIM_ERROR);
        }
        boundary_p->list[boundary_p->num-1].num = ibackward - ifoward + 1 + 1;
        boundary_p->list[boundary_p->num-1].list = NULL;
        if ((boundary_p->list[boundary_p->num-1].list=(TimVector*)TimAlloc(
              NULL, boundary_p->list[boundary_p->num-1].num, sizeof(TimVector))) == NULL)
        {
            fprintf(TimStderr, "TimMersynComputeBoundary: "
                   "Cannot allocate the extra list of vertices.%n");
            return (TIM_ERROR);
        }
        memcpy (&(boundary_p->list[boundary_p->num-1].list[0]),
               &(boundary_p->list[iboundary].list[ifoward]),
               (boundary_p->list[boundary_p->num-1].num-1) *
               sizeof(TimVector));
    }
    /* Point ifoward and ibackward are present in both lists */
    /* within the new list add (or substrat) 180 degrees */
    /*-----*/
    if (boundary_p->list[iboundary].list[ifoward].x <
        boundary_p->list[iboundary].list[ifoward+1].x)
    {
        boundary_p->list[boundary_p->num-1].list[0].x =
            boundary_p->list[boundary_p->num-1].list[0].x + 2 * TIM_PI;
        boundary_p->list[boundary_p->num-1].list[1].
}
}

boundary_p->list[boundary_p->num-1].list[0].x =
    boundary_p->list[boundary_p->num-1].list[1].list[0].x + 2 * TIM_PI;
}
else
{
    boundary_p->list[boundary_p->num-1].list[0].x =
        boundary_p->list[boundary_p->num-1].list[1].list[0].x - 2 * TIM_PI;
    boundary_p->list[boundary_p->num-1].list[1].list[0].x =
        boundary_p->list[boundary_p->num-1].list[1].list[1].list[0].x =
        boundary_p->list[boundary_p->num-1].list[1].list[1].list[1].list[0].x - 2 * TIM_PI;
}
}

/* Close the new list duplicating the first point at the end */
/*-----*/
memcpy (&(boundary_p->list[boundary_p->num-1].list[0],
          &(boundary_p->list[boundary_p->num-1].list[0]),
          sizeof(TimVector));
/* Remove the points within the current list */
/*-----*/
for (i=ibackward; i<boundary_p->list[iboundary].num; i++)
{
    memcpy (
        &boundary_p->list[iboundary].list[i-(ibackward-ifoward)+1],
        &boundary_p->list[iboundary].list[i],
        sizeof(TimVector));
}

boundary_p->list[iboundary].num = boundary_p->list[iboundary].num -
        (ibackward - ifoward - 1);
boundary_p->list[iboundary].list = (TimVector*)TimAlloc(
    boundary_p->list[iboundary].list, boundary_p->list[iboundary].num,
    sizeof(TimVector));
/*-----*/
Current boundary becomes the new one
/*-----*/
iboundary = iboundary + 1;
ifoward = 0;
ibackward = boundary_p->list[iboundary].num - 1;
} /* Case of -180 / +180 break */
ifoward = ifoward + 1;
} /* Detect the breaks -180 / +180 degrees */
/*-----*/
/* Print out coordinates within a ".geo" file */
/*-----*/
#endif
{
    TimFILE *tim_fp; /* "MER...NI.geo" file pointer */

    sprintf(buf, "%s.geo", meris_file->name);
    if ((tim_fp=TimOpen(buf,TIM_WRITE_ONLY)) == NULL)
    {
        fprintf(TimStderr, "TimMersynComputeBoundary: Cannot open \"%s\" file.\n",
                buf);
        return (TIM_ERROR);
    }
    for (iboundary=0; iboundary<boundary_p->num; iboundary++)
    {
        for (ipoint=0; ipoint<boundary_p->list[iboundary].num; ipoint++)
        {
            TimFprintf (tim_fp, "%12.8f %12.8f\n",
                        boundary_p->list[iboundary].list[ipoint].x * 180.0 / TIM_PI,
                        boundary_p->list[iboundary].list[ipoint].y * 180.0 / TIM_PI);
        }
        TimFprintf (tim_fp, "END\n");
    }
    TimClose (tim_fp);
    tim_fp = NULL;
}
#endif
/*-----*/
/* Loop on boundary points conversion: Geographic -> Destination projection */
/*-----*/
for (iboundary=0; iboundary<boundary_p->num; iboundary++)
{
    for (ipoint=0; ipoint<boundary_p->list[iboundary].num; ipoint++)
    {
        prj_coordinate.x = boundary_p->list[iboundary].list[ipoint].x;
        prj_coordinate.y = boundary_p->list[iboundary].list[ipoint].y;
        prj_coordinate.z = 0.0;
        if (TimRiConvertCoordinate(prj_coordinate,geographic_projection,
                                   &prj_coordinate,synthesis_projection) != TIM_OK)
        {
            fprintf(TimStderr, "TimMersynComputeBoundary: "
                   "Cannot convert coordinates of boundary point #d (%f,%f).\n",
                   ipoint,
                   boundary_p->list[iboundary].list[ipoint].x,
                   boundary_p->list[iboundary].list[ipoint].y);
            return (TIM_ERROR);
        }
        boundary_p->list[iboundary].list[ipoint].x = prj_coordinate.x;
        boundary_p->list[iboundary].list[ipoint].y = prj_coordinate.y;
    }
} /* Loop on boundary points conversion */
/*-----*/
/* Return "OK" status */
/*-----*/
return (TIM_OK);
} /* TimMersynComputeBoundary */
}

***** TimMersynComputeIntersectionsWithBoundary computes the intersection between/
/* the current horizontal line and the boundary of the segment.
/*-----*/
/* Intersection points will be stored in the "intersection" list passed in */
/* parameter.
/*-----*/
/* TimMersynComputeIntersectionsWithBoundary will also determine if the first */
/* point to be processed on the line (0.0,y_current) is inside a polygon or */
/* not.
/*-----*/
int TimMersynComputeIntersectionsWithBoundary
{
    double y_current, /* curr.point Y-coord in output proj. */
    TimPolyVectorList *boundary_p, /* envelope of MERIS segment */
    TimFloatList *intersection_p, /* list of intersect. segment % line */
    int is_inside_p, /* point is inside segment" flag */
    int current_intersection_p /* intersection to be reached */
}
else
{
    y_current,boundary_p,intersection_p,is_inside_p,current_intersection_p);
    double y_current;
    TimPolyVectorList *boundary_p;
    TimFloatList *intersection_p;
    int is_inside_p;
    int current_intersection_p;
}
#endif

```



```

        }

#endif /* TIM_PRF */
    facet_search_all = facet_search_all + 1;
#endif /* Case of failure -> Test all the facets */

#ifndef TIM_PRF
    current_clock = clock();
    elapsed_time_facet = elapsed_time_facet +
        (current_clock - time_facet);
#endif

/*=====
 * Compute coordinates of the source point within the segment
 *=====
if (is_found)
{
    *mer_x_p = (*iline_facet_p + *delta_facet_x_p) *
        TIM_FMT_ENVISAT_MERIS_SPECIAL.linesPerTp;
    *mer_y_p = (*ipixel_facet_p + *delta_facet_y_p) *
        TIM_FMT_ENVISAT_MERIS_SPECIAL.samplesPerTp;
}

/*=====
 * Return "IS_FOUND" status
 *=====
return (is_found);
} /* TimMersynlocationInverse */

*****+
/* TimMersynGetAltitudeFromDem read the altitude value from the list of DEMs.
 */
/* Altitude is always read from the first DEM first. If the location of the
 * point of interest is out of this DEM or if the value found is background,
 * altitude is read from the second in the list, and so on...
 */
/* TimMersynGetAltitudeFromDem performs a bi-linear interpolation from the 4
 * nearest neighbours of the point of interest.
 */
/* TimMersynGetAltitudeFromDem return:
 * 1. TIM_TRUE if an altitude has been found in one DEM,
 * 2. TIM_FALSE if no altitude in whatever DEM has been found and
 * 3. TIM_ERROR if an error occurred.
 */
*****+
int TimMersynGetAltitudeFromDem
#ifndef TIM_ANSI_PROTOTYPE
(
    double longitude,           /* X-coord of point to be processed */
    double latitude,           /* Y-coord of point to be processed */
    TimPrjProjection *geographic_projection, /* projection structure */
    TimDEMList *dem_p,          /* DEMs in order they have to be read */
    double *altitude_p          /* altitude to be initialized */
)
#else
(longitude,latitude,geographic_projection,dem_p,altitude_p)
double longitude;
double latitude;
TimPrjProjection *geographic_projection;
TimDEMList *dem_p;
double *altitude_p;
#endif
{
    /* Local variables
     */
    static TimBuf*projection *dem_projection=NULL; /* DEM proj. struct. list */
    static TimBufferInt *dem_buf=NULL; /* DEM direct buffer list */
    TimPrjCoordinate *prj_coordinate; /* conversion prj coordinate struct */
    int idem; /* index among DEMs in list */
    double x_dem; /* X-coord of interest point in DEM */
    double y_dem; /* Y-coord of interest point in DEM */
    int i0; /* truncated value of x_dem */
    int j0; /* truncated value of y_dem */
    TimRDouble dx; /* decimal part of x_dem coordinate */
    TimRDouble dy; /* decimal part of y_dem coordinate */
    TimRDouble z1; /* 1st nearest pixel value in input */
    TimRDouble z2; /* 2nd nearest pixel value in input */
    TimRDouble z3; /* 3rd nearest pixel value in input */
    TimRDouble z4; /* 4th nearest pixel value in input */

    /* For the first call, initialise the projection structures of each DEM */
    if (dem_projection == NULL)
    {
        if ((dem_projection=(TimPrjProjection*)TimAlloc(NULL,
            dem_p->num,sizeof(TimPrjProjection))) == NULL)
            fprintf (TimStderr,"TimMersynGetAltitudeFromDem: "
                "Cannot allocate DEM projection list.\n");
        return (TIM_ERROR);
    }
    for (idem=0; idem<dem_p->num; idem++)
    {
        dem_projection[idem] = NULL;
        if (TimPrjAllocProjection(dem_p->list[idem]->projection,NULL,
            &dem_projection[idem])) != TIM_OK
        {
            fprintf (TimStderr,"TimMersynGetAltitudeFromDem: "
                "Cannot allocate projection structure for DEM '\\"%s\\".\n",
                dem_p->list[idem]->name);
            return (TIM_ERROR);
        }
    }
    /* For the first call, initialise the direct buffer of each DEM */
    if (dem_buf == NULL)
    {
        if ((dem_buf=(TimBufferInt*)TimAlloc(NULL,
            dem_p->num,sizeof(TimBufferInt*)) == NULL)
            fprintf (TimStderr,"TimMersynGetAltitudeFromDem: "
                "Cannot allocate DEM buffer list.\n");
        return (TIM_ERROR);
    }
    for (idem=0; idem<dem_p->num; idem++)
    {
        dem_buf[idem] = NULL;
        if ((dem_buf[idem]=(TimBufferInt*)TimAllocBufferDirect(
            TIM_DATA_TYPE_INT)) == NULL)
        {
            fprintf (TimStderr,"TimMersynGetAltitudeFromDem: "
                "Cannot allocate buffer structure for DEM '\\"%s\\".\n",
                dem_p->list[idem]->name);
            return (TIM_ERROR);
        }
    }
}

/*=====
 * Loop on DEMs
 *=====
for (idem=0; idem<dem_p->num; idem++)
{
    /* Convert (longitude,latitude) coordinates to DEM projection
     */
    prj_coordinate.x = longitude;
    prj_coordinate.y = latitude;
    prj_coordinate.z = 0.0;
    if (TimPrjConvertCoordinate(&prj_coordinate,geographic_projection,
        &prj_coordinate,dem_projection[idem]) != TIM_OK)
    {
        fprintf (TimStderr,"TimMersynGetAltitudeFromDem: "
            "Cannot convert geographic coordinates to projection "
            "'%s' of DEM '\\"%s\\".\n",dem_p->list[idem]->name,
            dem_p->list[idem]->name);
        return (TIM_ERROR);
    }
    x_dem = (dem_p->list[idem]->origin.y - prj_coordinate.y) /
        dem_p->list[idem]->pixelHeight;
    y_dem = (prj_coordinate.x - dem_p->list[idem]->origin.x) /
        dem_p->list[idem]->pixelWidth;
    i0 = x_dem;
    j0 = y_dem;

    /* Check that point is within the DEM
     */
    if ((i0 >= 0) && (i0 < dem_p->list[idem]->lineNumber - 1) &&
        (j0 >= 0) && (j0 < dem_p->list[idem]->pixelNumber - 1))
    {
        /* Read the four neighbours around the point of interest
         */
        if (TimReadImageDirect (TimFile(dem_p->list[idem]),i0,2,j0,2,1,0,1,
            TIM_SAMPLING_METHOD_NEAREST_NEIGHBOUR,NULL,
            (TimBuffer*)dem_buf[idem]) != TIM_OK)
        {
            fprintf (TimStderr,"TimMersynGetAltitudeFromDem: "
                "Cannot extract window ( %d 2 %d 2 ) from DEM '\\"%s\\".\n",
                i0,j0,dem_p->list[idem]->name);
            return (TIM_ERROR);
        }
    }
    /* Check that pixel is not background
     */
    z1 = TimValueDirect(dem_buf[idem],0,0);
    z2 = TimValueDirect(dem_buf[idem],0,1);
    z3 = TimValueDirect(dem_buf[idem],1,0);
    z4 = TimValueDirect(dem_buf[idem],1,1);
    if ((! (dem_p->list[idem]->backgroundFlag)) ||
        ((z1 != dem_p->list[idem]->background) &&
        (z2 != dem_p->list[idem]->background) &&
        (z3 != dem_p->list[idem]->background) &&
        (z4 != dem_p->list[idem]->background)))
    {
        /* Convert altitudes to scientific values
         */
        z1 = z1 * dem_p->list[idem]->radioFactor +
            dem_p->list[idem]->radioshift;
        z2 = z2 * dem_p->list[idem]->radioFactor +
            dem_p->list[idem]->radioshift;
        z3 = z3 * dem_p->list[idem]->radioFactor +
            dem_p->list[idem]->radioshift;
        z4 = z4 * dem_p->list[idem]->radioFactor +
            dem_p->list[idem]->radioshift;

        /* Compute bi-linear interpolation
         */
        dx = x_dem - i0;
        dy = y_dem - j0;
        *altitude_p = z1 + dy * (z2 - z1) +
            dx * (z3 + dy * (z4 - z3) -
            z1 - dy * (z2 - z1));
    }
    /* Return "IS_FOUND" status
     */
    return (TIM_TRUE);
}
/* Check that point is within the DEM */
} /* Loop on DEMs */
/* Return "NOT_FOUND" status
 */
return (TIM_FALSE);
} /* TimMersynGetAltitudeFromDem */

*****+
/* TimMersynLocationDirect computes the geographic coordinates of the point
 * ('mer_x0,mer_y0,altitude) given in MERIS segment reference system.
 */
/* TiePointSynLocationDirect applies the parallax correction interpolating the
 * viewing angle from the tie-points grid.
 */
*****+
int TimMersynLocationDirect
#ifndef TIM_ANSI_PROTOTYPE
(
    double mer_x,           /* X-coordinates in MERIS segment */
    double mer_y,           /* Y-coordinates in MERIS segment */
    double altitude,         /* Z-coordinates in MERIS segment */
    int iline_facet,          /* number of the tie-point frame */
    int ipixel_facet,         /* number of the tie-point column */
    double delta_facet_x,      /* X-coordinates within facet [0,1] */
    double delta_facet_y,      /* Y-coordinates within facet [0,1] */
    double *longitude_p,        /* longitude to be computed */
    double *latitude_p,        /* latitude to be computed */
)
#else
(mer_x,mer_y,altitude,iline_facet,ipixel_facet,delta_facet_x,delta_facet_y,
    longitude_p,latitude_p)
double mer_x;
double mer_y;
double altitude;
int iline_facet;
int ipixel_facet;
double delta_facet_x;
double delta_facet_y;
double *longitude_p;
double *latitude_p;
#endif
{
    /* Local variables
     */
    double longitude; /* X-coord interpolated from tie-point*/
}

```

```

double      latitude;          /* Y-coord interpolated from tie-point*/
double      viewing_zenith;    /* viewing angle from vertical */
double      viewing_azimuth;   /* viewing angle from north */
double      dx;                /* parallax module */
double      dlon;              /* longitude correction */
double      dlat;              /* latitude correction */

/*=====
 * Interpolate the geodetic coordinates
 *=====
 */
/*=====
 * Longitude
 *=====
 */
longitude =
(1 - delta_facet_x) * (1 - delta_facet_y) *
TIM_FMT_ENVISAT_MERIS_SPECIAL.tiePointLine.list[
iline_facet].longitude[ipixel_facet] +
(1 - delta_facet_x) * delta_facet_y *
TIM_FMT_ENVISAT_MERIS_SPECIAL.tiePointLine.list[
iline_facet].longitude[ipixel_facet+1] +
delta_facet_x * (1 - delta_facet_y) *
TIM_FMT_ENVISAT_MERIS_SPECIAL.tiePointLine.list[
iline_facet+1].longitude[ipixel_facet] +
delta_facet_x * delta_facet_y *
TIM_FMT_ENVISAT_MERIS_SPECIAL.tiePointLine.list[
iline_facet+1].longitude[ipixel_facet+1];
/*=====
 * Latitude
 *=====
 */
/*=====
 * Latitude
 *=====
 */
latitude =
(1 - delta_facet_x) * (1 - delta_facet_y) *
TIM_FMT_ENVISAT_MERIS_SPECIAL.tiePointLine.list[
iline_facet].latitude[ipixel_facet] +
(1 - delta_facet_x) * delta_facet_y *
TIM_FMT_ENVISAT_MERIS_SPECIAL.tiePointLine.list[
iline_facet].latitude[ipixel_facet+1] +
delta_facet_x * (1 - delta_facet_y) *
TIM_FMT_ENVISAT_MERIS_SPECIAL.tiePointLine.list[
iline_facet+1].latitude[ipixel_facet] +
delta_facet_x * delta_facet_y *
TIM_FMT_ENVISAT_MERIS_SPECIAL.tiePointLine.list[
iline_facet+1].latitude[ipixel_facet+1];
/*=====
 * Interpolate the viewing angle
 *=====
 */
/*=====
 * Viewing zenith
 *=====
 */
viewing_zenith =
(1 - delta_facet_x) * (1 - delta_facet_y) *
TIM_FMT_ENVISAT_MERIS_SPECIAL.tiePointLine.list[
iline_facet].viewingZenith[ipixel_facet] +
(1 - delta_facet_x) * delta_facet_y *
TIM_FMT_ENVISAT_MERIS_SPECIAL.tiePointLine.list[
iline_facet].viewingZenith[ipixel_facet+1] +
delta_facet_x * (1 - delta_facet_y) *
TIM_FMT_ENVISAT_MERIS_SPECIAL.tiePointLine.list[
iline_facet+1].viewingZenith[ipixel_facet] +
delta_facet_x * delta_facet_y *
TIM_FMT_ENVISAT_MERIS_SPECIAL.tiePointLine.list[
iline_facet+1].viewingZenith[ipixel_facet+1];
/*=====
 * Viewing azimuth
 *=====
 */
viewing_azimuth =
(1 - delta_facet_x) * (1 - delta_facet_y) *
TIM_FMT_ENVISAT_MERIS_SPECIAL.tiePointLine.list[
iline_facet].viewingAzimuth[ipixel_facet] +
(1 - delta_facet_x) * delta_facet_y *
TIM_FMT_ENVISAT_MERIS_SPECIAL.tiePointLine.list[
iline_facet].viewingAzimuth[ipixel_facet+1] +
delta_facet_x * (1 - delta_facet_y) *
TIM_FMT_ENVISAT_MERIS_SPECIAL.tiePointLine.list[
iline_facet+1].viewingAzimuth[ipixel_facet] +
delta_facet_x * delta_facet_y *
TIM_FMT_ENVISAT_MERIS_SPECIAL.tiePointLine.list[
iline_facet+1].viewingAzimuth[ipixel_facet+1];

#ifndef TIM_BNCH
if (bench_index != -1)
{
  TIM_MERSYN_BENCH[bench_index].viewingZenith = viewing_zenith;
  TIM_MERSYN_BENCH[bench_index].viewingAzimuth = viewing_azimuth;
}
#endif

/*=====
 * Compute the longitude and latitude corrections
 *=====
 */
dx = altitude * tan(viewing_zenith);
dlat = dx * cos(viewing_azimuth) / TIM_MERSYN_MEAN_EARTH_RADIUS;
dlon = dx * sin(viewing_azimuth) /
(TIM_MERSYN_MEAN_EARTH_RADIUS * cos(latitude));

/*=====
 * Apply geodetic corrections
 *=====
 */
longitude_p = longitude + dlon;
latitude_p = latitude + dlat;

/*=====
 * Return "Ok" status
 *=====
 */
/*=====
 * Return
 *=====
 */
return (TIM_OK);
} /* TimMersynLocationDirect */

```

APPENDIX D – ORTHORECTIFICATION BENCHMARK

This section contains a second version of the log of MERSYN execution (version 02.05) when applied to MERIS FR scene MER_FR_1PNUPA20030921_092341_000000982020_00079_08149_0534.N1 of Italy and using the GETASSE30 DEM above WGS84 ellipsoid directive to produce 25 control points for unitary testing (see e-mail of Norman FOMFERRA, Brockmann Consult on 27/08/2004).

This second version makes suite the comments of Norman FOMFERRA (see R-7) that lead to the modification of equations 6a and 6b.

Print out of the benchmark values is processed compiling the MERSYN program provided in 0 with the “TIM_BENCH” compilation directive.

These values are also stored within a MS EXCEL file “VT-P194-DOC-001-E-01-04.xls” that may be provided upon demand.

D.1 Benchmark points distribution

As shown in fig. 65, benchmark points have been dispatched within the output image to encompass cases with different viewing angles and different elevations.

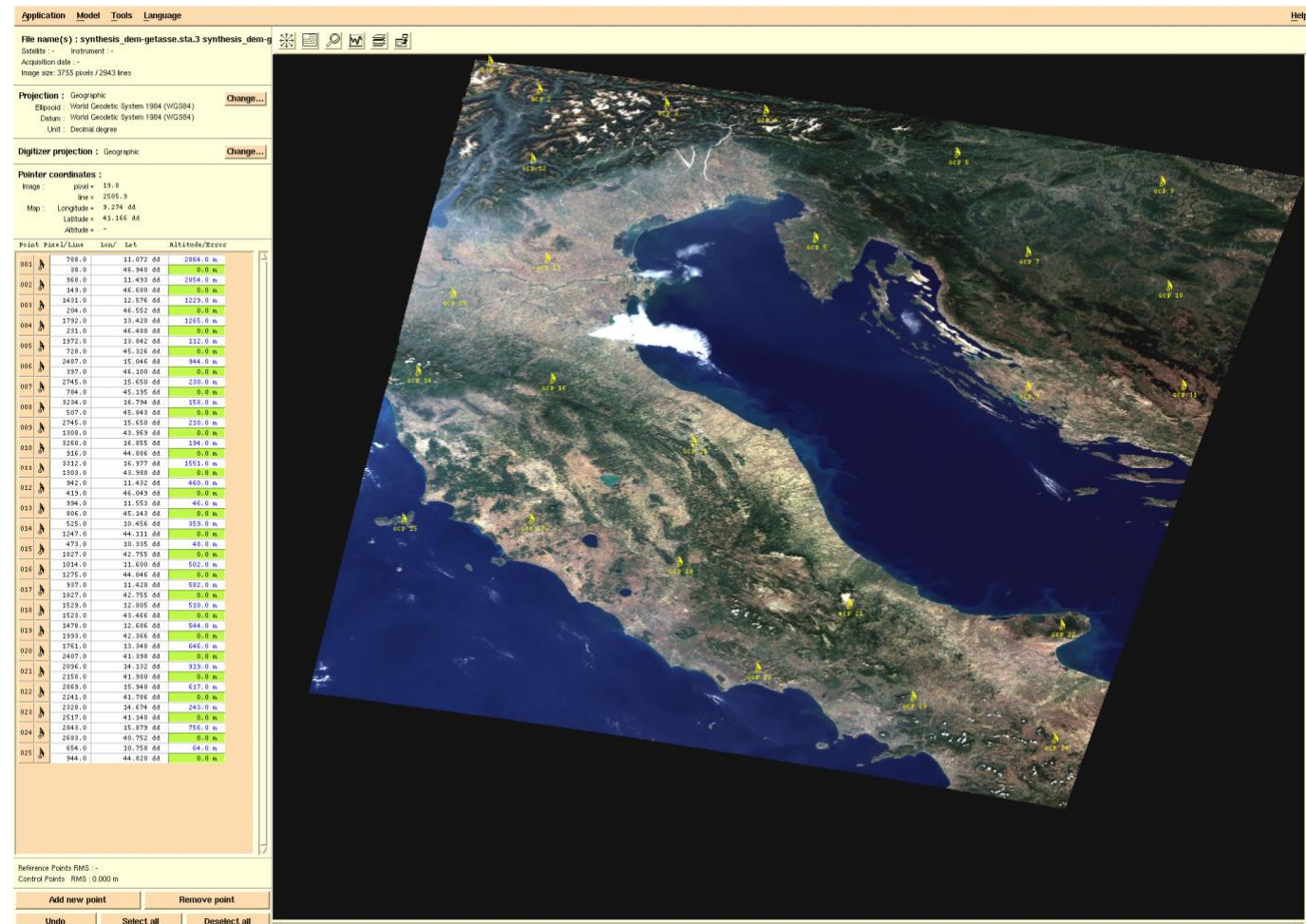


fig. 65 - Distribution of benchmark points.

D.2 Benchmark values

Values are stored within the following columns:

Nb	is a sequential number of the benchmark point.
(line,column)	are the coordinates of the benchmark point within the output (geocoded) image.
(Easting,Northing)	are the coordinates of the benchmark point within the coordinates reference system of the output image : “Plate Carrée – WGS 1984”.
(longitude,latitude)	are the coordinates of the benchmark point within the geodetic reference system (also called “ <i>geographic coordinates</i> ”).
elevation	is the elevation computed by a bi-linear interpolation from the four nearest neighbours at the benchmark point location found within the GETASSE30 DEM. These values are given above WGS 1984 ellipsoid.
view zenith/azimuth	are the two angles interpolated within the tie-point grid at the location of the benchmark point.
longitude/latitude corrections	are the parallax corrections computed taking into account the viewing angles and the point elevation.
MERIS origin (line,column)	are the coordinates of the antecedent of the benchmark point found within the input MERIS scene not taking into account the elevation.
MERIS antecedent (line,column)	are the coordinates of the antecedent of the benchmark point found within the input MERIS scene taking into account the elevation and after having processed the prediction/correction loop.

Nb	line	column	Easting	Northing	longitude	latitude	elevation	view zenith	view azimuth	longitude correction	latitude correction	MERIS origin line	MERIS origin column	MERIS antecedent line	MERIS antecedent column
0	38	788	1230413.2	5216575.0	11.071550	46.939981	2841	38.825	99.946	0.029666	-0.003551	12.362	2098.622	12.375	2107.442
1	149	968	1277213.2	5187715.0	11.492668	46.680292	2036	36.737	100.298	0.019604	-0.002443	90.297	1957.374	90.302	1963.237
2	204	1431	1397593.2	5173415.0	12.575875	46.551617	1424	31.672	101.089	0.011273	-0.001519	85.682	1633.586	85.684	1636.974
3	231	1792	1491453.2	5166395.0	13.420450	46.488449	1436	27.462	101.695	0.009548	-0.001361	65.485	1383.903	65.488	1386.782
4	728	1972	1538253.2	5037175.0	13.841568	45.325697	164	23.385	102.166	0.000884	-0.000134	473.198	1158.107	473.198	1158.380
5	397	2487	1672153.2	5123235.0	15.046432	46.100085	985	18.091	102.895	0.004068	-0.000646	118.239	877.737	118.240	878.979
6	784	2745	1739233.2	5022615.0	15.650033	45.194683	252	12.812	103.431	0.000710	-0.000119	414.628	613.340	414.628	613.561
7	507	3234	1866373.2	5094635.0	16.794069	45.842736	158	7.285	104.152	0.000252	-0.000044	105.166	345.520	105.166	345.598
8	1308	2745	1739233.2	4886375.0	15.650033	43.968763	215	10.309	103.573	0.000474	-0.000082	864.013	490.957	864.013	491.107
9	916	3260	1873133.2	4988295.0	16.854897	44.885863	196	4.804	104.297	0.000203	-0.000037	450.513	227.214	450.513	227.278

Nb	line	column	Easting	Northing	longitude	latitude	elevation	view zenith	view azimuth	longitude correction	latitude correction	MERIS origin line	MERIS origin column	MERIS antecedent line	MERIS antecedent column
10	1303	3312	1886653.2	4887675.0	16.976554	43.980461	1516	2.016	104.478	0.000646	-0.000120	772.409	94.983	772.409	95.189
11	419	942	1270453.2	5117515.0	11.431840	46.048616	522	36.219	100.377	0.004872	-0.000619	329.537	1926.552	329.536	1928.026
12	806	994	1283973.2	5016895.0	11.553496	45.143213	47	34.585	100.619	0.000402	-0.000053	661.958	1820.076	661.958	1820.200
13	1247	525	1162033.2	4902235.0	10.456251	44.111475	459	38.335	100.049	0.004474	-0.000569	1101.176	2070.374	1101.176	2071.773
14	1827	473	1148513.2	4751435.0	10.334594	42.754541	48	37.390	100.208	0.000442	-0.000058	1614.970	2005.610	1614.970	2005.751
15	1275	1014	1289173.2	4894955.0	11.600287	44.045968	559	33.026	100.830	0.004465	-0.000614	1068.898	1718.696	1068.900	1720.097
16	1827	937	1269153.2	4751435.0	11.420142	42.754541	588	32.249	100.918	0.004465	-0.000632	1559.338	1669.616	1559.338	1671.048
17	1523	1529	1423073.2	4830475.0	12.805151	43.465761	473	26.044	101.727	0.002805	-0.000423	1219.772	1304.177	1219.772	1305.069
18	1993	1478	1409813.2	4708275.0	12.685834	42.366177	583	24.994	101.805	0.003241	-0.000500	1633.713	1244.989	1633.714	1246.038
19	2407	1761	1483393.2	4600635.0	13.347924	41.397607	637	19.533	102.362	0.002647	-0.000435	1952.375	951.629	1952.377	952.501
20	2158	2096	1570493.2	4665375.0	14.131671	41.980152	919	15.805	102.796	0.003069	-0.000518	1689.644	760.930	1689.646	761.933
21	2241	2869	1771473.2	4643795.0	15.940137	41.785970	662	3.816	103.997	0.000517	-0.000096	1642.937	180.101	1642.937	180.271
22	2517	2328	1630813.2	4572035.0	14.674444	41.140257	304	10.719	103.244	0.000669	-0.000119	1963.413	510.395	1963.413	510.617
23	2683	2843	1764713.2	4528875.0	15.879308	40.751893	780	1.953	104.063	0.000306	-0.000058	2024.333	92.061	2024.333	92.164
24	944	654	1195573.2	4981015.0	10.758052	44.820356	66	37.769	100.131	0.000634	-0.000080	821.305	2032.557	821.305	2032.753

APPENDIX E – TIE-POINT VALUES

This section contains the values for the first and last (36th for FR or 71st for RR) tie-point of some lines (sampling factor of 8) and the last one (36th for FR or undefined for RR, see example E.15).

E.1 scene01-01/MER_FR__1PNUPA20030921_092217_000000982020_00079_08149_0354.N1

Viewing vectors found in the tie-points ADS enable registering the viewing geometry.

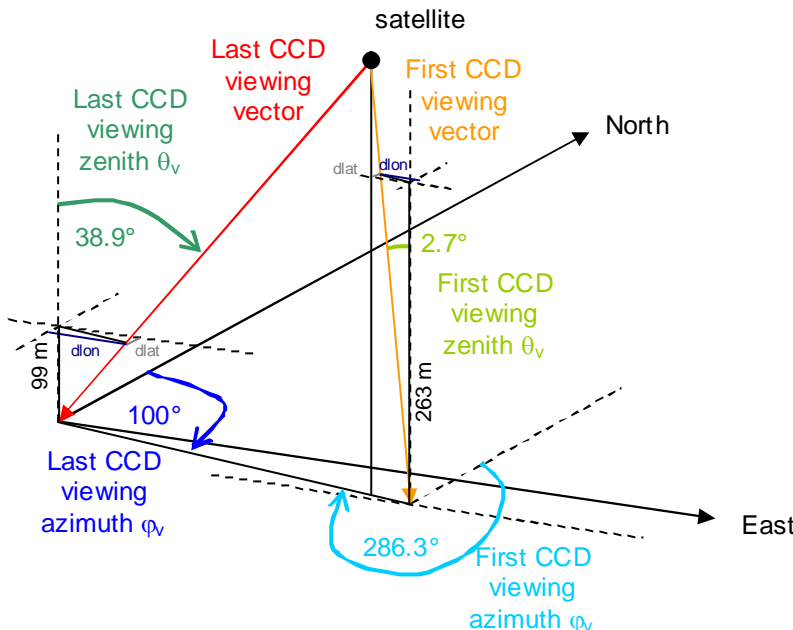


fig. 66 - First and last viewing vectors of the first tie-points line.

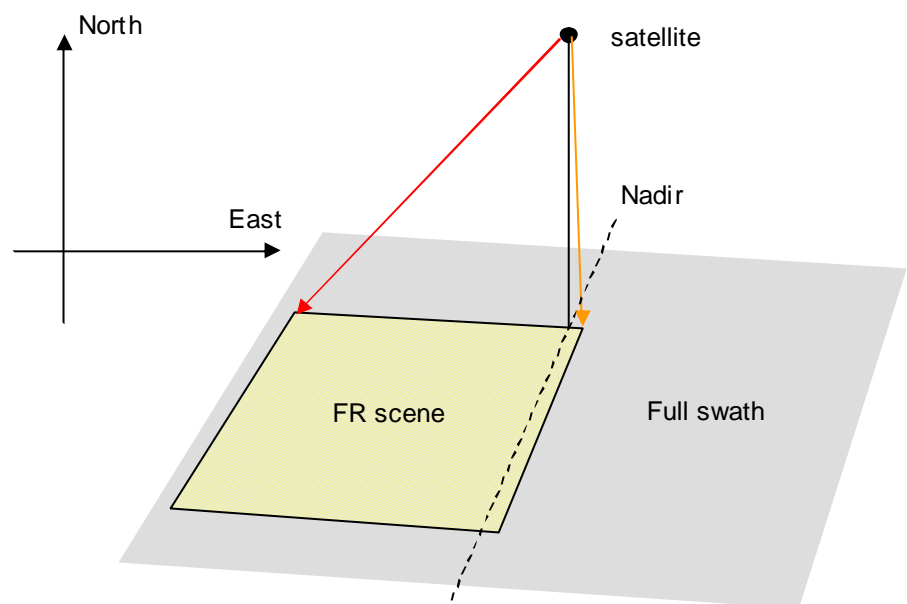


fig. 67 - Location of the FR scene within the full swath in geodetic geometry.

Figure fig. 66 here above illustrates the viewing vector values of the first and last tie-point in the first tie-point line found within the third data set ("Tie-point ADS"). Do not forget that tie-points are ordered from Esat to West. These values let suppose that the FR scene is located on the left side of the full swath as illustrated in fig. 67.

The parallax defect is also provided as "corrected latitude and longitude" According to the MERIS Level 1 Detailed Processing Model (R-3), these corrections are computed using the equation 2.

$$\begin{aligned}
 dx &= Z_{F,J} \times \tan(\theta_{vF,J}) \\
 dlat_{F,J} &= \frac{dx \times \cos(\phi_{vF,J})}{R_e} \\
 dlon_{F,J} &= \frac{-dx \times \sin(\phi_{vF,J})}{R_e \times \cos(\phi_{F,J})}
 \end{aligned} \quad \text{Eq. 2}$$

Where:

- dx is the modulus of the parallax error.
- $dlat_{F,J}$ is the latitude correction of tie-point (F,J).
- $dlon_{F,J}$ is the longitude correction of tie-point (F,J).
- $Z_{F,J}$ is the DEM elevation of tie-point (F,J).
- $\theta_{vF,J}$ is the zenith of the viewing angle of tie-point (F,J).
- $\phi_{vF,J}$ is the azimuth of the viewing angle of tie-point (F,J).
- $\phi_{F,J}$ is the geodetic latitude of tie-point (F,J).
- R_e is the mean Earth radius ($R_e = 6\,370\,997.0$ metres)

In our example, see the bold values of the first line of data dumped here below.

FIRST TIE-POINT

$$\begin{aligned}
 dx &= Z_{F,J} \times \tan(\theta_{vF,J}) = 263 \times \tan(2.7^\circ) = 12.403 \text{ m} \\
 dlat_{F,J} &= \frac{dx \times \cos(\phi_{vF,J})}{R_e} = \frac{12.403 \times \cos(286.3^\circ)}{6370997} = 0.000031306^\circ \\
 dlon_{F,J} &= \frac{-dx \times \sin(\phi_{vF,J})}{R_e \times \cos(\phi_{F,J})} = \frac{-12.403 \times \sin(286.3^\circ)}{6370997 \times \cos(50.742379^\circ)} = 0.000169181^\circ
 \end{aligned}$$

LAST TIE-POINT

$$\begin{aligned}
 dx &= Z_{F,J} \times \tan(\theta_{vF,J}) = 99 \times \tan(38.9^\circ) = 79.883 \text{ m} \\
 dlat_{F,J} &= \frac{dx \times \cos(\phi_{vF,J})}{R_e} = \frac{79.883 \times \cos(100.0^\circ)}{6370997} = -0.000124750^\circ \\
 dlon_{F,J} &= \frac{-dx \times \sin(\phi_{vF,J})}{R_e \times \cos(\phi_{F,J})} = \frac{-79.883 \times \sin(100.0^\circ)}{6370997 \times \cos(51.937422^\circ)} = -0.001147541^\circ
 \end{aligned}$$

Sign of the latitude correction (dlat) is not compliant with the sign of longitude correction (dlon). In the case these quantities have to be considered as "CORRECTIONS TO BE ADDED" to the original values (see eq. 6b') and not to be subtracted as previously in eq. 6b, expression of dlon computation should be changed as:

$$dlon_{F,J} = \frac{dx \times \sin(\phi_{vF,J})}{R_e \times \cos(\phi_{F,J})} \quad \text{Eq. 2c'}$$

$$\begin{aligned}
 \lambda_{\text{corrected}} &\leftarrow \lambda_{\text{origin}} + dlon_{F,J} \\
 \varphi_{\text{corrected}} &\leftarrow \varphi_{\text{origin}} + dlat_{F,J}
 \end{aligned} \quad \text{Eq. 6b'}$$

DATA SET #3 - "Tie points ADS":

No.	Date	FIRST (Lat., Lon.)	Alt. Rough.	Corr. Lat. Lon.	Sun (Zen., Azi.)	View (Zen., Azi.)
1	117451337.241756	(50.742379, 20.514153)	263	27 31 1e-6 169 1e-6	(52.0, 157.9)	(2.7, 286.3)
9	117451359.768220	(49.435929, 19.924214)	642	91 75 1e-6	403 1e-6 (51.0, 156.9)	(2.7, 286.0)
17	117451382.294684	(48.127118, 19.360172)	196	42 22 1e-6	120 1e-6 (49.9, 155.9)	(2.7, 285.7)
25	117451404.821148	(46.816133, 18.819646)	159	20 18 1e-6	95 1e-6 (48.8, 154.9)	(2.7, 285.5)
33	117451427.347612	(45.503143, 18.300527)	95	10 10 1e-6	55 1e-6 (47.8, 153.8)	(2.7, 285.2)
36	117451435.795036	(45.010286, 18.110986)	164	49 18 1e-6	95 1e-6 (47.4, 153.4)	(2.7, 285.1)

LAST (Lat., Lon.)	Alt. Rough.	Corr. Lat. Lon.	Sun (Zen., Azi.)	View (Zen., Azi.)
(51.937422 , 12.372044)	99	11 -124 1e-6 -1146 1e-6	(55.4, 148.6)	(38.9, 100.0)
(50.615694, 12.001195)	433	33 -543 1e-6	-4876 1e-6 (54.4, 147.8)	(38.9, 100.0)
(49.293239, 11.641344)	536	20 -671 1e-6	-5875 1e-6 (53.3, 147.0)	(38.9, 99.9)
(47.970091, 11.291352)	634	19 -794 1e-6	-6771 1e-6 (52.3, 146.1)	(38.9, 99.9)
(46.646280, 10.950213)	1315	442 -1647 1e-6	-13703 1e-6 (51.3, 145.3)	(38.9, 99.9)
(46.149686, 10.824383)	1364	358 -1709 1e-6	-14086 1e-6 (51.0, 144.9)	(38.9, 99.9)

E.2 scene01-02/MER_FR__1PNUPA20030921_092220_000000982020_00079_08149_0398.N1

DATA SET #3 - "Tie points ADS":

No.	Date	FIRST (Lat., Lon.)	Alt. Rough.	Corr. Lat. Lon.	Sun (Zen., Azi.)	View (Zen., Azi.)	LAST (Lat., Lon.)	Alt. Rough.	Corr. Lat. Lon.	Sun (Zen., Azi.)	View (Zen., Azi.)		
1	117451340.058163	(49.074601, 27.223613)	300	27	797 1e-6	3090 1e-6 (49.1, 166.0)	(38.9, 291.5)	(50.743669, 19.533811)	271	29	-31 1e-6	-175 1e-6 (52.3, 156.7)	(2.7, 105.6)
9	117451362.584627	(47.800010, 26.479166)	255	22	662 1e-6	2572 1e-6 (48.0, 164.9)	(38.9, 291.0)	(49.433965, 18.970195)	769	175	-86 1e-6	-485 1e-6 (51.2, 155.8)	(2.7, 105.3)
17	117451385.111091	(46.520884, 25.769594)	806	48	2046 1e-6	7965 1e-6 (46.9, 163.8)	(38.9, 290.5)	(48.122164, 18.430685)	199	24	-22 1e-6	-122 1e-6 (50.1, 154.7)	(2.7, 105.1)
25	117451407.637555	(45.237598, 25.091987)	700	76	1738 1e-6	6782 1e-6 (45.8, 162.6)	(38.9, 290.0)	(46.808431, 17.913047)	188	31	-20 1e-6	-113 1e-6 (49.1, 153.7)	(2.7, 104.8)
33	117451430.164019	(43.950485, 24.443732)	78	7	189 1e-6	741 1e-6 (44.7, 161.5)	(38.9, 289.6)	(45.492911, 17.415303)	427	169	-45 1e-6	-251 1e-6 (48.0, 152.7)	(2.7, 104.6)
36	117451438.611443	(43.466894, 24.207718)	137	60	330 1e-6	1293 1e-6 (44.2, 161.0)	(38.9, 289.4)	(44.999157, 17.233411)	213	56	-22 1e-6	-124 1e-6 (47.6, 152.3)	(2.7, 104.5)

E.3 scene01-03/MER_FR__1PNUPA20030921_092327_000000982020_00079_08149_0394.N1

DATA SET #3 - "Tie points ADS":

No.	Date	FIRST (Lat., Lon.)	Alt. Rough.	Corr. Lat. Lon.	Sun (Zen., Azi.)	View (Zen., Azi.)	LAST (Lat., Lon.)	Alt. Rough.	Corr. Lat. Lon.	Sun (Zen., Azi.)	View (Zen., Azi.)		
1	117451407.636284	(46.612105, 18.963019)	93	7	15 1e-6	83 1e-6 (48.6, 155.0)	(4.1, 285.6)	(47.778675, 11.466962)	609	165	-750 1e-6	-6269 1e-6 (52.1, 146.3)	(38.0, 100.1)
9	117451430.162748	(45.299488, 18.441791)	101	2	17 1e-6	88 1e-6 (47.5, 153.9)	(4.1, 285.3)	(46.454782, 11.121505)	1164	222	-1433 1e-6	-11692 1e-6 (51.1, 145.4)	(38.0, 100.1)
17	117451452.689212	(43.984986, 17.940157)	830	189	138 1e-6	711 1e-6 (46.5, 152.9)	(4.1, 285.1)	(45.130236, 10.784263)	20	0	-24 1e-6	-196 1e-6 (50.1, 144.5)	(38.0, 100.1)
25	117451475.215676	(42.668733, 17.456441)	-80	0	0 1e-6	0 1e-6 (45.4, 151.8)	(4.1, 284.9)	(43.805064, 10.454420)	176	81	-217 1e-6	-1688 1e-6 (49.1, 143.5)	(38.0, 100.1)
33	117451497.742140	(41.350854, 16.989140)	-128	0	0 1e-6	0 1e-6 (44.4, 150.6)	(4.1, 284.7)	(42.479293, 10.131249)	-91	0	0 1e-6	0 1e-6 (48.2, 142.6)	(38.0, 100.1)
36	117451506.189564	(40.856253, 16.817854)	362	28	58 1e-6	296 1e-6 (44.0, 150.2)	(4.1, 284.6)	(41.981979, 10.011643)	-567	0	0 1e-6	0 1e-6 (47.8, 142.2)	(38.0, 100.1)

E.4 scene01-04/MER_FR__1PNUPA20030921_092341_000000982020_00079_08149_0534.N1

DATA SET #3 - "Tie points ADS":

No.	Date	FIRST (Lat., Lon.)	Alt. Rough.	Corr. Lat. Lon.	Sun (Zen., Azi.)	View (Zen., Azi.)	LAST (Lat., Lon.)	Alt. Rough.	Corr. Lat. Lon.	Sun (Zen., Azi.)	View (Zen., Azi.)		
1	117451421.714409	(45.909863, 18.014693)	98	3	0 1e-6	0 1e-6 (48.2, 153.6)	(0.0, 182.0)	(47.028196, 10.603496)	1476	382	-1907 1e-6	-16512 1e-6 (51.8, 145.0)	(40.7, 99.6)
9	117451444.240873	(44.594348, 17.519381)	591	159	0 1e-6	0 1e-6 (47.2, 152.5)	(0.0, 181.9)	(45.703992, 10.278711)	850	227	-1101 1e-6	-9284 1e-6 (50.8, 144.1)	(40.7, 99.6)
17	117451466.767337	(43.277165, 17.041762)	417	32	0 1e-6	0 1e-6 (46.1, 151.4)	(0.0, 181.9)	(44.379209, 9.960598)	744	75	-967 1e-6	-7942 1e-6 (49.8, 143.2)	(40.7, 99.7)
25	117451489.293801	(41.958432, 16.580328)	-110	0	0 1e-6	0 1e-6 (45.1, 150.3)	(0.0, 181.9)	(43.053869, 9.648478)	-366	0	0 1e-6	0 1e-6 (48.9, 142.3)	(40.7, 99.7)
33	117451511.820265	(40.638252, 16.133722)	540	177	0 1e-6	0 1e-6 (44.1, 149.2)	(0.0, 181.8)	(41.727992, 9.341743)	116	23	-152 1e-6	-1186 1e-6 (47.9, 141.3)	(40.7, 99.7)
36	117451520.267689	(40.142832, 15.969815)	1053	209	0 1e-6	0 1e-6 (43.7, 148.8)	(0.0, 181.8)	(41.230654, 9.227991)	79	54	-103 1e-6	-801 1e-6 (47.6, 140.9)	(40.7, 99.8)

E.5 scene01-05/MER_FR__1PNUPA20030925_103640_000000982020_00137_08207_0539.N1

DATA SET #3 - "Tie points ADS":

No.	Date	FIRST (Lat., Lon.)	Alt. Rough.	Corr. Lat. Lon.	Sun (Zen., Azi.)	View (Zen., Azi.)	LAST (Lat., Lon.)	Alt. Rough.	Corr. Lat. Lon.	Sun (Zen., Azi.)	View (Zen., Azi.)		
1	117801400.752079	(51.545466, 3.970685)	-2	0	0 1e-6	0 1e-6 (53.8, 161.5)	(12.0, 287.9)	(52.871546, -4.276685)	-12	0	0 1e-6	0 1e-6 (57.0, 152.2)	(32.1, 101.4)
9	117801423.278543	(50.247548, 3.315102)	55	13	31 1e-6	157 1e-6 (52.7, 160.5)	(12.0, 287.5)	(51.551705, -4.707541)	-38	0	0 1e-6	0 1e-6 (55.9, 151.4)	(32.1, 101.3)
17	117801445.805007	(48.946594, 2.690314)	72	27	40 1e-6	201 1e-6 (51.6, 159.5)	(12.0, 287.1)	(50.230855, -5.122747)	75	50	-82 1e-6	-649 1e-6 (54.9, 150.5)	(32.1, 101.2)
25	117801468.331471	(47.642858, 2.093492)	135	6	74 1e-6	368 1e-6 (50.5, 158.5)	(12.0, 286.8)	(48.909059, -5.523896)	-121	0	0 1e-6	0 1e-6 (53.8, 149.7)	(32.1, 101.1)
33	117801490.857935	(46.336567, 1.522125)	311	32	169 1e-6	829 1e-6 (49.4, 157.5)	(12.0, 286.5)	(47.586371, -5.912392)	-140	0	0 1e-6	0 1e-6 (52.8, 148.9)	(32.1, 101.1)
36	117801499.305359	(45.846090, 1.313961)	333	38	180 1e-6	881 1e-6 (49.0, 157.1)	(12.0, 286.4)	(47.090144, -6.055074)	-1669	0	0 1e-6	0 1e-6 (52.4, 148.5)	(32.1, 101.0)



VisioTerra

Envisat MERIS

Geometry Handbook

reference VT-P194-DOC-001-E

issue 1 revision 5

date 06/07/2005

page 101 of 115

E.6 scene01-06/MER_FR__1PNUPA20030926_100615_000000982020_00151_08221_0538.N1

DATA SET #3 - "Tie points ADS":

No.	Date	FIRST (Lat., Lon.)	Alt. Rough.	Corr. Lat. Lon.	Sun (Zen., Azi.)	View (Zen., Azi.)	LAST (Lat., Lon.)	Alt. Rough.	Corr. Lat. Lon.	Sun (Zen., Azi.)	View (Zen., Azi.)
1	117885975.564369	(46.131973, 15.246156)	432 134	1178 1e-6	4509 1e-6 (48.3, 165.1)	(40.7, 290.7)	(47.752857, 7.968492)	907 96	0 1e-6	0 1e-6 (51.5, 156.3)	(0.0, 182.1)
9	117885998.090833	(44.850067, 14.567378)	-90 0	0 1e-6	0 1e-6 (47.2, 164.0)	(40.7, 290.2)	(46.439901, 7.445472)	1549 398	0 1e-6	0 1e-6 (50.4, 155.3)	(0.0, 182.1)
17	117886020.617297	(43.564274, 13.917832)	-55 0	0 1e-6	0 1e-6 (46.0, 162.9)	(40.7, 289.7)	(45.125091, 6.942563)	1579 352	0 1e-6	0 1e-6 (49.3, 154.3)	(0.0, 182.0)
25	117886043.143761	(42.274895, 13.295207)	1103 373	2824 1e-6	10886 1e-6 (44.9, 161.8)	(40.7, 289.3)	(43.808563, 6.458004)	939 98	0 1e-6	0 1e-6 (48.3, 153.3)	(0.0, 182.0)
33	117886065.670225	(40.982206, 12.697413)	-694 0	0 1e-6	0 1e-6 (43.8, 160.7)	(40.7, 288.9)	(42.490438, 5.990218)	-2420 0	0 1e-6	0 1e-6 (47.2, 152.3)	(0.0, 182.0)
36	117886074.117649	(40.496644, 12.479252)	-2251 0	0 1e-6	0 1e-6 (43.4, 160.3)	(40.7, 288.8)	(41.995752, 5.818829)	-2399 0	0 1e-6	0 1e-6 (46.8, 151.9)	(0.0, 181.9)

E.7 scene01-07/MER_FR__1PNUPA20031010_092709_000000982020_00351_08421_0536.N1

DATA SET #3 - "Tie points ADS":

No.	Date	FIRST (Lat., Lon.)	Alt. Rough.	Corr. Lat. Lon.	Sun (Zen., Azi.)	View (Zen., Azi.)	LAST (Lat., Lon.)	Alt. Rough.	Corr. Lat. Lon.	Sun (Zen., Azi.)	View (Zen., Azi.)
1	119093229.243887	(43.298630, 18.667244)	1584 288	1035 1e-6	4917 1e-6 (52.0, 159.2)	(14.6, 286.1)	(44.541324, 11.619780)	13 10	-13 1e-6	-93 1e-6 (55.3, 151.3)	(30.0, 101.3)
9	119093251.770351	(41.986534, 18.156891)	-1196 0	0 1e-6	0 1e-6 (50.9, 158.3)	(14.6, 285.9)	(43.216211, 11.255751)	246 80	-248 1e-6	-1723 1e-6 (54.2, 150.6)	(30.0, 101.2)
17	119093274.296815	(40.672518, 17.664457)	143 14	90 1e-6	427 1e-6 (49.8, 157.4)	(14.7, 285.6)	(41.890343, 10.900534)	-1365 0	0 1e-6	0 1e-6 (53.1, 149.8)	(30.0, 101.2)
25	119093296.823279	(39.356718, 17.188507)	-447 0	0 1e-6	0 1e-6 (48.7, 156.5)	(14.7, 285.4)	(40.563758, 10.553316)	-1832 0	0 1e-6	0 1e-6 (52.1, 149.0)	(30.0, 101.2)
33	119093319.349743	(38.039257, 16.727746)	-1717 0	0 1e-6	0 1e-6 (47.6, 155.6)	(14.7, 285.2)	(39.236493, 10.213367)	-1629 0	0 1e-6	0 1e-6 (51.1, 148.1)	(30.1, 101.1)
36	119093327.797167	(37.544803, 16.558633)	-2377 0	0 1e-6	0 1e-6 (47.2, 155.2)	(14.7, 285.1)	(38.738600, 10.087623)	-2016 0	0 1e-6	0 1e-6 (50.7, 147.8)	(30.1, 101.1)

E.8 scene01-08/MER_FR__1PNUPA20031010_092717_000000502020_00351_08421_0453.N1

Warning : This product has not the expected number of tie-point lines.

DATA SET #3 - "Tie points ADS":

No.	Date	FIRST (Lat., Lon.)	Alt. Rough.	Corr. Lat. Lon.	Sun (Zen., Azi.)	View (Zen., Azi.)	LAST (Lat., Lon.)	Alt. Rough.	Corr. Lat. Lon.	Sun (Zen., Azi.)	View (Zen., Azi.)
1	119093237.693105	(43.734696, 13.508266)	-26 0	0 1e-6	0 1e-6 (53.9, 153.3)	(18.4, 102.6)	(44.266045, 9.846784)	540 187	-665 1e-6	-5220 1e-6 (55.6, 149.3)	(38.0, 100.1)
9	119093260.219569	(42.410958, 13.104730)	1206 238	-786 1e-6	-4785 1e-6 (52.8, 152.5)	(18.4, 102.5)	(42.940479, 9.521488)	-128 0	0 1e-6	0 1e-6 (54.6, 148.5)	(38.0, 100.1)
17	119093282.746033	(41.086229, 12.712415)	-457 0	0 1e-6	0 1e-6 (51.8, 151.6)	(18.4, 102.5)	(41.614330, 9.202422)	442 65	-547 1e-6	-4095 1e-6 (53.5, 147.8)	(38.0, 100.1)
19	119093288.377649	(40.754899, 12.615973)	-2261 0	0 1e-6	0 1e-6 (51.5, 151.4)	(18.4, 102.4)	(41.282704, 9.123556)	-55 0	0 1e-6	0 1e-6 (53.3, 147.6)	(38.0, 100.1)

E.9 scene01-09/MER_FR__1PNUPA20031207_104236_000000982022_00180_09252_0537.N1

DATA SET #3 - "Tie points ADS":

No.	Date	FIRST (Lat., Lon.)	Alt. Rough.	Corr. Lat. Lon.	Sun (Zen., Azi.)	View (Zen., Azi.)	LAST (Lat., Lon.)	Alt. Rough.	Corr. Lat. Lon.	Sun (Zen., Azi.)	View (Zen., Azi.)
1	124108956.659803	(49.653164, 7.216756)	409 50	1055 1e-6	4122 1e-6 (72.8, 170.4)	(37.9, 291.6)	(51.323409, -0.566129)	47 25	-8 1e-6	-46 1e-6 (75.5, 163.1)	(4.1, 105.6)
9	124108979.186267	(48.379342, 6.461337)	320 17	806 1e-6	3156 1e-6 (71.6, 169.7)	(37.9, 291.0)	(50.013974, -1.134740)	-60 0	0 1e-6	0 1e-6 (74.4, 162.6)	(4.1, 105.3)
17	124109001.712731	(47.100896, 5.741857)	250 13	615 1e-6	2415 1e-6 (70.4, 169.0)	(38.0, 290.5)	(48.702428, -1.678617)	-7 0	0 1e-6	0 1e-6 (73.2, 162.0)	(4.1, 105.0)
25	124109024.239195	(45.818209, 5.055281)	195 18	469 1e-6	1846 1e-6 (69.2, 168.3)	(38.0, 290.1)	(47.388935, -2.200081)	10 3	-1 1e-6	-9 1e-6 (72.1, 161.5)	(4.1, 104.8)
33	124109046.765659	(44.531627, 4.398887)	262 55	618 1e-6	2432 1e-6 (68.1, 167.7)	(38.0, 289.6)	(46.073645, -2.701183)	-104 0	0 1e-6	0 1e-6 (70.9, 161.0)	(4.1, 104.6)
36	124109055.213083	(44.048219, 4.160015)	137 34	320 1e-6	1263 1e-6 (67.6, 167.4)	(38.0, 289.5)	(45.579975, -2.884227)	-87 0	0 1e-6	0 1e-6 (70.5, 160.8)	(4.1, 104.5)

E.10 scene01-10/MER_FR_1PNUPA20031208_101129_000000982022_00194_09266_0535.N1

DATA SET #3 - "Tie points ADS":

No.	Date	FIRST (Lat., Lon.)	Alt. Rough.	Corr. Lat. Lon.	Sun (Zen., Azi.)	View (Zen., Azi.)	LAST (Lat., Lon.)	Alt. Rough.	Corr. Lat. Lon.	Sun (Zen., Azi.)	View (Zen., Azi.)
1	124193489.202554	(49.271664, 8.360204)	106 4	32 le-6	165 le-6 (73.5, 163.9)	(6.7, 286.5)	(50.497857, 0.477256)	-44 0	0 le-6	0 le-6 (76.4, 156.7)	(36.1, 100.5)
9	124193511.729018	(47.965088, 7.780743)	324 157	96 le-6	494 le-6 (72.3, 163.4)	(6.7, 286.2)	(49.175646, 0.098816)	123 22	-146 le-6	-1213 le-6 (75.2, 156.3)	(36.1, 100.5)
17	124193534.255482	(46.656169, 7.225743)	1439 193	420 le-6	2147 le-6 (71.2, 162.8)	(6.7, 285.9)	(47.852658, -0.268492)	44 6	-52 le-6	-423 le-6 (74.1, 155.9)	(36.1, 100.4)
25	124193556.781946	(45.345087, 6.693028)	2153 390	619 le-6	3142 le-6 (70.0, 162.3)	(6.7, 285.7)	(46.528933, -0.625784)	106 15	-125 le-6	-994 le-6 (72.9, 155.5)	(36.1, 100.4)
33	124193579.308410	(44.032007, 6.180659)	747 231	211 le-6	1067 le-6 (68.9, 161.7)	(6.8, 285.4)	(45.204505, -0.974050)	21 2	-24 le-6	-192 le-6 (71.8, 155.1)	(36.1, 100.4)
36	124193587.755834	(43.539117, 5.993407)	319 51	89 le-6	452 le-6 (68.4, 161.5)	(6.8, 285.3)	(44.707670, -1.102505)	-5 0	0 le-6	0 le-6 (71.4, 155.0)	(36.1, 100.4)

E.11 scene02-01/MER_FR_1PNDPA20040302_103942_000000982024_00409_10483_1126.N1

DATA SET #3 - "Tie points ADS":

No.	Date	FIRST (Lat., Lon.)	Alt. Rough.	Corr. Lat. Lon.	Sun (Zen., Azi.)	View (Zen., Azi.)	LAST (Lat., Lon.)	Alt. Rough.	Corr. Lat. Lon.	Sun (Zen., Azi.)	View (Zen., Azi.)
1	131539182.139727	(49.625284, 8.164910)	245 61	658 le-6	2547 le-6 (58.1, 162.5)	(38.8, 291.7)	(51.310939, 0.393494)	98 10	-11 le-6	-64 le-6 (61.5, 154.1)	(2.7, 105.8)
9	131539204.666191	(48.352861, 7.404165)	483 94	1267 le-6	4915 le-6 (57.0, 161.4)	(38.9, 291.2)	(50.002262, -0.181561)	-49 0	0 le-6	0 le-6 (60.4, 153.3)	(2.7, 105.5)
17	131539227.192655	(47.075725, 6.679666)	1044 177	2676 le-6	10406 le-6 (55.9, 160.4)	(38.9, 290.7)	(48.691410, -0.731444)	233 45	-25 le-6	-144 le-6 (59.4, 152.5)	(2.7, 105.2)
25	131539249.719119	(45.794270, 5.988361)	438 341	1098 le-6	4279 le-6 (54.9, 159.4)	(38.9, 290.2)	(47.378555, -1.258509)	39 19	-4 le-6	-23 le-6 (58.4, 151.6)	(2.7, 104.9)
33	131539272.245583	(44.508844, 5.327512)	826 254	2027 le-6	7915 le-6 (53.8, 158.4)	(38.9, 289.8)	(46.063849, -1.764842)	-40 0	0 le-6	0 le-6 (57.4, 150.8)	(2.7, 104.7)
36	131539280.693007	(44.025851, 5.087037)	173 144	421 le-6	1646 le-6 (53.4, 158.1)	(38.9, 289.6)	(45.570386, -1.949758)	-75 0	0 le-6	0 le-6 (57.0, 150.4)	(2.7, 104.6)

E.12 scene02-02/MER_FR_1PNDPA20040302_103942_000000982024_00409_10483_1126.N1

DATA SET #3 - "Tie points ADS":

No.	Date	FIRST (Lat., Lon.)	Alt. Rough.	Corr. Lat. Lon.	Sun (Zen., Azi.)	View (Zen., Azi.)	LAST (Lat., Lon.)	Alt. Rough.	Corr. Lat. Lon.	Sun (Zen., Azi.)	View (Zen., Azi.)
1	131539182.139727	(51.145019, 1.308982)	59 0	7 le-6	38 le-6 (61.1, 155.1)	(2.7, 286.5)	(52.345710, -6.903788)	88 14	-110 le-6	-1028 le-6 (64.6, 146.7)	(38.8, 100.0)
9	131539204.666191	(49.839405, 0.710308)	14 17	1 le-6	8 le-6 (60.0, 154.2)	(2.7, 286.1)	(51.024262, -7.278522)	-97 0	0 le-6	0 le-6 (63.6, 146.0)	(38.9, 100.0)
17	131539227.192655	(48.531364, 0.138334)	248 9	28 le-6	153 le-6 (59.0, 153.4)	(2.7, 285.8)	(49.702075, -7.641864)	-127 0	0 le-6	0 le-6 (62.6, 145.4)	(38.9, 100.0)
25	131539249.719119	(47.221091, -0.409409)	60 13	6 le-6	36 le-6 (58.0, 152.5)	(2.7, 285.6)	(48.379184, -7.994999)	-147 0	0 le-6	0 le-6 (61.6, 144.7)	(38.9, 99.9)
33	131539272.245583	(45.908761, -0.935113)	15 12	1 le-6	8 le-6 (57.0, 151.6)	(2.7, 285.3)	(47.055620, -8.338972)	-4187 0	0 le-6	0 le-6 (60.6, 144.0)	(38.9, 99.9)
36	131539280.693007	(45.416139, -1.126975)	11 7	1 le-6	6 le-6 (56.6, 151.3)	(2.7, 285.2)	(46.559115, -8.465792)	-4784 0	0 le-6	0 le-6 (60.3, 143.7)	(38.9, 99.9)

E.13 scene02-03/MER_FR_1PNDPA20040302_104117_000000982024_00409_10483_1131.N1

DATA SET #3 - "Tie points ADS":

No.	Date	FIRST (Lat., Lon.)	Alt. Rough.	Corr. Lat. Lon.	Sun (Zen., Azi.)	View (Zen., Azi.)	LAST (Lat., Lon.)	Alt. Rough.	Corr. Lat. Lon.	Sun (Zen., Azi.)	View (Zen., Azi.)
1	131539277.874097	(44.187083, 5.166854)	619 265	1511 le-6	5903 le-6 (53.6, 158.2)	(38.9, 289.7)	(45.735081, -1.888340)	-62 0	0 le-6	0 le-6 (57.1, 150.5)	(2.7, 104.7)
9	131539300.400561	(42.897134, 4.540645)	-525 0	0 le-6	0 le-6 (52.5, 157.2)	(38.9, 289.2)	(44.418253, -2.371344)	-1344 0	0 le-6	0 le-6 (56.1, 149.7)	(2.7, 104.5)
17	131539322.927025	(41.603879, 3.939703)	-2125 0	0 le-6	0 le-6 (51.5, 156.2)	(38.9, 288.8)	(43.099862, -2.837508)	649 186	-68 le-6	-367 le-6 (55.1, 148.8)	(2.7, 104.3)
25	131539345.453489	(40.307565, 3.362081)	-1509 0	0 le-6	0 le-6 (50.5, 155.1)	(38.9, 288.5)	(41.780015, -3.288272)	1001 25	-104 le-6	-555 le-6 (54.1, 147.9)	(2.7, 104.1)
33	131539367.979953	(39.008419, 2.806016)	-166 0	0 le-6	0 le-6 (49.4, 154.1)	(38.9, 288.1)	(40.458810, -3.724928)	681 22	-70 le-6	-370 le-6 (53.2, 147.0)	(2.7, 104.0)
36	131539376.427377	(38.520551, 2.602718)	-2043 0	0 le-6	0 le-6 (49.0, 153.7)	(38.9, 288.0)	(39.963026, -3.885279)	472 41	-48 le-6	-254 le-6 (52.8, 146.6)	(2.7, 103.9)



VisioTerra

Envisat MERIS

Geometry Handbook

reference VT-P194-DOC-001-E

issue 1 revision 5

date 06/07/2005

page 103 of 115

E.14 scene02-04/MER_FR_1PNPDE20040328_102200_00000982025_00280_10855_0002.N1

DATA SET #3 - "Tie points ADS":																							
No.	Date	FIRST (Lat., Lon.)	Alt.	Rough.	Corr.	Lat.	Lon.	Sun (Zen., Azi.)	View (Zen., Azi.)	LAST (Lat., Lon.)	Alt.	Rough.	Corr.	Lat.	Lon.	Sun (Zen., Azi.)	View (Zen., Azi.)						
1	133784520.248060	(51.198988, 13.715287)	164	32	473	1e-6	1807	1e-6 (49.0, 164.0)	(39.7, 292.7)	(52.950155, 5.704595)	-2	0	0	1e-6	0	1e-6 (52.4, 154.4)	(1.4, 106.4)						
9	133784542.774524	(49.934628, 12.898227)	651	37	1830	1e-6	7017	1e-6 (48.0, 162.7)	(39.7, 292.1)	(51.645319, 5.087028)	10	1	0	1e-6	-3	1e-6 (51.4, 153.3)	(1.4, 106.0)						
17	133784565.300988	(48.664890, 12.122121)	464	26	1273	1e-6	4895	1e-6 (46.9, 161.5)	(39.8, 291.5)	(50.337982, 4.498547)	175	20	-10	1e-6	-56	1e-6 (50.4, 152.2)	(1.4, 105.7)						
25	133784587.827452	(47.390239, 11.383432)	1809	613	4851	1e-6	18691	1e-6 (45.8, 160.2)	(39.8, 291.0)	(49.028355, 3.936351)	120	33	-6	1e-6	-37	1e-6 (49.4, 151.1)	(1.4, 105.4)						
33	133784610.353916	(46.111086, 10.679000)	1503	319	3941	1e-6	15220	1e-6 (44.8, 158.9)	(39.8, 290.5)	(47.716621, 3.397969)	247	34	-13	1e-6	-75	1e-6 (48.4, 150.0)	(1.4, 105.2)						
36	133784618.801340	(45.630319, 10.423082)	404	46	1050	1e-6	4061	1e-6 (44.4, 158.4)	(39.8, 290.3)	(47.224212, 3.201762)	254	26	-14	1e-6	-76	1e-6 (48.0, 149.6)	(1.4, 105.1)						

E.15 MER_RR_1PNPDK20030408_093303_000023202015_00208_05773_0848.N1

This product has been generated on February 2003 and contains a defect that has been fixed in the processor: Latitude and longitude corrections are not expressed in 10^{-6} degrees as stated in document R-2 but in 10^{-6} radians.

DATA SET #3 - "Tie points ADS":																							
No.	Date	FIRST (Lat., Lon.)	Alt.	Rough.	Corr.	Lat.	Lon.	Sun (Zen., Azi.)	View (Zen., Azi.)	LAST (Lat., Lon.)	Alt.	Rough.	Corr.	Lat.	Lon.	Sun (Zen., Azi.)	View (Zen., Azi.)						
1	103109583.820036	(69.010207, 47.018145)	-51	0	-4	1e-6	-14	1e-6 (62.2, 191.0)	(40.5, 311.8)	(74.042619, 17.620962)	-242	0	7	1e-6	114	1e-6 (67.9, 158.9)	(40.5, 103.8)						
9	103109606.346500	(67.975274, 44.591548)	20	11	1	1e-6	5	1e-6 (61.1, 188.4)	(40.5, 309.6)	(72.747260, 16.535418)	-437	0	13	1e-6	192	1e-6 (66.8, 157.7)	(40.5, 103.1)						
17	103109628.872964	(66.908355, 42.372819)	-7	1	0	1e-6	-1	1e-6 (59.9, 186.1)	(40.5, 307.6)	(71.447998, 15.575876)	-1293	0	37	1e-6	532	1e-6 (65.7, 156.5)	(40.5, 102.5)						
25	103109651.399428	(65.813653, 40.339576)	-8	27	0	1e-6	-2	1e-6 (58.7, 183.9)	(40.5, 305.8)	(70.145543, 14.717798)	-2501	0	69	1e-6	966	1e-6 (64.6, 155.4)	(40.5, 102.0)						
33	103109673.925892	(64.694747, 38.471623)	-1	16	0	1e-6	0	1e-6 (57.6, 181.9)	(40.5, 304.2)	(68.840428, 13.942550)	-91	0	2	1e-6	33	1e-6 (63.5, 154.4)	(40.5, 101.5)						
41	103109696.452356	(63.554680, 36.750928)	180	30	13	1e-6	45	1e-6 (56.4, 180.0)	(40.5, 302.7)	(67.530606, 13.235743)	-238	0	6	1e-6	82	1e-6 (62.5, 153.5)	(40.5, 101.2)						
49	103109718.978820	(62.396046, 35.161501)	60	23	4	1e-6	14	1e-6 (55.3, 178.2)	(40.5, 301.3)	(66.223758, 12.586091)	-71	75	1	1e-6	23	1e-6 (61.4, 152.5)	(40.5, 100.9)						
57	103109741.505284	(61.221061, 33.689225)	120	19	8	1e-6	28	1e-6 (54.1, 176.5)	(40.5, 300.0)	(64.912769, 11.984627)	233	77	-5	1e-6	-72	1e-6 (60.3, 151.6)	(40.5, 100.6)						
65	103109764.031748	(60.031621, 32.321670)	10	9	0	1e-6	2	1e-6 (53.0, 174.8)	(40.5, 298.9)	(63.600293, 11.424131)	442	65	-10	1e-6	-131	1e-6 (59.3, 150.7)	(40.5, 100.4)						
73	103109786.558212	(58.829354, 31.047899)	50	6	3	1e-6	11	1e-6 (51.9, 173.2)	(40.6, 297.8)	(62.286487, 10.898731)	647	83	-15	1e-6	-184	1e-6 (58.3, 149.8)	(40.6, 100.2)						
81	103109809.084676	(57.615663, 29.858292)	64	11	3	1e-6	14	1e-6 (50.7, 171.7)	(40.6, 296.9)	(60.971483, 10.403599)	635	88	-14	1e-6	-173	1e-6 (57.2, 149.0)	(40.6, 100.1)						
89	103109831.611140	(56.391762, 28.744384)	148	11	8	1e-6	32	1e-6 (49.6, 170.3)	(40.6, 296.0)	(59.655387, 9.934729)	195	92	-4	1e-6	-51	1e-6 (56.2, 148.1)	(40.6, 100.0)						
97	103109854.312018	(55.149121, 27.690865)	173	5	9	1e-6	36	1e-6 (48.5, 168.8)	(40.6, 295.1)	(58.328084, 9.485400)	-635	0	14	1e-6	160	1e-6 (55.2, 147.2)	(40.6, 99.9)						
105	103109876.838482	(53.907758, 26.707302)	207	12	11	1e-6	43	1e-6 (47.4, 167.4)	(40.6, 294.4)	(57.010045, 9.059673)	4	0	0	1e-6	0	1e-6 (54.2, 146.3)	(40.6, 99.8)						
113	103109899.364946	(52.658958, 25.779529)	148	5	7	1e-6	30	1e-6 (46.3, 166.0)	(40.6, 293.6)	(55.691137, 8.651612)	25	4	0	1e-6	-5	1e-6 (53.2, 145.4)	(40.6, 99.7)						
121	103109921.891401	(51.403423, 24.902395)	166	7	8	1e-6	33	1e-6 (45.2, 164.6)	(40.6, 293.0)	(54.371413, 8.259167)	-12	0	0	1e-6	2	1e-6 (52.2, 144.5)	(40.6, 99.7)						
129	103109944.417874	(50.141770, 24.071324)	221	14	11	1e-6	42	1e-6 (44.1, 163.2)	(40.6, 292.4)	(53.050918, 7.880573)	12	4	0	1e-6	-2	1e-6 (51.2, 143.5)	(40.6, 99.6)						
137	103109966.944338	(48.874542, 23.282246)	788	90	39	1e-6	149	1e-6 (43.0, 161.9)	(40.6, 291.8)	(51.729692, 7.514298)	80	13	-1	1e-6	-17	1e-6 (50.3, 142.5)	(40.6, 99.6)						
145	103109989.470802	(47.602224, 22.531532)	127	10	6	1e-6	23	1e-6 (42.0, 160.5)	(40.6, 291.2)	(50.407669, 7.159013)	467	47	-10	1e-6	-97	1e-6 (49.3, 141.5)	(40.6, 99.6)						
153	103110011.997266	(46.325245, 21.815938)	155	132	7	1e-6	28	1e-6 (40.9, 159.1)	(40.6, 290.7)	(49.085180, 6.813549)	268	16	-6	1e-6	-54	1e-6 (48.4, 140.5)	(40.6, 99.6)						
161	103110034.523730	(45.043987, 21.132555)	103	22	4	1e-6	18	1e-6 (39.9, 157.6)	(40.7, 290.3)	(47.761952, 6.476881)	335	12	-7	1e-6	-66	1e-6 (47.5, 139.4)	(40.7, 99.6)						
169	103110057.050194	(43.758792, 20.478773)	324	116	14	1e-6	56	1e-6 (38.9, 156.2)	(40.7, 289.8)	(46.438111, 6.148100)	1288	259	-29	1e-6	-248	1e-6 (46.6, 138.3)	(40.7, 99.6)						
177	103110079.576658	(42.469970, 19.852244)	1694	429	75	1e-6	292	1e-6 (37.9, 154.7)	(40.7, 289.4)	(45.113678, 5.826400)	496	410	-11	1e-6	-93	1e-6 (45.7, 137.2)	(40.7, 99.7)						
185	103110102.103122	(41.177797, 19.250847)	-85	0	-3	1e-6	-14	1e-6 (36.9, 153.2)	(40.7, 289.0)	(43.788677, 5.511059)	541	48	-12	1e-6	-99	1e-6 (44.9, 136.0)	(40.7, 99.7)						
193	103110124.632316	(39.882367, 18.672597)	-128	0	-5	1e-6	-21	1e-6 (35.9, 151.6)	(40.7, 288.6)	(42.462966, 5.201393)	-1915	0	43	1e-6	345	1e-6 (44.0, 134.8)	(40.7, 99.7)						
201	103110147.158780	(38.584220, 18.115900)	-2583	0	-109	1e-6	-424	1e-6 (34.9, 150.0)	(40.7, 288.3)	(41.136887, 4.896896)	-2581	0	59	1e-6	456	1e-6 (43.2, 133.6)	(40.7, 99.8)						
209	103110169.685244	(37.283408, 17.579107)	-2866	0	-119	1e-6	-463	1e-6 (34.0, 148.3)	(40.7, 287.9)	(39.810298, 4.597003)	-792	0	18	1e-6	137	1e-6 (42.4, 132.3)	(40.7, 99.8)						
217	103110192.211708	(35.980119, 17.060785)	-3596	0	-147	1e-6	-572	1e-6 (33.1, 146.5)	(40.7, 287.6)	(38.483217, 4.301234)	-2584	0	59	1e-6	439	1e-6 (41.7, 130.9)	(40.7, 99.9)						
225	103110214.738172	(34.674525, 16.559626)	-1544	0	-62	1e-6	-242	1e-6 (32.2, 144.7)	(40.7, 287.3)	(37.155664, 4.009153)	-2339	0	54	1e-6	391	1e-6 (40.9, 129.5)	(40.7, 99.9)						
233	103110237.264636	(33.366786, 16.074438)	-1212	0	-48	1e-6	-187	1e-6 (31.3, 142.8)	(40.7, 287.0)	(35.827656, 3.720359)	664	20	-15	1e-6	-109	1e-6 (40.2, 128.1)	(40.7, 100.0)						
241	103110259.791100	(32.057047, 15.604127)	-64	0	-2	1e-6	-9	1e-6 (30.5, 140.9)	(40.7, 286.7)	(34.499212, 3.434483)	1038	32	-24	1e-6	-167	1e-6 (39.5, 126.6)	(40.7, 100.0)						
249	103110282.317564	(30.745443, 15.147690)	152	22	5	1e-6	22	1e-6 (29.7															



VisioTerra

reference VT-P194-DOC-001-E

Envisat MERIS

Geometry Handbook

issue 1 revision 5

date 06/07/2005

page 104 of 115

257	103110304.844028	(29.432101, 14.704209)	344	17	13 1e-6	51 1e-6 (28.9, 136.7)	(40.8, 286.2)	(31.841091, 2.870148)	689	18	-16 1e-6	-108 1e-6 (38.3, 123.5)	(40.8, 100.2)
265	103110327.370492	(28.117135, 14.272835)	546	18	20 1e-6	80 1e-6 (28.2, 134.4)	(40.8, 286.0)	(30.511453, 2.591077)	453	7	-10 1e-6	-70 1e-6 (37.7, 121.8)	(40.8, 100.3)
273	103110349.896956	(26.800654, 13.852787)	504	21	18 1e-6	73 1e-6 (27.5, 132.1)	(40.8, 285.8)	(29.181457, 2.313696)	471	12	-11 1e-6	-71 1e-6 (37.1, 120.2)	(40.8, 100.3)
281	103110372.423200	(25.492760, 13.443343)	646	3	23 1e-6	93 1e-6 (26.8, 129.6)	(40.8, 285.5)	(27.851122, 2.037744)	529	23	-12 1e-6	-79 1e-6 (36.6, 118.4)	(40.8, 100.4)
289	103110394.948708	(24.163617, 13.043857)	717	6	25 1e-6	102 1e-6 (26.2, 127.1)	(40.8, 285.3)	(26.520540, 1.762992)	152	2	-3 1e-6	-22 1e-6 (36.1, 116.6)	(40.8, 100.5)
297	103110417.475172	(22.843176, 12.653666)	767	12	27 1e-6	108 1e-6 (25.7, 124.4)	(40.8, 285.1)	(25.189593, 1.489176)	305	26	-7 1e-6	-44 1e-6 (35.7, 114.8)	(40.8, 100.6)
305	103110440.001636	(21.521591, 12.272217)	719	4	25 1e-6	101 1e-6 (25.2, 121.7)	(40.8, 284.9)	(23.858374, 1.216089)	306	7	-7 1e-6	-44 1e-6 (35.3, 112.9)	(40.8, 100.7)
313	103110462.528100	(20.198940, 11.898976)	400	6	13 1e-6	55 1e-6 (24.7, 118.9)	(40.8, 284.8)	(22.526905, 0.943519)	360	1	-9 1e-6	-51 1e-6 (35.0, 111.0)	(40.8, 100.7)
321	103110485.054564	(18.875300, 11.533442)	555	3	18 1e-6	77 1e-6 (24.4, 115.9)	(40.8, 284.6)	(21.195211, 0.671259)	382	3	-9 1e-6	-54 1e-6 (34.7, 109.1)	(40.8, 100.8)
329	103110507.581028	(17.550742, 11.175152)	411	0	13 1e-6	56 1e-6 (24.0, 112.9)	(40.8, 284.4)	(19.863315, 0.399112)	381	2	-9 1e-6	-53 1e-6 (34.4, 107.1)	(40.8, 100.9)
337	103110530.107492	(16.225334, 10.823668)	397	6	13 1e-6	54 1e-6 (23.8, 109.9)	(40.8, 284.2)	(18.531245, 0.126886)	403	2	-10 1e-6	-56 1e-6 (34.2, 105.1)	(40.8, 101.0)
345	103110552.633956	(14.899140, 10.478584)	437	4	14 1e-6	59 1e-6 (23.6, 106.8)	(40.8, 284.1)	(17.199026, -0.145608)	324	3	-8 1e-6	-45 1e-6 (34.1, 103.1)	(40.8, 101.1)
353	103110575.160420	(13.572225, 10.139516)	465	12	15 1e-6	63 1e-6 (23.5, 103.6)	(40.8, 283.9)	(15.866684, -0.418554)	386	9	-10 1e-6	-53 1e-6 (33.9, 101.0)	(40.8, 101.2)
361	103110597.686884	(12.244646, 9.806103)	361	5	11 1e-6	48 1e-6 (23.4, 100.5)	(40.8, 283.8)	(14.532450, -0.692135)	302	12	-8 1e-6	-41 1e-6 (33.9, 99.0)	(40.8, 101.3)
369	103110620.213348	(10.916460, 9.478006)	610	24	19 1e-6	81 1e-6 (23.5, 97.3)	(40.8, 283.6)	(13.201750, -0.966529)	303	12	-8 1e-6	-41 1e-6 (33.9, 96.9)	(40.8, 101.4)
377	103110642.739812	(9.587724, 9.154905)	1139	12	35 1e-6	152 1e-6 (23.5, 94.2)	(40.8, 283.5)	(11.869216, -1.241915)	273	0	-7 1e-6	-37 1e-6 (33.9, 94.9)	(40.8, 101.5)
385	103110665.269006	(8.258327, 8.836457)	170	6	5 1e-6	22 1e-6 (23.7, 91.1)	(40.8, 283.3)	(10.536516, -0.518506)	152	19	-4 1e-6	-20 1e-6 (34.0, 92.9)	(40.8, 101.6)
393	103110687.795470	(6.928644, 8.522453)	152	4	4 1e-6	20 1e-6 (23.9, 88.0)	(40.8, 283.2)	(9.204005, -1.796414)	178	6	-4 1e-6	-23 1e-6 (34.1, 90.9)	(40.8, 101.7)
401	103110710.321934	(5.598562, 8.212579)	152	14	4 1e-6	20 1e-6 (24.2, 85.1)	(40.8, 283.0)	(7.871554, -2.075851)	229	23	-6 1e-6	-30 1e-6 (34.3, 88.9)	(40.8, 101.8)
409	103110732.848398	(4.268129, 7.906576)	-4	0	0 1e-6	0 1e-6 (24.6, 82.2)	(40.8, 282.9)	(6.539196, -0.357001)	146	77	-4 1e-6	-19 1e-6 (34.6, 86.9)	(40.8, 101.9)
417	103110755.374862	(2.937389, 7.604195)	-2314	0	-69 1e-6	-306 1e-6 (25.0, 79.4)	(40.8, 282.8)	(5.206967, -2.640048)	41	1	-1 1e-6	-5 1e-6 (34.8, 85.0)	(40.8, 102.1)
425	103110777.901326	(1.606388, 7.305199)	-1644	0	-48 1e-6	-217 1e-6 (25.5, 76.7)	(40.8, 282.7)	(3.874902, -2.925181)	-2916	0	83 1e-6	387 1e-6 (35.2, 83.1)	(40.8, 102.2)
433	103110800.427790	(0.275169, 7.009358)	-2809	0	-82 1e-6	-371 1e-6 (26.0, 74.2)	(40.8, 282.5)	(2.543036, -3.212592)	-4979	0	143 1e-6	660 1e-6 (35.5, 81.3)	(40.8, 102.3)
441	103110822.954254	(-1.056227, 6.716454)	-3197	0	-93 1e-6	-423 1e-6 (26.6, 71.7)	(40.8, 282.4)	(1.211409, -3.502478)	-5006	0	145 1e-6	662 1e-6 (36.0, 79.5)	(40.8, 102.4)
449	103110845.480718	(-2.387761, 6.426274)	-3625	0	-104 1e-6	-480 1e-6 (27.2, 69.4)	(40.8, 282.3)	(-0.119941, -3.795045)	-5006	0	147 1e-6	662 1e-6 (36.4, 77.8)	(40.8, 102.5)
457	103110868.007182	(-3.719394, 6.138614)	-4544	0	-129 1e-6	-603 1e-6 (27.9, 67.1)	(40.8, 282.2)	(-1.450976, -4.090501)	-5000	0	148 1e-6	661 1e-6 (36.9, 76.1)	(40.8, 102.6)
465	103110890.533646	(-5.051087, 5.853275)	-4817	0	-136 1e-6	-640 1e-6 (28.6, 65.0)	(40.8, 282.1)	(-2.781653, -4.389063)	-4803	0	143 1e-6	635 1e-6 (37.4, 74.5)	(40.8, 102.8)
473	103110913.060110	(-6.382805, 5.570063)	-4885	0	-137 1e-6	-651 1e-6 (29.4, 63.0)	(40.8, 282.0)	(-4.111930, -4.690959)	-4402	0	133 1e-6	582 1e-6 (38.0, 72.9)	(40.8, 102.9)
481	103110935.585398	(-7.714442, 5.288802)	-5090	0	-141 1e-6	-680 1e-6 (30.1, 61.2)	(40.7, 281.8)	(-5.441695, -4.996407)	-4740	0	144 1e-6	627 1e-6 (38.6, 71.4)	(40.7, 103.0)
489	103110958.111862	(-9.046103, 5.009279)	-5289	0	-145 1e-6	-709 1e-6 (31.0, 59.4)	(40.7, 281.7)	(-6.771040, -5.305685)	-4410	0	135 1e-6	585 1e-6 (39.3, 70.0)	(40.7, 103.2)
497	103110980.638326	(-10.377686, 4.731325)	-5416	0	-147 1e-6	-729 1e-6 (31.8, 57.7)	(40.7, 281.6)	(-8.098551, -5.619034)	-4600	0	143 1e-6	611 1e-6 (39.9, 68.6)	(40.7, 103.3)
505	103111003.164790	(-11.709158, 4.454759)	-5467	0	-147 1e-6	-739 1e-6 (32.7, 56.1)	(40.7, 281.5)	(-9.428079, -5.936724)	-4299	0	135 1e-6	573 1e-6 (40.6, 67.3)	(40.7, 103.4)
513	103111025.691254	(-13.040488, 4.179403)	-5429	0	-145 1e-6	-738 1e-6 (33.6, 54.6)	(40.7, 281.4)	(-10.755675, -6.259039)	-4438	0	140 1e-6	593 1e-6 (41.4, 66.0)	(40.7, 103.6)
521	103111048.217178	(-14.371647, 3.905077)	-5434	0	-144 1e-6	-743 1e-6 (34.5, 53.2)	(40.7, 281.3)	(-12.082587, -6.586279)	-4405	0	141 1e-6	591 1e-6 (42.1, 64.8)	(40.7, 103.7)
529	103111070.744182	(-15.702605, 3.631604)	-5437	0	-142 1e-6	-748 1e-6 (35.5, 51.9)	(40.7, 281.2)	(-13.408761, -6.918758)	-3984	0	129 1e-6	536 1e-6 (42.9, 63.7)	(40.7, 103.9)
537	103111093.270646	(-17.033335, 3.358804)	-5403	0	-140 1e-6	-748 1e-6 (36.4, 50.7)	(40.7, 281.1)	(-14.734143, -7.256813)	-4198	0	137 1e-6	568 1e-6 (43.7, 62.6)	(40.7, 104.0)
545	103111115.797110	(-18.363809, 3.086495)	-5407	0	-139 1e-6	-754 1e-6 (37.4, 49.5)	(40.6, 281.0)	(-16.058674, -7.600796)	-4331	0	143 1e-6	589 1e-6 (44.6, 61.6)	(40.6, 104.2)
553	103111138.323574	(-19.694000, 2.814495)	-5376	0	-137 1e-6	-755 1e-6 (38.4, 48.5)	(40.6, 280.9)	(-17.382294, -7.951087)	-4194	0	140 1e-6	574 1e-6 (45.4, 60.6)	(40.6, 104.4)
561	103111160.850038	(-21.023885, 2.542617)	-5388	0	-136 1e-6	-764 1e-6 (39.4, 47.4)	(40.6, 280.9)	(-18.704940, -8.308085)	-3829	0	129 1e-6	527 1e-6 (46.3, 59.7)	(40.6, 104.5)
569	103111183.376502	(-22.353439, 2.270668)	-5181	0	-130 1e-6	-741 1e-6 (40.5, 46.5)	(40.6, 280.8)	(-20.026546, -6.672218)	-3715	0	127 1e-6	515 1e-6 (47.2, 58.8)	(40.6, 104.7)
577	103111205.905696	(-23.682798, 1.998420)	-5244	0	-130 1e-6	-757 1e-6 (41.5, 45.6)	(40.6, 280.7)	(-21.347203, -9.043991)	-3992	0	138 1e-6	557 1e-6 (48.1, 58.0)	(40.6, 104.9)
585	103111228.432160	(-25.011619, 1.725736)	-5155	0	-127 1e-6	-752 1e-6 (42.6, 44.7)	(40.6, 280.6)	(-22.666518, -9.423801)	-4085	0	143 1e-6	575 1e-6 (49.0, 57.3)	(40.6, 105.1)
593	103111250.958624	(-26.340042, 1.452371)	-5241	0	-128 1e-6	-773 1e-6 (43.6, 43.9)	(40.6, 280.5)	(-23.984574, -9.812219)	-4182	0	148 1e-6	593 1e-6 (50.0, 56.6)	(40.6, 105.3)
601	103111273.485088	(-27.668044, 1.178107)	-4589	0	-111 1e-6	-684 1e-6 (44.7, 43.2)	(40.5, 280.4)	(-25.301289, -10.209809)	-4038	0	145 1e-6	578 1e-6 (50.9, 55.9)	(40.5, 105.5)
609	103111296.011552	(-28.995607, 0.902712)	-4421	0	-106 1e-6	-667 1e-6 (45.8, 42.5)	(40.5, 280.3)	(-26.615678, -10.617177)	-3976	0	144 1e-6	574 1e-6 (51.9, 55.3)	(40.5, 105.7)
617	103111318.538016	(-30.322710, 0.625946)	-2517	0	-60 1e-6	-385 1e-6 (46.9, 41.9)	(40.5, 280.3)	(-27.930350, -11.034978)	-3569	0	131 1e-6	521 1e-6 (52.9, 54.8)	(40.5, 106.0)
625													

721	103111611.384778	(-47.525514, -3.243639)	-4239	0	-94	1e-6	-823	1e-6	(61.5, 36.8)	(40.3, 279.6)	(-44.814626, -17.839679)	-3510	0	161	1e-6	618	1e-6	(66.7, 51.8)	(40.3, 110.2)
729	103111633.911242	(-48.844383, -3.578024)	-3947	0	-87	1e-6	-786	1e-6	(62.7, 36.6)	(40.2, 279.6)	(-46.092284, -18.515580)	-3976	0	186	1e-6	713	1e-6	(67.8, 51.9)	(40.2, 110.6)
737	103111656.437706	(-50.162529, -3.920955)	-2962	0	-65	1e-6	-606	1e-6	(63.9, 36.5)	(40.2, 279.6)	(-47.365666, -19.222939)	-4000	0	191	1e-6	732	1e-6	(68.9, 52.0)	(40.2, 111.1)
745	103111678.964170	(-51.479928, -4.273426)	-2400	0	-53	1e-6	-504	1e-6	(65.0, 36.4)	(40.2, 279.6)	(-48.634404, -19.964570)	-3326	0	163	1e-6	621	1e-6	(70.0, 52.2)	(40.2, 111.7)
753	103111701.490634	(-52.796553, -4.636560)	-2033	0	-45	1e-6	-440	1e-6	(66.2, 36.3)	(40.2, 279.6)	(-49.898088, -20.743613)	-4096	0	205	1e-6	781	1e-6	(71.2, 52.5)	(40.2, 112.2)
761	103111724.017098	(-54.112373, -5.011641)	-2463	0	-54	1e-6	-549	1e-6	(67.3, 36.2)	(40.2, 279.7)	(-51.156253, -21.563575)	-4540	0	233	1e-6	885	1e-6	(72.3, 52.8)	(40.2, 112.9)
769	103111746.718167	(-55.437543, -5.403206)	-2992	0	-66	1e-6	-689	1e-6	(68.5, 36.2)	(40.2, 279.7)	(-52.418057, -22.435275)	-4501	0	238	1e-6	897	1e-6	(73.4, 53.2)	(40.2, 113.5)
777	103111769.244631	(-56.751636, -5.806939)	-3104	0	-69	1e-6	-739	1e-6	(69.7, 36.2)	(40.1, 279.8)	(-53.663494, -23.349747)	-4018	0	218	1e-6	819	1e-6	(74.6, 53.7)	(40.1, 114.2)
785	103111791.771095	(-58.064801, -6.227764)	-4006	0	-90	1e-6	-988	1e-6	(70.8, 36.3)	(40.1, 279.8)	(-54.901622, -24.318486)	-3991	0	223	1e-6	833	1e-6	(75.7, 54.2)	(40.1, 115.0)
793	103111814.297559	(-59.376981, -6.667977)	-4999	0	-114	1e-6	-1279	1e-6	(72.0, 36.3)	(40.1, 279.9)	(-56.131674, -25.347094)	-7005	0	403	1e-6	1498	1e-6	(76.9, 54.8)	(40.1, 115.8)
801	103111836.824023	(-60.688109, -7.130273)	-5220	0	-120	1e-6	-1389	1e-6	(73.2, 36.5)	(40.1, 280.1)	(-57.352774, -26.441906)	-1893	0	112	1e-6	414	1e-6	(78.0, 55.5)	(40.1, 116.7)
809	103111859.350487	(-61.998105, -7.617840)	-5204	0	-121	1e-6	-1442	1e-6	(74.3, 36.6)	(40.1, 280.2)	(-58.563918, -27.610088)	-3209	0	196	1e-6	721	1e-6	(79.2, 56.2)	(40.1, 117.6)
817	103111881.876951	(-63.306870, -8.134481)	-5228	0	-124	1e-6	-1513	1e-6	(75.5, 36.8)	(40.1, 280.4)	(-59.763948, -28.859770)	-2518	0	159	1e-6	580	1e-6	(80.3, 57.1)	(40.1, 118.6)
825	103111904.403415	(-64.614286, -8.684763)	-5193	0	-125	1e-6	-1573	1e-6	(76.7, 37.1)	(40.1, 280.6)	(-60.951527, -30.200177)	-4133	0	271	1e-6	976	1e-6	(81.5, 58.1)	(40.1, 119.8)

APPENDIX F - QUALITY CONTROLS OF ACE AND GETASSE30

F.1 Differences between GPS points and ACE DEM – Nearest neighbour

DEM ".../DEM_ACE/ACE_30sec/EUROPA_WGS84" controlled by "EUVN_ETRF.BLH" GCPs:

NUMBER OF GCPs IN INPUT : 192
 NUMBER OF PROCESSED GCPs : 144 (75.0%)
 NUMBER OF GCPs OUTSIDE THE DEM : 48 (25.0%)
 ELEVATION DIFFERENCES :
 . ARITHMETIC MEAN : -2201.149
 . QUADRATIC MEAN : 12109.911
 . STANDARD DEVIATION : 11908.186
 . MINIMUM : -65001.139
 . MAXIMUM : 325.560

GCP #	EASTING	NORTHING	GCP	ELEVAT.	DEM	ELEVAT.	DIFFERENCE	21 :	-6.205649	36.464351	84.180	51.000	>	33.180
1 :	17.073455	52.276957		124.366	78.000	->	46.366	21 :	11.877930	45.406732	84.043	16.000	->	68.043
2 :	4.359235	50.797807		149.668	101.000	->	48.668	22 :	-3.951976	40.443603	647.362	595.000	->	52.362
3 :	8.972749	39.135881		238.378	142.000	->	96.378	23 :	18.367308	57.653880	79.787	31.000	->	48.787
4 :	3.399645	50.933714		63.894	15.000	->	48.894	24 :	12.878888	49.144195	666.026	587.000	->	79.026
5 :	4.594950	50.094902		282.695	148.000	->	134.695	25 :	7.465296	46.877115	956.342	850.000	->	106.342
6 :	0.492343	40.820895		107.810	6.000	->	101.810	26 :	15.598375	48.654545	457.606	393.000	->	64.606
7 :	14.785635	49.913677		592.594	466.000	->	126.594	27 :	13.683435	46.554197	687.372	568.000	->	119.372
8 :	6.920585	43.754725		1319.310	1260.000	->	59.310	28 :	12.082992	47.496026	630.059	531.000	->	99.059
9 :	15.493466	47.067107		538.290	430.000	->	108.290	29 :	23.394726	42.556098	1119.560	794.000	->	325.560
10 :	0.336269	50.867308		76.489	14.000	->	62.489	30 :	27.909290	43.192709	38.243	5.000	->	33.243
11 :	21.031561	52.097275		141.447	112.000	->	29.447	31 :	21.035229	52.474971	139.882	79.000	->	60.882
12 :	5.809620	52.178407		96.846	53.000	->	43.846	32 :	4.358834	50.798668	157.470	101.000	->	56.470
13 :	20.669911	53.892409		187.031	145.000	->	42.031	33 :	7.668582	47.567070	504.933	475.000	->	29.933
14 :	16.704471	40.649120		535.657	471.000	->	64.657	34 :	7.209528	45.958605	1683.440	1918.000	->	-234.560
15 :	11.646799	44.519965		50.057	10.000	->	40.057	35 :	6.102058	46.454101	1258.260	1213.000	->	45.260
16 :	14.989779	36.876079		126.244	101.000	->	25.244	36 :	8.670456	46.659734	2094.220	2176.000	->	-81.780
17 :	11.925486	57.395302		45.547	13.000	->	32.547	37 :	8.498912	47.713004	563.324	498.000	->	65.324
18 :	19.281520	47.789608		291.748	209.000	->	82.748	38 :	8.940319	45.851463	429.707	360.000	->	69.707
19 :	13.066073	52.379286		144.420	30.000	->	114.420	39 :	10.100730	46.698581	1612.690	1519.000	->	93.690
20 :	24.058785	56.948625		34.702	0.000	->	34.702	40 :	14.969324	50.817232	338.631	320.000	->	18.631



VisioTerra

Envisat MERIS

Geometry Handbook

reference VT-P194-DOC-001-E

issue 1 revision 5

date 06/07/2005

page 107 of 115

42 :	13.666705	49.462587	547.358	518.000 ->	29.358	85 :	18.060776	42.657912	46.673	21.000 ->	25.673
43 :	17.246431	49.505901	303.702	259.000 ->	44.702	86 :	18.711655	45.153943	146.095	76.000 ->	70.095
44 :	15.935217	49.858445	427.682	396.000 ->	31.682	87 :	16.438445	43.506635	47.627	1.000 ->	46.627
45 :	11.228598	52.335512	153.490	87.000 ->	66.490	88 :	15.978647	45.806199	160.909	120.000 ->	40.909
46 :	9.681841	50.508463	334.877	282.000 ->	52.877	89 :	15.679620	44.845120	713.172	657.000 ->	56.172
47 :	6.761590	50.673819	217.982	168.000 ->	49.982	90 :	21.632365	48.377004	155.772	117.000 ->	38.772
48 :	9.283692	48.400209	760.506	723.000 ->	37.506	91 :	20.670770	46.319570	142.470	91.000 ->	51.470
49 :	7.295758	49.914766	526.493	450.000 ->	76.493	92 :	18.619237	47.255668	234.628	159.000 ->	75.628
50 :	12.487501	50.840896	334.308	283.000 ->	51.308	93 :	-9.583063	51.871472	62.621	72.000 ->	-9.379
51 :	11.141565	48.917419	597.626	533.000 ->	64.626	94 :	-6.541173	53.711583	135.615	68.000 ->	67.615
52 :	8.007257	52.363932	128.934	62.000 ->	66.934	95 :	-7.339016	55.371616	82.705	1.000 ->	81.705
53 :	12.088951	54.177972	49.546	3.000 ->	46.546	96 :	16.867878	41.132069	63.116	2.000 ->	61.116
54 :	23.932619	38.078547	514.553	392.000 ->	122.553	97 :	15.094687	37.501178	51.971	9.000 ->	42.971
55 :	12.499933	55.738882	87.938	28.000 ->	59.938	98 :	11.788148	42.096242	57.488	7.000 ->	50.488
56 :	12.499819	55.738824	86.715	40.000 ->	46.715	99 :	14.850322	40.649523	86.635	28.000 ->	58.635
57 :	27.248784	57.842324	107.504	96.000 ->	11.504	100 :	8.925651	44.412079	49.339	48.000 ->	1.339
58 :	24.380271	59.463565	84.272	29.000 ->	55.272	101 :	11.075102	42.871680	68.406	105.000 ->	-36.594
59 :	-2.459192	36.852473	125.048	137.000 ->	-11.952	102 :	11.231004	43.803827	144.673	56.000 ->	88.673
60 :	2.157415	41.350939	67.660	10.000 ->	57.660	103 :	12.452550	41.922461	201.931	36.000 ->	165.931
61 :	-1.024620	41.721528	269.634	194.000 ->	75.634	104 :	14.213193	42.464939	68.747	2.000 ->	66.747
62 :	-8.398931	43.364369	66.957	1.000 ->	65.957	105 :	13.759409	45.647203	56.199	18.000 ->	38.199
63 :	2.624605	39.552594	59.085	2.000 ->	57.085	106 :	9.115185	39.210538	60.143	13.000 ->	47.143
64 :	-4.110514	38.686741	763.213	700.000 ->	63.213	107 :	5.810079	52.178523	89.310	53.000 ->	36.310
65 :	22.976524	59.822697	24.858	1.000 ->	23.858	108 :	23.371464	55.913575	164.821	136.000 ->	28.821
66 :	-0.561842	44.815672	53.915	5.000 ->	48.915	109 :	25.298666	54.653125	240.831	169.000 ->	71.831
67 :	3.735284	46.620143	257.485	236.000 ->	21.485	110 :	24.410065	57.315888	26.406	12.000 ->	14.406
68 :	-4.503849	48.407887	104.411	46.000 ->	58.411	111 :	21.000909	56.514952	36.258	2.000 ->	34.258
69 :	0.105997	49.481896	53.632	65035.000 ->	-64981.368	112 :	21.851980	57.554411	40.611	6.000 ->	34.611
70 :	6.128414	48.762776	241.724	194.000 ->	47.724	113 :	-4.249170	40.427214	815.088	831.000 ->	-15.912
71 :	2.424987	48.844424	126.148	58.000 ->	68.148	114 :	22.863652	42.001531	1264.160	1111.000 ->	153.160
72 :	-0.199389	46.990445	133.433	87.000 ->	46.433	115 :	11.441623	59.125635	141.486	90.000 ->	51.486
73 :	-1.685527	55.212790	144.401	79.000 ->	65.401	116 :	11.925486	57.395302	45.558	13.000 ->	32.558
74 :	-2.782971	56.478513	57.779	1.000 ->	56.779	117 :	9.784687	47.515331	1090.310	825.000 ->	265.310
75 :	-1.450672	50.930791	98.586	10.000 ->	88.586	118 :	19.201822	50.512247	367.231	300.000 ->	67.231
76 :	-2.386369	54.446576	356.112	304.000 ->	52.112	119 :	15.552539	52.578390	101.438	38.000 ->	63.438
77 :	-1.192268	52.940670	98.465	32.000 ->	66.465	120 :	22.359563	53.734044	154.602	120.000 ->	34.602
78 :	25.566236	40.928037	182.585	126.000 ->	56.585	121 :	18.326514	54.827479	70.796	65035.000 ->	-64964.204
79 :	20.664811	39.734223	598.607	571.000 ->	27.607	122 :	16.853840	54.587695	33.861	65035.000 ->	-65001.139
80 :	21.320333	37.644130	26.885	1.000 ->	25.885	123 :	-6.941155	41.022116	221.752	144.000 ->	77.752
81 :	15.493466	47.067165	540.068	430.000 ->	110.068	124 :	-7.051678	38.878854	229.935	166.000 ->	63.935
82 :	0.335639	50.867421	70.809	14.000 ->	56.809	125 :	-8.707011	41.196354	70.070	29.000 ->	41.070
83 :	14.585901	45.255471	182.398	163.000 ->	19.398	126 :	-8.668737	37.100047	55.347	35.000 ->	20.347
84 :	15.570243	45.578563	268.988	185.000 ->	83.988	127 :	27.204036	47.242718	222.944	67.000 ->	155.944



reference VT-P194-DOC-001-E

Envisat MERIS

Geometry Handbook

issue 1 revision 5

date 06/07/2005

page 108 of 115

128 :	21.345945	45.738362	140.156	95.000 ->	45.156	137 :	18.884517	49.165908	415.054	507.000 ->	-91.946
129 :	28.624054	44.588148	156.390	106.000 ->	50.390	138 :	1.480752	43.560778	207.106	145.000 ->	62.106
130 :	11.217940	58.353462	45.196	65035.000 ->	-64989.804	139 :	26.717480	38.426617	58.650	10.000 ->	48.650
131 :	18.090914	59.322331	35.084	65035.000 ->	-64999.916	140 :	22.452611	48.562870	273.801	201.000 ->	72.801
132 :	15.185443	46.286396	342.172	316.000 ->	26.172	141 :	18.367308	57.653880	79.788	31.000 ->	48.788
133 :	16.476891	46.565884	385.191	281.000 ->	104.191	142 :	6.604485	52.914599	82.275	17.000 ->	65.275
134 :	13.643386	45.503793	323.127	124.000 ->	199.127	143 :	12.878487	49.143966	660.272	587.000 ->	73.272
135 :	18.729417	47.836647	261.732	232.000 ->	29.732	144 :	12.878945	49.144253	665.937	587.000 ->	78.937
136 :	20.323501	49.034587	743.178	689.000 ->	54.178						

F.2 Differences between GPS points and GETASSE30 DEM – Nearest neighbour

DEM ".../DEM_GETASSE30/EUROPA_WGS84" controlled by "EUVN_ETRF.BLH" GCPs:

NUMBER OF GCPs IN INPUT : 217
NUMBER OF PROCESSED GCPs : 169 (77.9%)
NUMBER OF GCPs OUTSIDE THE DEM : 48 (22.1%)
ELEVATION DIFFERENCES :
. ARITHMETIC MEAN : 10.828
. QUADRATIC MEAN : 32.368
. STANDARD DEVIATION : 30.503
. MINIMUM : -127.560
. MAXIMUM : 100.931

GCP #	EASTING	NORTHING	GCP	ELEVAT.	DEM	ELEVAT.	DIFFERENCE	15 :	11.646799	44.519965	50.057	49.000 ->	1.057
1 :	17.073455	52.276957	124.366	111.000 ->	13.366	16 :	14.989779	36.876079	126.244	152.000 ->	-25.756		
2 :	4.359235	50.797807	149.668	134.000 ->	15.668	17 :	11.925486	57.395302	45.547	36.000 ->	9.547		
3 :	8.972749	39.135881	238.378	162.000 ->	76.378	18 :	19.281520	47.789608	291.748	299.000 ->	-7.252		
4 :	3.399645	50.933714	63.894	55.000 ->	8.894	19 :	13.066073	52.379286	144.420	105.000 ->	39.420		
5 :	4.594950	50.094902	282.695	217.000 ->	65.695	20 :	24.058785	56.948625	34.702	33.000 ->	1.702		
6 :	0.492343	40.820895	107.810	58.000 ->	49.810	21 :	-6.205649	36.464351	84.180	66.000 ->	18.180		
7 :	14.785635	49.913677	592.594	555.000 ->	37.594	22 :	11.877930	45.406732	84.043	63.000 ->	21.043		
8 :	6.920585	43.754725	1319.310	1303.000 ->	16.310	23 :	-3.951976	40.443603	647.362	668.000 ->	-20.638		
9 :	15.493466	47.067107	538.290	472.000 ->	66.290	24 :	18.367308	57.653880	79.787	80.000 ->	-0.213		
10 :	0.336269	50.867308	76.489	52.000 ->	24.489	25 :	12.878888	49.144195	666.026	627.000 ->	39.026		
11 :	21.031561	52.097275	141.447	135.000 ->	6.447	26 :	7.465296	46.877115	956.342	908.000 ->	48.342		
12 :	5.809620	52.178407	96.846	82.000 ->	14.846	27 :	15.598375	48.654545	457.606	440.000 ->	17.606		
13 :	20.669911	53.892409	187.031	180.000 ->	7.031	28 :	13.683435	46.554197	687.372	677.000 ->	10.372		
14 :	16.704471	40.649120	535.657	500.000 ->	35.657	29 :	12.082992	47.496026	630.059	569.000 ->	61.059		



VisioTerra

Envisat MERIS

Geometry Handbook

reference VT-P194-DOC-001-E

issue 1 revision 5

date 06/07/2005

page 109 of 115

30 :	2.927413	51.234919	54.461	48.000 ->	6.461	73 :	22.976524	59.822697	24.858	29.000 ->	-4.142
31 :	27.482093	42.483503	41.743	38.000 ->	3.743	74 :	8.762702	41.927389	96.797	48.000 ->	48.797
32 :	23.394726	42.556098	1119.560	1029.000 ->	90.560	75 :	-0.561842	44.815672	53.915	53.000 ->	0.915
33 :	27.7909290	43.192709	38.243	37.000 ->	1.243	76 :	3.735284	46.620143	257.485	258.000 ->	-0.515
34 :	21.035229	52.474971	139.882	131.000 ->	8.882	77 :	-4.503849	48.407887	104.411	97.000 ->	7.411
35 :	4.358834	50.798668	157.470	134.000 ->	23.470	78 :	0.105997	49.481896	53.632	49.000 ->	4.632
36 :	7.668582	47.567070	504.933	480.000 ->	24.933	79 :	5.353775	43.278770	61.797	49.000 ->	12.797
37 :	7.209528	45.958605	1683.440	1811.000 ->	-127.560	80 :	6.128414	48.762776	241.724	246.000 ->	-4.276
38 :	6.102058	46.454101	1258.260	1363.000 ->	-104.740	81 :	2.424987	48.844424	126.148	94.000 ->	32.148
39 :	8.670456	46.659734	2094.220	2214.000 ->	-119.780	82 :	-1.681746	43.395136	54.264	80.000 ->	-25.736
40 :	8.498912	47.713004	563.324	541.000 ->	22.324	83 :	-0.199389	46.990445	133.433	133.000 ->	0.433
41 :	8.940319	45.851463	429.707	406.000 ->	23.707	84 :	-1.685527	55.212790	144.401	136.000 ->	8.401
42 :	10.100730	46.698581	1612.690	1578.000 ->	34.690	85 :	-5.924040	54.622245	67.897	55.000 ->	12.897
43 :	14.969324	50.817232	338.631	360.000 ->	-21.369	86 :	-2.782971	56.478513	57.779	51.000 ->	6.779
44 :	13.666705	49.462587	547.358	599.000 ->	-51.642	87 :	-5.355838	36.131807	45.469	42.000 ->	3.469
45 :	17.246431	49.505901	303.702	284.000 ->	19.702	88 :	-1.450672	50.930791	98.586	67.000 ->	31.586
46 :	15.935217	49.858445	427.682	424.000 ->	3.682	89 :	-2.386369	54.446576	356.112	353.000 ->	3.112
47 :	11.228598	52.335512	153.490	146.000 ->	7.490	90 :	-5.542908	50.102924	57.507	53.000 ->	4.507
48 :	9.681841	50.508463	334.877	330.000 ->	4.877	91 :	-1.192268	52.940670	98.465	77.000 ->	21.465
49 :	8.717037	53.868059	45.021	40.000 ->	5.021	92 :	25.566236	40.928037	182.585	246.000 ->	-63.415
50 :	6.761590	50.673819	217.982	217.000 ->	0.982	93 :	20.664811	39.734223	598.607	566.000 ->	32.607
51 :	9.283692	48.400209	760.506	743.000 ->	17.506	94 :	21.320333	37.644130	26.885	23.000 ->	3.885
52 :	7.295758	49.914766	526.493	509.000 ->	17.493	95 :	15.493466	47.067165	540.068	472.000 ->	68.068
53 :	12.487501	50.840896	334.308	327.000 ->	7.308	96 :	0.335639	50.867421	70.809	52.000 ->	18.809
54 :	11.141565	48.917419	597.626	586.000 ->	11.626	97 :	14.585901	45.255471	182.398	168.000 ->	14.398
55 :	8.007257	52.363932	128.934	121.000 ->	7.934	98 :	15.570243	45.578563	268.988	199.000 ->	69.988
56 :	12.088951	54.177972	49.546	42.000 ->	7.546	99 :	18.060776	42.657912	46.673	67.000 ->	-20.327
57 :	23.932619	38.078547	514.553	519.000 ->	-4.447	100 :	18.711655	45.153943	146.095	128.000 ->	18.095
58 :	12.499933	55.738882	87.938	81.000 ->	6.938	101 :	16.438445	43.506635	47.627	56.000 ->	-8.373
59 :	9.962361	57.595037	42.208	53.000 ->	-10.792	102 :	15.978647	45.806199	160.909	164.000 ->	-3.091
60 :	8.439783	55.460139	43.303	40.000 ->	3.303	103 :	13.629348	45.084043	53.589	53.000 ->	0.589
61 :	11.924512	54.572108	40.619	38.000 ->	2.619	104 :	15.679620	44.845120	713.172	758.000 ->	-44.828
62 :	12.499819	55.738824	86.715	81.000 ->	5.715	105 :	21.632365	48.377004	155.772	135.000 ->	20.772
63 :	27.248784	57.842324	107.504	110.000 ->	-2.496	106 :	20.670770	46.319570	142.470	128.000 ->	14.470
64 :	24.380271	59.463565	84.272	51.000 ->	33.272	107 :	18.619237	47.255668	234.628	228.000 ->	6.628
65 :	-0.481227	38.338897	60.347	49.000 ->	11.347	108 :	-9.583063	51.871472	62.621	73.000 ->	-10.379
66 :	-2.459192	36.852473	125.048	87.000 ->	38.048	109 :	-6.541173	53.711583	135.615	94.000 ->	41.615
67 :	2.157415	41.350939	67.660	49.000 ->	18.660	110 :	-7.339016	55.371616	82.705	67.000 ->	15.705
68 :	-1.024620	41.721528	269.634	258.000 ->	11.634	111 :	16.867878	41.132069	63.116	47.000 ->	16.116
69 :	-8.398931	43.364369	66.957	61.000 ->	5.957	112 :	15.094687	37.501178	51.971	50.000 ->	1.971
70 :	2.624605	39.552594	59.085	49.000 ->	10.085	113 :	11.788148	42.096242	57.488	70.000 ->	-12.512
71 :	-4.110514	38.686741	763.213	732.000 ->	31.213	114 :	14.850322	40.649523	86.635	77.000 ->	9.635
72 :	-3.789428	43.461426	59.281	50.000 ->	9.281	115 :	8.925651	44.412079	49.339	58.000 ->	-8.661

116 :	11.075102	42.871680	68.406	111.000 ->	-42.594	143 :	-6.941155	41.022116	221.752	229.000 ->	-7.248
117 :	11.231004	43.803827	144.673	98.000 ->	46.673	144 :	-9.426130	38.690064	65.808	53.000 ->	12.808
118 :	12.452550	41.922461	201.931	101.000 ->	100.931	145 :	-7.051678	38.878854	229.935	222.000 ->	7.935
119 :	14.213193	42.464939	68.747	48.000 ->	20.747	146 :	-8.707011	41.196354	70.070	73.000 ->	-2.930
120 :	13.759409	45.647203	56.199	68.000 ->	-11.801	147 :	-8.668737	37.100047	55.347	52.000 ->	3.347
121 :	9.115185	39.210538	60.143	50.000 ->	10.143	148 :	27.204036	47.242718	222.944	177.000 ->	45.944
122 :	5.810079	52.178523	89.310	82.000 ->	7.310	149 :	28.659006	44.168573	37.216	33.000 ->	4.216
123 :	23.371464	55.913575	164.821	157.000 ->	7.821	150 :	21.345945	45.738362	140.156	132.000 ->	8.156
124 :	25.298666	54.653125	240.831	222.000 ->	18.831	151 :	28.624054	44.588148	156.390	143.000 ->	13.390
125 :	21.083013	55.729771	29.329	24.000 ->	5.329	152 :	15.589036	56.104256	35.189	32.000 ->	3.189
126 :	24.410065	57.315888	26.406	28.000 ->	-1.594	153 :	11.217940	58.353462	45.196	36.000 ->	9.196
127 :	21.000909	56.514952	36.258	28.000 ->	8.258	154 :	18.090914	59.322331	35.084	30.000 ->	5.084
128 :	21.537941	57.395876	27.941	31.000 ->	-3.059	155 :	15.185443	46.286396	342.172	321.000 ->	21.172
129 :	21.851980	57.554411	40.611	37.000 ->	3.611	156 :	16.476891	46.565884	385.191	316.000 ->	69.191
130 :	-4.249170	40.427214	815.088	843.000 ->	-27.912	157 :	13.643386	45.503793	323.127	261.000 ->	62.127
131 :	22.863652	42.001531	1264.160	1203.000 ->	61.160	158 :	18.729417	47.836647	261.732	185.000 ->	76.732
132 :	7.554792	58.006474	43.822	40.000 ->	3.822	159 :	20.323501	49.034587	743.178	688.000 ->	55.178
133 :	5.768998	58.961827	45.534	43.000 ->	2.534	160 :	18.884517	49.165908	415.054	480.000 ->	-64.946
134 :	11.441623	59.125635	141.486	147.000 ->	-5.514	161 :	5.219359	53.362711	56.091	41.000 ->	15.091
135 :	11.925486	57.395302	45.558	36.000 ->	9.558	162 :	1.480752	43.560778	207.106	194.000 ->	13.106
136 :	9.784687	47.515331	1090.310	1029.000 ->	61.310	163 :	27.845061	40.390488	40.005	38.000 ->	2.005
137 :	19.201822	50.512247	367.231	370.000 ->	-2.769	164 :	26.717480	38.426617	58.650	80.000 ->	-21.350
138 :	15.552539	52.578390	101.438	99.000 ->	2.438	165 :	22.452611	48.562870	273.801	237.000 ->	36.801
139 :	22.359563	53.734044	154.602	153.000 ->	1.602	166 :	18.367308	57.653880	79.788	80.000 ->	-0.212
140 :	18.326514	54.827479	70.796	70.000 ->	0.796	167 :	6.604485	52.914599	82.275	65.000 ->	17.275
141 :	14.226771	53.927591	42.205	44.000 ->	-1.795	168 :	12.878487	49.143966	660.272	627.000 ->	33.272
142 :	16.853840	54.587695	33.861	32.000 ->	1.861	169 :	12.878945	49.144253	665.937	627.000 ->	38.937

F.3 Differences between GPS points and GETASSE30 DEM – Bi-linear

DEM ".../DEM_GETASSE30/EUROPA_WGS84" controlled by "EUVN_ETRF.BLH" GCPs:

NUMBER OF GCPs IN INPUT :	217
NUMBER OF PROCESSED GCPs :	169 (77.9%)
NUMBER OF GCPs OUTSIDE THE DEM :	48 (22.1%)
ELEVATION DIFFERENCES :	
. ARITHMETIC MEAN :	11.304
. QUADRATIC MEAN :	34.017
. STANDARD DEVIATION :	32.083
. MINIMUM :	-181.091



VisioTerra

Envisat MERIS

Geometry Handbook

reference VT-P194-DOC-001-E

issue 1 revision 5

date 06/07/2005

page 111 of 115

. MAXIMUM : 125.763

GCP #	EASTING	NORTHING	GCP	ELEVAT.	DEM	ELEVAT.	DIFFERENCE	41 :	8.940319	45.851463	429.707	403.264 ->	26.443
1 :	17.073455	52.276957	124.366	112.812 ->	11.554	42 :	10.100730	46.698581	1612.690	1634.494 ->	-21.804		
2 :	4.359235	50.797807	149.668	133.450 ->	16.218	43 :	14.969324	50.817232	338.631	361.892 ->	-23.261		
3 :	8.972749	39.135881	238.378	167.832 ->	70.546	44 :	13.666705	49.462587	547.358	571.505 ->	-24.147		
4 :	3.399645	50.933714	63.894	54.994 ->	8.900	45 :	17.246431	49.505901	303.702	280.865 ->	22.837		
5 :	4.594950	50.094902	282.695	243.019 ->	39.676	46 :	15.935217	49.858445	427.682	424.213 ->	3.469		
6 :	0.492343	40.820895	107.810	64.683 ->	43.127	47 :	11.228598	52.335512	153.490	143.051 ->	10.439		
7 :	14.785635	49.913677	592.594	529.154 ->	63.440	48 :	9.681841	50.508463	334.877	328.023 ->	6.854		
8 :	6.920585	43.754725	1319.310	1241.729 ->	77.581	49 :	8.717037	53.868059	45.021	39.806 ->	5.215		
9 :	15.493466	47.067107	538.290	479.032 ->	59.258	50 :	6.761590	50.673819	217.982	216.771 ->	1.211		
10 :	0.336269	50.867308	76.489	55.476 ->	21.013	51 :	9.283692	48.400209	760.506	743.031 ->	17.475		
11 :	21.031561	52.097275	141.447	136.241 ->	5.206	52 :	7.295758	49.914766	526.493	498.273 ->	28.220		
12 :	5.809620	52.178407	96.846	83.807 ->	13.039	53 :	12.487501	50.840896	334.308	331.205 ->	3.103		
13 :	20.669911	53.892409	187.031	179.426 ->	7.605	54 :	11.141565	48.917419	597.626	586.354 ->	11.272		
14 :	16.704471	40.649120	535.657	504.194 ->	31.463	55 :	8.007257	52.363932	128.934	121.713 ->	7.221		
15 :	11.646799	44.519965	50.057	48.379 ->	1.678	56 :	12.088951	54.177972	49.546	39.988 ->	9.558		
16 :	14.989779	36.876079	126.244	147.778 ->	-21.534	57 :	23.932619	38.078547	514.553	501.339 ->	13.214		
17 :	11.925486	57.395302	45.547	39.760 ->	5.787	58 :	12.499933	55.738882	87.938	77.902 ->	10.036		
18 :	19.281520	47.789608	291.748	307.604 ->	-15.856	59 :	9.962361	57.595037	42.208	45.916 ->	-3.708		
19 :	13.066073	52.379286	144.420	113.480 ->	30.940	60 :	8.439783	55.460139	43.303	40.000 ->	3.303		
20 :	24.058785	56.948625	34.702	33.045 ->	1.657	61 :	11.924512	54.572108	40.619	38.000 ->	2.619		
21 :	-6.205649	36.464351	84.180	60.023 ->	24.157	62 :	12.499819	55.738824	86.715	77.843 ->	8.872		
22 :	11.877930	45.406732	84.043	60.589 ->	23.454	63 :	27.248784	57.842324	107.504	109.946 ->	-2.442		
23 :	-3.951976	40.443603	647.362	664.634 ->	-17.272	64 :	24.380271	59.463565	84.272	54.129 ->	30.143		
24 :	18.367308	57.653880	79.787	78.403 ->	1.384	65 :	-0.481227	38.338897	60.347	49.000 ->	11.347		
25 :	12.878888	49.144195	666.026	627.837 ->	38.189	66 :	-2.459192	36.852473	125.048	96.173 ->	28.875		
26 :	7.465296	46.877115	956.342	909.589 ->	46.753	67 :	2.157415	41.350939	67.660	50.107 ->	17.553		
27 :	15.598375	48.654545	457.606	435.192 ->	22.414	68 :	-1.024620	41.721528	269.634	260.437 ->	9.197		
28 :	13.683435	46.554197	687.372	654.312 ->	33.060	69 :	-8.398931	43.364369	66.957	66.484 ->	0.473		
29 :	12.082992	47.496026	630.059	575.422 ->	54.637	70 :	2.624605	39.552594	59.085	49.587 ->	9.498		
30 :	2.927413	51.234919	54.461	47.669 ->	6.792	71 :	-4.110514	38.686741	763.213	744.151 ->	19.062		
31 :	27.482093	42.483503	41.743	38.000 ->	3.743	72 :	-3.789428	43.461426	59.281	50.000 ->	9.281		
32 :	23.394726	42.556098	1119.560	993.797 ->	125.763	73 :	22.976524	59.822697	24.858	24.827 ->	0.031		
33 :	27.909290	43.192709	38.243	37.494 ->	0.749	74 :	8.762702	41.927389	96.797	48.000 ->	48.797		
34 :	21.035229	52.474971	139.882	130.440 ->	9.442	75 :	-0.561842	44.815672	53.915	54.821 ->	-0.906		
35 :	4.358834	50.798668	157.470	133.594 ->	23.876	76 :	3.735284	46.620143	257.485	263.942 ->	-6.457		
36 :	7.668582	47.567070	504.933	482.512 ->	22.421	77 :	-4.503849	48.407887	104.411	96.610 ->	7.801		
37 :	7.209528	45.958605	1683.440	1864.531 ->	-181.091	78 :	0.105997	49.481896	53.632	47.181 ->	6.451		
38 :	6.102058	46.454101	1258.260	1317.040 ->	-58.780	79 :	5.353775	43.278770	61.797	60.163 ->	1.634		
39 :	8.670456	46.659734	2094.220	2153.840 ->	-59.620	80 :	6.128414	48.762776	241.724	270.605 ->	-28.881		
40 :	8.498912	47.713004	563.324	527.537 ->	35.787	81 :	2.424987	48.844424	126.148	94.967 ->	31.181		



VisioTerra

reference VT-P194-DOC-001-E

Envisat MERIS

issue 1 revision 5

date 06/07/2005

page 112 of 115

Geometry Handbook

82 :	-1.681746	43.395136	54.264	66.099 ->	-11.835	125 :	21.083013	55.729771	29.329	22.736 ->	6.593
83 :	-0.199389	46.990445	133.433	133.753 ->	-0.320	126 :	24.410065	57.315888	26.406	28.816 ->	-2.410
84 :	-1.685527	55.212790	144.401	136.748 ->	7.653	127 :	21.000909	56.514952	36.258	28.494 ->	7.764
85 :	-5.924040	54.622245	67.897	55.000 ->	12.897	128 :	21.537941	57.395876	27.941	26.148 ->	1.793
86 :	-2.782971	56.478513	57.779	53.485 ->	4.294	129 :	21.851980	57.554411	40.611	34.225 ->	6.386
87 :	-5.355838	36.131807	45.469	100.590 ->	-55.121	130 :	-4.249170	40.427214	815.088	846.380 ->	-31.292
88 :	-1.450672	50.930791	98.586	63.803 ->	34.783	131 :	22.863652	42.001531	1264.160	1184.369 ->	79.791
89 :	-2.386369	54.446576	356.112	371.459 ->	-15.347	132 :	7.554792	58.006474	43.822	40.000 ->	3.822
90 :	-5.542908	50.102924	57.507	59.768 ->	-2.261	133 :	5.768998	58.961827	45.534	43.000 ->	2.534
91 :	-1.192268	52.940670	98.465	78.145 ->	20.320	134 :	11.441623	59.125635	141.486	145.177 ->	-3.691
92 :	25.566236	40.928037	182.585	220.174 ->	-37.589	135 :	11.925486	57.395302	45.558	39.760 ->	5.798
93 :	20.664811	39.734223	598.607	571.592 ->	27.015	136 :	9.784687	47.515331	1090.310	995.169 ->	95.141
94 :	21.320333	37.644130	26.885	23.635 ->	3.250	137 :	19.201822	50.512247	367.231	370.119 ->	-2.888
95 :	15.493466	47.067165	540.068	479.125 ->	60.943	138 :	15.552539	52.578390	101.438	99.488 ->	1.950
96 :	0.335639	50.867421	70.809	55.130 ->	15.679	139 :	22.359563	53.734044	154.602	151.982 ->	2.621
97 :	14.585901	45.255471	182.398	143.241 ->	39.157	140 :	18.326514	54.827479	70.796	68.668 ->	2.128
98 :	15.570243	45.578563	268.988	209.594 ->	59.394	141 :	14.226771	53.927591	42.205	41.296 ->	0.909
99 :	18.060776	42.657912	46.673	72.476 ->	-25.803	142 :	16.853840	54.587695	33.861	33.459 ->	0.402
100 :	18.711655	45.153943	146.095	129.914 ->	16.181	143 :	-6.941155	41.022116	221.752	234.550 ->	-12.798
101 :	16.438445	43.506635	47.627	51.167 ->	-3.540	144 :	-9.426130	38.690064	65.808	53.000 ->	12.808
102 :	15.978647	45.806199	160.909	161.905 ->	-0.996	145 :	-7.051678	38.878854	229.935	223.962 ->	5.973
103 :	13.629348	45.084043	53.589	48.099 ->	5.490	146 :	-8.707011	41.196354	70.070	65.635 ->	4.435
104 :	15.679620	44.845120	713.172	742.703 ->	-29.531	147 :	-8.668737	37.100047	55.347	58.280 ->	-2.933
105 :	21.632365	48.377004	155.772	143.887 ->	11.885	148 :	27.204036	47.242718	222.944	170.510 ->	52.434
106 :	20.670770	46.319570	142.470	128.664 ->	13.806	149 :	28.659006	44.168573	37.216	33.000 ->	4.216
107 :	18.619237	47.255668	234.628	213.072 ->	21.556	150 :	21.345945	45.738362	140.156	131.592 ->	8.564
108 :	-9.583063	51.871472	62.621	110.272 ->	-47.651	151 :	28.624054	44.588148	156.390	140.789 ->	15.601
109 :	-6.541173	53.711583	135.615	112.329 ->	23.286	152 :	15.589036	56.104256	35.189	32.000 ->	3.189
110 :	-7.339016	55.371616	82.705	69.613 ->	13.092	153 :	11.217940	58.353462	45.196	39.091 ->	6.105
111 :	16.867878	41.132069	63.116	47.181 ->	15.935	154 :	18.090914	59.322331	35.084	35.917 ->	-0.833
112 :	15.094687	37.501178	51.971	47.658 ->	4.313	155 :	15.185443	46.286396	342.172	329.825 ->	12.347
113 :	11.788148	42.096242	57.488	56.876 ->	0.612	156 :	16.476891	46.565884	385.191	308.600 ->	76.591
114 :	14.850322	40.649523	86.635	76.209 ->	10.426	157 :	13.643386	45.503793	323.127	253.943 ->	69.184
115 :	8.925651	44.412079	49.339	67.432 ->	-18.093	158 :	18.729417	47.836647	261.732	196.757 ->	64.975
116 :	11.075102	42.871680	68.406	106.220 ->	-37.814	159 :	20.323501	49.034587	743.178	695.092 ->	48.086
117 :	11.231004	43.803827	144.673	100.100 ->	44.573	160 :	18.884517	49.165908	415.054	491.704 ->	-76.650
118 :	12.452550	41.922461	201.931	87.465 ->	114.466	161 :	5.219359	53.362711	56.091	41.000 ->	15.091
119 :	14.213193	42.464939	68.747	49.105 ->	19.642	162 :	1.480752	43.560778	207.106	195.826 ->	11.280
120 :	13.759409	45.647203	56.199	66.645 ->	-10.446	163 :	27.845061	40.390488	40.005	38.000 ->	2.005
121 :	9.115185	39.210538	60.143	51.356 ->	8.787	164 :	26.717480	38.426617	58.650	71.158 ->	-12.508
122 :	5.810079	52.178523	89.310	84.083 ->	5.227	165 :	22.452611	48.562870	273.801	218.340 ->	55.461
123 :	23.371464	55.913575	164.821	155.374 ->	9.447	166 :	18.367308	57.653880	79.788	78.403 ->	1.385
124 :	25.298666	54.653125	240.831	224.789 ->	16.042	167 :	6.604485	52.914599	82.275	65.656 ->	16.619

168 :	12.878487	49.143966	660.272	627.916 ->	32.356	169 :	12.878945	49.144253	665.937	627.881 ->	38.056
-------	-----------	-----------	---------	------------	--------	-------	-----------	-----------	---------	------------	--------

F.4 Differences between GPS points and GETASSE30 DEM – Bi-cubic

DEM ".../DEM_GETASSE30/EUROPA_WGS84" controlled by "EUVN_ETRF.BLH" GCPs:

NUMBER OF GCPs IN INPUT : 217
 NUMBER OF PROCESSED GCPs : 169 (77.9%)
 NUMBER OF GCPs OUTSIDE THE DEM : 48 (22.1%)
 ELEVATION DIFFERENCES :
 . ARITHMETIC MEAN : 12.008
 . QUADRATIC MEAN : 32.915
 . STANDARD DEVIATION : 30.646
 . MINIMUM : -172.570
 . MAXIMUM : 127.387

GCP #	EASTING	NORTHING	GCP	ELEVAT.	DEM	ELEVAT.	DIFFERENCE	23 :	-3.951976	40.443603	647.362	662.525 ->	-15.163
1 :	17.073455	52.276957	124.366	112.723 ->	11.643	24 :	18.367308	57.653880	79.787	78.621 ->	1.166		
2 :	4.359235	50.797807	149.668	132.284 ->	17.384	25 :	12.878888	49.144195	666.026	633.368 ->	32.658		
3 :	8.972749	39.135881	238.378	166.796 ->	71.582	26 :	7.465296	46.877115	956.342	913.803 ->	42.539		
4 :	3.399645	50.933714	63.894	55.095 ->	8.799	27 :	15.598375	48.654545	457.606	441.081 ->	16.525		
5 :	4.594950	50.094902	282.695	237.366 ->	45.329	28 :	13.683435	46.554197	687.372	650.284 ->	37.088		
6 :	0.492343	40.820895	107.810	63.524 ->	44.286	29 :	12.082992	47.496026	630.059	557.365 ->	72.694		
7 :	14.785635	49.913677	592.594	533.833 ->	58.761	30 :	2.927413	51.234919	54.461	47.558 ->	6.903		
8 :	6.920585	43.754725	1319.310	1245.788 ->	73.522	31 :	27.482093	42.483503	41.743	37.998 ->	3.745		
9 :	15.493466	47.067107	538.290	479.585 ->	58.705	32 :	23.394726	42.556098	1119.560	992.173 ->	127.387		
10 :	0.336269	50.867308	76.489	54.938 ->	21.551	33 :	27.909290	43.192709	38.243	37.181 ->	1.062		
11 :	21.031561	52.097275	141.447	136.975 ->	4.472	34 :	21.035229	52.474971	139.882	130.629 ->	9.253		
12 :	5.809620	52.178407	96.846	82.618 ->	14.228	35 :	4.358834	50.798668	157.470	132.994 ->	24.476		
13 :	20.669911	53.892409	187.031	179.789 ->	7.242	36 :	7.668582	47.567070	504.933	485.308 ->	19.625		
14 :	16.704471	40.649120	535.657	504.578 ->	31.079	37 :	7.209528	45.958605	1683.440	1856.010 ->	-172.570		
15 :	11.646799	44.519965	50.057	48.275 ->	1.782	38 :	6.102058	46.454101	1258.260	1307.717 ->	-49.457		
16 :	14.989779	36.876079	126.244	148.171 ->	-21.927	39 :	8.670456	46.659734	2094.220	2137.401 ->	-43.181		
17 :	11.925486	57.395302	45.547	40.469 ->	5.078	40 :	8.498912	47.713004	563.324	525.685 ->	37.639		
18 :	19.281520	47.789608	291.748	307.550 ->	-15.802	41 :	8.940319	45.851463	429.707	398.204 ->	31.503		
19 :	13.066073	52.379286	144.420	114.260 ->	30.160	42 :	10.100730	46.698581	1612.690	1596.687 ->	16.003		
20 :	24.058785	56.948625	34.702	33.212 ->	1.490	43 :	14.969324	50.817232	338.631	360.229 ->	-21.598		
21 :	-6.205649	36.464351	84.180	62.822 ->	21.358	44 :	13.666705	49.462587	547.358	572.080 ->	-24.722		
22 :	11.877930	45.406732	84.043	60.980 ->	23.063	45 :	17.246431	49.505901	303.702	283.528 ->	20.174		



VisioTerra

Envisat MERIS

Geometry Handbook

reference VT-P194-DOC-001-E

issue 1 revision 5

date 06/07/2005

page 114 of 115

46 :	15.935217	49.858445	427.682	421.547 ->	6.135	89 :	-2.386369	54.446576	356.112	373.204 ->	-17.092
47 :	11.228598	52.335512	153.490	142.074 ->	11.416	90 :	-5.542908	50.102924	57.507	57.362 ->	0.145
48 :	9.681841	50.508463	334.877	328.169 ->	6.708	91 :	-1.192268	52.940670	98.465	77.148 ->	21.317
49 :	8.717037	53.868059	45.021	39.868 ->	5.153	92 :	25.566236	40.928037	182.585	219.439 ->	-36.854
50 :	6.761590	50.673819	217.982	217.091 ->	0.891	93 :	20.664811	39.734223	598.607	568.993 ->	29.614
51 :	9.283692	48.400209	760.506	742.933 ->	17.573	94 :	21.320333	37.644130	26.885	21.683 ->	5.202
52 :	7.295758	49.914766	526.493	500.350 ->	26.142	95 :	15.493466	47.067165	540.068	479.585 ->	60.483
53 :	12.487501	50.840896	334.308	331.907 ->	2.401	96 :	0.335639	50.867421	70.809	54.185 ->	16.624
54 :	11.141565	48.917419	597.626	586.403 ->	11.223	97 :	14.585901	45.255471	182.398	148.040 ->	34.358
55 :	8.007257	52.363932	128.934	119.959 ->	8.975	98 :	15.570243	45.578563	268.988	213.595 ->	55.393
56 :	12.088951	54.177972	49.546	40.534 ->	9.012	99 :	18.060776	42.657912	46.673	73.635 ->	-26.962
57 :	23.932619	38.078547	514.553	495.031 ->	19.522	100 :	18.711655	45.153943	146.095	131.279 ->	14.816
58 :	12.499933	55.738882	87.938	79.685 ->	8.253	101 :	16.438445	43.506635	47.627	49.399 ->	-1.772
59 :	9.962361	57.595037	42.208	46.441 ->	-4.233	102 :	15.978647	45.806199	160.909	161.443 ->	-0.534
60 :	8.439783	55.460139	43.303	39.611 ->	3.692	103 :	13.629348	45.084043	53.589	47.210 ->	6.379
61 :	11.924512	54.572108	40.619	38.075 ->	2.544	104 :	15.679620	44.845120	713.172	736.048 ->	-22.876
62 :	12.499819	55.738824	86.715	79.685 ->	7.030	105 :	21.632365	48.377004	155.772	140.266 ->	15.506
63 :	27.248784	57.842324	107.504	109.971 ->	-2.467	106 :	20.670770	46.319570	142.470	128.596 ->	13.874
64 :	24.380271	59.463565	84.272	55.676 ->	28.596	107 :	18.619237	47.255668	234.628	215.137 ->	19.491
65 :	-0.481227	38.338897	60.347	46.192 ->	14.155	108 :	-9.583063	51.871472	62.621	101.853 ->	-39.232
66 :	-2.459192	36.852473	125.048	94.285 ->	30.763	109 :	-6.541173	53.711583	135.615	108.040 ->	27.575
67 :	2.157415	41.350939	67.660	48.808 ->	18.852	110 :	-7.339016	55.371616	82.705	69.699 ->	13.006
68 :	-1.024620	41.721528	269.634	260.769 ->	8.865	111 :	16.867878	41.132069	63.116	46.953 ->	16.163
69 :	-8.398931	43.364369	66.957	62.806 ->	4.151	112 :	15.094687	37.501178	51.971	47.473 ->	4.498
70 :	2.624605	39.552594	59.085	49.099 ->	9.986	113 :	11.788148	42.096242	57.488	55.702 ->	1.786
71 :	-4.110514	38.686741	763.213	740.724 ->	22.489	114 :	14.850322	40.649523	86.635	76.195 ->	10.440
72 :	-3.789428	43.461426	59.281	48.260 ->	11.021	115 :	8.925651	44.412079	49.339	61.144 ->	-11.805
73 :	22.976524	59.822697	24.858	26.119 ->	-1.261	116 :	11.075102	42.871680	68.406	111.298 ->	-42.892
74 :	8.762702	41.927389	96.797	45.929 ->	50.868	117 :	11.231004	43.803827	144.673	99.837 ->	44.836
75 :	-0.561842	44.815672	53.915	54.871 ->	-0.956	118 :	12.452550	41.922461	201.931	83.302 ->	118.629
76 :	3.735284	46.620143	257.485	263.692 ->	-6.207	119 :	14.213193	42.464939	68.747	48.891 ->	19.856
77 :	-4.503849	48.407887	104.411	97.902 ->	6.509	120 :	13.759409	45.647203	56.199	69.730 ->	-13.531
78 :	0.105997	49.481896	53.632	47.363 ->	6.269	121 :	9.115185	39.210538	60.143	50.483 ->	9.660
79 :	5.353775	43.278770	61.797	56.707 ->	5.090	122 :	5.810079	52.178523	89.310	83.347 ->	5.963
80 :	6.128414	48.762776	241.724	262.970 ->	-21.246	123 :	23.371464	55.913575	164.821	155.424 ->	9.397
81 :	2.424987	48.844424	126.148	94.233 ->	31.915	124 :	25.298666	54.653125	240.831	226.470 ->	14.361
82 :	-1.681746	43.395136	54.264	65.093 ->	-10.829	125 :	21.083013	55.729771	29.329	22.435 ->	6.894
83 :	-0.199389	46.990445	133.433	134.083 ->	-0.650	126 :	24.410065	57.315888	26.406	29.183 ->	-2.777
84 :	-1.685527	55.212790	144.401	138.244 ->	6.157	127 :	21.000909	56.514952	36.258	29.052 ->	7.206
85 :	-5.924040	54.622245	67.897	53.946 ->	13.951	128 :	21.537941	57.395876	27.941	26.503 ->	1.438
86 :	-2.782971	56.478513	57.779	53.560 ->	4.219	129 :	21.851980	57.554411	40.611	34.141 ->	6.470
87 :	-5.355838	36.131807	45.469	88.148 ->	-42.679	130 :	-4.249170	40.427214	815.088	842.403 ->	-27.315
88 :	-1.450672	50.930791	98.586	63.465 ->	35.121	131 :	22.863652	42.001531	1264.160	1196.877 ->	67.283



VisioTerra

Envisat MERIS

Geometry Handbook

reference VT-P194-DOC-001-E

issue 1 revision 5

date 06/07/2005

page 115 of 115

132 :	7.554792	58.006474	43.822	37.857 ->	5.965	151 :	28.624054	44.588148	156.390	142.725 ->	13.665
133 :	5.768998	58.961827	45.534	42.585 ->	2.949	152 :	15.589036	56.104256	35.189	32.004 ->	3.185
134 :	11.441623	59.125635	141.486	146.211 ->	-4.725	153 :	11.217940	58.353462	45.196	39.917 ->	5.279
135 :	11.925486	57.395302	45.558	40.469 ->	5.088	154 :	18.090914	59.322331	35.084	34.771 ->	0.313
136 :	9.784687	47.515331	1090.310	1008.774 ->	81.536	155 :	15.185443	46.286396	342.172	323.922 ->	18.250
137 :	19.201822	50.512247	367.231	371.068 ->	-3.837	156 :	16.476891	46.565884	385.191	308.686 ->	76.505
138 :	15.552539	52.578390	101.438	98.918 ->	2.520	157 :	13.643386	45.503793	323.127	261.656 ->	61.471
139 :	22.359563	53.734044	154.602	152.159 ->	2.443	158 :	18.729417	47.836647	261.732	191.301 ->	70.431
140 :	18.326514	54.827479	70.796	69.929 ->	0.867	159 :	20.323501	49.034587	743.178	692.453 ->	50.725
141 :	14.226771	53.927591	42.205	41.565 ->	0.640	160 :	18.884517	49.165908	415.054	485.528 ->	-70.474
142 :	16.853840	54.587695	33.861	32.685 ->	1.176	161 :	5.219359	53.362711	56.091	39.798 ->	16.293
143 :	-6.941155	41.022116	221.752	232.939 ->	-11.187	162 :	1.480752	43.560778	207.106	195.360 ->	11.746
144 :	-9.426130	38.690064	65.808	51.780 ->	14.028	163 :	27.845061	40.390488	40.005	37.030 ->	2.975
145 :	-7.051678	38.878854	229.935	224.384 ->	5.551	164 :	26.717480	38.426617	58.650	71.807 ->	-13.157
146 :	-8.707011	41.196354	70.070	65.521 ->	4.549	165 :	22.452611	48.562870	273.801	223.232 ->	50.569
147 :	-8.668737	37.100047	55.347	56.649 ->	-1.302	166 :	18.367308	57.653880	79.788	78.621 ->	1.167
148 :	27.204036	47.242718	222.944	175.060 ->	47.884	167 :	6.604485	52.914599	82.275	65.809 ->	16.466
149 :	28.659006	44.168573	37.216	32.986 ->	4.230	168 :	12.878487	49.143966	660.272	633.368 ->	26.904
150 :	21.345945	45.738362	140.156	131.726 ->	8.430	169 :	12.878945	49.144253	665.937	633.368 ->	32.569